

AD-A056 090

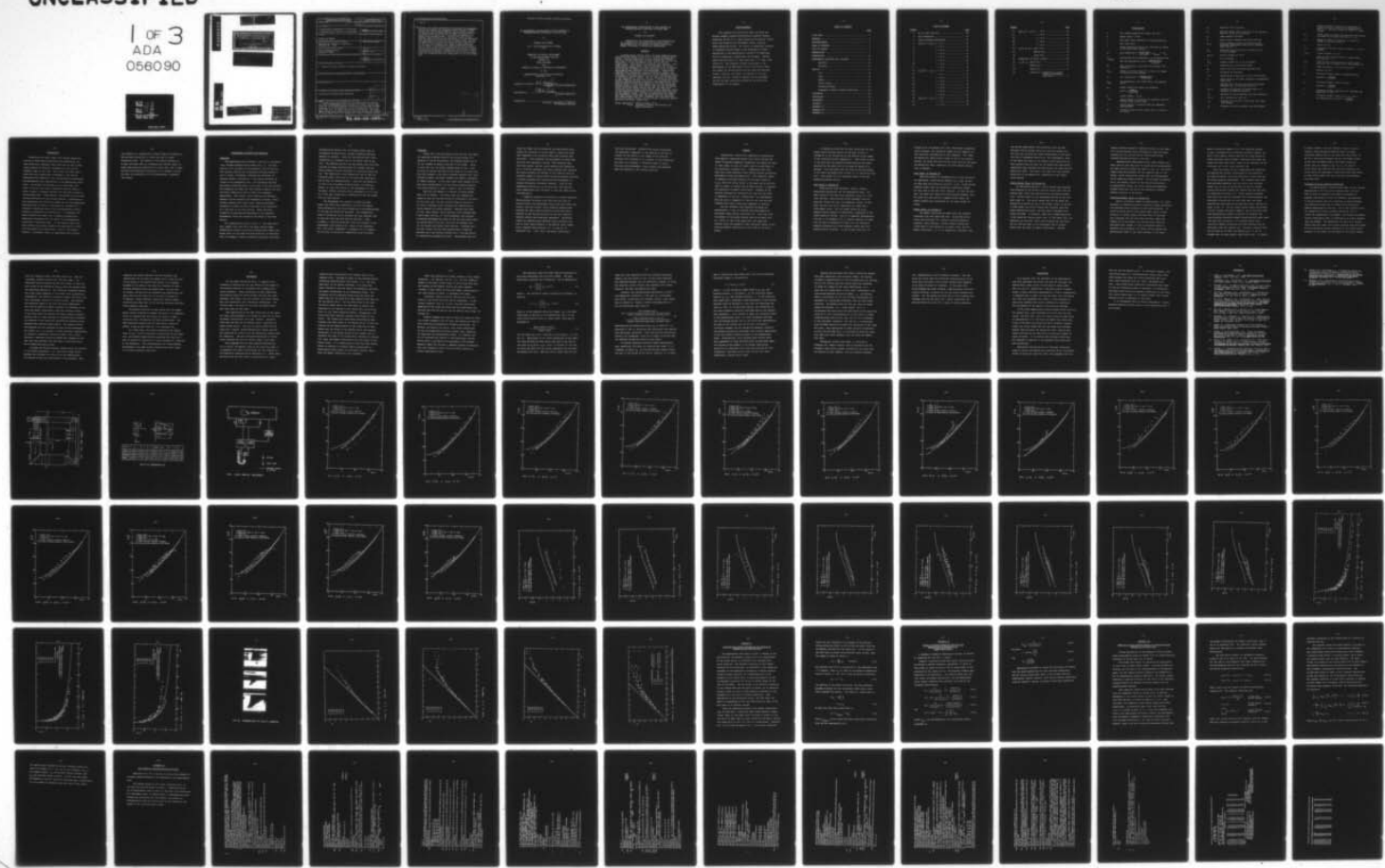
MASSACHUSETTS INST OF TECH CAMBRIDGE DEPT OF OCEAN E--ETC F/G 20/4  
AN EXPERIMENTAL INVESTIGATION OF WALL EFFECTS ON SUPERCAVITATION--ETC(U)  
AUG 77 M R MAIXNER

N00014-76-C-0358

NL

UNCLASSIFIED

1 OF 3  
ADA  
056090



AD A 056090

LEVEL

AN EXPERIMENTAL INVESTIGATION OF  
WALL EFFECTS ON SUPERCAVITATING  
HYDROFOILS OF FINITE SPAN,

by

(10) Michael Rex/Maixner

M.I.T.

(9) Master's Thesis

(11) August 1977

(12) 214 p.

(15) NDAF 14-76-C-4358

(16) RPP911

(17) SR009011

AD No.  
DDC FILE COPY

DISTRIBUTION STATEMENT A  
Approved for public release  
Distribution Unlimited

406 856  
DDC  
RECEIVED  
JUL 11 1978  
REF ID: A

REPORT DOCUMENTATION PAGE			READ INSTRUCTIONS BEFORE COMPLETING FORM
1. REPORT NUMBER	2. GOVT ACQUISITION NUMBER	3. RECIPIENT'S CATALOG NUMBER	
4. TITLE (and Subtitle)  An Experimental Investigation of Wall Effects on Supercavitating Hydrofoils of Finite Span.		5. TYPE OF REPORT & PERIOD COVERED  Thesis	
7. AUTHOR(s)  Michael Rex MAIXNER		8. CONTRACT OR GRANT NUMBER(s)	
9. PERFORMING ORGANIZATION NAME AND ADDRESS  Massachusetts Institute of Technology Cambridge, MA 02139		10. PROGRAM ELEMENT, PROJECT, TASK AREA & WORK UNIT NUMBERS	
11. CONTROLLING OFFICE NAME AND ADDRESS  Naval Postgraduate School Monterey, CA 93940		12. REPORT DATE  AUG 77	
14. MONITORING AGENCY NAME & ADDRESS (if different from Controlling Office)		13. NUMBER OF PAGES  211	
16. DISTRIBUTION STATEMENT (of this Report)  A. Approved for public release; distribution unlimited.		15. SECURITY CLASS. (of this report)  UNCLASS	
17. DISTRIBUTION STATEMENT (of the abstract entered in Block 20, if different from Report)		15a. DECLASSIFICATION/DOWNGRADING SCHEDULE	
18. SUPPLEMENTARY NOTES			
19. KEY WORDS (Continue on reverse side if necessary and identify by block number)  Wall effects, supercavitating, hydrofoils			
20. ABSTRACT (Continue on reverse side if necessary and identify by block number)  A geometrically similar family of three supercavitating hydrofoils was tested in the M.I.T. variable pressure water tunnel. The half-span foils were of elliptical planform; the ratio of foil half-span to tunnel height was 1/4 for the small foil, 1/2 for the medium foil, and 3/4 for the largest foil. The tunnel was of square cross section. Lift, drag, moment, tunnel speed, ambient pressure, and cavity pressure were measured for attack angles from 8 to 21 degrees and a variety of ambient pressure			

(Cont'd)

settings; cavity length measurements were obtained from photographs.) Results were compared with theoretical results obtained by Leehey, and also with a more detailed numerical lifting surface procedure developed by Jiang and Leehey. For the small and medium foils, it was sufficient to correct only for the effect on downwash of the images of the trailing vortices. The large foil data, however, required further correction; upon application of the same corrections which were applied to the data for the two smaller foils, the force and moment data for the large foil plotted slightly lower than did the data for the two smaller foils, while the cavity length data for the large foil indicated cavity lengths significantly larger than for either of the theoretical predictions or the cavity length data for the two smaller foils. Through the application of existing two-dimensional corrections, the force data for the large foil were brought into close agreement with the force data for the two smaller foils, but no suitable correction factors exist for the cavity length data.



Approved for public release; distribution unlimited.

AN EXPERIMENTAL INVESTIGATION OF WALL EFFECTS ON  
SUPERCAVITATING HYDROFOILS OF FINITE SPAN

by

MICHAEL REX MAIXNER

B.S., United States Naval Academy  
(1972)

SUBMITTED IN PARTIAL FULFILLMENT  
OF THE REQUIREMENTS FOR THE  
DEGREES OF  
OCEAN ENGINEER  
AND  
MASTER OF SCIENCE IN MECHANICAL ENGINEERING

at the

L MASSACHUSETTS INSTITUTE OF TECHNOLOGY  
(September 1977)

Signature of Author ..... M.R. Maixner .....  
Department of Ocean Engineering

Certified by ..... Patrick Lechner .....  
Thesis Supervisor

Accepted by .....  
Chairman, Departmental Committee  
on Graduate Students

AN EXPERIMENTAL INVESTIGATION OF WALL EFFECTS ON  
SUPERCAVITATING HYDROFOILS OF FINITE SPAN

by

MICHAEL REX MAIXNER

Submitted to the Department of Ocean Engineering  
on 12 August 1977 in partial fulfillment of the  
requirements for the Degrees of Ocean Engineer and  
Master of Science in Mechanical Engineering.

ABSTRACT

A geometrically similar family of three supercavitating hydrofoils was tested in the M.I.T. variable pressure water tunnel. The half-span foils were of elliptical planform; the ratio of foil half-span to tunnel height was 1/4 for the small foil, 1/2 for the medium foil, and 3/4 for the largest foil. The tunnel was of square cross section. Lift, drag, moment, tunnel speed, ambient pressure, and cavity pressure were measured for attack angles from 8 to 21 degrees and a variety of ambient pressure settings; cavity length measurements were obtained from photographs. Results were compared with theoretical results obtained by Leehey, and also with a more detailed numerical lifting surface procedure developed by Jiang and Leehey. For the small and medium foils, it was sufficient to correct only for the effect on downwash of the images of the trailing vortices. The large foil data, however, required further correction; upon application of the same corrections which were applied to the data for the two smaller foils, the force and moment data for the large foil plotted slightly lower than did the data for the two smaller foils, while the cavity length data for the large foil indicated cavity lengths significantly larger than for either of the theoretical predictions or the cavity length data for the two smaller foils. Through the application of existing two-dimensional corrections, the force data for the large foil were brought into close agreement with the force data for the two smaller foils, but no suitable correction factors exist for the cavity length data.

Thesis Supervisor: Patrick Leehey, Ph.D.

Title: Professor of Naval Architecture and  
Applied Mechanics

ACKNOWLEDGMENTS

This research was carried out under the Naval Sea Systems Command, General Hydromechanics Research Program, Subproject SR 009 01 01, administered by the David W. Taylor Naval Ship Research and Development Center, Contract Number N00014-76-C-0358. The author is exceedingly grateful to Professor Patrick Leehey of the Department of Ocean Engineering at the Massachusetts Institute of Technology for his inspiration, suggestions, and guidance. Special thanks are also due to S. Dean Lewis and C. W. Jiang, also from M.I.T., who rendered valuable assistance in the performance of the experiments, and to Miss Cheryl Gibson for typing the various drafts and for enduring countless errors. Finally, the author is indebted to his wife, Gretchen, for her unfailing support and encouragement and for the many sacrifices endured by her during the preparation of this report.

TABLE OF CONTENTS

	<u>Page</u>
TITLE PAGE .....	1
ABSTRACT .....	2
ACKNOWLEDGMENTS .....	3
TABLE OF CONTENTS .....	4
LIST OF FIGURES .....	5
NOMENCLATURE .....	7
INTRODUCTION .....	10
EXPERIMENTAL APPARATUS AND PROCEDURE .....	12
Apparatus .....	12
Procedure .....	14
RESULTS .....	17
Lift .....	18
Drag .....	19
Moment .....	19
Cavity Length .....	20
Cavitation Number .....	21
Influence of Static Pressure Controller .....	23
DISCUSSION .....	26
CONCLUSIONS .....	34
REFERENCES .....	36
APPENDIX I .....	73
APPENDIX II .....	75
APPENDIX III .....	77
APPENDIX IV .....	81

LIST OF FIGURES

<u>Figure</u>		<u>Page</u>
1	M.I.T. Test Facility .....	38
2	Foil Dimensions .....	39
3	Static Pressure Measurement .....	40
4	$C_L/\alpha_T$ vs. $\sigma_C/\alpha_T$ , $\alpha = 8.0^\circ$ .....	41
5	$\alpha = 9.5^\circ$ .....	42
6	$\alpha = 11.0^\circ$ .....	43
7	$\alpha = 12.0^\circ$ .....	44
8	$\alpha = 14.0^\circ$ .....	45
9	$\alpha = 16.0^\circ$ .....	46
10	$\alpha = 18.0^\circ$ .....	47
11	$\alpha = 21.0^\circ$ .....	48
12	$C_D/\alpha_T^2$ vs. $\sigma_C/\alpha_T$ , $\alpha = 8.0^\circ$ .....	49
13	$\alpha = 9.5^\circ$ .....	50
14	$\alpha = 11.0^\circ$ .....	51
15	$\alpha = 12.0^\circ$ .....	52
16	$\alpha = 14.0^\circ$ .....	53
17	$\alpha = 16.0^\circ$ .....	54
18	$\alpha = 18.0^\circ$ .....	55
19	$\alpha = 21.0^\circ$ .....	56
20	$C_M/\alpha_T$ vs. $\sigma_C/\alpha_T$ , $\alpha = 8.0^\circ$ .....	57
21	$\alpha = 9.5^\circ$ .....	58
22	$\alpha = 11.0^\circ$ .....	59

<u>Figure</u>		<u>Page</u>
23	$C_M/\alpha_T$ vs. $\sigma_C/\alpha_T$ , $\alpha = 12.0^\circ$ .....	60
24	$\alpha = 14.0^\circ$ .....	61
25	$\alpha = 16.0^\circ$ .....	62
26	$\alpha = 18.0^\circ$ .....	63
27	$\alpha = 21.0^\circ$ .....	64
28	$\sigma_C/\alpha_T$ vs. $L/c$ , Small Foil .....	65
29	Medium Foil .....	66
30	Large Foil .....	67
31	Comparison of Cavity Lengths .....	68
32	$\sigma_C$ vs. $\sigma_V$ , Small Foil .....	69
33	Medium Foil .....	70
34	Large Foil .....	71
35	Large Foil: Comparison of Cavity Pressure Measurement Techniques .....	72

NOMENCLATURE

a	foil leading edge bevel length; see Fig. 2
A	aspect ratio = $2s^2/S$
c	foil mean chord, measured at centroid position
C	foil root chord
$\delta$	tunnel correction factor for influence of images of trailing vortex system
$C_D$	drag coefficient = $\frac{\text{total drag}}{(1/2)\rho U^2 S} = C_{D_{\text{uncor}}} + \Delta C_{D_i}$
$C_{D_{\text{uncor}}}$	uncorrected drag coefficient, as calculated from the raw experimental data = $\frac{\text{measured drag}}{(1/2)\rho U^2 S}$
$C'_D$	drag coefficient, corrected for blockage; see equation (1)
$\Delta C_{D_i}$	change in induced drag due to effect of images of trailing vortex system
$C_L$	lift coefficient = $\frac{\text{measured lift}}{(1/2)\rho U^2 S}$
$C_{L_{2D}}$	two-dimensional lift coefficient; see equation (II-5)
$C_M$	moment coefficient about the midchord point = $\frac{\text{moment}}{(1/2)\rho U^2 S c}$
H	tunnel height = 51 cm
$\ell(z)$	cavity length as a function of spanwise position; measured from leading edge
L	cavity length at centroid position; measured from midchord
$P_b$	minimum pressure along tunnel wall in vicinity of cavity

$p_c$	measured cavity pressure
$p_\infty$	upstream tunnel static pressure at the spanwise position of the foil centroid
$p_v$	vapor pressure of water
$\tilde{p}$	tunnel static pressure controller setting
$p_{U,D}$	static pressure signal to controller from upstream, downstream tunnel static pressure taps; see Fig. 3
$q_{ij}$	strength of discrete source located in the $(i,j)$ -th element
$q(x,z)$	source strength at $(x,z)$
$s$	foil half-span
$\Delta s_{ij}$	element length for $(i,j)$ -th element
$S$	planform area of half-span model
$S_o$	tunnel test section cross-sectional area
$t$	thickness of hydrofoil
$u,v$	perturbation velocities in the $x,y$ -directions
$U$	water velocity one meter upstream of dynamometer shaft axis
$V$	maximum water velocity (at point of minimum pressure, $p_b$ ) in vicinity of cavity
$x_l(z)$	chordwise coordinate of leading edge as a function of spanwise position
$x_T$	distance of cavity pressure tap from midchord
$x,y,z$	foil coordinates; see Fig. 2
$z_C$	distance of centroid of half-span foil model from midspan
$z_T$	distance of cavity pressure tap from midspan

$\alpha$	geometric angle of attack with reference to tunnel side wall; when used in Appendices II and III, $\alpha$ indicates angle of attack in a free stream
$\alpha_T$	"true" angle of attack, as corrected for effects of images of trailing vortices = $\alpha + \Delta\alpha_i$
$\Delta\alpha_i$	change in angle of attack due to effect of images of trailing vortices
$\gamma$	$\arctan (2\alpha/\sigma_c)$
$\gamma_{ij}$	strength of discrete vortex located in $(i,j)$ -th element
$\gamma(x,z)$	vortex strength at $(x,z)$
$\lambda$	ratio of foil frontal width to tunnel width; see equation (3)
$\lambda_{3D}$	ratio of foil frontal area to tunnel cross-sectional area (without foil); see equation (4)
$\xi, \zeta$	dummy variables in the $x, z$ -directions
$\rho$	density of water
$\sigma_c$	cavitation number based on measured cavity pressure = $\frac{P_\infty - P_c}{(1/2) \rho U^2}$
$\sigma_v$	cavitation number, based on vapor pressure = $\frac{P_\infty - P_v}{(1/2) \rho U^2}$
$\sigma'$	cavitation number, corrected for blockage; see equations (2) and (5)
$\sigma''$	cavitation number, based on $P_b$ , $P_c$ , and $V$ , the maximum water velocity = $\frac{P_b - P_c}{(1/2) \rho V^2}$

INTRODUCTION

Corrections for water tunnel wall effects during the testing of subcavitating hydrofoils are essentially the same corrections developed fifty years ago for use in wind tunnel testing of airfoils; references [1] and [2] are standard texts in this area. Only within the last twenty years have wall effects been considered in the case of supercavitating hydrofoils, with the majority of theoretical and experimental work concentrated on two-dimensional hydrofoils. The problem of blockage can be significant; the shape of the foil and cavity combination must be known in order to apply a blockage correction of the type utilized in subcavitating flow. Unfortunately, this proves to be an area of great difficulty in the various theories. Corrections to drag coefficient and cavitation number for the two-dimensional pure-drag case are given in references [3] through [7]; a nonlinear theoretical model of the two-dimensional lifting problem is formulated in reference [6]. In reference [8], Baker converts this model into a computer program which numerically calculates the wall effect on two-dimensional hydrofoils of arbitrary shape. It was hoped by Baker that these results would prove adequate for application to flows over high aspect ratio hydrofoils. Prior to the current research, a systematic series of experiments which exhibit

wall effects on a geometrically similar family of hydrofoils had not been carried out in either the two- or three-dimensional case. The purpose of the present research is to make available data on a geometrically similar family of three supercavitating hydrofoils of finite span, and to apply existing two-dimensional corrections in an attempt to bring the data into agreement with three-dimensional, unbounded flow theory.

### EXPERIMENTAL APPARATUS AND PROCEDURE

#### Apparatus

The experiments were conducted in the M.I.T. recirculating, variable pressure water tunnel (Fig. 1). The test section is 51 cm square in cross-section, and 147 cm long. Test section velocity was continuously variable between 0 and 9.1 m/sec; a manometer indicated the difference in pressure across a contraction in the tunnel one meter upstream of the dynamometer axis. This manometer had been previously calibrated using a pitot tube in the test section. The assumption was made that the blockage caused by the foil and cavity combination did not affect the manometer appreciably. Test section static pressure was variable between 60 mm Hg absolute and atmospheric pressure; static pressure readings were taken using a mercury manometer connected to either or both of two taps on the centerline of a side wall of the test section. These taps were located 62 cm upstream and downstream of the hydrofoil dynamometer, which was located at the center of the test section.

Foil dimensions are given in Fig. 2. The three half-span, aspect ratio five foils had sharp leading edges. Geometrically similar elliptical planforms were chosen even though foils of this type were more difficult to fabricate than, for example, foils of rectangular planform; elliptical

planform foils exhibit less tip loading effect than do rectangular planform foils, thereby rendering them more amenable to analysis. Each foil was drilled with a hole terminating in a pressure tap on the cavity side of the foil. The medium-sized foil was the aspect ratio five foil utilized by Leehey and Stellinger [9], except that the cavity pressure tap was relocated to a position nearer the tip. The composition of the medium foil was of type 304 stainless steel, while that of the small and large foils was of type 614 aluminum bronze. Each foil was welded to its own 10.16 cm diameter mounting plate; the mounting plates, in turn, were bolted to the dynamometer so that the small, medium, and large foils protruded 1/4, 1/2, and 3/4 of the way, respectively, downward from the top window into the test section.

The dynamometer was capable of measuring three moment and three force components, but only the moment about midchord and the forces tangential to and perpendicular to the span and chord were measured. Zero geometrical angle of attack was set by aligning the flat (wetted) side of each foil with the test section side wall. Upon alignment, a sighting telescope, which was attached to the dynamometer, was aligned with a scale on the laboratory wall; this scale, graduated in increments of 0.05 degree, was utilized in setting the geometrical angle of attack.

Procedure

Before test runs were begun on any one day, the tunnel was operated at medium velocity for twenty minutes at a pressure of 300 mm Hg absolute; this removed almost all of the air trapped in remote locations of the tunnel. Prior to each test run, the bubble chamber shown in Fig. 3 was utilized to collect and draw off any gases or air which may have been trapped in the static pressure sensing line; once cleared of gases, the bubble chamber was merely a reservoir of common pressure. On the other hand, small amounts of air were bled intermittently into the cavity pressure sensing line during testing in order to keep it free of moisture.

Each foil was tested at a variety of attack angles from 8 to 21 degrees. The lower limit of 8 degrees was chosen so that the cavities would not terminate on the foil. For all test runs, the test section velocity was set at 8.5 m/sec, whereupon static pressure was reduced until a cavity covered the entire planform. Readings were taken of lift, drag, moment, static pressure (with pressure taps U and D open; see Fig. 3), cavity pressure, and velocity. A Polaroid photograph was taken of the foil and cavity from the wetted side of the foil, utilizing an exposure time of 1/40 second with bottom flood lighting. Pressure tap D was then closed, and the same readingstaken; reopening pressure tap D and closing pressure tap U, the same series of readings was repeated once more. (Photographs were not

taken for these last two pressure tap combinations since hardly any variation in cavity shape or length was noted when compared to the situation where both pressure taps were open.) This completed the measurement of three data points at one controller setting. Both pressure taps were then opened, and the static pressure was reduced by 20 to 30 mm Hg, whereupon the above procedure was repeated. The static pressure was reduced in this fashion until an excessive number of recirculated cavitation bubbles resulted in either extremely poor conditions for photography or rapidly fluctuating instrument readings. Prior to and immediately following a run of this type, the room and water temperatures were recorded, as were the tares on the instrumentation.

A computer program was utilized in the data reduction. Wetted surface frictional drag (for each foil and its mounting plate) and dynamometer shaft twist were taken into account, and test section static pressure readings were modified for static head difference to give the static pressure at the vertical position of the foil centroid. (Gravity effects were otherwise neglected.) Cavitation number was computed using measured cavity pressure, and also by using vapor pressure at the ambient water temperature (computed using equation (2) on page 151 of reference [10]). Lift, drag, and moment coefficients

were also calculated. Standard wind tunnel corrections (as described in Appendix I) were applied to the data to account for the effect of the images of the trailing vortices; this resulted in an increase in drag coefficient and also in an increase in effective angle of attack. Utilizing the photographs, cavity lengths were measured from the midchord at the centroid position.

### RESULTS

Experimental results were compared with predictions from Leehey's linearized theory [11], which utilizes the method of matched asymptotic expansions; the theory is valid to first order in angle of attack, and to second order in the reciprocal of aspect ratio. Comparisons were also made with a more detailed linear lifting surface calculation developed by Jiang and Leehey [12]. This numerical theory is expected to be more accurate at the lower values of  $\sigma_c/a_T$ , where the cavity length is the same size as the foil span or longer; it should also be more accurate, in general, for prediction of moment coefficients. Synopses of the theories developed in references [11] and [12] are given in Appendices II and III, respectively; the experimental data are given in Appendix IV, both in raw form and with standard wind tunnel corrections (Appendix I) applied.

The wall boundary layer momentum thickness was approximately 1.9 mm, as inferred from measurements by Stellinger under similar conditions [9]. Since less than two percent of the wetted surface area of the small foil was within 1.9 mm of the upper wall, the upper wall boundary layer was assumed to have negligible effect on the force and moment coefficients of all three of the foils tested.

It should be noted that the only correction for wall effect which has been applied to the data in Figs. 4 through 30 is the correction for the effects of the images of the trailing vortices (Appendix I). Also worthy of note is the fact that the supercavitating condition was never achieved for the small foil at an angle of attack of 8 degrees. This fact bears upon the lack of scaling evident in the force and moment data of Figs. 4, 12, and 20 for this foil. This matter will be considered again in the subsequent discussion section.

Lift (Figs. 4 through 11)

There was very good agreement, overall, between theoretical predictions and the experimental data. For small values of the similarity parameter  $\sigma_c/a_T$  (i.e., for long cavities), there was much better agreement with the numerical theory than with the asymptotic theory; in this case, the foil and cavity combination no longer has a large aspect ratio. For the higher values of  $\sigma_c/a_T$ , Leehey's theory appears to underpredict, especially at the higher angles of attack. This is in apparent contradiction with Fig. 4 of reference [9]; it should, however, be noted that the data of reference [9] were based on cavitation numbers calculated with vapor pressure rather than with measured cavity pressure. It can be seen from Figs. 32

through 35 of the present work that, when based on measured cavity pressure, the cavitation number will be smaller, so that the above contradiction is only apparent. The small and medium foil data plotted almost on top of one another, whereas the large foil data plotted lower than did the small and medium foil data, especially at attack angles greater than 11 degrees.

Drag (Figs. 12 through 19)

When the effects of streamwise foil or flow curvature are negligible, linear theory predicts  $C_D = \alpha_T C_L$ , so that the drag data are plotted as  $C_D/\alpha_T^2$  vs.  $\sigma_c/\alpha_T^2$ .  $C_D/\alpha_T^2$  plotted somewhat higher than the theoretical predictions except for very long or for very short cavities. As with the lift data, the small and medium foil data plotted together, with the large foil data plotting somewhat below these, the effect becoming more pronounced at the higher angles of attack.

Moment (Figs. 20 through 27)

The moment coefficient was taken about the midchord consistent with the right-hand rule. As pointed out by Leehey and Stellinger [9], Leehey's matched asymptotic expansion theory neglects lifting surface corrections (third order in the reciprocal of aspect ratio) for the moment coefficient. It is not surprising, therefore, that

the current experimental data agreed best with the more detailed lifting surface theory of Jiang and Leehey [12]. The load cell utilized for moment measurements on the small foil was of inadequate sensitivity, and consequently, much of the small foil data at the smaller attack angles may be less accurate than the data for the medium and large foils; comparisons must therefore be made between the large and the medium foil data. Once again, the large foil data plotted below that of the medium foil, especially at the larger attack angles.

Cavity Length (Figs. 28 through 31)

As mentioned previously, cavity lengths were measured from midchord at the centroid position rather than from the leading edge, since this convention was utilized by Leehey [11]. Cavity length ( $L$ ) was nondimensionalized on the foil mean chord ( $c$ ). The cavity length data for the small and medium foils plotted on top of one another (Figs. 28 and 29); in both cases, the cavity lengths were slightly less than those predicted by theory, but the overall agreement with theory was good. In contrast, there was a marked deviation in the large foil cavity length (Fig. 30) and shape (Fig. 31), especially at the root, where local blockage was the worst. The tip vortices seen in the photographs had no evident effect upon the force or moment coefficients. Neither

Leehey's matched asymptotic expansion theory nor the numerical lifting surface theory developed by Jiang and Leehey accounts for the roll-up effects which produced these isolated trailing vortices in the wake.

Representative photographs of the large, medium, and small foils at the same angle of attack and at approximately the same cavitation number are shown in Fig. 31. The cavity shapes shown were averaged over the exposure time of 1/40 second; visual observations showed that the instantaneous cavity shape was highly unsteady. For the small and medium foils, the general outline of the cavity was elliptical, as predicted by theory; the cavity length was undoubtedly reduced toward the tip due to the hydrostatic pressure gradient existing in the tunnel.

Cavitation Number (Figs. 32 through 35)

Below a cavitation number of approximately 0.4, there was almost no difference between cavitation number calculated with measured cavity pressure or with vapor pressure. It should be noted that in this region there exists a large variation in cavity length from very short to very long. This indicates that for even short cavities, where ram effects of the re-entrant jet from the cavity end have heretofore been thought to have a pronounced effect on measured cavity pressure, the actual cavity pressure was approximately equal to the vapor pressure of the water.

Above a cavitation number of 0.4, the disparity between  $\sigma_v$  and  $\sigma_c$  increased with increasing cavitation number; the data in this region, however, were only for large angles of attack and small cavity lengths, indicating that there may indeed have been some effect caused by the impinging of the re-entrant jet on the cavity pressure tap.

After the series of basic experiments was completed, ram effects were further investigated on the large foil by Jiang and Leehey, this time utilizing a total head tube for cavity pressure measurement. The L-shaped total head tube protruded downwards into the cavity from the upper tunnel wall so that it was parallel to the foil wetted surface and pointed towards the leading edge and away from the impinging re-entrant jet. Cavity pressure readings were taken with both the standard foil surface pressure tap previously utilized and the total head tube, and vapor pressure was calculated as was done previously; results are shown in Fig. 35. For the larger attack angles and shorter cavities (higher cavitation numbers), use of the total head tube significantly reduced re-entrant jet effects; the result was that cavitation numbers calculated with total head tube data were as much as 5 to 8 percent higher than cavitation numbers calculated with data obtained from the previously used foil surface tap. Although a similar check was not made on the small and medium foils, it can be assumed that the same general trend would occur. It should

be noted, however, that data points in Figs. 32 and 33 exhibit a more pronounced downward "hook" at higher cavitation numbers than do the large foil data (Figs. 34 and 35), a fact which accounts for the noticeable "hooks" in the lift and moment data at the higher angles of attack (see, for example, Figs. 10, 11, 26, and 27). If the total head tube had been utilized throughout the entire series of experiments, these deviations from theory at high attack angles and short cavities would probably have been less.

#### Influence of Static Pressure Controller

As stated earlier, readings were taken for the various combinations of the two static pressure taps; this was done in order to determine the effect of blockage on pressure and velocity at the two different tap positions. It was anticipated that this variation in static pressure tap combination would have no effect on the forces and moments experienced by the foil. Due to the location within the system of the static pressure controller (Fig. 3) (which was inadvertently overlooked), the forces and moments varied significantly when the combination of static pressure taps was changed. The explanation for this is as follows. Before data were taken, both static pressure taps were opened and the controller setting reduced to  $\tilde{p}$ ; the actual static pressure in the tunnel was decreased by the control system

until the combined signal from both taps was  $\tilde{p}$ . When the instrument readings settled out, data were taken. The downstream static pressure tap was then closed, so that the only signal to the controller was  $p_U$ , which was greater than the controller setting,  $\tilde{p}$ . The controller therefore lowered the actual static pressure in the tunnel until  $p_U$  equaled  $\tilde{p}$ . Consequently, the effective cavitation number (as seen by the foil) decreased, causing the cavity to grow. This reduced the effective camber of the foil and cavity combination; this loss of effective camber resulted in a reduction of the force and moment coefficients from their previous values. On the other hand, the measured cavitation number increased slightly due to a small decrease in measured cavity pressure; the presence of the controller prevented the measured static pressure from changing significantly. The opposite effect was observed with the upstream tap open and the downstream tap closed (i.e., an increase in force and moment coefficients, an increase in effective cavitation number, and a slight decrease in measured cavitation number when compared to the case when both pressure taps were open); there were only a few of these data points taken.

Although the desired pressure readings were not obtained in the current experiment (i.e., the actual tunnel static pressure was different for each of the tap combinations), the results do show the significance of the blockage. When

comparing the results obtained with the different tap combinations for the small and medium foils, there was very little change in the plotted data points; the increased blockage in the case of the large foil resulted in significantly different force and moment data. For the sake of clarity, the data for the different tap combinations are shown only for the large foil at an angle of attack of 14 degrees. Unless otherwise specified, further remarks concerning foil data will be for the data obtained with both static pressure taps open.

The general trend of the data agrees with the experimental results obtained by Kermeen (see page 37 of reference [13]); he observed that the longer the cavity in supercavitating flow, the smaller the force coefficients. The same conclusion follows from the theoretical results of Leehey, as may be seen from Fig. 4 of reference [9].

At a later time, the system indicated by the dashed lines in Fig. 3 will be utilized to obtain data on the large foil; the present system would be operated with only tap U open to provide an indication of static pressure at "infinity" to the controller. This configuration will allow pressure measurements to be made without affecting the input signal to the static pressure controller.

DISCUSSION

For the small and medium foils, it appears to be necessary to correct only for the effects of the images of the trailing vortices in accordance with standard wind tunnel procedure. These corrections to drag coefficient and effective angle of attack brought the data into good agreement with theory; the lift, moment, and cavity length data also agreed well with theoretical predictions. For the most part, the plots for the small and medium foils were very close to each other.

Upon application of the same corrections to the large foil data, good agreement with theory was seen for the force and moment coefficients; they were, however, generally lower than the data for the smaller foils, especially at higher attack angles. The plot of cavity length for the large foil, however, showed substantially longer cavities than predicted by either of the two theoretical models used for comparison. The most pronounced deviations in cavity length occurred for the long cavity (lower  $\sigma_c/a_T$ ) data.

When compared with the data obtained from the two smaller foils, the general trend of the large foil data is in agreement with Baker's predictions for wall effects on two-dimensional supercavitating hydrofoils [8]. Baker makes the point that the wall effect is negligible for tunnel

height-to-foil chord ratios ( $H/c$ ) greater than 10 for cambered foils. Although he makes no such generalizations concerning supercavitating flat plates, (i.e., the case applicable to the current research), it is seen from Figs. 4 through 27 that the effect of blockage on the force and moment coefficients is not exceedingly large. The following line of reasoning explains why the force and moment data for the large foil were somewhat lower than for the two smaller foils. For the three foils at the same cavitation number and at the same angle of attack, the magnitude of the velocity on the cavity wall of all three foils is  $c_c/2$  (from linearized theory); consequently, all three foils have identical pressure coefficients on the cavity. The largest foil experiences significantly more blockage than does either of the smaller foils, so that the velocity on the wetted surface of the large foil is much higher than for either of the smaller foils; the pressure coefficient on the wetted surface of the largest foil is therefore the least of all three foils, resulting in smaller lift, drag, and moment coefficients than for either of the smaller foils. It is interesting to note that this overall effect is contrary to blockage effects experienced in subcavitating water tunnel or wind tunnel testing, where force and moment coefficients are increased.

Baker also questions the sharp increase in wall effect predicted by Wu, Whitney, and Lin [6] for thin symmetric wedges or for small attack angles in the lifting flow case. The results of the present work do not show a marked increase in wall effect on force and moment coefficients at the lower angles of attack, in agreement with Baker.

Conversely, Baker's results indicate that the wall effect on the cavity plus wake can be tremendous. In the current research, this is, in fact, the most significant departure of the large foil data from the theoretical predictions and from the data of the two smaller foils (Figs. 28 through 30).

Several attempts were made to bring the large foil data into closer agreement with the small and medium foil data by using existing two-dimensional blockage corrections. Wu, Whitney, and Brennen [4] derive wall effect corrections for the two-dimensional pure-drag (wedge) case, employing the open-wake and Riabouchinsky models. Wu, Whitney, and Lin [6] consider wall effects in two-dimensional lifting cavity flows, a situation more applicable to the current research; Baker [8] utilizes a computer program to translate this into information which could be readily applied to correct experimental data.

The pure-drag, open-wake model employs corrections to both drag coefficient and cavitation number. The drag coefficient corrected for blockage,  $C_D'$ , can be expressed as

$$C_D' = \left[ \frac{1+\sigma'}{1+\sigma_c} \right] C_D + O(\lambda^2), \quad (1)$$

where  $\sigma'$ , the cavitation number corrected for blockage, is given by

$$\sigma' = \sigma_c - \left[ \frac{1+\sigma_c}{\sigma_c} \right] C_D \lambda + O(\lambda^2), \quad (2)$$

where  $\sigma_c$  is the measured cavitation number,  $C_D$  is the drag coefficient as defined in the nomenclature, and  $\lambda$  is the ratio of foil frontal width to tunnel width, which may be expressed as

$$\lambda = \frac{(\text{mean chord}) \times \sin(\alpha)}{\text{tunnel width}}. \quad (3)$$

For the large foil with  $\lambda$  defined in this fashion,  $\lambda \approx 0.30 \sin(\alpha)$ . Application of the above corrections to the large foil data shifted the data points down and to the left on the plots of  $C_D/\alpha_T^2$  vs.  $\sigma_c/\alpha_T$  (Figs. 12 through 19) but did not bring the data into any closer agreement with the small and medium foil data. When the cavity length data for the

large foil were replotted using the corrected cavitation numbers, the data points in Fig. 30 were moved downward; this downward movement was not sufficient, however, to bring the large foil cavity lengths into agreement with either theory or the small and medium foil data.

Actually, the straightforward application of such a two-dimensional correction to the case of a finite-span wing should overcorrect for blockage, making  $\lambda$  much larger than it should be. Perhaps a better representation of  $\lambda$  for the finite-span case would be

$$\begin{aligned}\lambda_{3D} &= \frac{\text{foil frontal area}}{\text{tunnel cross-sectional area (without foil)}} \\ &= \frac{(\text{foil planform area}) \times \sin (\alpha)}{\text{tunnel cross-sectional area (without foil)}}.\end{aligned}\quad (4)$$

Recalculating the corrections using  $\lambda_{3D}$  in place of  $\lambda$  in equations (1) and (2) would make the corrections even smaller than previously calculated. Since the previous corrections proved to be inadequate, there is no reason to believe that the modified corrections should be any better.

To correct measured cavitation number and measured drag coefficient utilizing the Riabouchinsky model, it is necessary to obtain  $p_b$ , the minimum pressure reading along the wall in the region of the cavity. Equation (1) is again

used to correct the drag coefficient, but now the corrected cavitation number is calculated as

$$\sigma' = (2/3)\sigma_c + (1/3)\sigma'' \quad (5)$$

where  $\sigma''$  is the cavitation number based on  $p_c$ ,  $p_b$ , and maximum velocity,  $V$ , and where  $\sigma_c$  is the cavitation number based on  $p_c$ ,  $p_\infty$ , and upstream velocity,  $U$ . It had originally been hoped that a reasonably close measurement of the minimum pressure could be obtained by using only the downstream tap (tap D in Fig. 3); as was shown earlier, the interaction of the static pressure controller precluded making this measurement accurately. In an attempt to apply the correction based on the Riabouchinsky model, the gross assumption was made that the maximum frontal area of the cavity was approximately the same as the frontal area of the foil; utilizing a continuity argument and the steady-flow Bernoulli equation, the pressure minimum was estimated, thus allowing application of the wall effect correction based on the Riabouchinsky model. Unfortunately, this procedure gave results which were comparable to those obtained using the open-wake model. The failure of both models in the current application should not be surprising since they were designed for two-dimensional, pure-drag cavity flows, and not for three-dimensional, lifting cavity flows.

Whereas the pure-drag wall effect corrections changed both drag coefficient and cavitation number, the results of Baker's computerization of the two-dimensional Wu, Whitney, and Lin [6] lifting case wall effect model are presented in terms of a change to the force coefficients (i.e., drag and lift coefficients in this case), referenced to the uncorrected measured cavitation number,  $\sigma_c$ . Accordingly, Baker's corrections to the lift and drag coefficients are expressed as a percentage difference from the free stream condition. He presents data for only one ratio of tunnel height-to-arclength (i.e., chord length),  $H/c = 4$ . Calculating this ratio using the mean chord of the large foil gives  $H/c \approx 3.33$ ; recalculating  $H/c$  as the ratio of tunnel cross-sectional area to foil area,  $H/c \approx 4.48$  is obtained. It was concluded, therefore, that the  $H/c = 4$  corrections given by Baker should be suitable for correction of the large foil data. Upon application of these additive corrections to both lift and drag data, it was found to bring the large foil data into close agreement with the small and medium foil data.

Because an infinite wake model is utilized in reference [8], Baker's results give no correction for the extremely large cavity lengths recorded for the large foil. His results do show, however, that as blockage increases,

the nondimensional cavity thickness increases. This was borne out nicely when the cavitation characteristics of the three foils utilized in the current research were compared at an angle of attack of 8 degrees. On the small foil, which produced the least blockage, supercavitation was never totally achieved, no matter how low the static pressure was brought. For the medium and large foils, which produced more blockage than did the small foil, cavity termination was achieved behind the foil over a range of static pressures.

CONCLUSIONS

As a general rule, the agreement of the experimental data with unbounded flow theory was good for the small and medium foils, whose ratios of half-span to tunnel width were 1/4 and 1/2, respectively, and whose ratios of tunnel height to mean chord were approximately 10 and 5, respectively. It appeared that in order to bring the small foil and medium foil data into agreement with theory, it was necessary to apply only standard wind tunnel procedures in correcting for the effects of the images of the trailing vortices.

Of the three geometrically similar aspect ratio five foils, the largest foil, which protruded 3/4 of the way into the tunnel, and which had a ratio of tunnel height to mean chord of approximately 3.33, had force and moment data which were close to the small and medium foil data, although slightly lower; the cavity length data for the large foil differed greatly from the small and medium foil data, showing much longer cavities for the same ratio of cavitation number to angle of attack. It is evident that blockage corrections are required in addition to the standard wind tunnel down-wash corrections.

Application and modification of blockage corrections based on various two-dimensional pure-drag cavity flow models failed to bring the large foil data into agreement with the

data for the two smaller foils. It was found, however, that corrections based on a two-dimensional lifting cavity flow model brought the large foil force coefficient data into much closer agreement with the small and medium foil data. While these force coefficient corrections were found to give an "engineering order of accuracy," no corrections have been found which give adequate corrections to the large foil cavity length data; it is clearly evident that further analytical work is necessary in this area.

It is recommended that for future experiments, a static pressure measuring system similar to that depicted in Fig. 3 be utilized.

REFERENCES

1. Pope, A., and Harper, J.J., Low Speed Wind Tunnel Testing. Wiley, New York, 1969.
2. Pankhurst, R.C., and Holder, D.W., Wind-Tunnel Technique. Sir Isaac Pitman & Sons, Ltd., London, 1965.
3. Whitney, A.K., "A Simple Correction Rule for Wall Effect in Two Dimensional Cavity Flows," Cavitation State of Knowledge, ASME, New York, 1969, p. 138.
4. Wu, T.Y., Whitney, A.K., and Brennen, C., "Cavity-Flow Wall Effects and Correction Rules," Journal of Fluid Mechanics, Vol. 49, Part 2, 1971, p. 223.
5. Wu, T.Y., Whitney, A.K., and Brennen, C., "Wall Effects in Cavity Flows and Their Correction Rules," Non-Steady Flow of Water at High Speeds, Proceedings of the IUTAM Symposium in Leningrad, June 22-26, 1971, Nauka Publishing House, Moscow, 1973, p. 461.
6. Wu, T.Y., Whitney, A.K., and Lin, J.D., "Final Report: Wall Effects in Cavity Flows," Calif. Inst. of Tech. Div. of Eng. & App. Sci. Report No.E-111A.5, 1969.
7. Whitney, A.K., Brennen, C., and Wu, T.Y., "Experimental Verification of Cavity-Flow Wall Effects and Correction Rules," Calif. Inst. of Tech. Div. of Eng. & App. Sci. Report No. E-97A-18, 1970.
8. Baker, E., "Analytical Prediction of Wall Effect on Fully Cavitating Lifting Foils, Using Nonlinear Theory," NSRDC Report 3688, 1972.
9. Leehey, P. and Stellinger, T.S., "Force and Moment Measurements of Supercavitating Hydrofoils of Finite Span with Comparison to Theory," Journal of Fluids Engineering, Vol. 97, No. 4, December 1975, p. 453.
10. Smith, L.B., Keyes, F.G., and Gerry, H.T., "The Vapor Pressure of Water, Part II, Steam Research Program," Proceedings of the American Academy of Arts and Sciences, published by the Society, Boston, Vol. 69, 1934, p. 137.
11. Leehey, P., "Supercavitating Hydrofoil of Finite Span," Non-Steady Flow of Water at High Speeds, Proceedings of the IUTAM Symposium in Leningrad, June 22-26, 1971, Nauka Publishing House, Moscow, 1973, p. 277.

12. Jiang, C.W., and Leehey, P., "A Numerical Method for Determining Forces and Moments on Supercavitating Hydrofoils of Finite Span," Proceedings of the Second International Conference on Numerical Ship Hydrodynamics, September 1977 (to be published).
13. Kermene, R.W., "Experimental Investigations of Three-Dimensional Effects on Cavitating Hydrofoils," Journal of Ship Research, Vol. 5, No. 2, September 1961, p. 22.

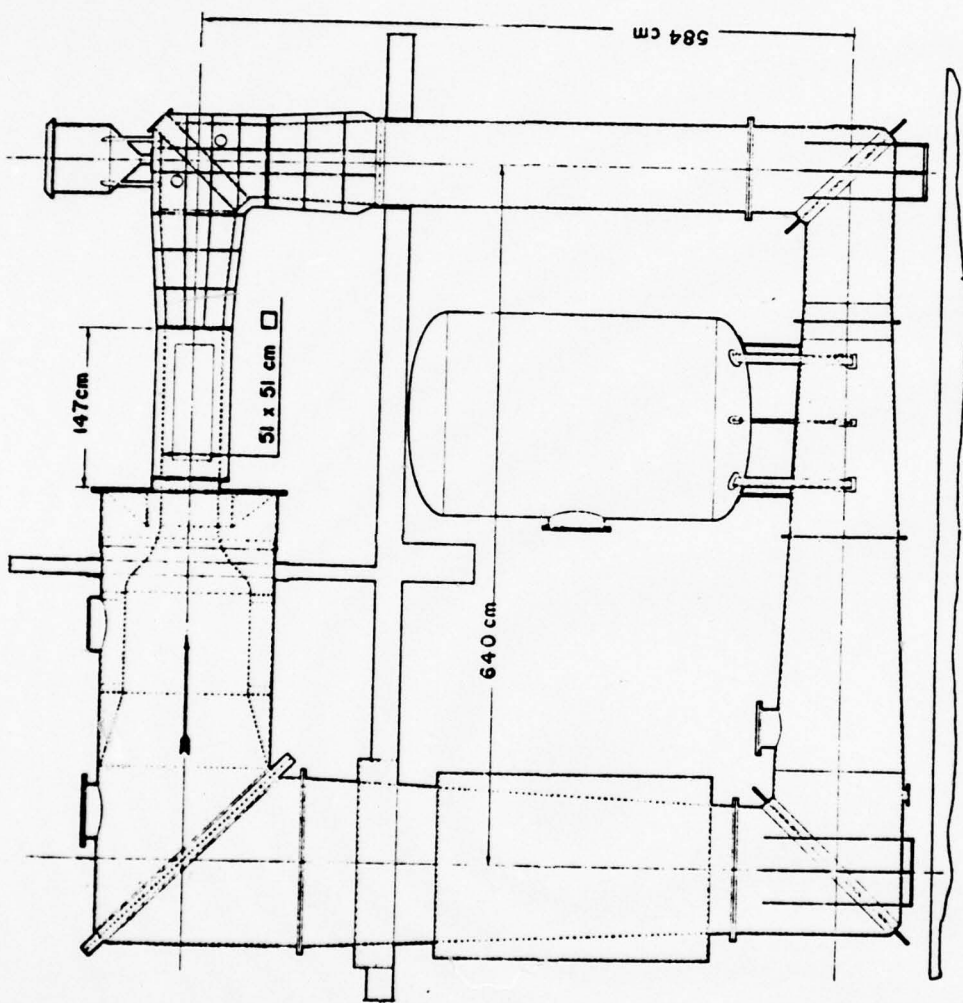
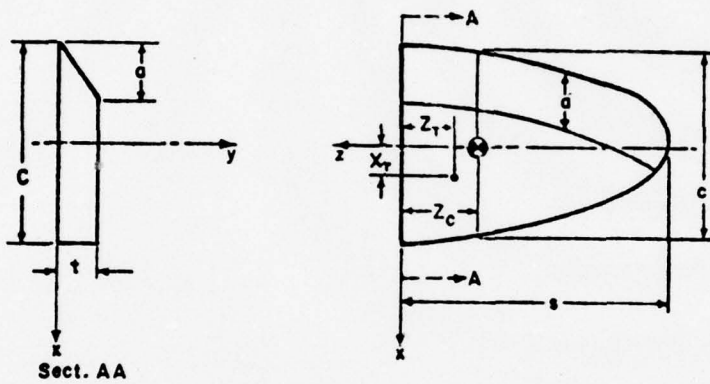


FIG. I : M.I.T. TEST FACILITY



FOIL	C	c	s	a	S(cm <sup>2</sup> )	Z <sub>c</sub>	Z <sub>T</sub>	x <sub>T</sub>	t
LARGE	19.50	15.33	38.10	7.65	580.6	16.17	12.55	2.54	1.60
MEDIUM	13.00	10.22	25.40	5.10	258.1	10.78	8.18	3.18	1.20
SMALL	6.50	5.11	12.70	2.55	64.5	5.39	4.67	1.43	.65

FIG. 2: FOIL DIMENSIONS (cm)

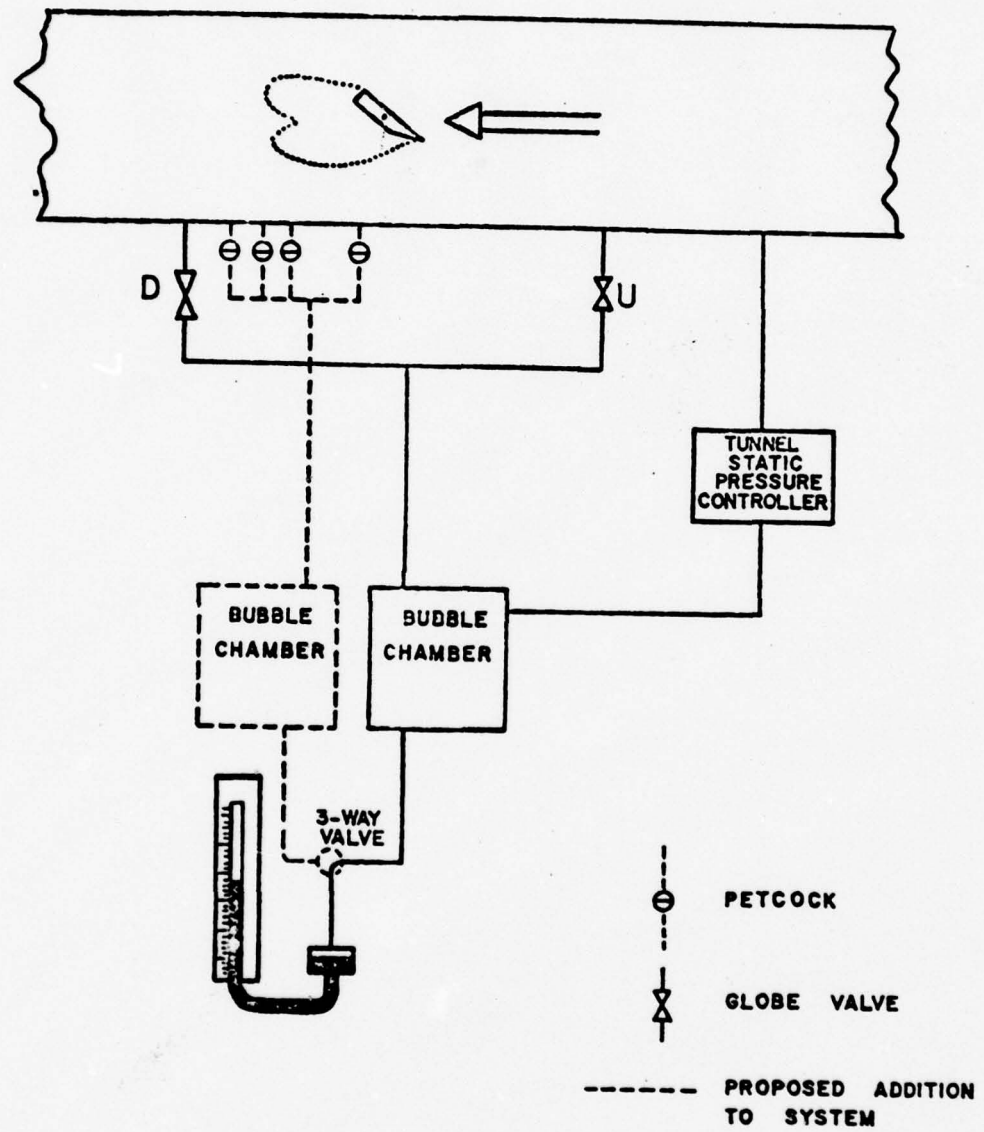


FIG.3 : STATIC PRESSURE MEASUREMENT

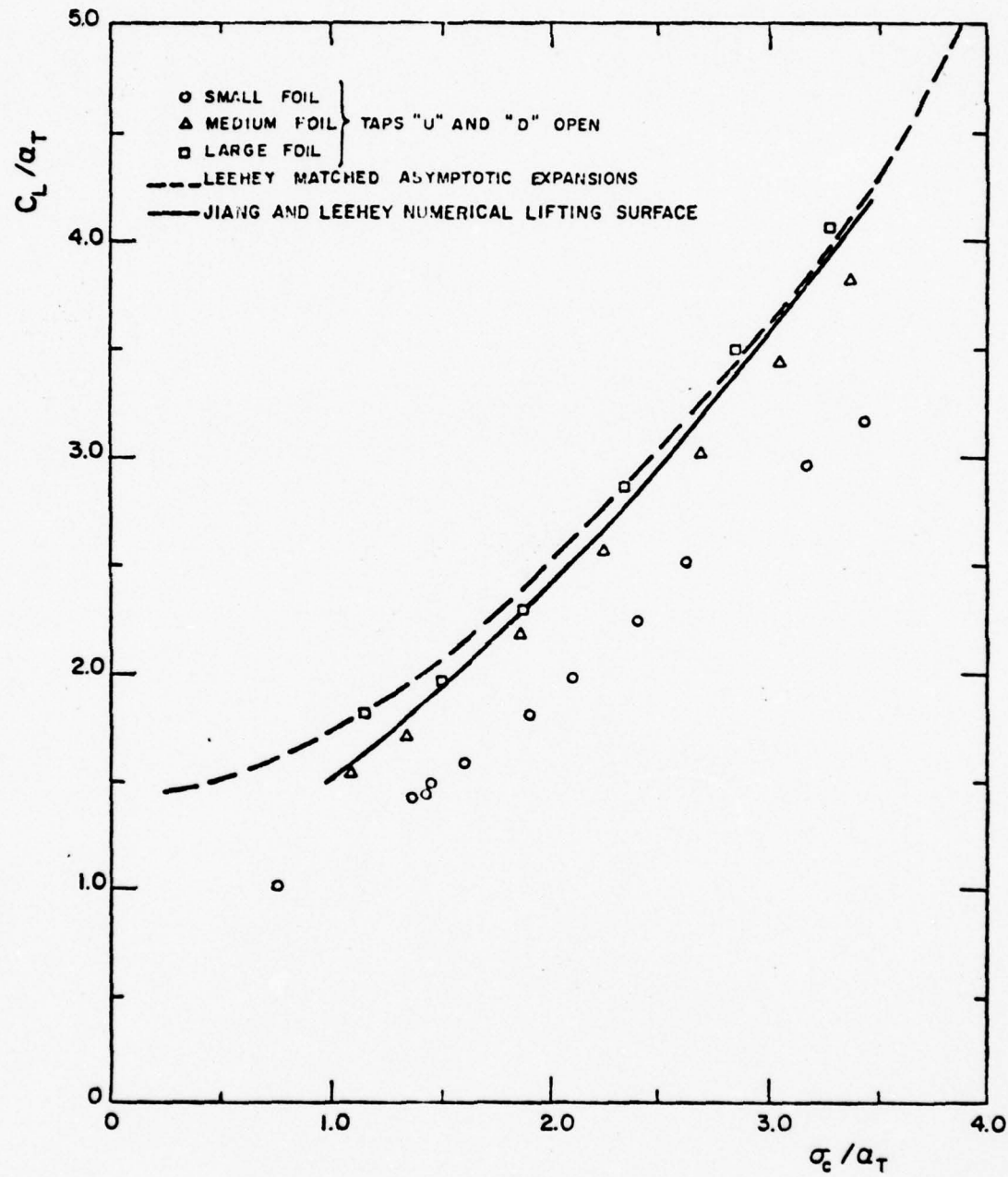


FIG. 4:  $C_L/a_T$  vs  $\sigma_c/a_T$ ,  $\alpha = 8.0^\circ$

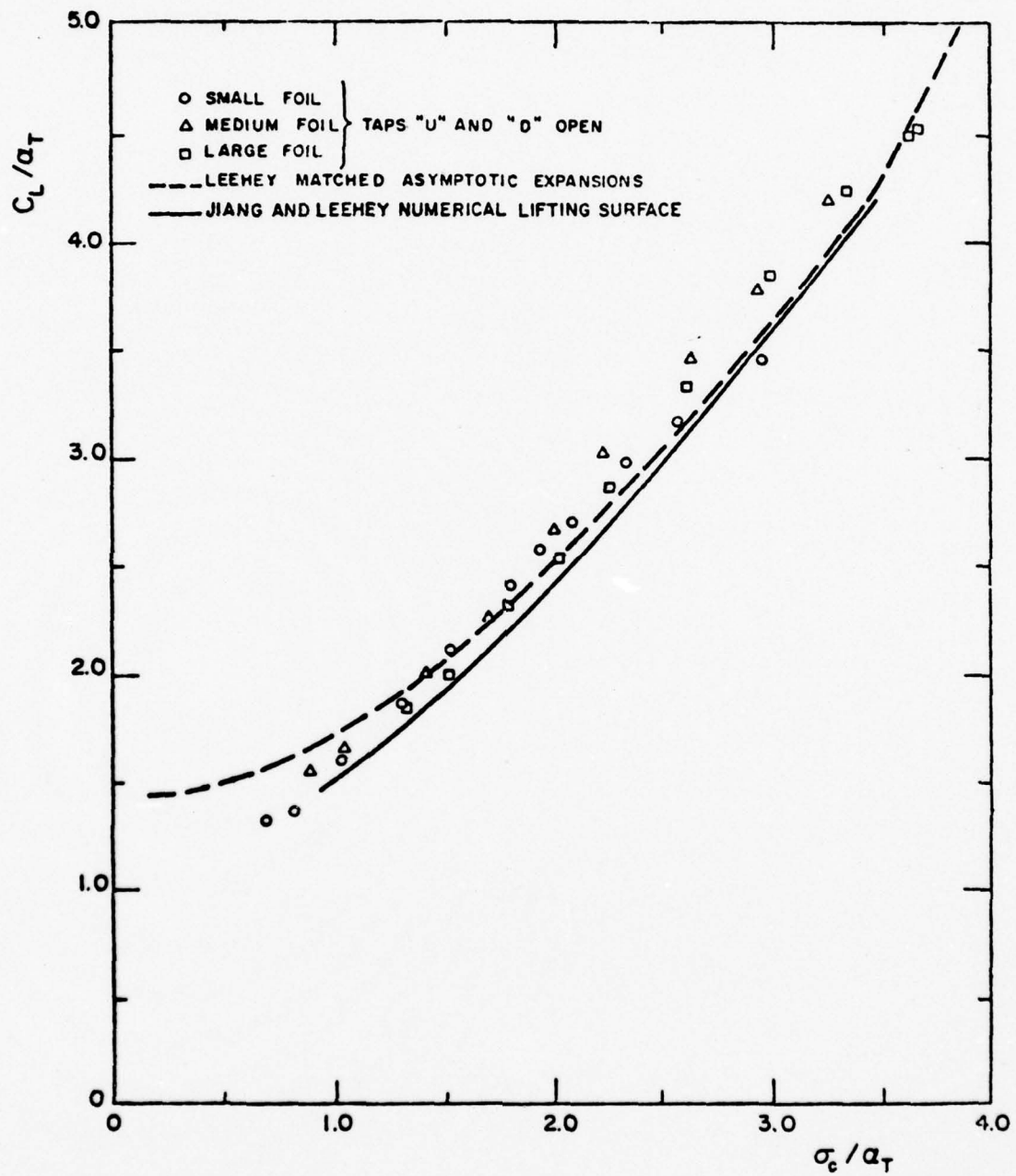


FIG. 5:  $C_L/a_T$  vs  $\sigma_c/a_T$ ,  $\alpha = 9.5^\circ$

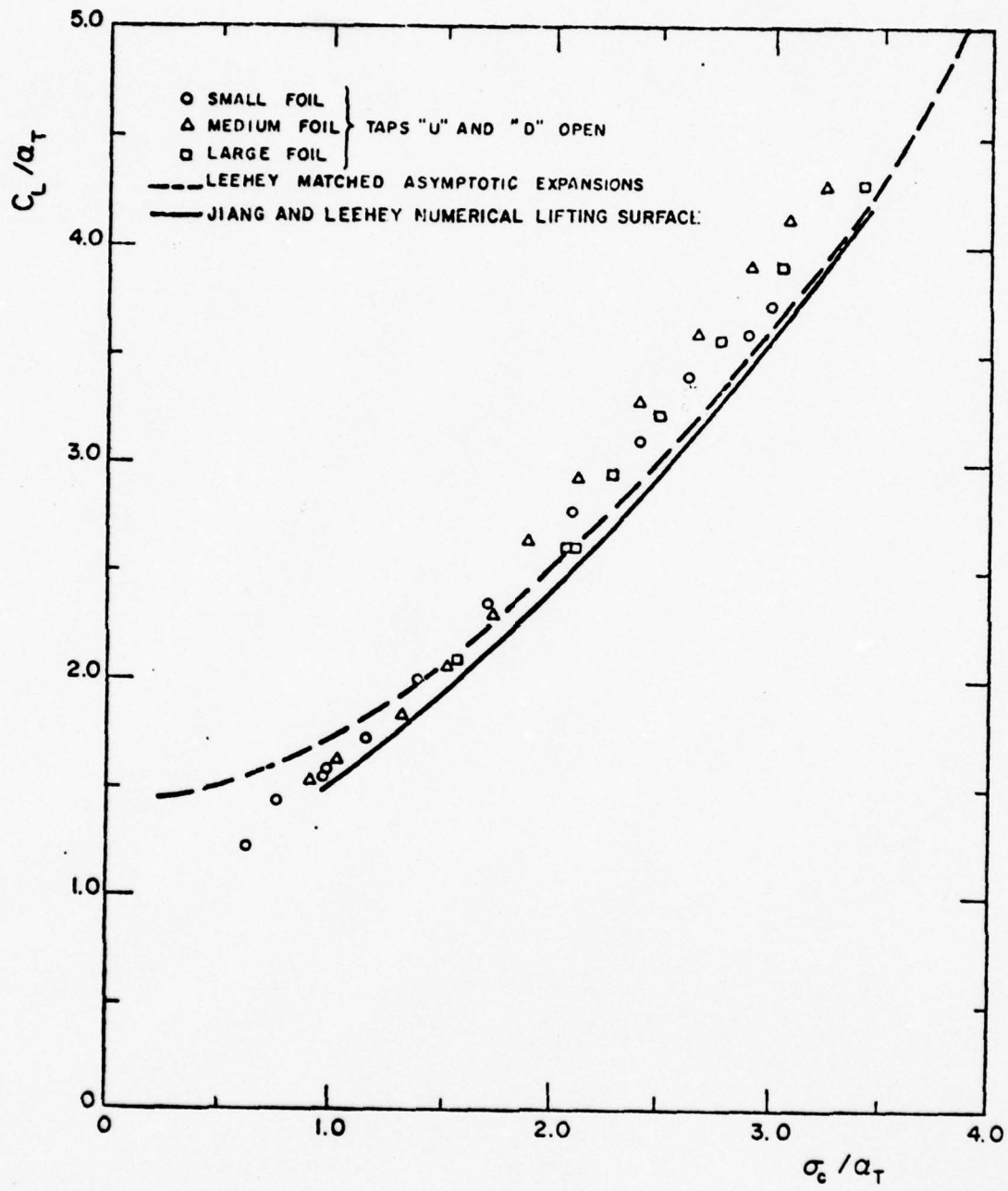


FIG. 6:  $C_L / \alpha_T$  vs  $\sigma_c / \alpha_T$ ,  $\alpha = 11.0^\circ$

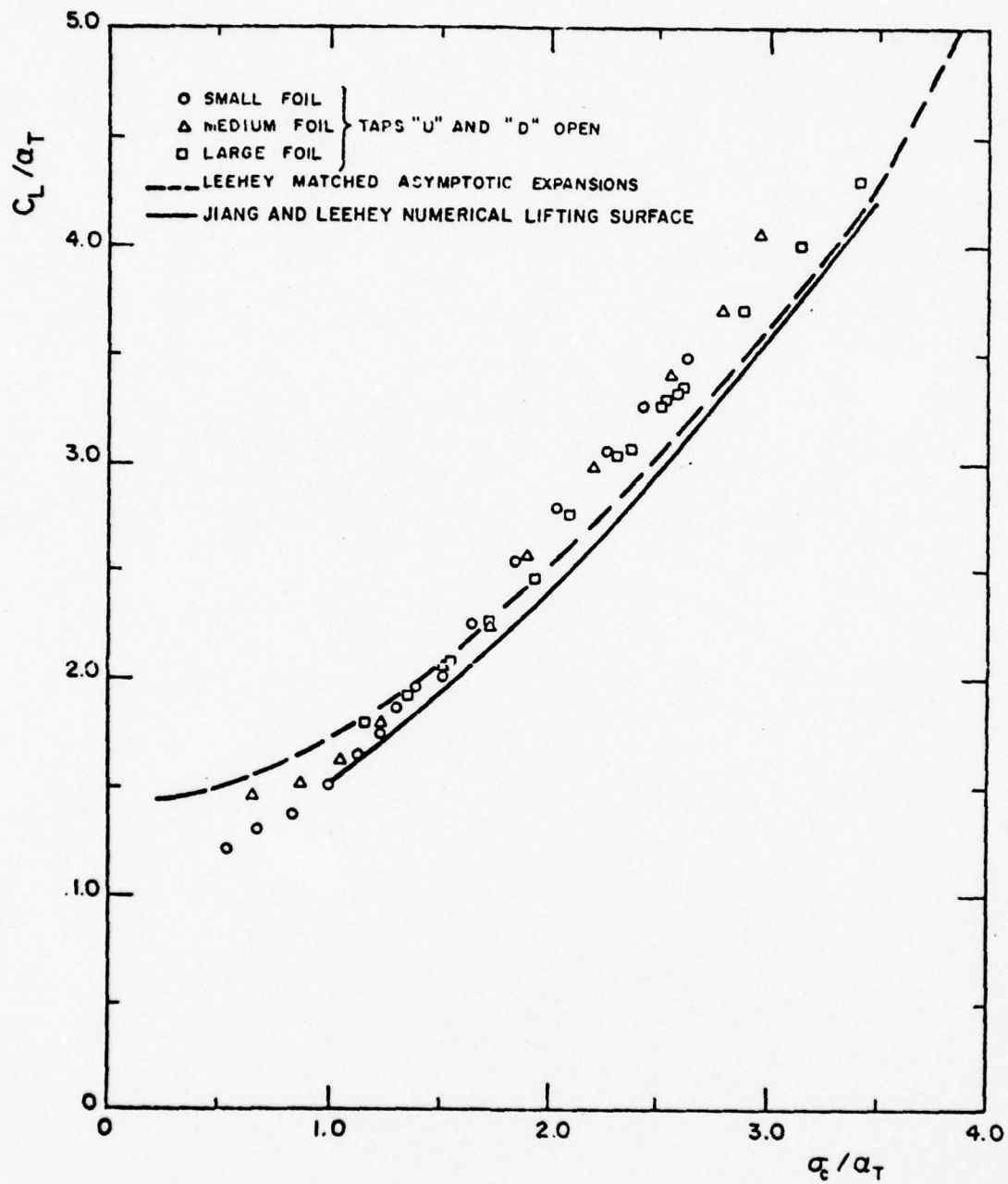


FIG. 7:  $C_L/a_T$  vs  $\sigma_c/a_T$ ,  $\alpha = 12.0^\circ$

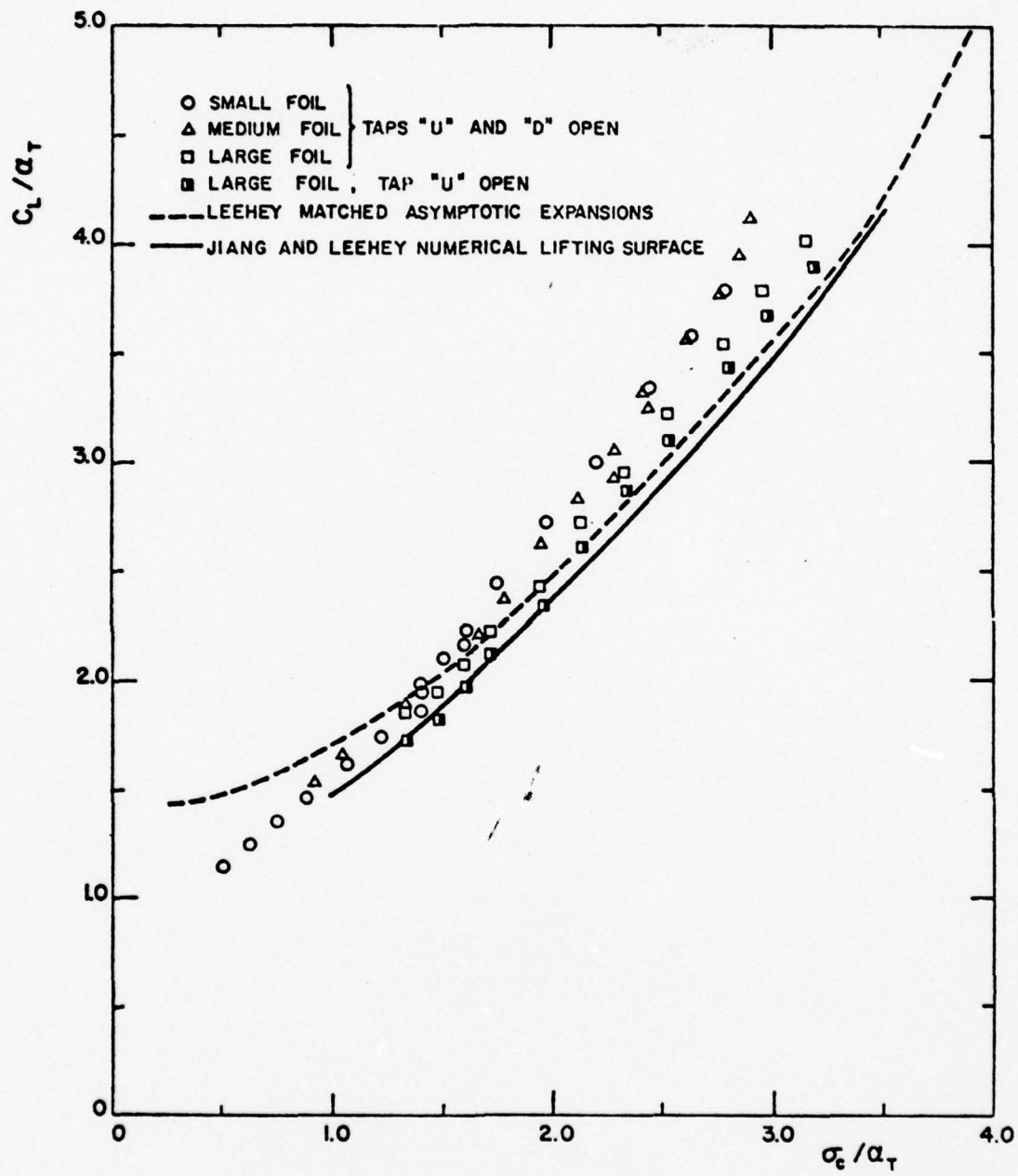


FIG. 8 :  $C_L / \alpha_T$  vs  $\sigma_e / \alpha_T$ ,  $\alpha = 14.0^\circ$

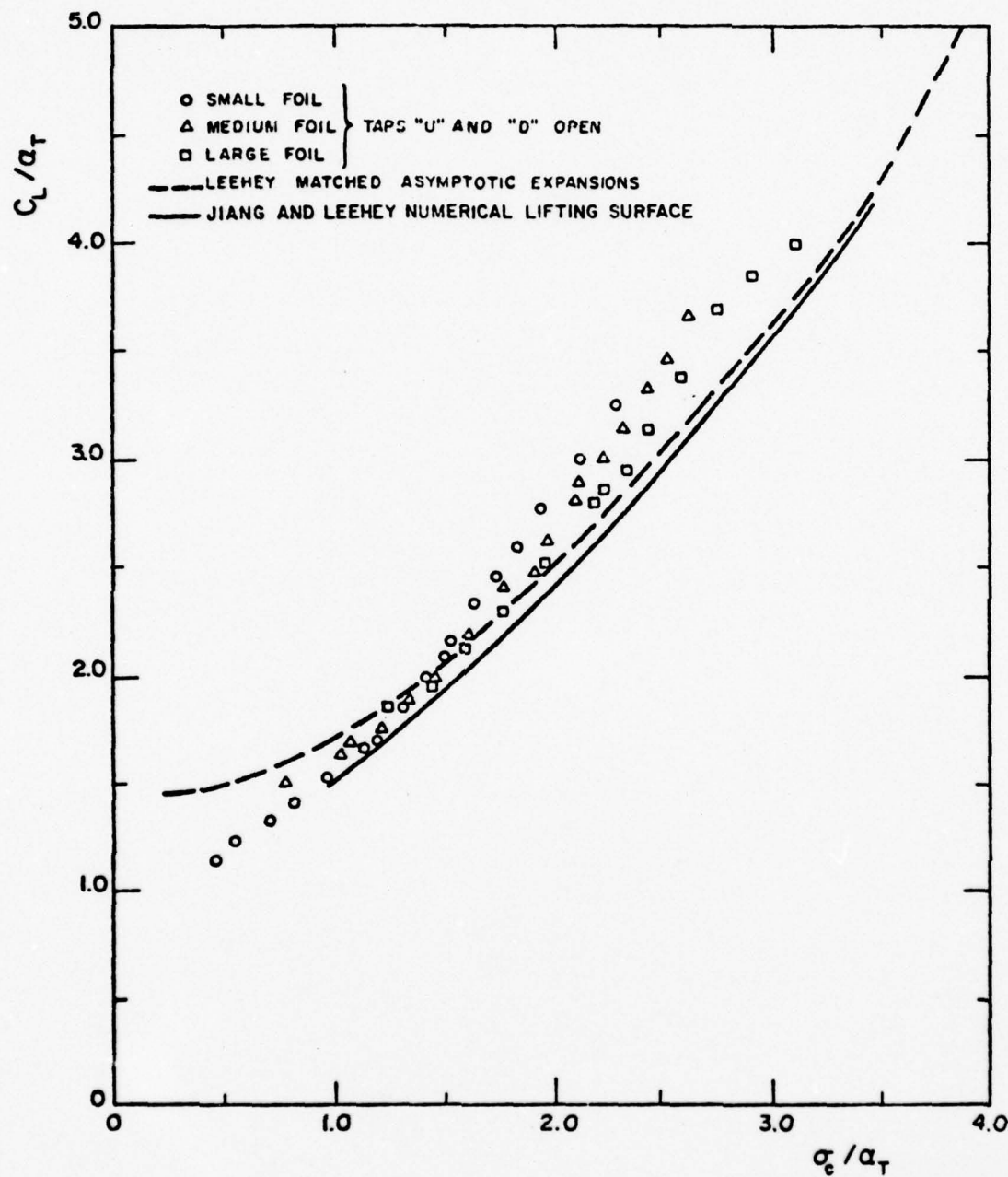


FIG. 9:  $C_L/a_T$  vs  $\sigma_c/a_T$ ,  $\alpha = 16.0^\circ$

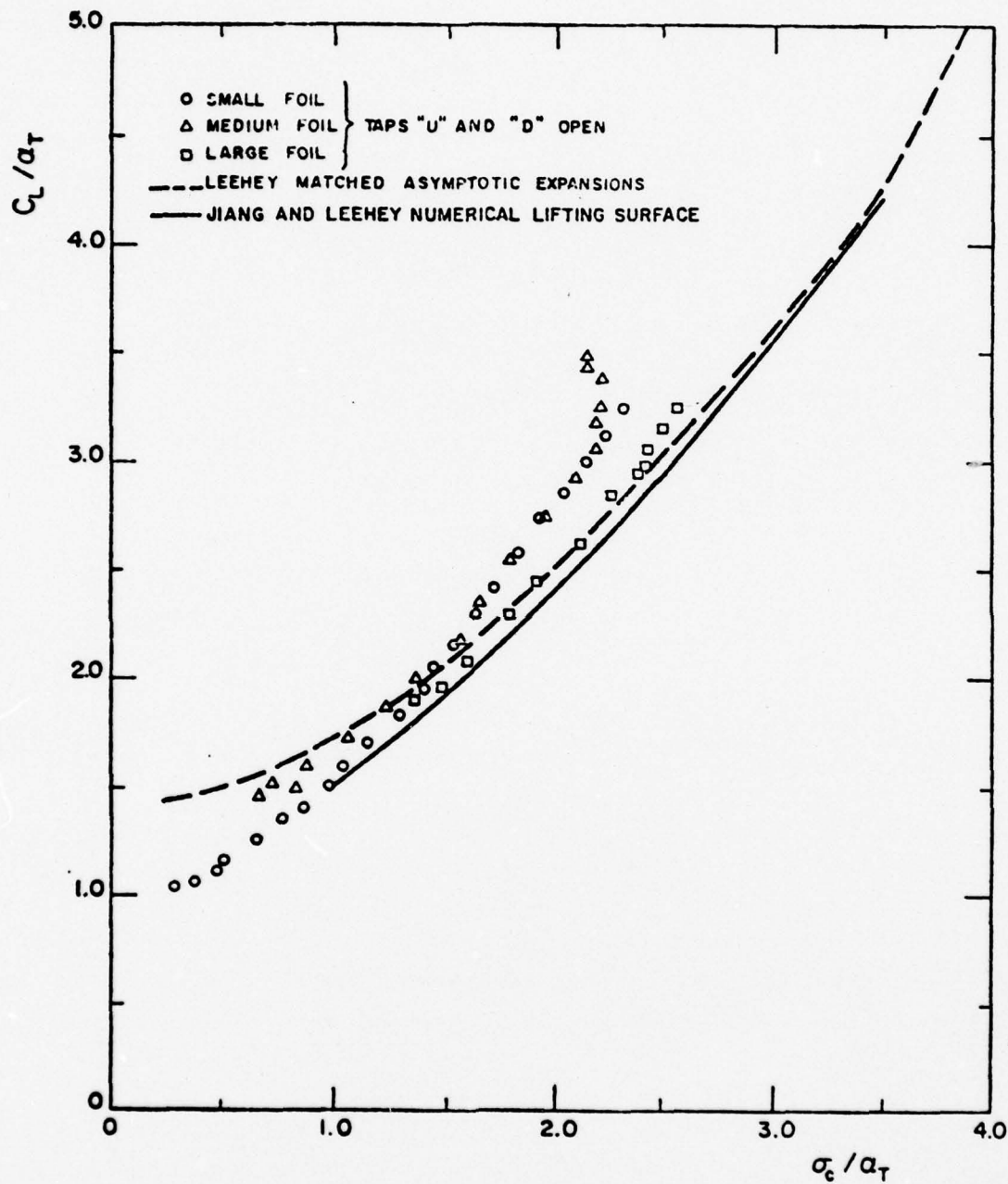


FIG. 10:  $C_L/a_T$  vs  $\sigma_c/a_T$ ,  $\alpha = 18.0^\circ$

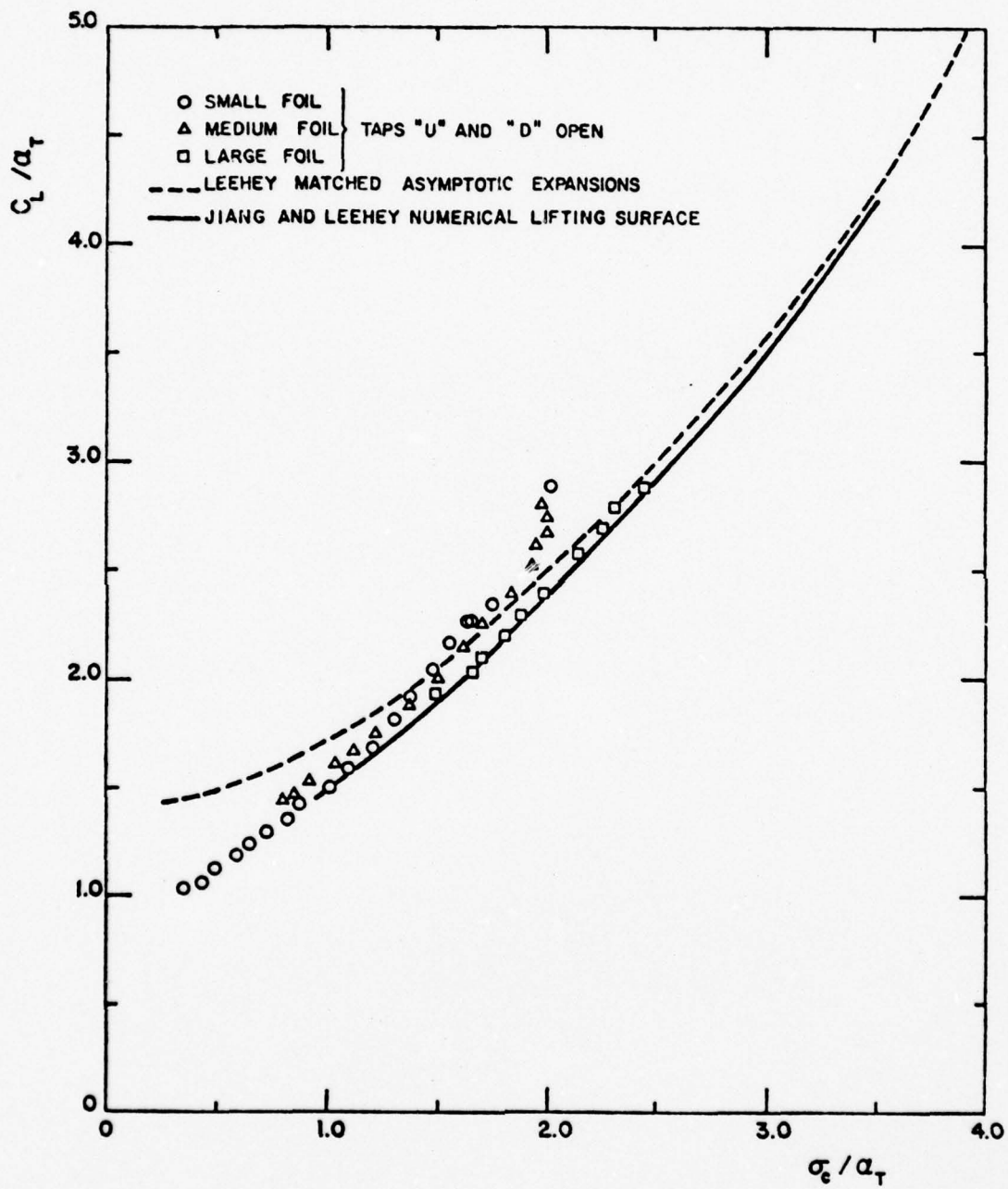


FIG. II:  $C_L/a_T$  vs  $\sigma_e/a_T$ ,  $\alpha = 21.0^\circ$

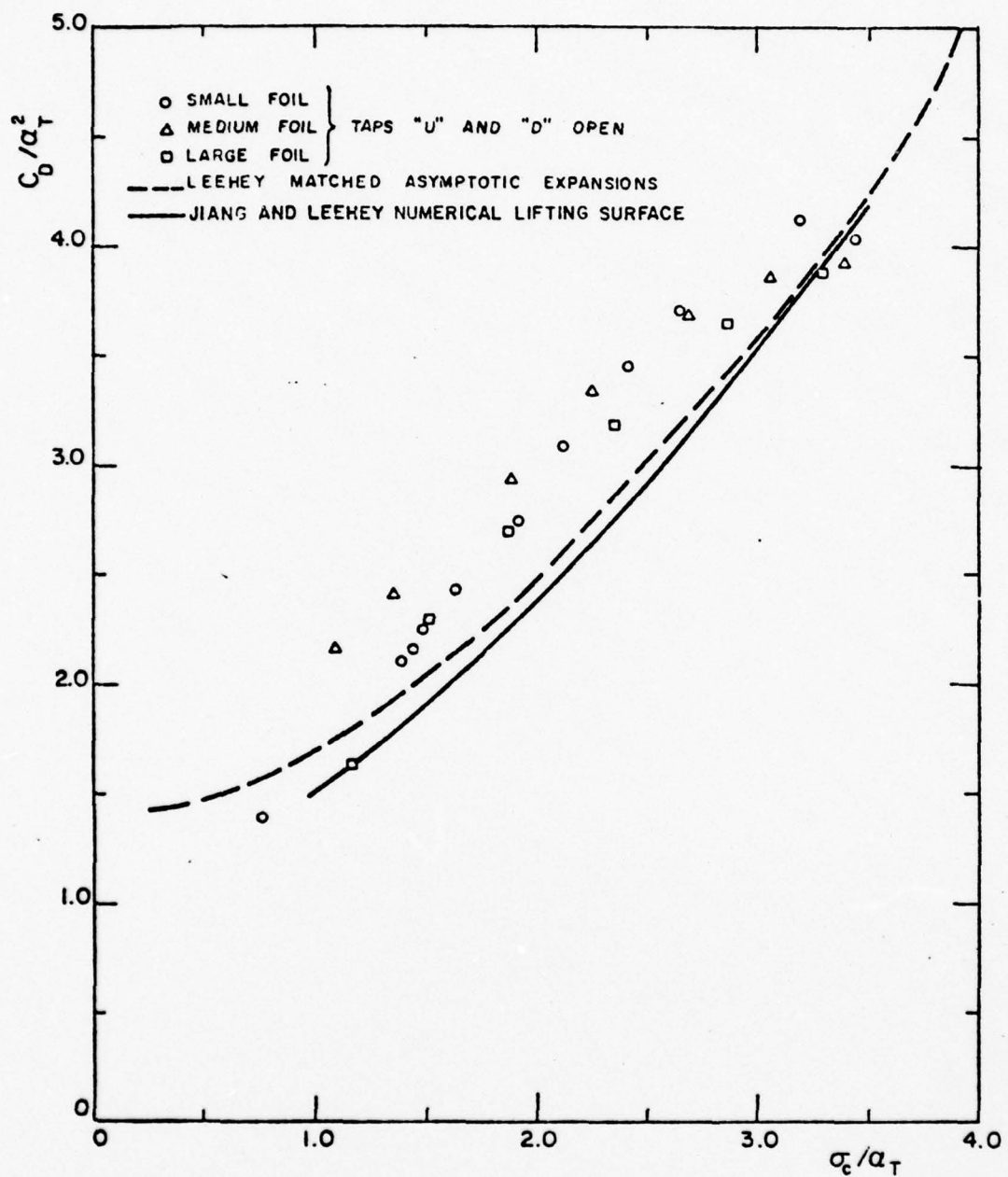


FIG. 12:  $C_D/a_T^2$  vs  $\sigma_c/a_T$ ,  $\alpha = 8.0^\circ$

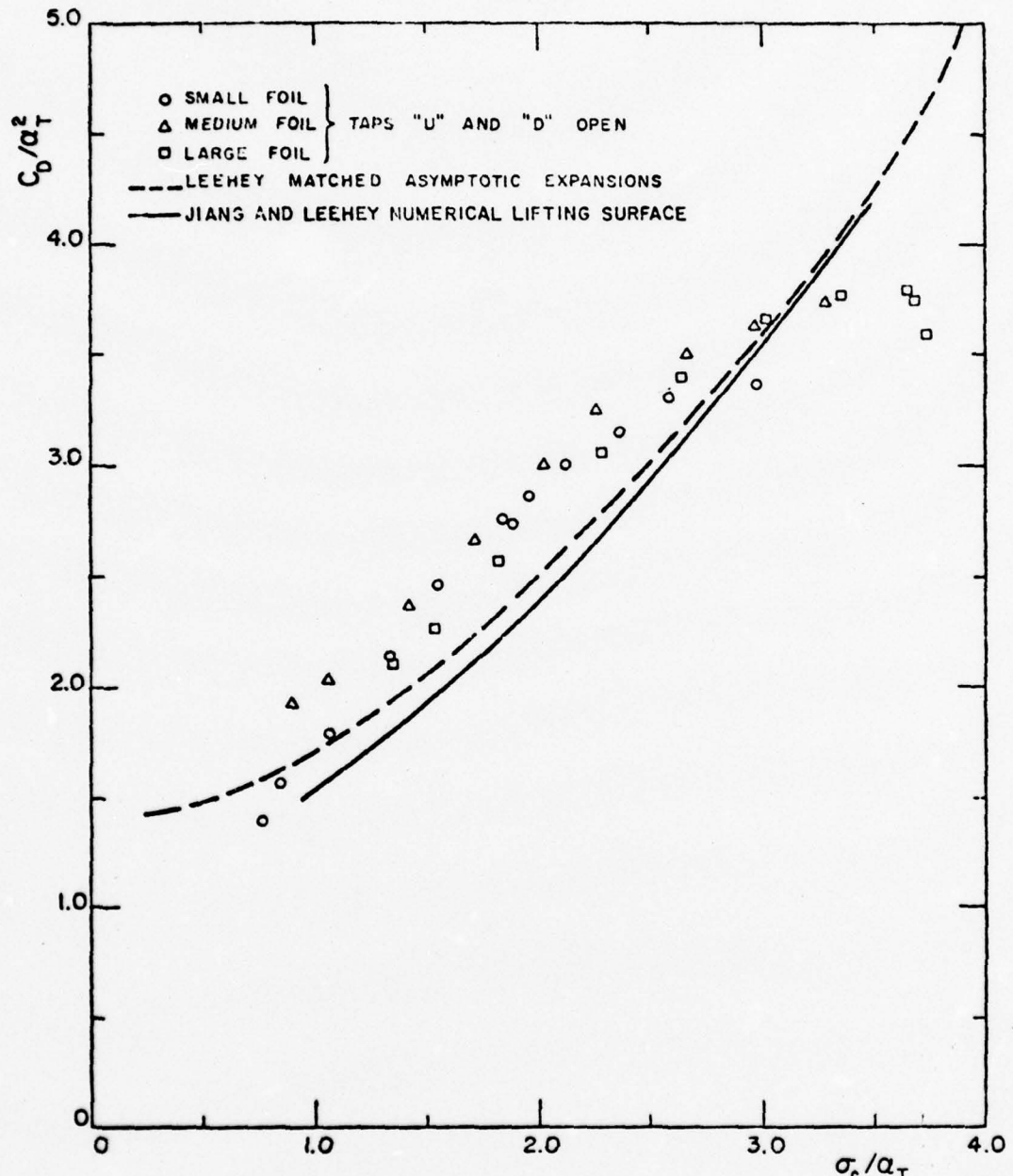


FIG. 13:  $C_D/a_T^2$  vs  $\sigma_c/a_T$ ,  $\alpha = 9.5^\circ$

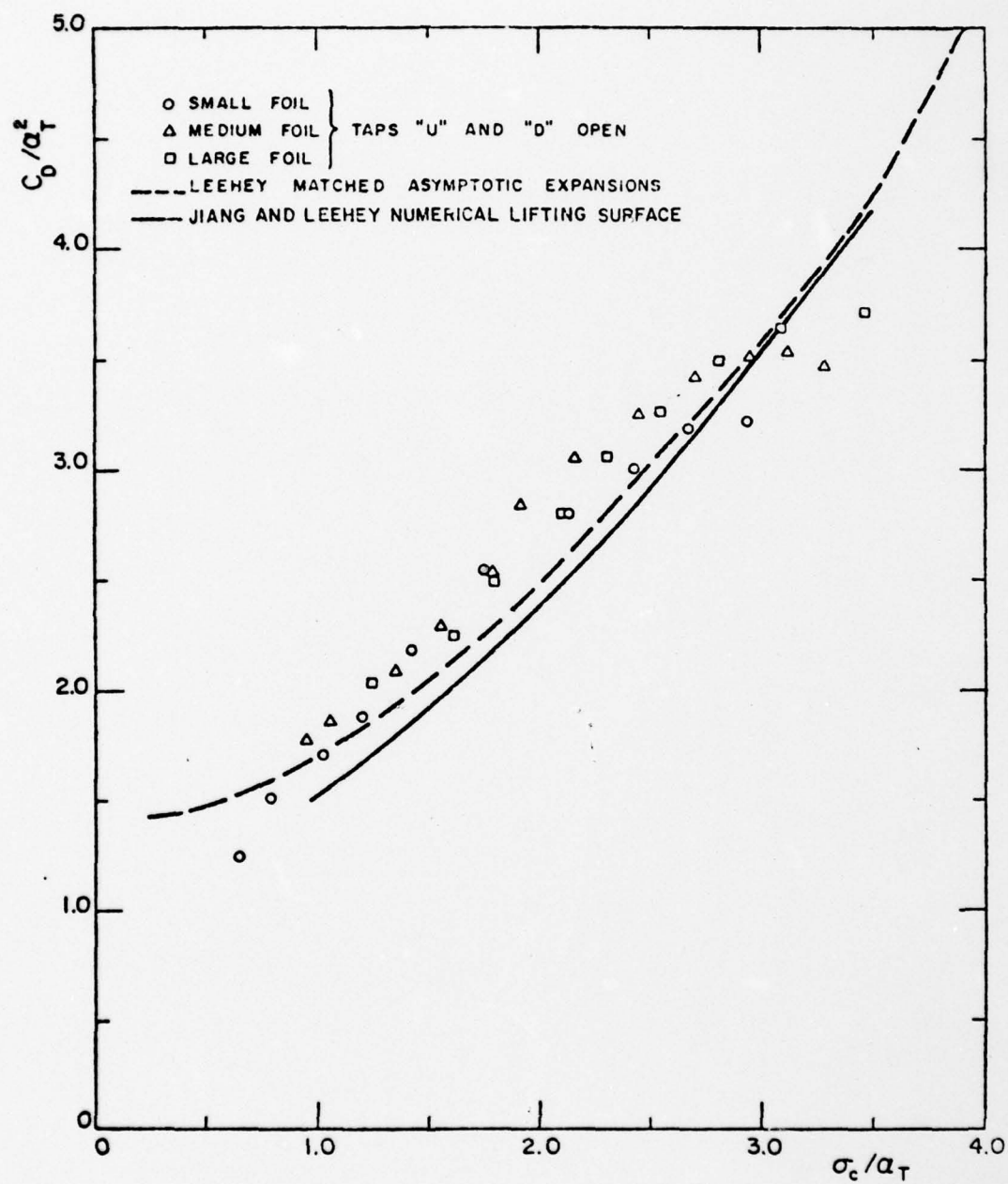


FIG. 14:  $C_D/a_T^2$  vs  $\sigma_c/a_T$ ,  $\alpha = 11.0^\circ$

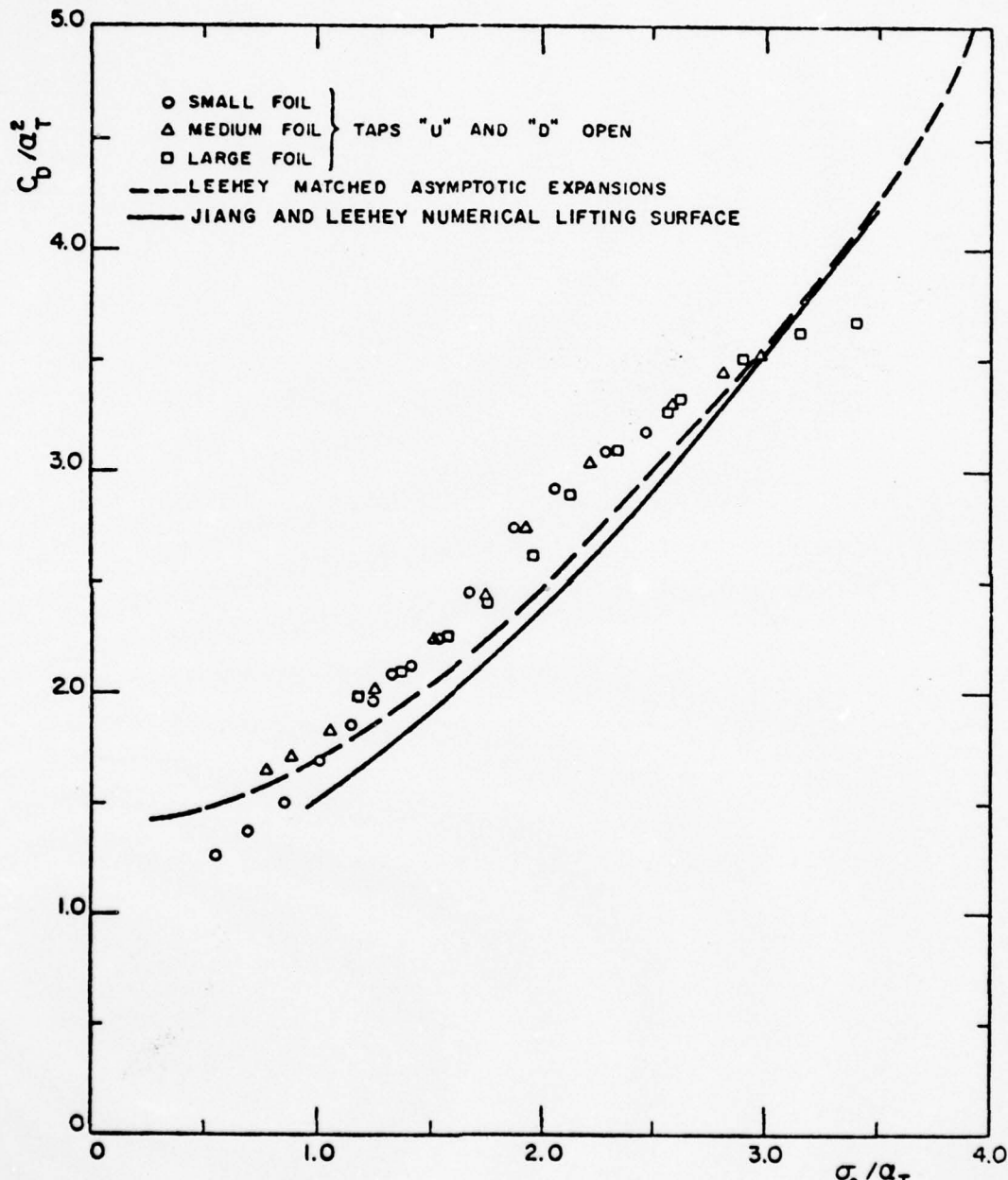


FIG. 15:  $C_D/a_T^2$  vs  $\sigma_c/a_T$ ,  $\alpha = 12.0^\circ$

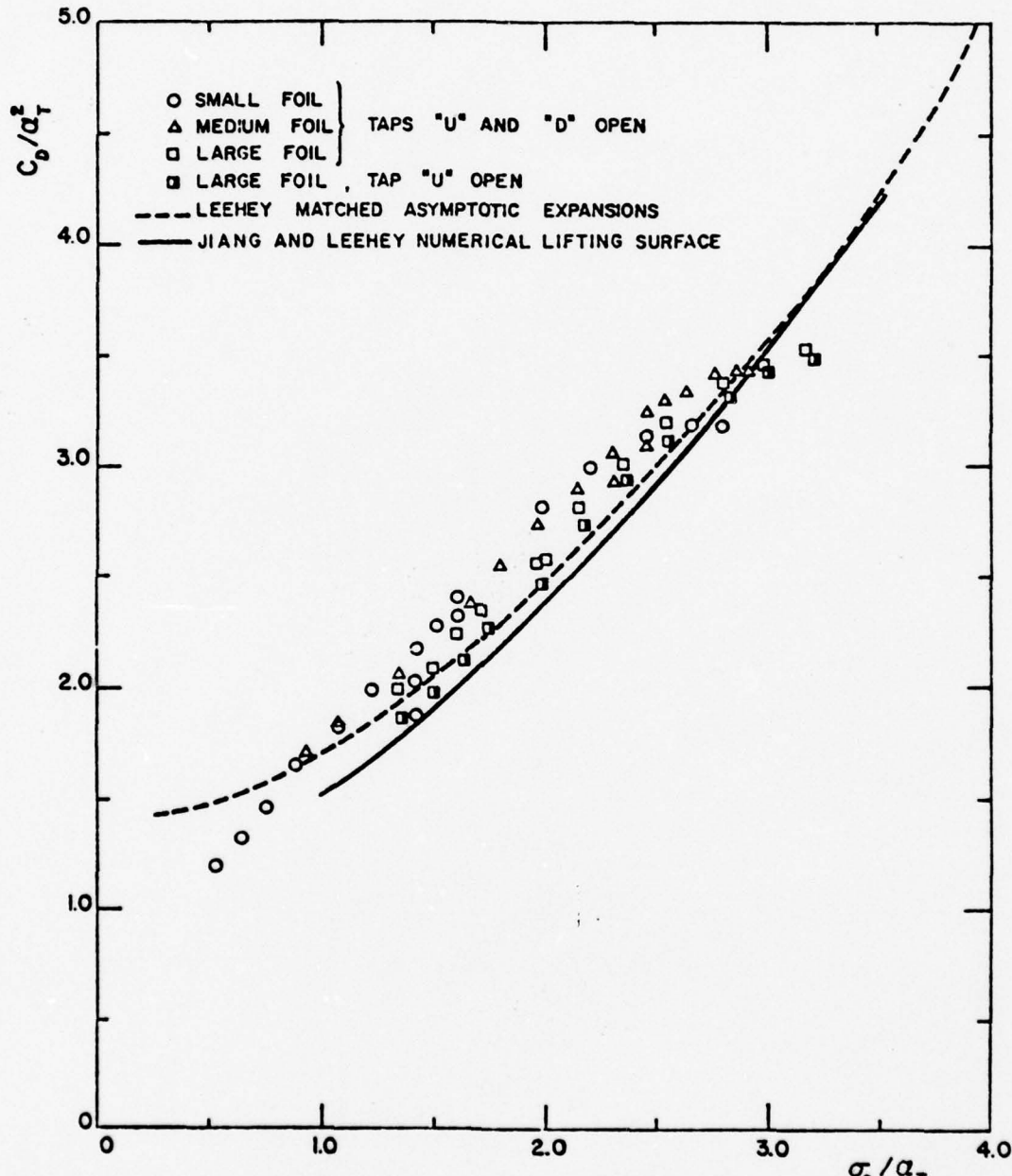


FIG.16:  $C_D/\alpha_T^2$  vs  $\sigma_c/\alpha_T$ ,  $\alpha=14.0^\circ$

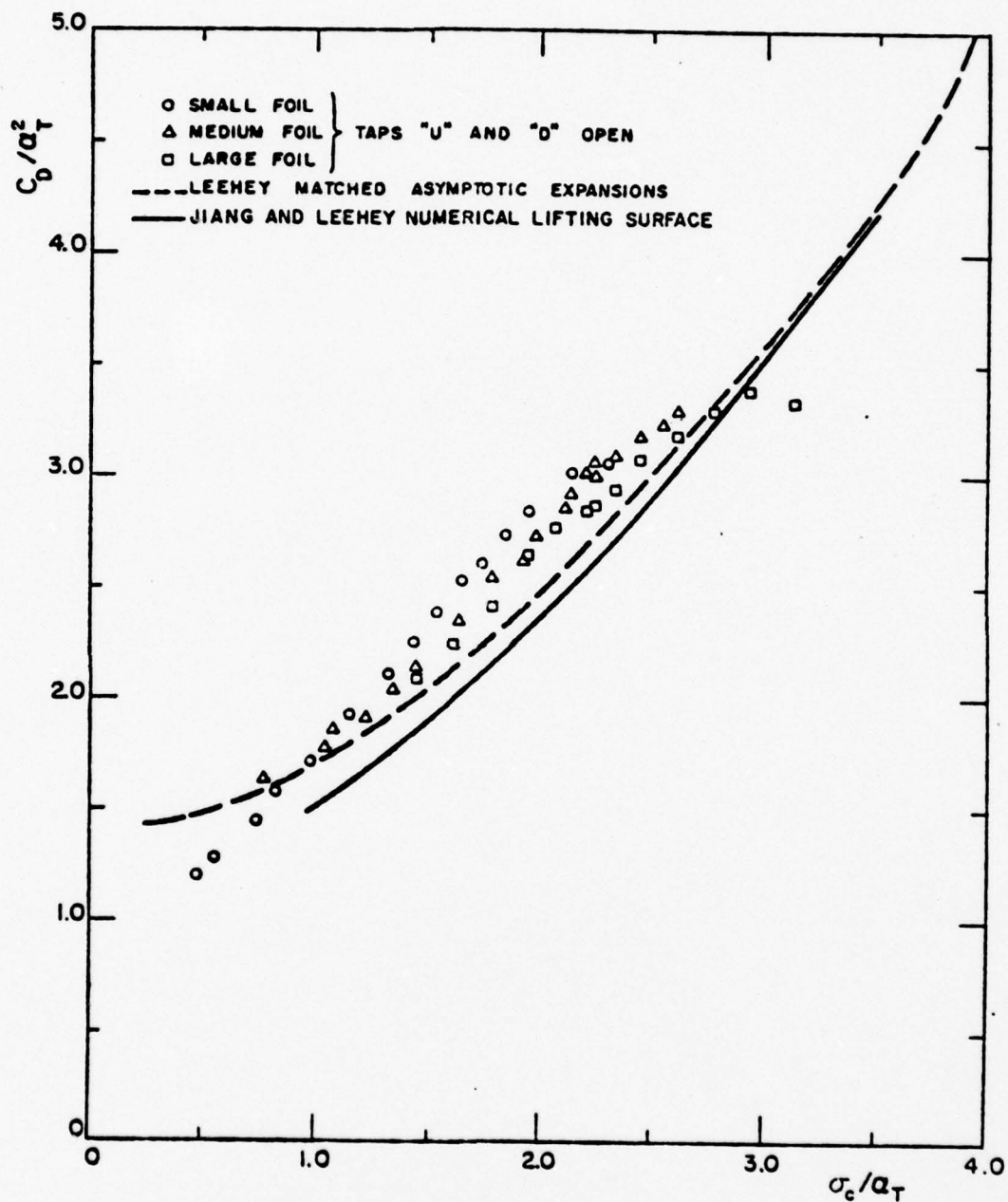


FIG. 17:  $C_D/a_T^2$  vs  $\sigma_e/a_T$ ,  $\alpha = 16.0^\circ$

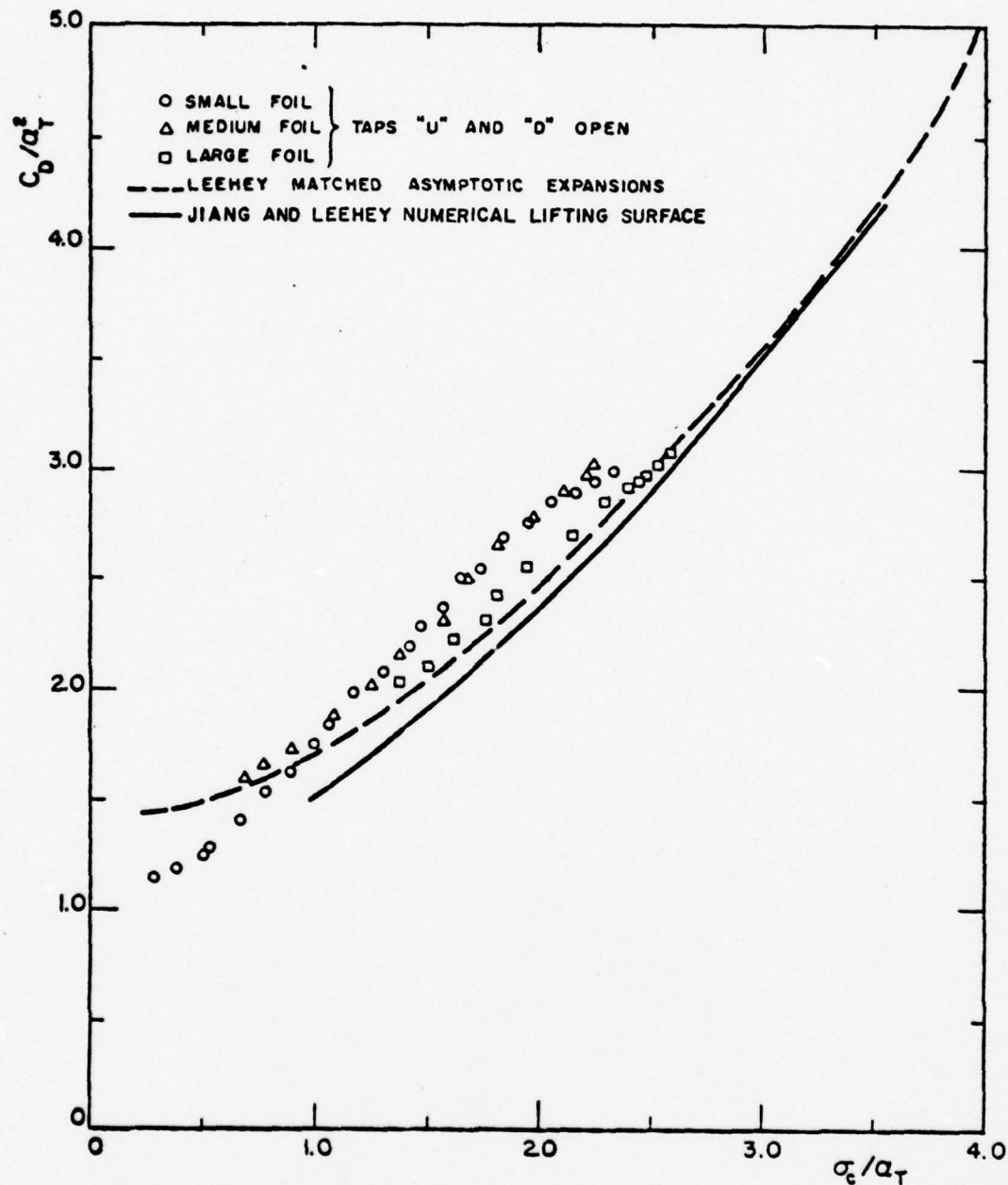


FIG. 18:  $C_D/a_T^2$  vs  $\sigma_c/a_T$ ,  $\alpha = 18.0^\circ$

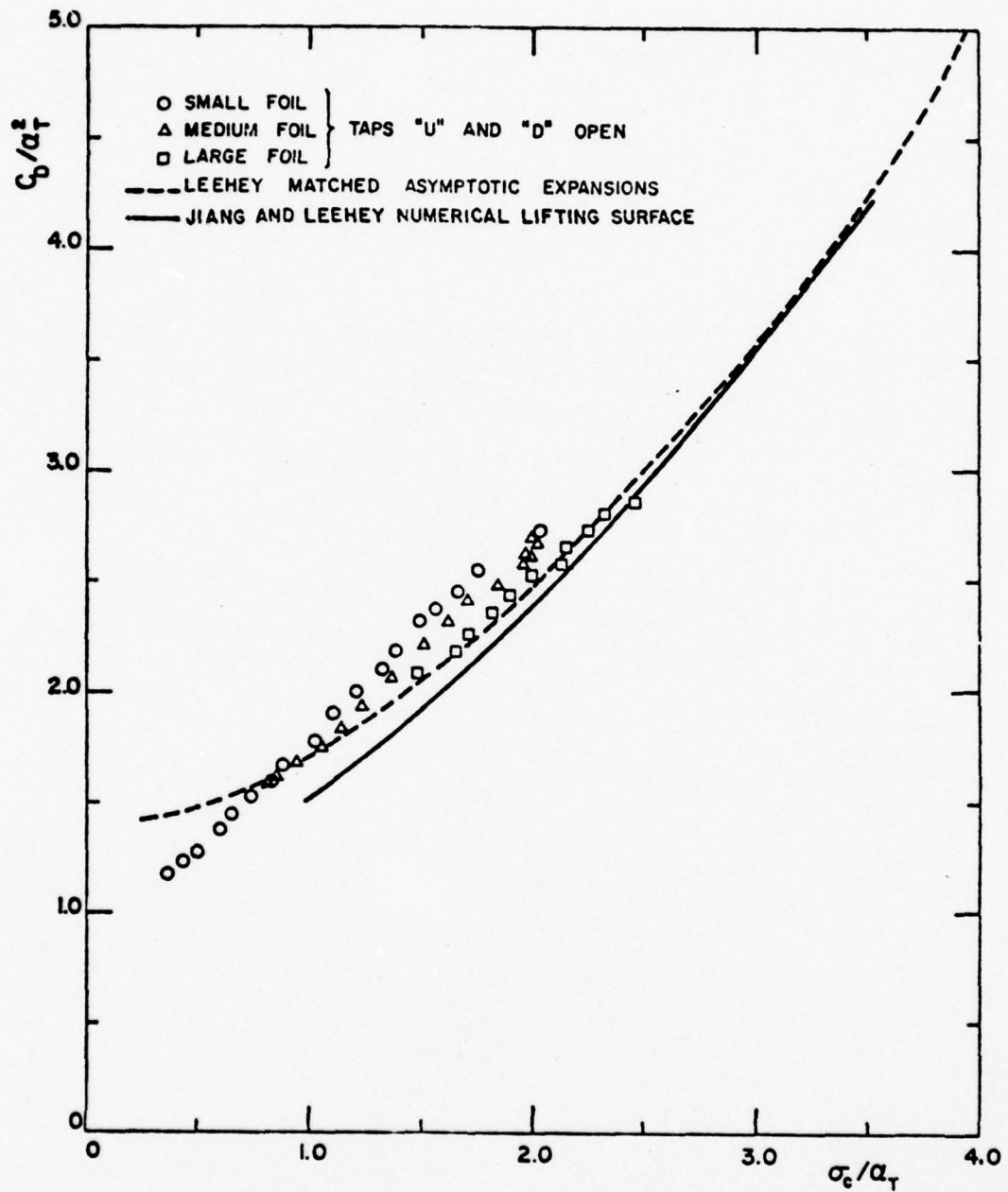


FIG. 19:  $C_D/a_T^2$  vs  $\sigma_e/a_T$ ,  $\alpha = 21.0^\circ$

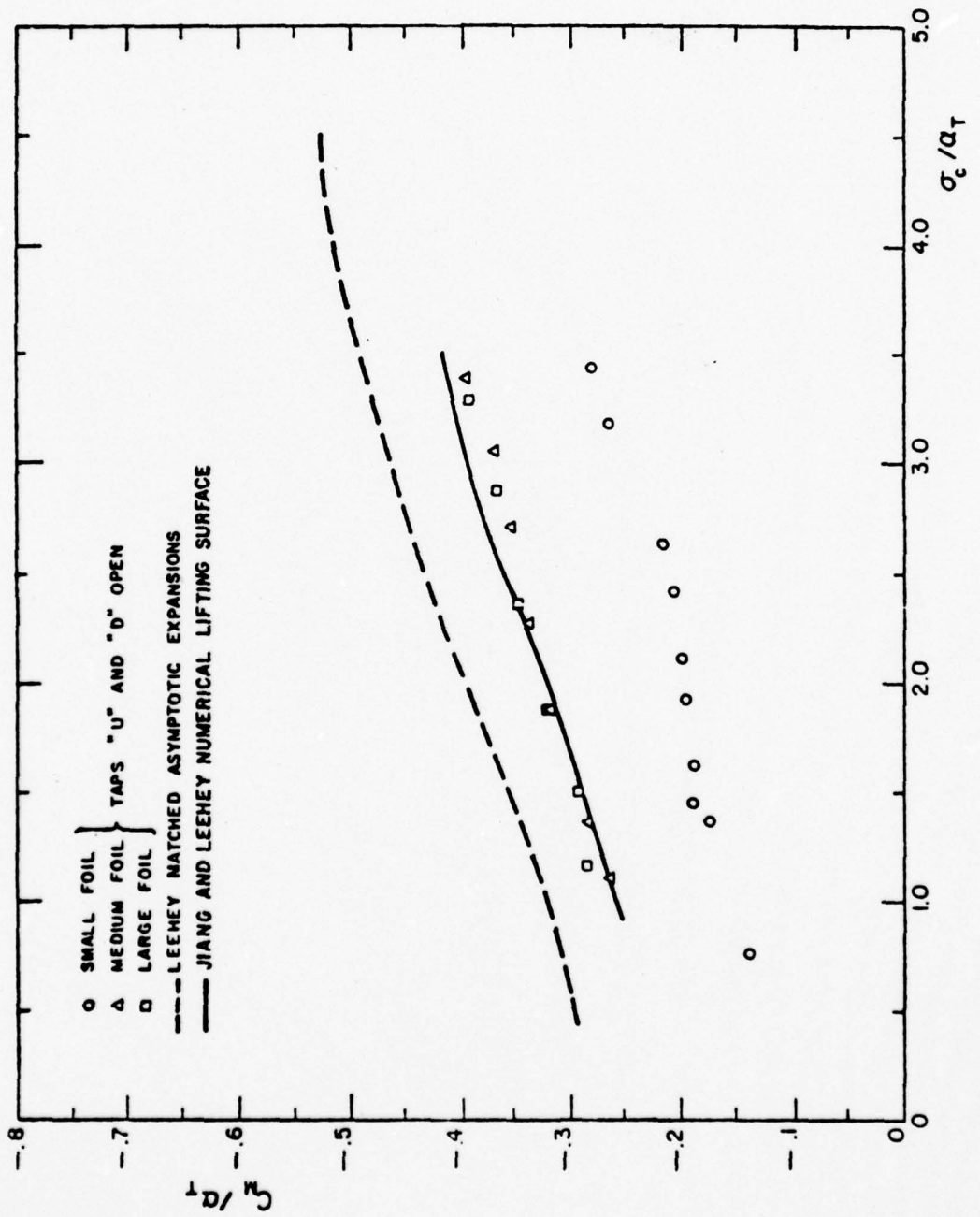


FIG. 20:  $C_w/a_T$  vs  $\sigma_e/a_T$  .  $\alpha = 8.0^\circ$

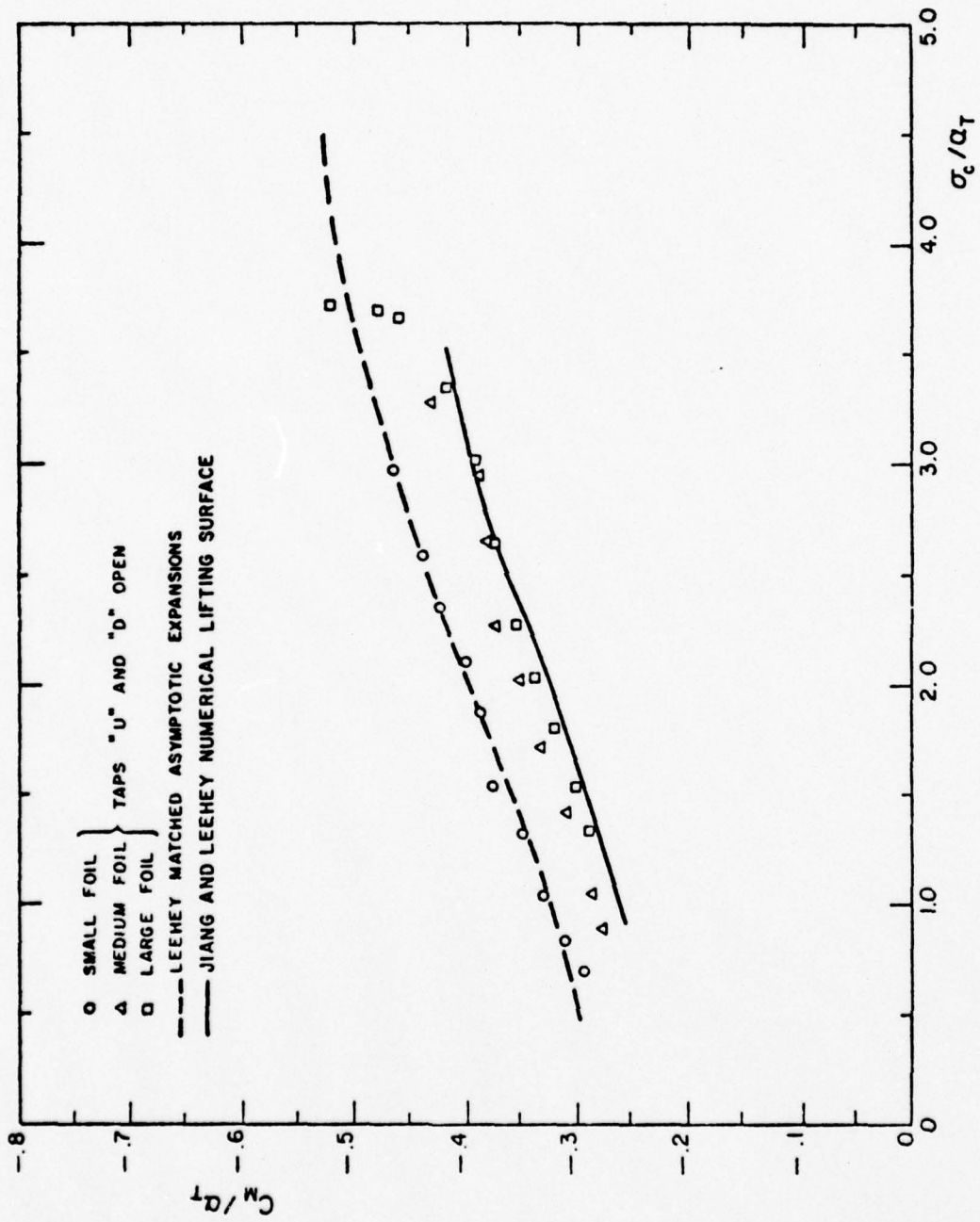


FIG. 21:  $C_M / \alpha_T$  vs  $\sigma_c / \alpha_T$ ,  $\alpha = 9.5^\circ$

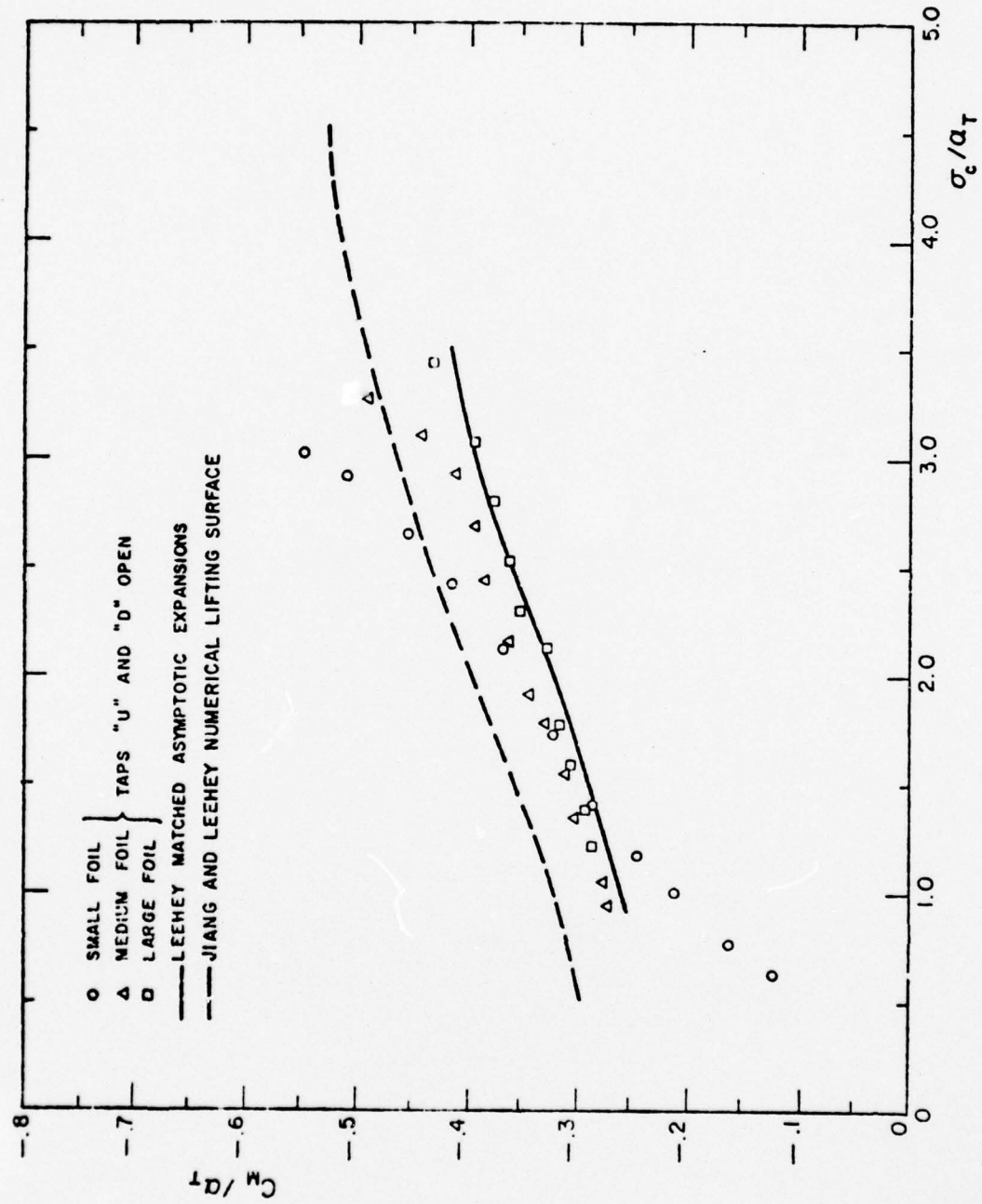


FIG. 22:  $C_w/a_T$  vs  $\sigma_c/a_T$ ,  $\alpha = 11.0^\circ$

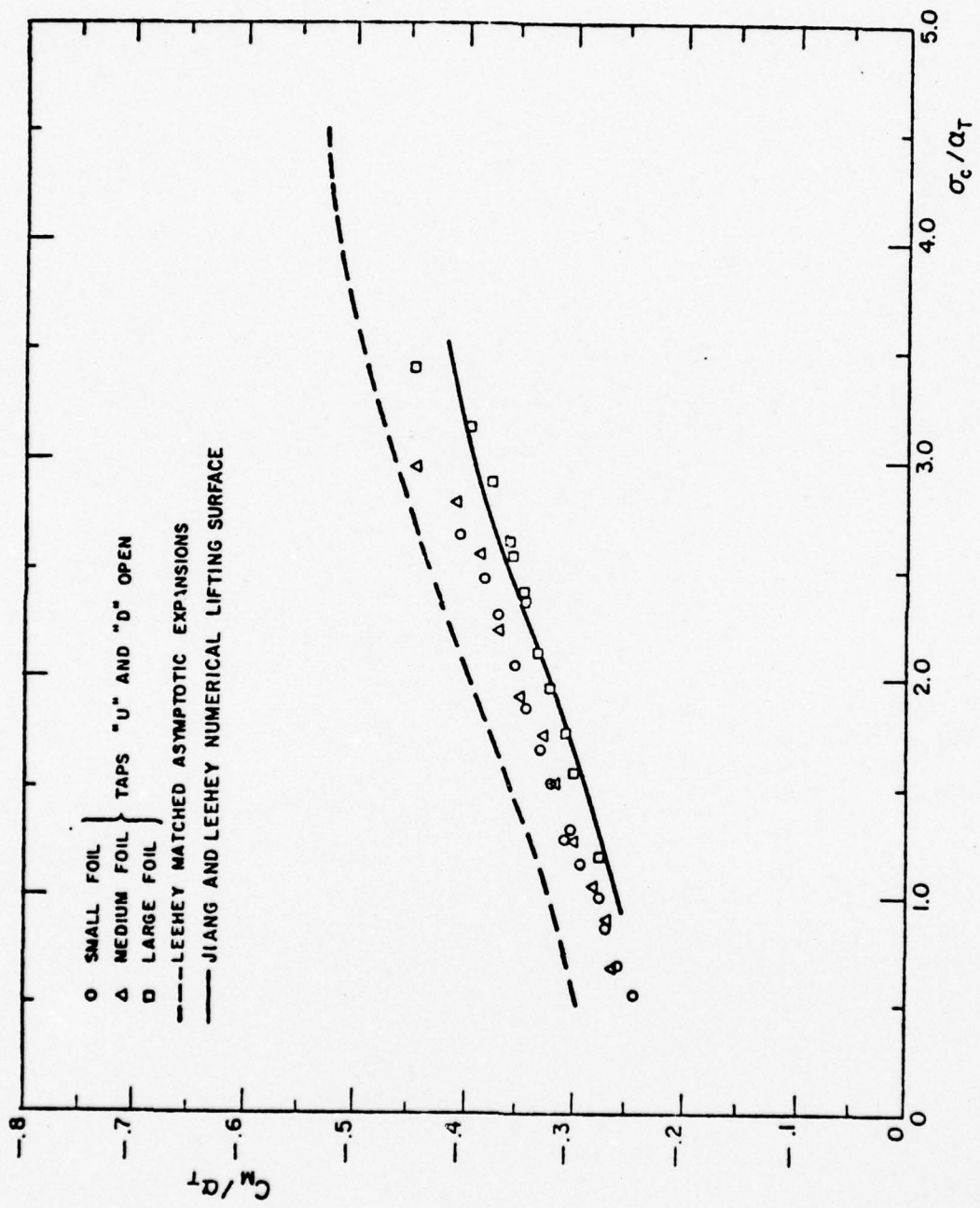


FIG. 23:  $C_L/q_T$  vs  $\sigma_c/q_T$ ,  $\alpha = 12.0^\circ$

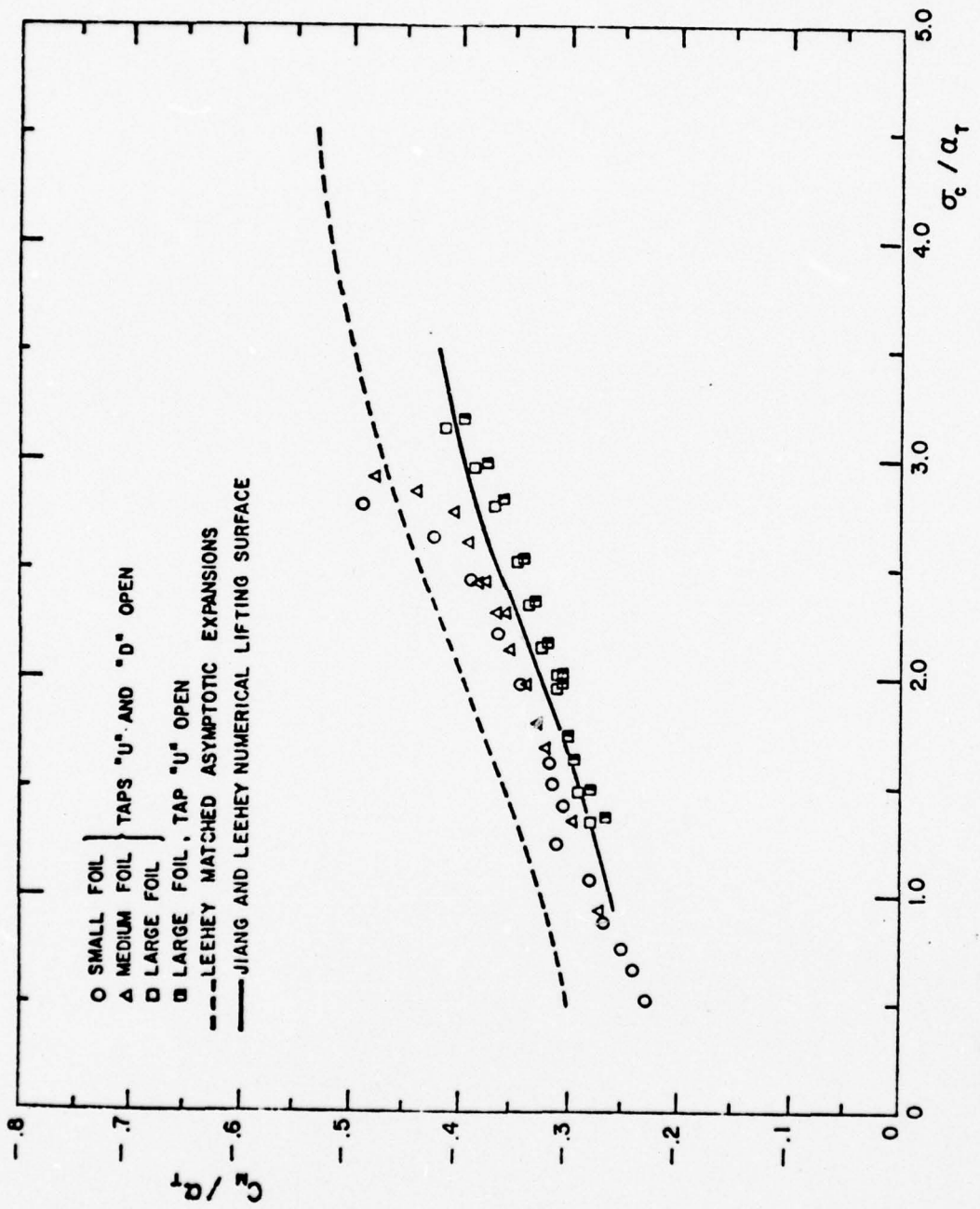


FIG. 24:  $C_w / \alpha_t$  vs.  $\sigma_e / \alpha_t$ ,  $\alpha = 14.0^\circ$

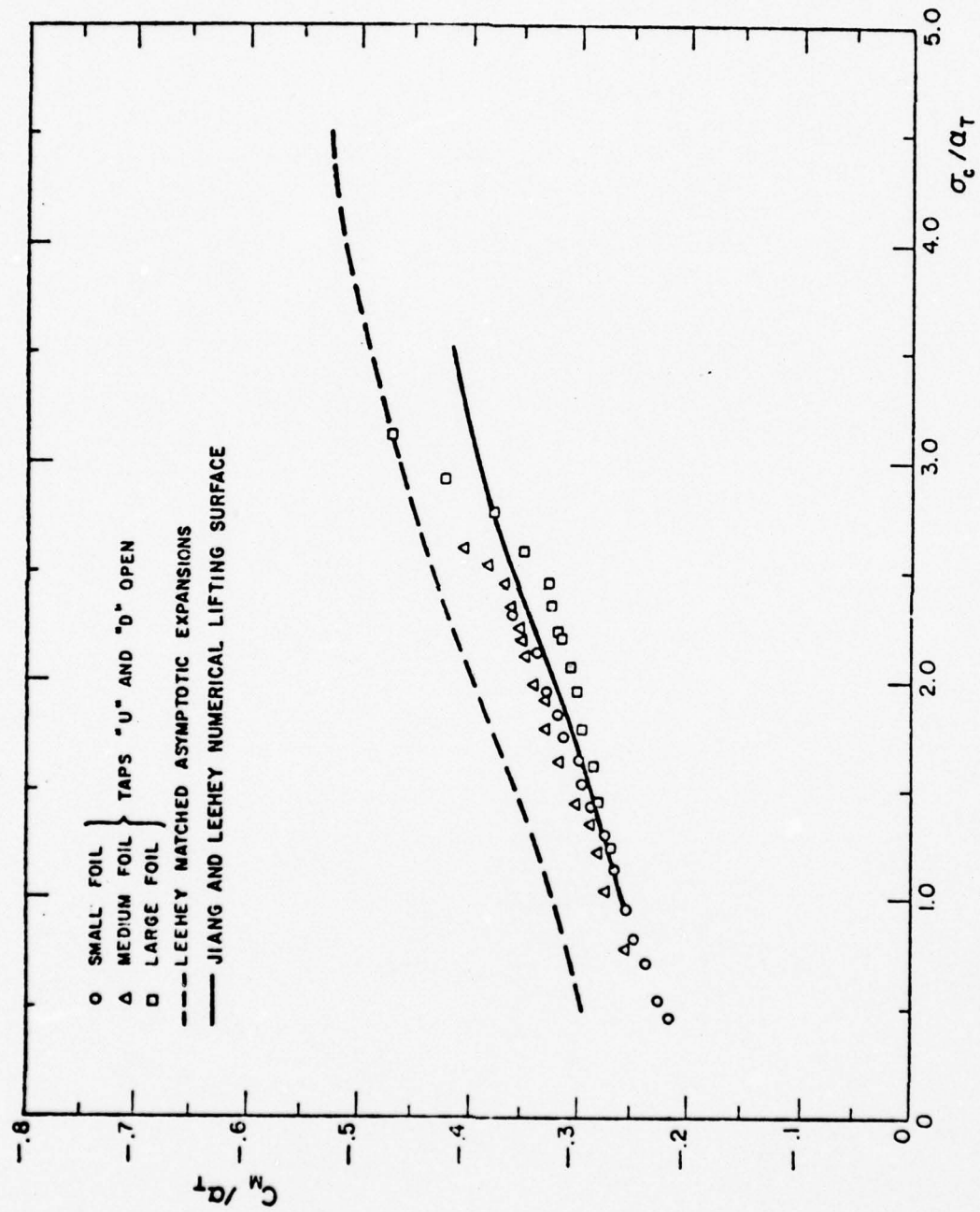


FIG. 25:  $C_M/a_T$  vs  $\sigma_c/a_T$ ,  $\alpha = 16.0^\circ$

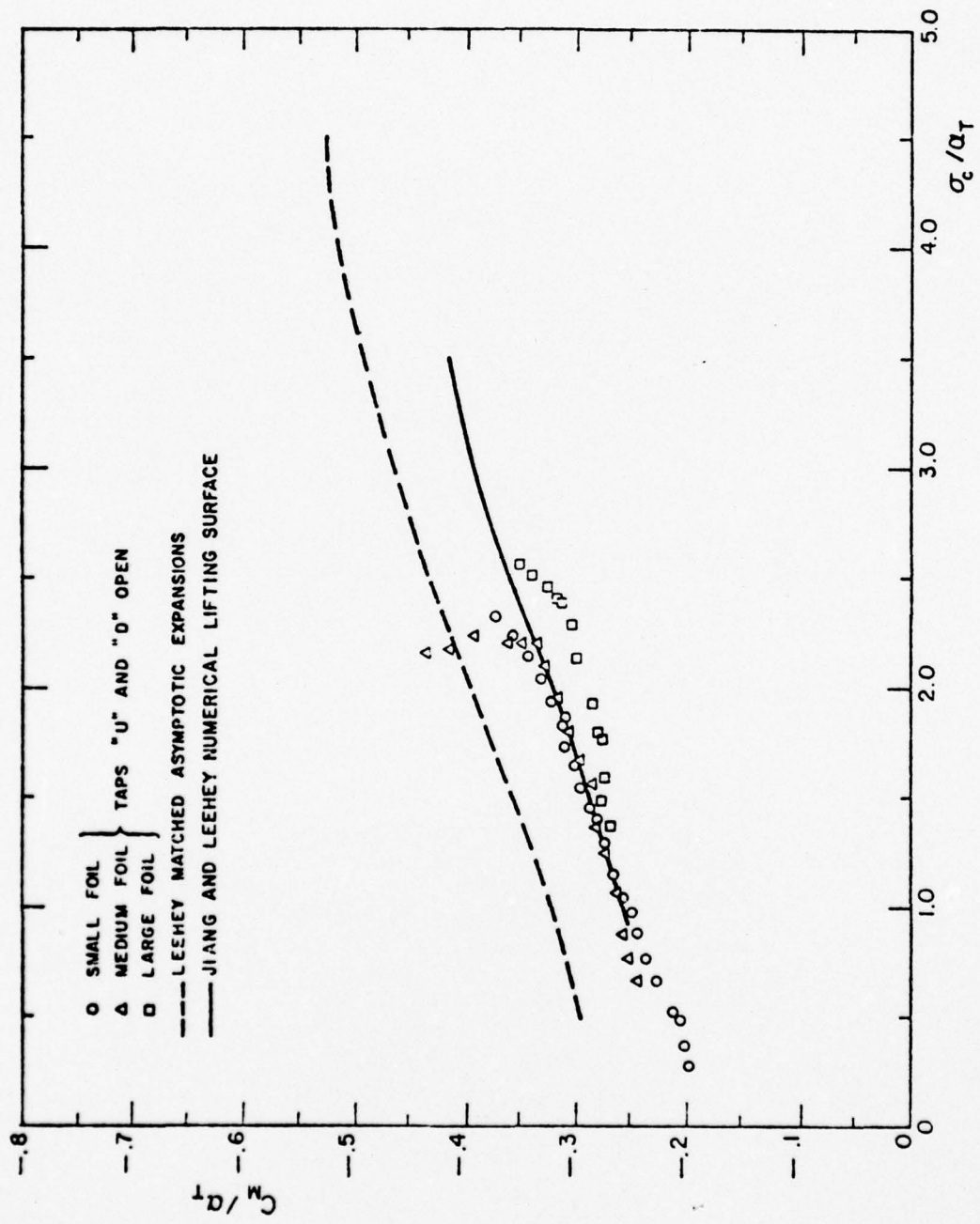


FIG. 26:  $C_M/a_T$  vs  $\sigma_c/a_T$ ,  $\alpha = 18.0^\circ$

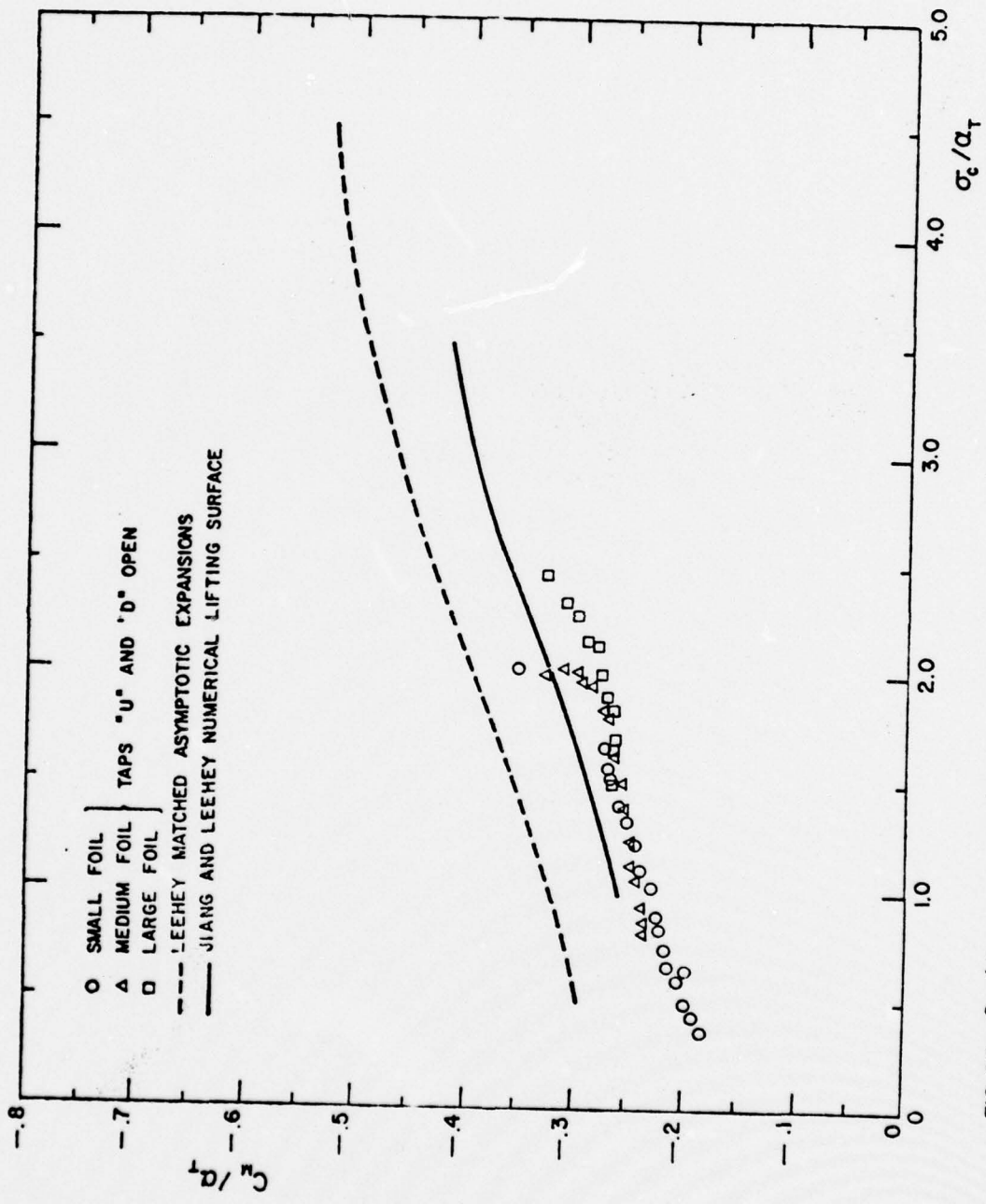


FIG. 27:  $C_L/a_T$  vs  $\sigma_e/a_T$ ,  $a = 21.0^\circ$

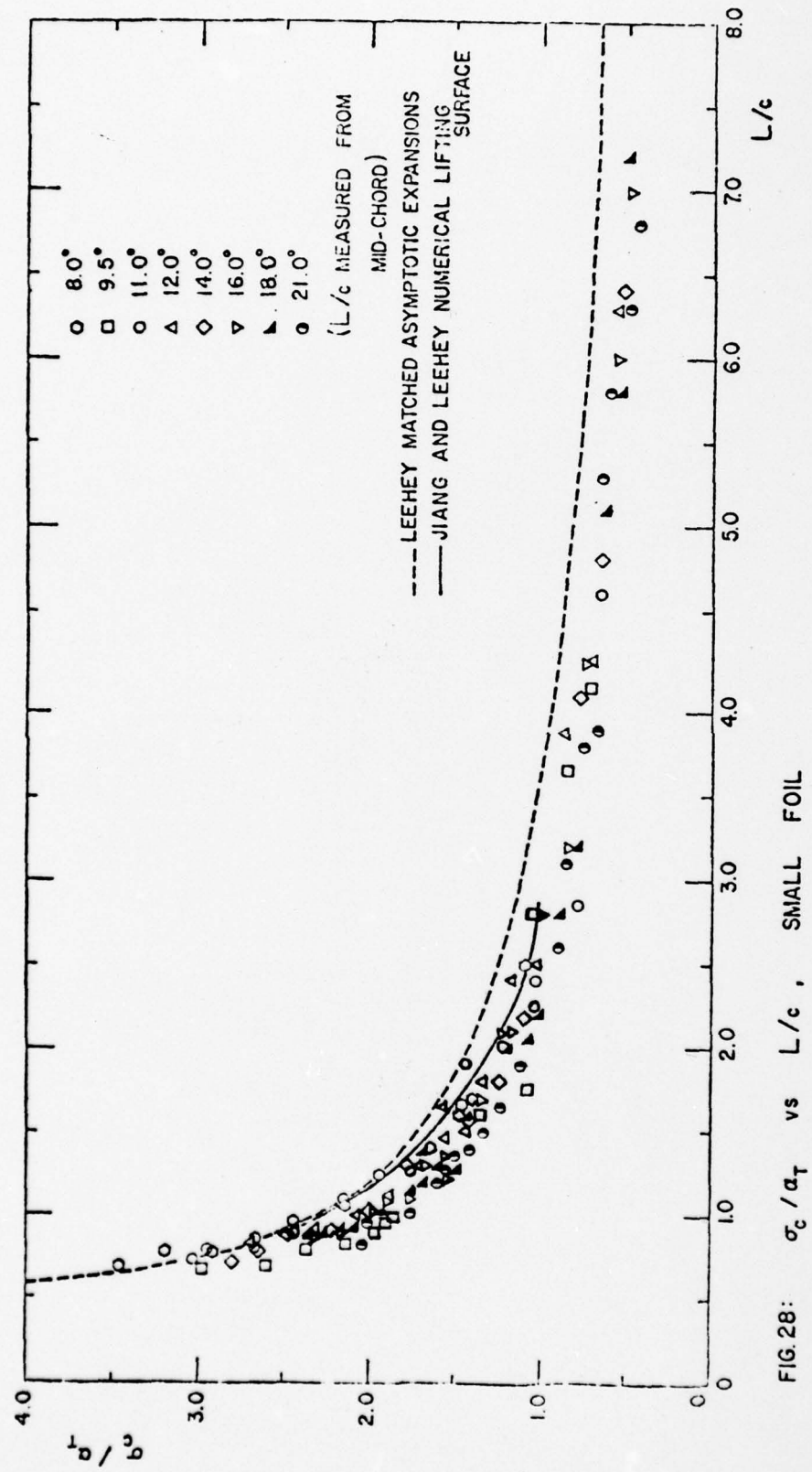


FIG. 28:  $\sigma_c / \sigma_T$  vs  $L/c$ , SMALL FOIL

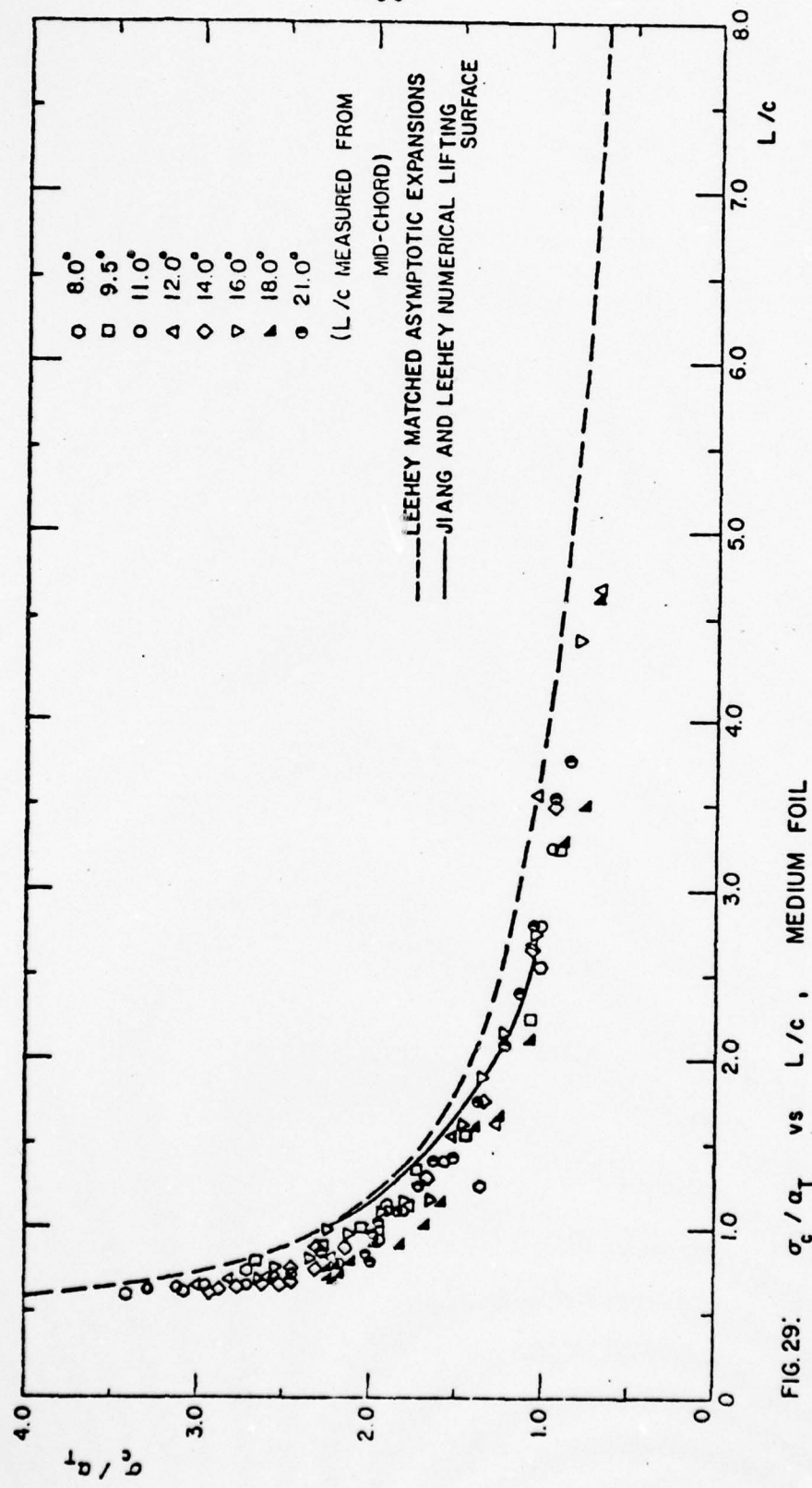


FIG. 29:  $\sigma_c / \sigma_T$  vs  $L/c$ , MEDIUM FOIL

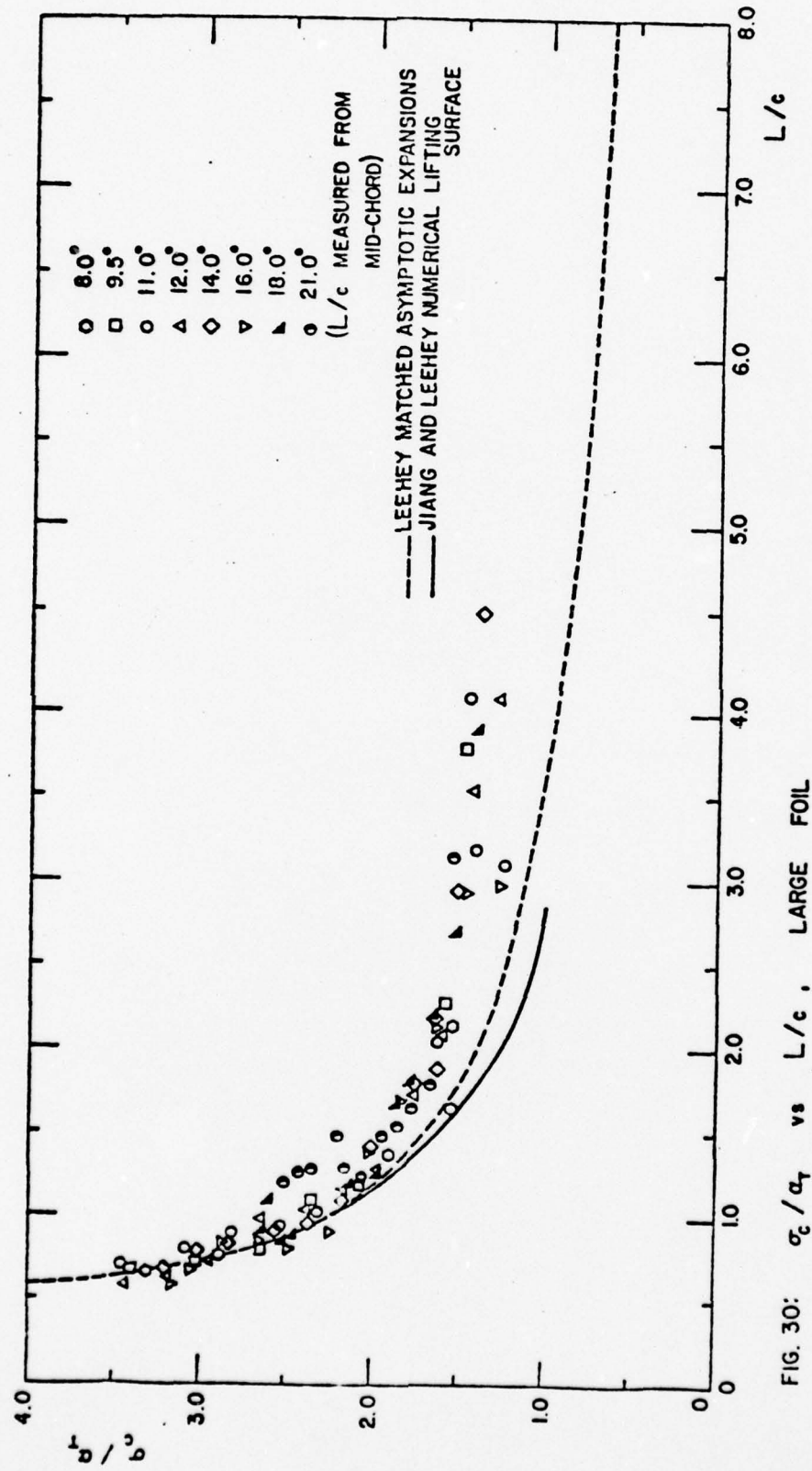
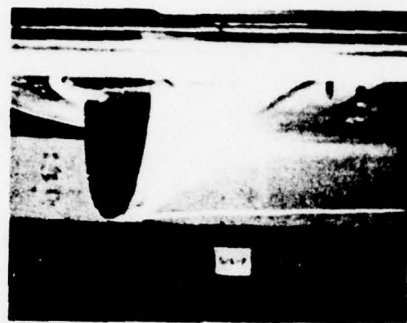
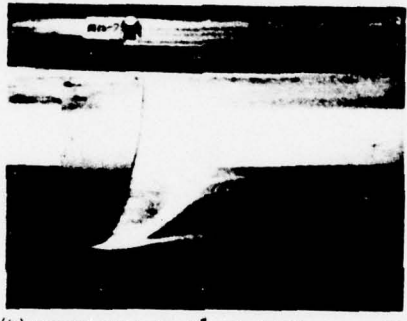


FIG. 30:  $\sigma_c / \alpha_l$  vs.  $L/c$ , LARGE FOIL



(a) SMALL FOIL:  $\alpha = 12^\circ$ ,  $\sigma_c = .3545$ ,  $L/c = 1.3$



(b) MEDIUM FOIL:  $\alpha = 12^\circ$ ,  $\sigma_c = .3473$ ,  $L/c = 1.55$



(c) LARGE FOIL:  $\alpha = 12^\circ$ ,  $\sigma_c = .3265$ ,  $L/c = 2.1$

FIG. 3I: COMPARISON OF CAVITY LENGTHS

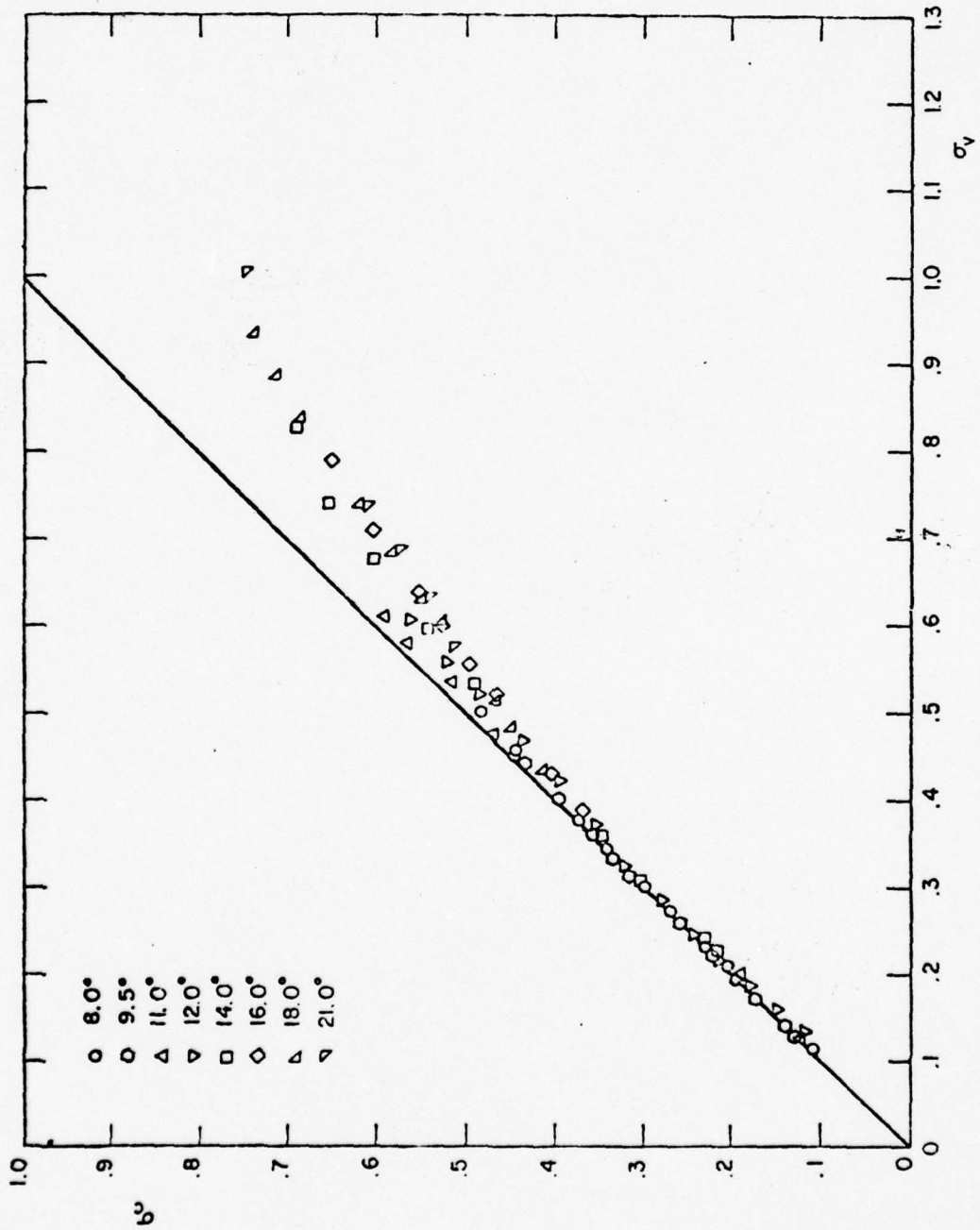


FIG. 32:  $\sigma_c$  vs  $\sigma_v$  • SMALL FOIL

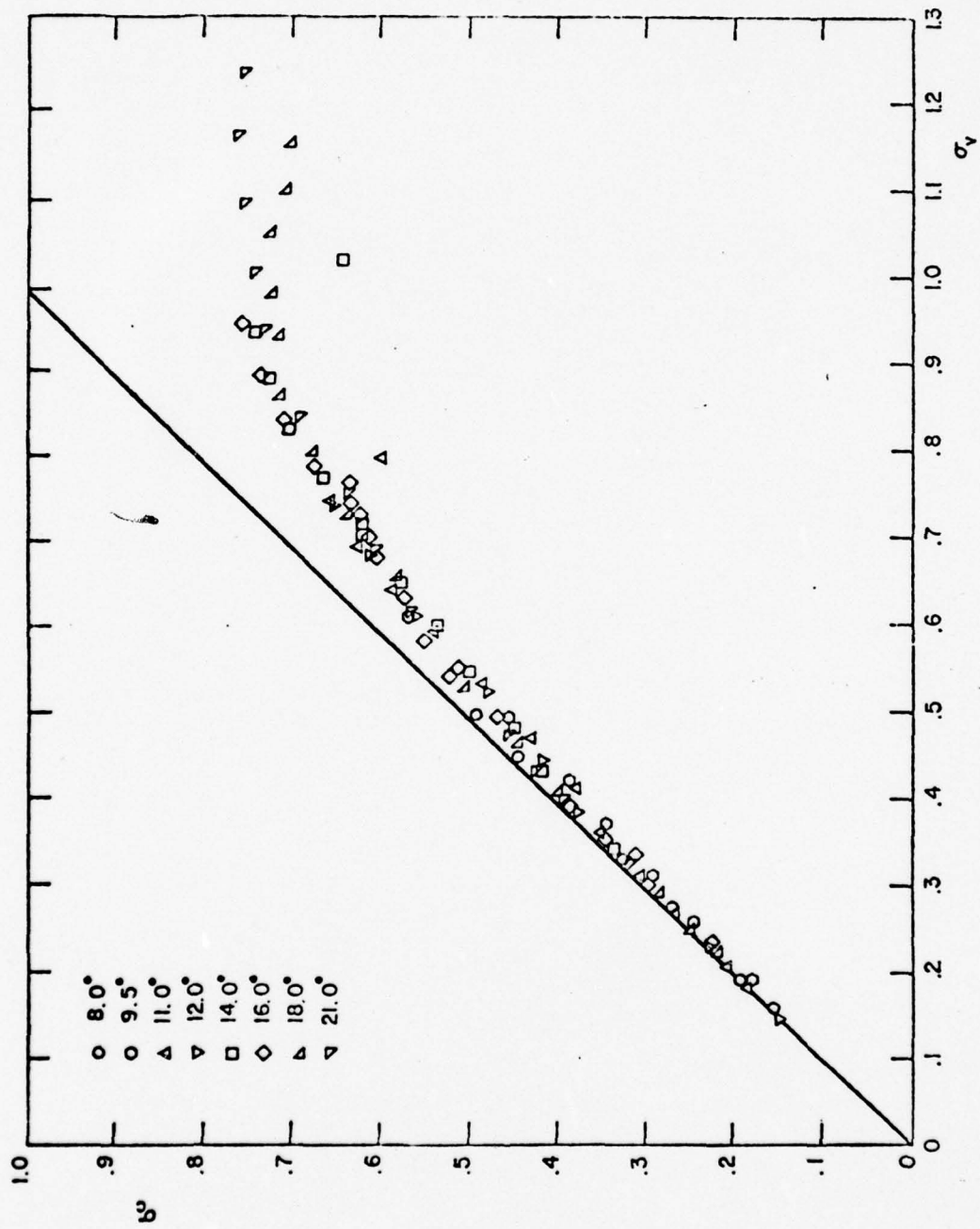


FIG. 33:  $\sigma_c$  vs  $\sigma_v$ , MEDIUM FOIL

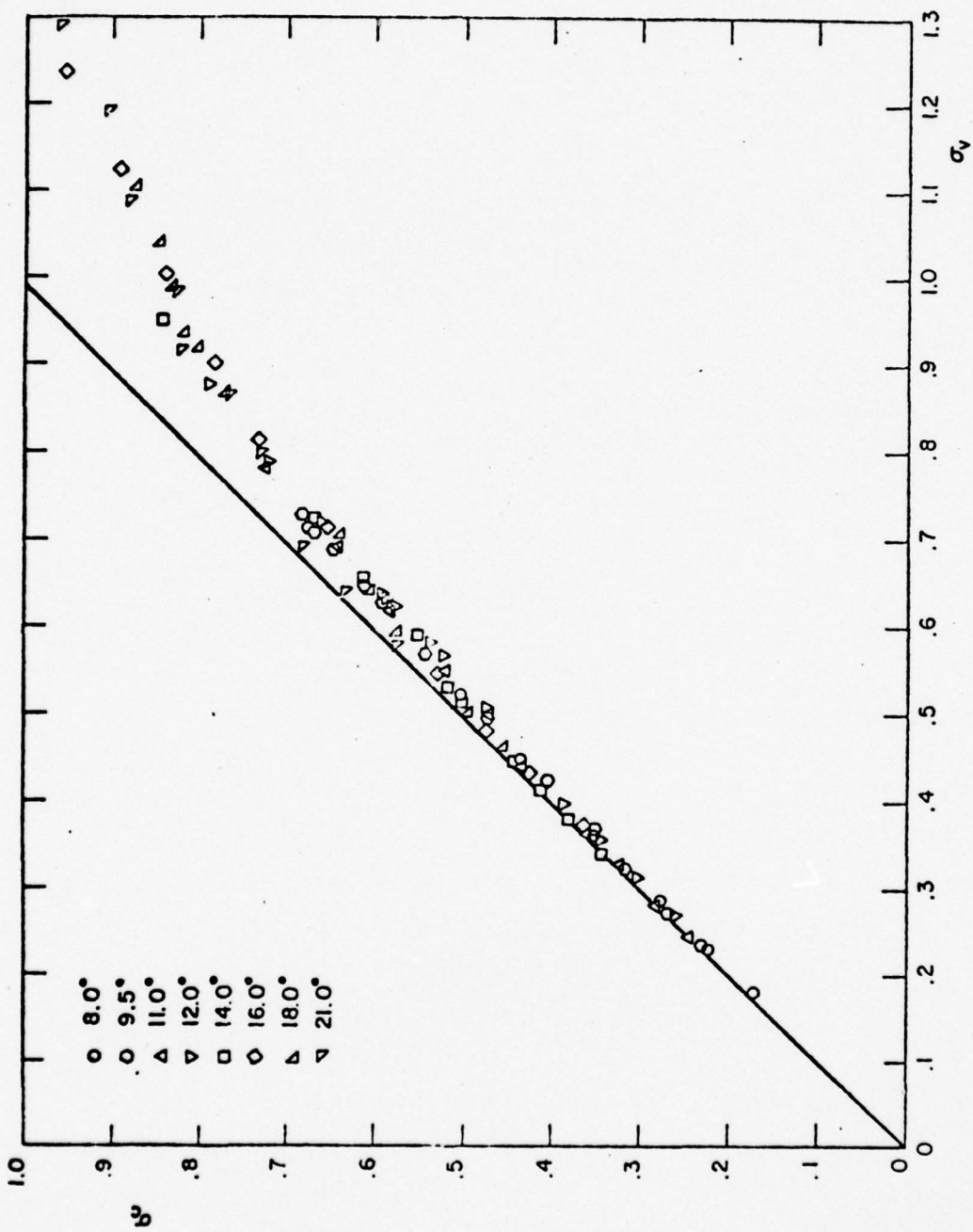


FIG. 34:  $\sigma_c$  vs  $\sigma_v$ , LARGE FOIL

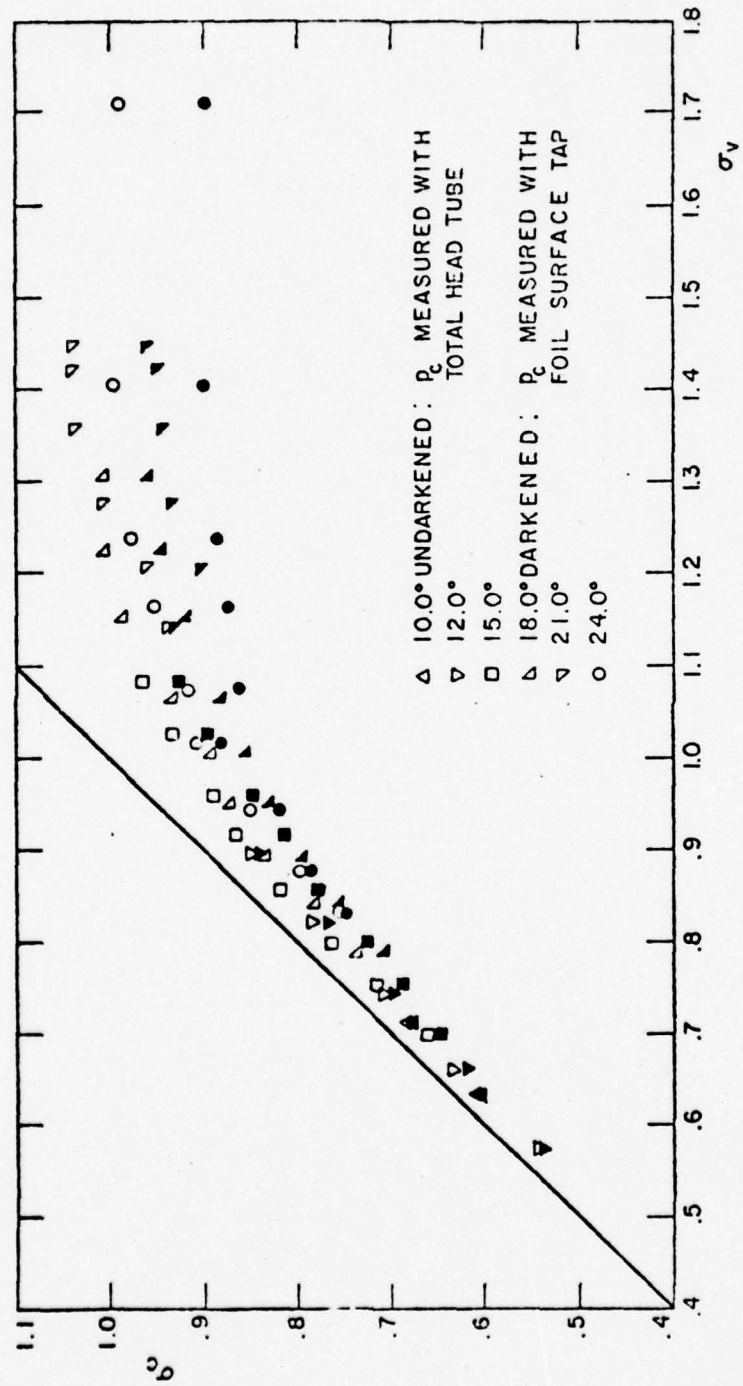


FIG. 35:  $\sigma_c$  vs  $\sigma_v$ , LARGE FOIL: COMPARISON OF CAVITY PRESSURE MEASUREMENT TECHNIQUES

APPENDIX I

Standard Wind Tunnel Corrections for Effects of  
Images of Trailing Vortices

The experimental data shown in Figs. 4 through 30 are corrected for the apparent upwash due to the interference of the tunnel walls, in accordance with standard wind tunnel practice. The boundary condition of zero normal velocity at the tunnel walls is satisfied in the analytical treatment of the problem by introducing a doubly infinite system of image vortices; the interference due to the presence of the tunnel walls is then calculated to be the interference caused by the series of vortex images on the flow at the model. The net result is an additive correction to the induced drag and the angle of attack (to be perfectly correct, there is also a slight negative correction to the measured lift, but this is usually neglected). Upon application of the correction factor, the flow about the model is transformed to the flow which would be seen if the foil were in an infinite stream.

Since the hydrofoils tested in the square tunnel were only of half-span, a full-span model would require a duplex tunnel (that is, one whose ratio of height to width is 1/2). The ratio of model span to tunnel width for the small, medium, and large foils is 1/4, 1/2, and 3/4, respectively. Entering Fig. 6.34 of Pope and Harper [1],  $\delta$ , the tunnel correction

factor for the influence of the images of the trailing vortex system was found to be 0.126 for the small, 0.104 for the medium, and 0.092 for the large foil. If the ratio of the foil area to tunnel cross-sectional area is  $S/S_o$ , then the change in angle of attack is

$$\Delta\alpha_i = \delta \frac{S}{S_o} C_L \quad (\text{radians}) \quad (\text{I-1})$$

The maximum value for  $\Delta\alpha_i$  encountered in the experiments was 1.47 degrees. When  $\Delta\alpha_i$  is added to the measured geometrical angle of attack,  $\alpha$ , the "true" angle of attack is obtained

$$\alpha_T = \alpha + \Delta\alpha_i \quad (\text{I-2})$$

(In addition to the above correction, the data reduction program accounted for the dynamometer shaft twist, which never exceeded 0.06 degree.) The change in induced drag is

$$\begin{aligned} \Delta C_{D_i} &= \delta \frac{S}{S_o} C_L^2 \\ &= \Delta\alpha_i C_L \end{aligned} \quad (\text{I-3})$$

so that the total drag coefficient is

$$C_D = C_{D_{\text{uncor}}} + \Delta C_{D_i} \quad (\text{I-4})$$

where  $C_{D_{\text{uncor}}}$  is the uncorrected drag coefficient calculated from the raw experimental data.

APPENDIX II

Leehey's Matched Asymptotic Solution for  
Supercavitating Hydrofoils of  
Large Aspect Ratio

A synopsis of Leehey's theoretical results, as derived in references [9] and [11], is given.

Leehey's linearized steady-flow theory, which utilizes the method of matched asymptotic expansions, is valid to first order in angle of attack, and to second order in the reciprocal of the aspect ratio. Gravitational effects were neglected in the derivation. The analysis shows that the lift, drag, and moment coefficients, and non-dimensional cavity length (measured from midchord) are given by the following relationships:

$$C_L = \frac{\pi\alpha}{\sin\gamma(1+\sin\gamma)} \left\{ 1 - \frac{2\sin\gamma-1}{A(1+\sin\gamma)} \right\}, \quad (\text{II-1})$$

$$C_D = \alpha C_L = \frac{\pi\alpha^2}{\sin\gamma(1+\sin\gamma)} \left\{ 1 - \frac{2\sin\gamma-1}{A(1+\sin\gamma)} \right\}, \quad (\text{II-2})$$

$$C_M = \frac{-4\alpha}{\pi(1+\sin\gamma)^2} \left\{ 1 - \frac{1-2\sin\gamma+2\sin^2\gamma}{A\sin\gamma(1+\sin\gamma)} \right\}, \quad (\text{II-3})$$

and

$$\frac{L}{c} = \sec^2\gamma - 1/2 - \frac{8}{\pi\alpha A} \left( \frac{\alpha}{C_L} \right)^2 C_{L_{2D}}, \quad (\text{II-4})$$

where  $C_{L_{2D}}$ , the two-dimensional lift coefficient may be expressed as

$$C_{L_{2D}} = \frac{\pi\alpha}{\sin\gamma(1+\sin\gamma)} , \quad (II-5)$$

and where

$$\gamma \equiv \arctan \left( \frac{2\alpha}{\sigma_c} \right) , \quad (II-6)$$

and

$$\sigma_c \equiv \frac{P_\infty - P_c}{(1/2)\rho U^2} . \quad (II-7)$$

Experiments performed by Leehey and Stellinger [9] showed that the above predictions for lift and drag coefficients and for cavity lengths were good; it was evident from the experimental results, however, that lifting surface corrections would be needed to improve the moment coefficient prediction.

### APPENDIX III

#### Numerical Lifting Surface Theory for Supercavitating Hydrofoils of Finite Span

A brief description of the numerical lifting surface theory developed by Jiang and Leehey [12] for supercavitating hydrofoils of finite span will be given.

The steady flow theory is linearized for application to thin wings at small attack angles. Discrete sources and vortices are utilized in the representation of the physical model, and the coupled integral equations are reduced to a set of simultaneous algebraic equations. The cavity closure condition is applied stripwise on the cavity in an iterative process to obtain the desired cavitation number over the supercavitated planform.

This numerical theory should prove to be more accurate than the asymptotic theory of Leehey [11]; an implicit assumption in the latter theory is that the cavity length is less than the span, so that for small  $\sigma_c/\alpha$  (i.e., long cavities), the numerical theory should indeed give better predictions. It should be noted, also, that for the  $\sigma/\alpha_T = 1.0$  curves in Figs. 4, 5, 7, and 8 of reference [9], there is an ever-present difference between the experimental data and Leehey's asymptotic theoretical predictions for lift and drag coefficients. For long and short cavities, however, there is an even stronger disagreement between data

and Leehey's predictions for moment coefficient (Figs. 9 and 10 of reference [9]). The numerical lifting surface theory was developed in an attempt to overcome these difficulties.

The foil-cavity surface is collapsed to become a region in the (x-z) plane of the foil. The relationships for the jump in the tangential and normal components of the perturbation velocity upon crossing the foil surface and cavity projection surface are:

$$u(x, z, +0) - u(x, z, -0) = -\gamma(x, z), \quad (\text{III-1})$$

$$v(x, z, +0) - v(x, z, -0) = q(x, z), \quad (\text{III-2})$$

where  $\gamma$  and  $q$  are the vortex and source distributions, respectively. The boundary conditions are:

$$v(x, z, -0) = \frac{dy(x, z, -0)}{dx} \quad \begin{matrix} \text{on the foil} \\ \text{wetted surface} \end{matrix} \quad (\text{III-3})$$

$$u = \sigma_c/2 \quad \begin{matrix} \text{on the cavity} \\ \text{boundary} \end{matrix} \quad (\text{III-4})$$

$$\int_{x_l(z)}^{\ell(z)} q(\xi, z) d\xi = 0 \quad \begin{matrix} \text{cavity closure} \\ \text{condition,} \end{matrix} \quad (\text{III-5})$$

where  $\ell(z)$  is the cavity length, measured from the leading edge as a function of spanwise position, and  $x_l(z)$  is the

chordwise coordinate of the leading edge as a function of spanwise position.

The discrete vortex and source method is utilized in the formulation of a series of simultaneous equations. Upon subdividing the projected surface into small elements, a discrete bound vortex, a trailing vortex, and a source are located within each of these elements. The bound vortex is situated on the quarter-chord line of each element, and induced velocities are calculated for all elements at their midspan, three-quarter chord positions. The concentrated source is taken to be a constant distribution across each element at its three-quarter chord position. The boundary condition of fixed cavity pressure is imposed on each element at its midspan, quarter-chord position. Utilizing these boundary conditions, the following equations are obtained:

$$\frac{1}{4\pi} \sum_{i,j} a_{ijkl} \frac{\gamma_{ij}}{\alpha} - \frac{1}{2} \frac{q_{kl}}{\alpha} = -1, \quad i = 1, \dots, M_1 \quad j = 1, \dots, N \quad (\text{III-6})$$

$$- \frac{\gamma_{kl}}{\alpha} + \frac{1}{2\pi} \sum_{i,j} b_{ijkl} \frac{q_{ij}}{\alpha} - \frac{\sigma_c}{\alpha} = 0, \quad i = 1, \dots, M \quad j = 1, \dots, N \quad (\text{III-7})$$

$\gamma_{kl} = 0 \text{ for } k > M_1$

$$\sum_i \frac{q_{ij}}{\alpha} \Delta s_{ij} = 0, \quad j = 1, \dots, N, \quad (\text{III-8})$$

where  $a_{ijkl}$  and  $b_{ijkl}$  are the v and u velocities at the  $(k, l)$

-th control point induced by the unit strength vortex and source at element  $(i,j)$ . For the  $(i,j)$ -th element,  $\Delta s_{ij}$  is the element length,  $\gamma_{ij}$  the discrete vortex strength, and  $q_{ij}$  the discrete source strength.  $M_1$  and  $N$  are the number of elements on the foil along the chord and span, respectively.  $M$  is the number of elements along the chord in the cavity.

APPENDIX IV

Data Reduction Program and Data Printout

Beginning on p. 82, a listing is given of the FORTRAN IV computer program utilized in the reduction of the experimental data.

The program output is also given, beginning on p. 92. For each foil at each angle of attack, a complete printout of the experimental data is given in raw form, with corrections for instrument tares, in reduced form, in nondimensional form without any corrections for wall effect, and finally in nondimensional form with corrections for the effects of the images of the trailing vortex system.

```
C HAIMMER SUPERCAVITATING HYDROPOIL DATA REDUCTION PROGRAM JUN 77. DERIVED
C FROM KERWIN/LEWIS/OPPENHEIM MK5 RUDDER DYNAMOMETER DATA REDUCTION PROGRAM
C JU 73 AND FROM STELLINGER PROGRAM JULY 74
INTERGER RS,S,BLANK
REAL NY,MIO,MYO,MZ,MZO,MPLAP,MAC,LDMAX,LDVAL,HY
DIMENSION IDENT(24),ZN(2),ZI(7,2,2),ZF(2),NTAP(50),NPILD(40),ANOM(4
10),ANGL(40),S(40,7),R(40,7),DZI(7,2),CL(40),CD(40),CH(40),CPL(40),
2CY(40),CNP(40),VC(5),VE(6),PM(3),C(14),CLD(40),CLSQ(40),RN(40),SI(
340),CO(40),VKEEP(40),TT(2),RUNNBR(40,2),PIHP(40),PCAV(40),TEMP(40),
4,CDL(40),SIGMAC(40),SIGNAV(40),SIGVOA(40),SIGCOA(40),CLOA(40),CDOA
5(40),NTAG(40),CNOA(40),CDOASQ(40)
DIMENSION TAPS(40),CAVLEN(40),COMMENT(40,3)
DIMENSION A(15,4),RHS(4),ANGD(40)
DATA KI/5/,KO/6/
DATA IDENT(19)/ CL ' /, IDENT(20) / CD ' /, IDENT(21) / CH ' /, IDENT(2
12) /' CMP' /, IDENT(23) /' CPL' /, IDENT(24) /' CY ' /
DATA VC/4-18934,2.60088,0.81646,-0.6214,4.7381,VE/.49386,.5,.46526
1.0.50638,*5,1.0/,RS/'R'/'BLANK'/
SIGMA(X1,X2,X3,X4)=(X2-X1)*288.*.01934/(X4*X3*X3)
READ(KI,103)(IDENT(N),N=1,18)
103 FORMAT(18A4)
1 READ(KI,104)(C(N),N=1,14),TWIST,SHAFT,ANWAPA,DDDO
104 FORMAT(7F10.5)
READ(KI,100)DP,NRT,NTT,AREA,SPAN,MAC,XMAC,ZMAC,AZL,DYCIR,VELINC
100 FORMAT(P5.2,2I5,8F5.2)
FUDGE=6.76
DELTA=-.092
IF(SPAN.LT.9.) GO TO 86
IF(SPAN.LT.14.) GO TO 85
GO TO 88
85 FUDGE=10.71
DELTA=.104
GO TO 88
86 FUDGE=14.66
DELTA=.126
88 IF(AREA.LE.0) GO TO 99
```

```
RHO=1.9574-0.00028*NFT
SCALE=1.000952-13.3E-6*NFT
PH(1)=1.474--.00071*NBT
PH(2)=24.5054-.00236*NBT
PH(3)=1.0

WRITE(KO,200) (IDENT(N),N=1,18)
200 FORMAT('1','1X,18A4//8X,' HYDROFOIL INPUT DATA' / 6X,'TR TT AREA
1SPAN MAC')
WRITE(KO,150) NRT,NTT,AREA,SPAN,HAC
150 FORMAT(4X,2I4,2P6.1,P6.2)
MYCOR=0
DYCOH=DYCOR
IP(DYCOR,LT.10.0) GC TO 30
DYCOH=99.
DYCOR=0.0
MYCOR=2
30 READ(KI,101) (ZK(K), (ZI(M,L,K), L=1,2), M=1,3), TT(K), K=1,2)
101 FORMAT(8P5.1)
WRITE(KO,201)
201 FORMAT(/, ZERO READINGS AND TUNNEL TEMP BEFORE AND AFTER'/' HANO
1M 1-N 1-R 2-N 2-R 3-N 3-R TT')
WRITE(KO,204) (ZM(K), ((ZI(M,L,K), L=1,2), M=1,3), TT(K), K=1,2)
204 FORMAT(P4.0,1X,P5.1,1X,P5.1,1X,P5.1,1X,P5.1,1X,P5.1,1X,P5.1,1X,P5.
11)
DO 69 K=1,2
DO 69 L=1,2
DO 69 M=4,7
69 ZI(M,L,K)=0.0
WRITE(KO,212) (C(N),N=1,3),TWIST,SHAFT
212 FORMAT(' CELL LBS/CT(NORMAL/REV) #1=' ,P7.5, ' #2=' ,P7.5, ' #3=' ,P7.
15/, ' TWIST=' ,P7.1, ' SHAFT DIA.= ' ,P5.2, ' IN')
WRITE(KO,202)
202 FORMAT(25X,'**INPUT DATA AS RECORDED**' //'
1' RUN NO MANOM S #1 S #2 S #3
2 PCAV')
DO 2 J=1,40
```

```
JT=J-1
READ (KI,102) (RUNNBR(J,N),N=1,2),NTAP(J),NPLD(J),ANOM(J),ANGL(J),
15(J,N),B(J,N),N=1,3),PINP(J),PCAV(J),NTAG(J),TAPS(J),CAVLEN(J),(CO
2NEWT(J,N),N=1,3)
102 FORMAT(2A4,2X,2I1,2X,P6.0,1X,P4.1,3(2X,A1,1X,P7.1),2X,2P5.0,13/A1,
1A4,3A4)
1P(ANOM(J),LE.0.0) GO TO 3
1P(NTAG(J),EQ.1) GO TO 444
1P(NTAG(J),EQ.2) GO TO 445
1P(NTAG(J),EQ.3) GO TO 446
WRITE(KO,203)(RUNNBR(J,N),N=1,2),TAPS(J),ANOM(J),(S(J,N),R(J,N),N=
11,3),PINP(J),PCAV(J)
203 FORMAT(1X,2A4,A1.4X,F5.0,4X,3(A1,P7.1,4X),2(P4.0,4X))
GO TO 2
444 WRITE(KO,944)(RUNNBR(J,N),N=1,2),TAPS(J),ANOM(J),(S(J,N),R(J,N),N=
11,3),PINP(J),PCAV(J)
944 FORMAT(1X,2A4,A1.4X,F5.0,4X,3(A1,P7.1,4X),2(P4.0,4X),'PC')
GO TO 2
445 WRITE(KO,945)(RUNNBR(J,N),N=1,2),TAPS(J),ANOM(J),(S(J,N),R(J,N),N=
11,3),PINP(J)
945 FORMAT(1X,2A4,A1.4X,F5.0,4X,3(A1,P7.1,4X),F4.0,4X,-----,4X,'PC(TW
1)')
GO TO 2
446 WRITE(KO,946)(RUNNBR(J,N),N=1,2),TAPS(J),ANOM(J),(S(J,N),R(J,N),N=
11,3),PINP(J)
946 FORMAT(1X,2A4,A1.4X,F5.0,4X,3(A1,P7.1,4X),F4.0,4X,-----,4X,'PW')
2 CONTINUE
GO TO 99
3 BUG=1.0/(JT-1)
WRITE(KO,938)
938 FORMAT(2X,'LEGEND',3X,'TR ROOM TEMPER (DEG FAHR)',20X,
1'LOAD CELL #1 LIPT (COUNTS)',/
2'11X,'TT TUNNEL "( " " )',31X,
2'*2 MOMENT ABOUT MIDCHORD (COUNTS)',/
3'9X,'AREA HALF-SPAN MODEL PLANFORM AREA (SQ IN)',15X,
3'*3 DRAG (COUNTS)',/
```

```
4 9X, 'SPAN FOIL HALF-SPAN (IN) ', 31X,
4 'PIMP STATIC PRESSURE (IN HG)', /
510X, 'MAC HEAN CHORD. MEAS. A MODUL CENTROID (IN)', 12X,
5 'PCAV CAVITY PRESSURE (IN HG)', /
6 8X, 'MANON VELOCITY MANOMETER BRADING (IN)', 17X,
6 'RUN NO Q-MI-Y: Q=FOIL TESTED (S=SMALL, H=NED, L=LARGE)', /
7 8X, 'TWIST SHAFT TWIST (DEGREES/IN-LB)', 37X,
7 'XIX=GEOGRAPHIC ATTACK ANGLE (DEGREES)', /
812X, 'S LOAD CELL POLARITY (N=NORMAL, R=REVERSE)', 27X,
8 'YT=RUN NUMBER, THIS FOIL @ THIS ANGLE'
DO 72 J=1,40
DO 72 H=4,7
S(J,H)=BLANK
R(J,H)=0.0
72 CONTINUE
DZM=(ZM(2)-ZM(1))*BUG
DZT=(TT(2)-TT(1))*BUG
DO 4 H=1,7
DO 4 L=1,2
DZI(H,L)=(ZI(H,L,2)-ZI(H,L,1))*BUG
DO 7 J=1,JT
4 IP(J, EQ, 1) GO TO 6
IP(NTAP(J), EQ, 0) NTAP(J)=NTAP(J-1)
IP(NPLD(J), EQ, 0) NPLD(J)=NPLD(J-1)
BUG=J-1
TEMP(J)=TT(1)+BUG*DZT
PINP(J)=PINP(J)-PUDGE
ANOM(J)=ANOM(J)-ZM(1)-BUG*DZM
ANGL(J)=ANGL(J)-AZL
DO 7 H=1,7
IP(S(1,H), EQ, BLANK) GO TO 27
IP(S(J,H), EQ, BLANK) S(J,H)=S(J-1,H)
IP(S(J,H), EQ, RS) GO TO 8
R(J,H)=R(J,H)-ZI(H,1,1)-BUG*DZI(H,1)
GO TO 7
8 R(J,H)=-R(J,H)+ZI(H,2,1)+BUG*DZI(H,2)
```

```
GO TO 7
27 R(J,M)=R(J,M)-ZI(M,1,1)-DZI(M,1)*BUG
7 CONTINUE
WRITE(KO,205) (IDENT(N),N=1,18)
19SEP73
205 FORMAT('1',1X,18A4//)
19SEP73
WRITE(KO,705)
705 FORMAT(' INPUT DATA CORRECTED FOR ZERO READINGS, SIGNS, AND HYDROS
1STATIC PRESSURE',// RUN NO      HANON   #1
#2
2   #3      PINP    PCAV')
DO 883 J=1,JT
IP (NTAG(J).GT.1) GO TO 882
WRITE(KO,991) (RUNNBR(J,N),N=1,2),ANOM(J),(R(J,N),N=1,3),PINP(J),P
1CAV(J)
991 FORMAT(1X,2A4,5X,P5.0,5X,2(P7.1,5X),P7.1,2(4X,F4.0))
GO TO 883
882 WRITE(KO,765) (RUNNBR(J,N),N=1,2),ANOM(J),(R(J,N),N=1,3),PINP(J)
765 FORMAT(1X,2A4,5X,P5.0,5X,2(P7.1,5X),P7.1,4X,F4.0,4X,1,-,-,-)
883 CONTINUE
33 WRITE(KO,207) (IDENT(N),N=1,18)
207 FORMAT('1',1X,18A4//)
607 WRITE(KO,707)
607 FORMAT(15X,"**HYDROFOIL DATA REDUCTION**//")
707 FORMAT(15X,"**HYDROFOIL DATA REDUCTION**//")
1* RUN NO ALPHA LIFT-LB DRAG-LB  NOM-INLB VEL-FPS*
BEAR=HAC/(12*3.9739*EXP(67.6832/NTT))
DO 9 J=1,JT
I=NTAP(J)
IP(I.LT.1.OR.I.GT.6) GO TO 99
K=NPLD(J)
IP(K.LT.1.OR.K.GT.3) GO TO 99
BUG=VB(I)
IP(NTAP(J) - PQ, 6) V=.039*ANOM(J)+.0103*ANOM(J)*EXP(-ANOM(J)/50.0)
IP(NTAP(J).NE.6) V=(ANOM(J)*PH(K)*SCALE/(VC(I)*RHO)) **BUG*
1(1.0+VELINC)
VKEEP(J)=V
PYHAPT=0.00327*SHAFT**2*V**2
PBOX I=C(1)*R(J,1)
```

```
IP (R(J,1) .LT. 0.0) PBOX1=C( 8)*R(J,1)
PBOX2=C(2)*R(J,2)
IP (R(J,2) .LT. 0.0) PBOX2=C( 9)*R(J,2)
PBOX3=C(3)*R(J,3)
IP (R(J,3) .LT. 0.0) PBOX3=C(10)*R(J,3)
PBOX4=C(4)*R(J,4)+PYHAFT*0.41477
IP (R(J,4) .LT. 0.0) PBOX4=C(11)*R(J,4)
PBOX5=C(5)*R(J,5)+PYHAFT*0.41477
IP (R(J,5) .LT. 0.0) PBOX5=C(12)*R(J,5)
PBOX6=C(6)*R(J,6)+PYHAFT*0.17045
IP (R(J,6) .LT. 0.0) PBOX6=C(13)*R(J,6)
PY=-PBOX3
PY=-PBOX4-PBOX5-PBOX6
PZ=-PBOX1-PBOX2
HX=4.725*(PBOX1+PBOX2)+6.062*(PBOX5-PBOX4)
HY=-18.0*PBOX2
HZ=17.034*PBOX6-4.725*(PBOX3-3.5*(PBOX4+PBOX5))
RAT=(ANGL(J) + AZL-DYCOR) * 0.0174532
C
RAT=0.0 FOR FIXED AXIS
RAT=0.0
SI(J)=SIN(RAT)
CO(J)=COS(RAT)
PYO=PY*CO(J)+PZ*SI(J)
PYO=PY
PZO=PZ*CO(J)-PY*SI(J)
HKO=HX*CO(J)+HZ*SI(J)
HYO=HY
HZO=HZ*CO(J)-HX*SI(J)
MPLAP=R(J,7)*C(7)
ANGD(J)=ANGL(J)+HYO/TWIST
SIE=SIN(ANGD(J)*3.14159/180.)
COE=COS(ANGD(J)*3.14159/180.)
WRITE(KO,206)(RUNNBR(J,H),H=1,2)*ANGD(J),PZO,PYO,HYO,",
206 FORMAT(1X,2A4,3X,P5.2,1X,P7.2,2X,P7.2,1X,P9.2,4X,P5.2)
RVS=0.5*RHO*AREA*V**2/144.0
SIE2=SIN(ANGD(J)*3.14159*0.5/180.)
```

```
COP2=COS (ANGD(J)*3.14159*0.5/180.)
CL(J)=PZ0/RVS+DDDQ*SIE2*144.0/AREA
CLS0(J)=CL(J)**2
RN(J)=V*BRAF
TAREA=AREA**4.*3.14159
RVSTAR=.5*BHO*TAREA*V**2/144.0
PRICTN=.0303*(RN(J)*1.E6)**(-1./7.)
PIO=PYO-RVSTAR*PRICTN
CD(J)=PYO/RVS-DDDQ*COP2*144./AREA
CLD(J)=CL(J)/CD(J)
CDL(J)=CD(J)/CL(J)
CM(J)=HYO/RVS/MAC+(CL(J)*COE+CD(J)*SIE)*XMAC/MAC+(CL(J)*COE-CD(J)*
1SIP)*ZMAC/MAC
SIGMAY(J)=SIGMA(PV(TEMP(J)),PINP(J),V,RHO)
SIGNAC(J)=SIGMA(PCA(V(J),PINP(J),V,RHO)
IP(HYO,NE.0.) GO TO 501
CPL(J)=0
GO TO 502
501 CONTINUE
CPL(J)=(MX0/PZO)/SPAN
502 CONTINUE
CY(J)=PYO/RVS
9 CMP(J)=-MPLAP/RVS/MAC
WRITE(KO,939)
939 FORMAT('0','1X','LEGEND','8X','VEL UPSTREAM VELOCITY (U)')
WRITE(KO,208)(IDENT(M),M=1,18)
208 FORMAT('1','1X',18A4//)
608 WRITE(KO,708)
708 FORMAT(5X,'**HYDROFOIL DATA IN NONDIMENSIONAL FORM (NO CORRECTION
1S APPLIED) *** /',RN NO ALPHA CL CDUNC CM
2 L/D D/L RN*10**-6')
WRITE(KO,209)((RUNNBR(J,M),M=1,2),ANGD(J),CL(J),CD(J),CM(J),CLD(J),
1,CDL(J),RN(J),J=1,JT)
209 FORMAT(1X,2A4,2X,P5.2,3X,P6.4,4X,P6.4,3X,P7.4,4X,P6.4,P10.
14)
DO 15 J=1,JT
```

```
ANGD (J) = ANGD (J) + DELTA * 180. * AREA * CL (J) / (400. * 3. 14159)
CD (J) = CD (J) + DELTA * AREA * CL (J) * CL (J) / 400.
SIGVOA (J) = SIGMAV (J) * 180. / (ANGD (J) * 3. 14159)
SIGCOA (J) = SIGMAC (J) * 180. / (ANGD (J) * 3. 14159)
CLOA (J) = CL (J) * 180. / (ANGD (J) * 3. 14159)
CDOA (J) = CD (J) * 180. / (ANGD (J) * 3. 14159)
CDL (J) = CD (J) / CL (J)
CMAO (J) = CM (J) * 180. / (ANGD (J) * 3. 14159)
CDOASQ (J) = CDOA (J) * 180. / (ANGD (J) * 3. 14159)

15    CLD (J) = CL (J) / CD (J)
      WRITE (KO, 940)
      940 FORMAT ('0. ', 1X, 'LEGEND', 5X, 'ALPHA GEOMETRIC ANGLP OF ATTACK CORRECT
1ED FOR SHAFT TWIST', /
216X, 'CL LIFT COEFFICIENT, NONDIMENSIONALIZED ON UPSTREAM VELOCITY
3AND MODEL PLANFORM AREA', /
413X, 'CDUNC CD (UNCORRECTED), THE UNCORRECTED DRAG COEFFICIENT AS C
5COMPUTED FROM MEASURED DRAG, AND NONDIMENSIONALIZED', /
619X, 'ON UPSTREAM VELOCITY AND MODEL PLANFORM AREA', /
716X, 'CM MOMENT COEFFICIENT, NONDIMENSIONALIZED ON UPSTREAM VELOCIT
8Y, MODEL PLANFORM AREA, AND MEAN CHORD', /
915X, 'L/D LIFT-TO-DRAG RATIO = CL/CDUNC', /
115X, 'D/L DRAG-TO-LIFT RATIO = CDUNC/CL', /
216X, 'RN REYNOLDS NUMBER, BASED ON MEAN CHORD')
      WRITE (KO, 211) (IDENT (N), N=1, 18)
      211 FORMAT ('1. ', 1X, 18A4 //)
      611 WRITE (KO, 711)
      711 FORMAT (23X, '**PRIOR DATA CORRECTED FOR EFFECTS OF IMAGES OF TRAIL
1ING VORTEX SYSTEM**', //
2*   RUN NO  ALPHAT   CL   CD   CM   (D/L) SIGV/AT SIGC/AT CL/A
3T   CD/AT2 CM/AT SIGV   SIGC   CAVLTH  COMMENTS/REMARKS')
      DO 63 J=1, JT
        IP (NTAG (J) - EQ. 1) GO TO 787
        IP (NTAG (J) - EQ. 2) GO TO 788
        IP (NTAG (J) - EQ. 3) GO TO 789
      WRITE (KO, 963) (RUNNBR (J, M), M=1, 2), TAPS (J), ANGD (J), CL (J), CD (J), CM (J)
1, CDL (J), SIGVOA (J), SIGCOA (J), CLOA (J), CDOASQ (J), SIGMAV (J), SI
```

2GMAC (J) , CAVLEN (J) , (COMENT (J,N) , N=1,3)  
963 FORMAT(1X,2A4,A1,1X,P5.2,5(2X,P5.3),1X,4 (2X,P5.3),1X,2 (P5.3,2X),1X  
1,A4,10X,3A4)  
GO TO 63

787 WRITE(KO,387) (RUNNBR (J,N) , N=1,2) , TAPS (J) , ANGD (J) , CL (J) , CD (J) , CM (J)  
1,CDL (J) , SIGVOA (J) , SIGCOA (J) , CLOA (J) , CDOASQ (J) , CMOA (J) , SIGMAV (J) , SI  
2GMAC (J) , CAVLEN (J) , (COMENT (J,N) , N=1,3)  
387 FORMAT(1X,2A4,A1,1X,P5.2,5(2X,P5.3),1X,4 (2X,P5.3),1X,2 (P5.3,2X),1X  
1,A4, PC, 6X,3A4)  
GO TO 63

788 WRITE(KO,388) (RUNNBR (J,N) , N=1,2) , TAPS (J) , ANGD (J) , CL (J) , CD (J) , CM (J)  
1,CDL (J) , CLOA (J) , CDOASQ (J) , CMOA (J) , CAVLEN (J) , (COMENT (J,N) , N=1,3)  
388 FORMAT(1X,2A4,A1,1X,P5.2,4 (2X,P5.3),2X, \*-----\*,3X, \*-----\*,3 (2X,P5.  
13),1X, \*-----\*,2X, \*-----\*,3X,A4, \* PC(TW) \* ,3A4)  
GO TO 63

789 WRITE(KO,389) (RUNNBR (J,N) , N=1,2) , TAPS (J) , ANGD (J) , CL (J) , CD (J) , CM (J)  
1,CDL (J) , CLOA (J) , CDOASQ (J) , CMOA (J) , CAVLEN (J) , (COMENT (J,N) , N=1,3)  
389 FORMAT(1X,2A4,A1,1X,P5.2,4 (2X,P5.3),2X, \*-----\*,3X, \*-----\*,3 (2X,P5.  
13),1X, \*-----\*,2X, \*-----\*,3X,A4, \* FW, 6X,3A4)  
63 CONTINUE  
WRITE(KO,439)

439 FORMAT("0","1X,"UNLESS OTHERWISE INDICATED. ALL DATA ARE FOR: "/19X,  
1\*1. SUPERCAVITATING FLOW." /19X,"2. BOTH STATIC PRESSURE TAPS OPE  
2N,"/1X," LEGEND" /10X,"\* ONLY UPSTREAM STATIC PRESSURE TAP UTILIZE  
3D"/18X,"\* ONLY DNSTREAM STATIC PRESSURE TAP UTILIZED" /17X,"PC PART  
4IALLY CAVITATING" /13X,"PC (TW) PARTIALLY CAVITATING (TAP WETTED) " /  
517X,"PW FULLY WETTED  
68X,"AT (ALPHAT) (TRUE) ANGLE OF ATTACK, CORRECTED FOR EFFECTS OF 1  
7MAGES OF TRAILING VORTICES" /16X,"AT2 ALPHAT\*\*2" /  
815X,"SIGC CAVITATION NUMBER COMPUTED WITH MEASURED CAVITY PRESSURE  
9"/15X,"SIGV CAVITATION NUMBER COMPUTED WITH CALCULATED VAPOR PRESS  
URE" /  
217X,"CD DRAG COEFFICIENT, CORRECTED FOR EFFECTS OF IMAGES OF TRAIL  
3ING VORTICES" /  
414X,"(D/L) CORRECTED DRAG-TO-LIFT RATIO = CD/CL" /  
513X,"CAVLTH CAVITY LENGTH MEASURED FROM MIDCHORD AT CENTROID POSIT

```
6ION. NONDIMENSIONALIZED ON MEAN CHORD*/  
720X, *(OBTAINED FROM PHOTOGRAPHS*) )  
GO TO 1  
STOP  
END  
99
```

```
FUNCTION PV(T)  
GIVES VAPOUR PRESSURE IN MMHG FOR TEMPERATURES BETWEEN 50 AND 300 DEGREES F  
(SEE EQUATION (2) ON PAGE 151 OF "THE VAPOR PRESSURE OF WATER:  
PART II: STEAM RESEARCH PROGRAM" BY SMITH, KEYES, AND GERRY IN  
THE PROC. AM. AC. ARTS & SCI., VOL 69, 1934, P. 137, REFERENCE (10))  
DEG=(5.*(T-32.)/9.)*273.16  
X=647.27-DEG  
A=3.2438+(5.8682E-3)*X+(1.1702E-8)*X*X*X  
B=1.+(.1878E-3)*X  
FOOP=X*A/(DEG*B)  
CRUD=218.167/(10.*FOOP)  
PV=14.6959*CRUD/.01934  
RETURN  
END
```

SEPER INVES OF WALL EFFECTS ON SUPERCAVITATING HYDROFOILS OF FINITE SPAN

HYDROFOIL INPUT DATA

TA TT AREA SPAN MAC

79 96 10.0 5.0 2.01

ZERO BEARINGS AND TUNNEL TEMP BEFORE AND AFTER

BAON 1-4 1-4 2-8 2-8 3-4 3-4 FT  
 0. 0.0 0.0 0.0 100.0 0.0 100.0 94.6  
 0. 0.0 0.0 0.0 99.5 0.0 101.0 97.0  
 CBL 1.85/CT(BORROW/REV) 0.1=0.10000 0.2=0.02030 0.3=0.04030  
 TWIST= 7200.0 SHAFT DIA=.1.501IN

INPUT DATA AS RECORDED\*

RUN NO.	BAON	S	01	S	02	S	03	PINP	PCAV
S-8-0-01	1439.	-235.0	R	111.2	R	218.0	R	194.	47.
S-8-0-02*	1433.	-230.0	R	111.1	R	219.0	R	194.	46.
S-8-0-03	1422.	-216.0	R	110.8	R	219.0	R	181.	45.
S-8-0-04*	1420.	-200.0	R	109.2	R	213.0	R	169.	44.
S-8-0-05	1408.	-160.0	R	108.3	R	207.0	R	158.	44.
S-8-0-06	1397.	-160.0	R	107.8	R	200.0	R	149.	44.
S-8-0-07	1400.	-142.0	R	107.5	R	191.0	R	138.	44.
S-8-0-08	1392.	-128.0	R	107.3	R	182.0	R	130.	44.
S-8-0-09	1395.	-112.0	R	106.9	R	174.0	R	119.	44.
S-8-0-10	1391.	-100.0	R	106.4	R	166.0	R	110.	44.
S-8-0-11*	1397.	-86.0	R	106.1	R	158.0	R	100.	45.
S-8-0-12	1400.	-76.0	R	105.1	R	150.0	R	90.	46.
S-8-0-13	1218.	-90.0	R	105.1	R	160.0	R	108.	46.
S-8-0-14	953.	-76.0	R	104.6	R	150.0	R	99.	46.
S-8-0-15	957.	-68.0	R	104.7	R	144.0	R	99.	46.
L2C8D	TA ROOM T2688A (0.5 FT)	( " )							
TT TUNNEL *	( " )								
AREA HALF-SPAN MODEL PLATEFORM AREA (SQ IN)									
SPAN POIL HALF-SPAN (IN)									
MAC CHORD, MEAS. A MODEL CENTROID (IN)									
BAON VELOCITY HARMONIC MEASUREMENT (IN/LB)									
TWIST SHAFT TWIST (DEGREES/IN-LB)									
S LOAD CELL POLARITY (R-NORMAL, R-REVERSE)									

LOAD CELL 01 LIPT (COUNTS)

TT TUNNEL \* ( " )

02 MOMENT ABOUT MIDCHORD (COUNTS)

03 DRAG (COUNTS)

PINP STATIC PRESSURE (IN HG)

PCAV CAVITY PRESSURE (IN HG)

RUN NO Q-ZX-YY: Q=POIL TESTED(S-SMALL, B-NRD, L-LARGE)

YY=GEOMETRIC ATTACK ANGLE (DEGREES)

\*=RUN NUMBER, THIS POIL & THIS ANGLE

## EFFECTS OF WALL EFFECTS ON SUPERCAVITATING HYDROPOOLS OF FINITE SPAN

## INPUT DATA CORRECTED FOR ZERO BRADING, SIGNS, AND HYDROSTATIC PRESSURE

BUS NO	RADON	01	02	03	PIBP	PCAV
S-0-0-01	1439.	-238.0	-11.2	-118.0	179.	67.
S-0-0-02	1433.	-230.0	-11.1	-118.9	179.	46.
S-0-0-03	1422.	-216.0	-10.5	-118.9	166.	65.
S-0-0-04	1420.	-200.0	-9.3	-112.8	158.	44.
S-0-0-05	1404.	-180.0	-8.4	-106.7	143.	64.
S-0-0-06	1397.	-160.0	-8.0	-99.6	138.	44.
S-0-0-07	1400.	-142.0	-7.7	-90.6	123.	44.
S-0-0-08	1392.	-128.0	-7.6	-81.5	115.	44.
S-0-0-09	1385.	-112.0	-7.2	-73.4	108.	44.
S-0-0-10	1391.	-100.0	-6.7	-65.8	95.	44.
S-0-0-11	1397.	-86.0	-6.5	-57.3	85.	45.
S-0-0-12	1340.	-76.0	-5.5	-49.2	75.	46.
S-0-0-13	1218.	-90.0	-5.5	-59.1	91.	46.
S-0-0-14	953.	-78.0	-5.1	-49.1	68.	46.
S-0-0-15	957.	-68.0	-5.2	-43.0	68.	46.

AD-A056 090

MASSACHUSETTS INST OF TECH CAMBRIDGE DEPT OF OCEAN E--ETC F/G 20/4  
AN EXPERIMENTAL INVESTIGATION OF WALL EFFECTS ON SUPERCAVITATION--ETC(U)  
AUG 77 M R MAIXNER

N00014-76-C-0358

NL

UNCLASSIFIED

2 OF 3  
ADA  
056090



PIPE LINES OF WALL EFFECTS ON SUPERCAVITATING HYDROFOILS OF PIVOT SPAN

HYDROFOIL DATA REDUCTION

RUN NO	ALPHA	LIPY-10	DRAG-10	BON-TIDS	VEL-PPS
S-8-0-01	8.00	23.63	4.76	8.21	28.05
S-8-0-02	8.00	23.23	4.79	8.19	27.99
S-8-0-03	8.00	21.82	4.79	3.98	27.89
S-8-0-04	8.00	20.19	6.55	3.50	27.88
S-8-0-05	8.00	18.18	4.30	3.18	27.73
S-8-0-06	8.00	16.17	4.02	3.00	27.66
S-8-0-07	8.00	14.36	3.65	2.90	27.69
S-8-0-08	8.00	12.96	3.28	2.84	27.62
S-8-0-09	8.00	11.35	2.96	2.70	27.55
S-8-0-10	8.00	10.14	2.63	2.53	27.61
S-8-0-11	8.00	8.73	2.31	2.43	27.66
S-8-0-12	8.00	7.51	1.98	2.07	28.06
S-8-0-13	8.00	9.12	2.38	2.08	25.96
S-8-0-14	8.00	7.51	1.98	1.91	23.16
S-8-0-15	8.00	6.91	1.73	1.96	23.20

LEGEND VEL UPSTREAM VELOCITY (ft)

**EFFECTS OF WALL EFFECTS ON SUPERCAVITATING HYDROPOILS OF FINITE SPAN**

**\*\*HYDROPOIL DATA IN NONDIMENSIONAL FORM (NO CORRECTIONS APPLIED) \*\***

TEST NO	ALPHA	CL	CDUNC	CB	L/D	D/L	Reynolds No
S-8-0-01	8.00	0.0002	0.0799	0.0397	5.6000	0.1783	0.5841
S-8-0-02	8.00	0.0023	0.0810	0.0397	5.4617	0.1831	0.5830
S-8-0-03	8.00	0.0103	0.0816	0.0376	5.1285	0.1950	0.5809
S-8-0-04	8.00	0.0187	0.0770	0.0338	5.0355	0.1986	0.5805
S-8-0-05	8.00	0.0327	0.0732	0.0307	4.8201	0.2075	0.5775
S-8-0-06	8.00	0.03151	0.0680	0.0291	4.6316	0.2158	0.5762
S-8-0-07	8.00	0.02798	0.0607	0.0281	4.6005	0.2174	0.5767
S-8-0-08	8.00	0.02538	0.0540	0.0276	4.6370	0.2129	0.5752
S-8-0-09	8.00	0.02210	0.0479	0.0264	4.6599	0.2146	0.5738
S-8-0-10	8.00	0.0195	0.0413	0.0246	4.8094	0.2079	0.5750
S-8-0-11	8.00	0.01703	0.0387	0.0236	4.9018	0.2039	0.5762
S-8-0-12	8.00	0.01424	0.0273	0.0195	5.2115	0.1919	0.5843
S-8-0-13	8.00	0.02019	0.0428	0.0229	4.7601	0.2101	0.5405
S-8-0-14	8.00	0.02088	0.0445	0.0264	4.6952	0.2130	0.4822
S-8-0-15	8.00	0.01915	0.0375	0.0270	5.1078	0.1958	0.4832

**LEGEND**

ALPHA GEOMETRIC ANGLE OF ATTACK CORRECTED FOR SHAFT TWIST  
 CL LIFT COEFFICIENT, NONDIMENSIONALIZED ON UPSTREAM VELOCITY AND MODEL PLATEFORM AREA  
 CDUNC CD (UNCORRECTED). THE DISCORRECTED DRAG COEFFICIENT AS COMPUTED FROM MEASURED DRAG, AND NONDIMENSIONALIZED  
 ON UPSTREAM VELOCITY AND MODEL PLATEFORM AREA  
 CB MOMENT COEFFICIENT, NONDIMENSIONALIZED ON UPSTREAM VELOCITY. MODEL PLATEFORM AREA, AND Mean CHORD  
 L/D LIFT-TO-DRAG RATIO = CL/CDUNC  
 D/L DRAG-TO-LIFT RATIO = CDUNC/CL  
 Re REYNOLDS NUMBER, BASED ON Mean CHORD

STEPS IN ALL EFFECTS ON SUPERCAVITATING HYDROFOILS OF FINITE SPAN

~~APPENDIX DATA CORRECTED FOR EFFECTS OF IMAGES OF TRAILING VORTEX SYSTEMS~~

BUS NO	ALPHAT	CL	CD	CA	(D/L)	SIGV	SIGC	CAVLT	CAVLT	CAVLT	CAVLT
						AT	AT	AT	AT	AT	AT
S-0-0-1	8.08	0.448	0.081	0.080	0.180	3.580	3.441	3.177	4.089	0.282	0.505
S-0-0-2*	8.08	0.462	0.092	0.040	0.184	3.481	3.136	3.102	0.281	0.506	0.491
S-0-0-3	8.08	0.416	0.082	0.038	0.196	3.269	3.192	2.968	4.133	0.267	0.461
S-0-0-4*	8.07	0.398	0.077	0.033	0.200	2.953	2.909	2.752	3.904	0.237	0.416
S-0-0-5	8.06	0.353	0.074	0.031	0.209	2.688	2.648	2.506	3.713	0.218	0.378
S-0-0-6	8.06	0.315	0.068	0.029	0.219	2.455	2.422	2.241	3.454	0.207	0.345
S-0-0-7	8.05	0.279	0.061	0.028	0.218	2.152	2.124	1.988	3.088	0.200	0.302
S-0-0-8	8.05	0.253	0.054	0.028	0.218	1.943	1.921	1.805	2.746	0.197	0.273
S-0-0-9	8.04	0.223	0.048	0.026	0.215	1.649	1.634	1.509	2.438	0.188	0.231
S-0-0-10	8.04	0.198	0.041	0.025	0.209	1.395	1.385	1.415	2.104	0.176	0.196
S-0-0-11*	8.03	0.170	0.035	0.024	0.204	1.115	1.085	1.215	1.772	0.168	0.156
S-0-0-12	8.03	0.182	0.027	0.019	0.192	0.817	0.768	1.017	1.396	0.139	0.118
S-0-0-13	8.04	0.202	0.003	0.023	0.211	1.496	1.445	1.419	2.162	0.163	0.210
S-0-0-14	8.04	0.209	0.045	0.026	0.214	1.525	1.471	1.489	2.267	0.188	0.218
S-0-0-15	8.03	0.191	0.036	0.027	0.196	1.511	1.465	1.365	1.912	0.192	0.212
						—	—	—	—	—	—

UNLESS OTHERWISE INDICATED, ALL DATA ARE FOR:

1. SUPERCAVITATING PLOW.
2. BOTH STATIC PRESSURE TAPS OPEN.

LEGEND

- \* ONLY UPSTREAM STATIC PRESSURE TAP UTILIZED
- PC PARTIALLY CAVITATING
- PC(1) PARTIALLY CAVITATING (TAP WETTED)
- PN FULLY WETTED
- AT (ALPHAT) (TRUE) ANGLE OF ATTACK, CORRECTED FOR EFFECTS OF IMAGES OF TRAILING VORTICES
- AT2 ALPHAT\*2
- SIGC CAVITATION NUMBER COMPUTED WITH REASDARD CAVITY PRESSURE
- SIGV CAVITATION NUMBER COMPUTED WITH CALCULATED VAPOR PRESSURE
- CD DRAG COEFFICIENT, CORRECTED FOR EFFECTS OF IMAGES OF TRAILING VORTICES
- (D/L) CORRECTED DRAG-TO-LIFT RATIO = CD/CL
- CAVLT CAVITY LENGTH MEASURED FROM MIDCHORD AT CENTROID POSITION, NONDIMENSIONALIZED ON MEAN CHORD (OBTAINED FROM PHOTOGRAPHS)

HIPER TESTS OF WALL EFFECTS ON SUPERCAVITATING HYDROPOILS OF FINITE SPAN

HIPERPOIL INPUT DATA  
 T# TT AREA SPAN MAC  
 75 91 10.0 5.0 2.01

ZERO SETTINGS AND TUNNEL TEMP BEFORE AND AFTER

MANOA 1-H 1-H 2-E 2-E 3-H 3-H TT  
 0. 0.0 0.0 100.0 0.0 100.0 90.0  
 0. 0.0 0.0 98.0 0.0 101.0 92.0  
 CAVL LBS/CF (NORMAL/REV) 61=0.10000 62=0.02090 63=0.04030  
 TWIST= 7200.0 SMART DIA.= 1.50IN

\*\*INPUT DATA AS RECORDED\*\*

RUN NO	MANOA	S	61	62	S	63	PINP	PCAV
S-9.5-01	1429.	-298.0	R	122.0	R	235.0	189.	39.
S-9.5-02*	1427.	-298.0	R	121.9	R	234.0	188.	39.
S-9.5-03	1420.	-272.0	R	120.3	R	232.0	171.	39.
S-9.5-04*	1406.	-270.0	R	119.0	R	229.0	171.	39.
S-9.5-05	1400.	-252.0	R	119.0	R	225.0	159.	39.
S-9.5-06	1399.	-228.0	R	117.8	R	220.0	148.	39.
S-9.5-07	1399.	-202.0	R	117.0	R	210.0	136.	38.
S-9.5-08	1390.	-176.0	R	116.3	R	200.0	121.	38.
S-9.5-09	1385.	-154.0	R	114.8	R	188.0	111.	38.
S-9.5-10	1385.	-132.0	R	113.8	R	176.0	99.	38.
S-9.5-11*	1398.	-126.0	R	113.2	R	173.0	99.	38.
S-9.5-12	1400.	-118.0	R	112.8	R	169.0	90.	38.
S-9.5-13	1407.	-110.0	R	111.9	R	163.0	87.	38.
S-9.5-14	940.	-150.0	R	112.2	R	180.0	115.	80.
S-9.5-15	1213.	-178.0	R	114.7	R	198.0	126.	40.

LEGEND TO ROOM TEMPP (DEG FAHR)

TT TUNNEL " " "

AREA HALF-SPAN MODEL PLATEFORM AREA (SQ IN)

SPAN FOIL HALF-SPAN (IN)

MAC BEAM CHORD, MEAS. @ MODEL CENTEROID (IN)

MANON VELOCITY MACHINER READING (IN)

TWIST SHARP TWIST (DEGREES/IN-LB)

S LOAD CELL POLARITY (N=NORMAL, R=REVERSE)

LOAD CELL 01 LIPT (COUNTS)

02 MOMENT ABOUT MIDCHORD (COUNTS)

03 DRAG (COUNTS)

PINP STATIC PRESSURE (IN HG)

PCAV CAVITY PRESSURE (IN HG)

NUM NO Q-III-IV: Q=POIL TESTED(SMALL, MEDIUM, L=Large)  
 XIN=GEOMETRIC ATTACK ANGLZ (DEGREES)  
 YY=BURN NUMBER. THIS FOIL @ THIS ANGLE

INPUT LINES OF WALL EFFECTS ON SUPERCAVITATING HYDROPOOLS OF FINITE SPAN

INPUT DATA CORRECTED FOR ZERO GRADIENTS, SIGNS, AND HYDROSTATIC PRESSURE

BUN NO	BARON	01	02	03	PINP	PCAV
S-9.5-01	1429-	-298.0	-12.0	-135.0	179.	39.
S-9.5-02	1627-	-298.0	-72.0	-113.9	173.	39.
S-9.5-03	1620-	-272.0	-20.6	-131.9	156.	39.
S-9.5-04	1606-	-270.0	-19.4	-128.8	158.	39.
S-9.5-05	1600-	-252.0	-19.6	-124.7	146.	39.
S-9.5-06	1399-	-228.0	-18.5	-119.6	133.	39.
S-9.5-07	1398-	-202.0	-17.9	-109.6	121.	38.
S-9.5-08	1390-	-176.0	-17.3	-99.5	106.	38.
S-9.5-09	1365-	-154.0	-15.9	-87.4	96.	38.
S-9.5-10	1385-	-132.0	-15.1	-75.4	84.	38.
S-9.5-11	1394-	-126.0	-11.6	-72.3	84.	38.
S-9.5-12	1608-	-118.0	-10.4	-69.2	75.	38.
S-9.5-13	1607-	-110.0	-13.6	-62.1	72.	38.
S-9.5-14	980-	-150.0	-18.1	-79.1	100.	40.
S-9.5-15	1213-	-170.0	-16.7	-97.0	111.	40.

TABLE I  
EFFECTS OF WALL EFFECTS ON SUPERCavitating Hydrofoils of Finite Span

• HYDROFOIL DATA REDUCTION •

Sub No.	ALPHA	LIFT-LB	DRAG-LB	BOR-INLB	VEL-FPS
S-9.5-01	9.50	30.26	5.44	0.28	27.98
S-9.5-02	9.50	30.26	5.40	0.29	27.96
S-9.5-03	9.50	27.63	5.31	7.74	27.89
S-9.5-04	9.50	27.41	5.19	7.31	27.76
S-9.5-05	9.50	25.61	5.03	7.36	27.71
S-9.5-06	9.50	23.19	4.82	6.97	27.70
S-9.5-07	9.50	20.57	4.42	6.72	27.65
S-9.5-08	9.50	17.96	4.01	6.51	27.62
S-9.5-09	9.50	15.73	3.52	6.00	27.57
S-9.5-10	9.50	13.52	3.04	5.68	27.57
S-9.5-11	9.50	12.91	2.91	5.50	27.65
S-9.5-12	9.50	11.70	2.75	5.61	27.75
S-9.5-13	9.50	11.28	2.50	5.12	27.77
S-9.5-14	9.50	15.29	3.19	5.29	23.02
S-9.5-15	9.50	18.15	3.91	6.28	25.92

LEGEND      VEL UPSTREAM VELOCITY (U)

EFFECTS OF WALL EFFECTS ON SUPERCAVITATING HYDROPOILS OF FINITE SPAN

••HYDROPOIL DATA IN NONDIMENSIONAL FORM (NO CORRECTIONS APPLIED)••

RUN NO	ALPHA	CL	CDUNC	CH	L/D	D/L	Re <sup>0.5</sup>
S-9.5-01	9.50	0.5764	0.0913	0.0784	6.1771	0.1619	0.5605
S-9.5-02	9.50	0.5772	0.0926	0.0787	6.2314	0.1605	0.5601
S-9.5-03	9.50	0.5298	0.0915	0.0738	5.7864	0.1720	0.5588
S-9.5-04	9.50	0.5300	0.0900	0.0703	5.8864	0.1639	0.5563
S-9.5-05	9.50	0.4972	0.0872	0.0711	5.6989	0.1755	0.5552
S-9.5-06	9.50	0.4505	0.0813	0.0673	5.4053	0.1850	0.5550
S-9.5-07	9.50	0.4010	0.0757	0.0651	5.2950	0.1889	0.5549
S-9.5-08	9.50	0.3511	0.0680	0.0633	5.1601	0.1918	0.5533
S-9.5-09	9.50	0.3085	0.0588	0.0585	5.2514	0.1900	0.5524
S-9.5-10	9.50	0.2650	0.0592	0.0554	5.3855	0.1857	0.5525
S-9.5-11	9.50	0.2516	0.0664	0.0534	5.4162	0.1846	0.5540
S-9.5-12	9.50	0.2266	0.0529	0.0521	5.2813	0.1893	0.5559
S-9.5-13	9.50	0.2181	0.0361	0.0492	5.7288	0.1746	0.5564
S-9.5-14	9.50	0.4302	0.0790	0.0740	5.4460	0.1837	0.4612
S-9.5-15	9.50	0.4027	0.0763	0.0693	5.2777	0.1895	0.5193

LEGEND

ALPHA GEOMETRIC ANGLE OF ATTACK CORRECTED FOR SHAFT THRUST

CL LIFT COEFFICIENT, NONDIMENSIONALIZED ON UPSTREAM VELOCITY AND MODEL PLATEFORM AREA

CDUNC CDUNC(CORRECTED), THE UNCORRECTED DRAG COEFFICIENT AS COMPUTED FROM MEASURED DBAG, AND NONDIMENSIONALIZED ON UPSTREAM VELOCITY AND MODEL PLATEFORM AREA

CH AERONAUT COEFFICIENT, NONDIMENSIONALIZED ON UPSTREAM VELOCITY, MODEL PLATEFORM AREA, AND REYN CHORD

L/D LIFT-TO-DRAG RATIO = CL/CDUNC

D/L DRAG-TO-LIFT RATIO = CDUNC/CL

AS REYNOLDS NUMBER, BASED ON REYN CHORD

**DATA TAKES OF WALL EFFECTS ON SUPERCAVITATING HYDROFOILS OF FINITE SPAN**

**APPENDIX DATA CORRECTED FOR EFFECTS OF IMAGES OF TRAILING VORTICES SYSTEMS\***

RUN NO	ALPHAT	CL	CD	CB	(D/L)	SIGC/AT	SIGC/AT CL/AT	CD/AT2	CB/AT	SIGT	SIGC	CAVLTN	COUNTS/MEASURES
S-9.5-0-1	9.61	0.576	0.694	0.078	0.168	3.038	2.978	3.357	0.468	0.509	0.499	0.68	
S-9.5-0-2*	9.61	0.577	0.696	0.079	0.162	3.016	2.956	3.383	0.469	0.506	0.496	0.68	
S-9.5-0-3	9.60	0.529	0.692	0.074	0.174	2.653	2.596	3.161	3.293	0.441	0.444	0.435	0.70
S-9.5-0-4*	9.60	0.530	0.691	0.070	0.172	2.719	2.665	3.164	3.281	0.420	0.455	0.446	0.70
S-9.5-0-5	9.59	0.497	0.688	0.071	0.177	2.413	2.383	2.970	3.182	0.425	0.408	0.396	0.60
S-9.5-0-6	9.58	0.450	0.684	0.068	0.186	2.166	2.120	2.594	3.002	0.403	0.362	0.354	0.63
S-9.5-0-7	9.57	0.401	0.676	0.065	0.190	1.901	1.880	2.400	2.731	0.390	0.318	0.318	0.55
S-9.5-0-8	9.56	0.351	0.668	0.063	0.195	1.565	1.508	2.103	2.455	0.379	0.261	0.258	1.30
S-9.5-0-9	9.56	0.369	0.659	0.059	0.191	1.380	1.327	1.050	2.123	0.351	0.228	0.221	1.60
S-9.5-10	9.55	0.265	0.609	0.055	0.187	1.064	1.055	1.590	1.780	0.332	0.177	0.176	1.75
S-9.5-11*	9.55	0.252	0.607	0.053	0.185	1.054	1.049	1.510	1.680	0.320	0.176	0.175	2.80
S-9.5-12	9.54	0.221	0.603	0.052	0.190	0.892	0.880	1.260	1.553	0.313	0.180	0.140	3.65
S-9.5-13	9.54	0.218	0.608	0.049	0.175	0.769	0.771	1.310	1.378	0.296	0.128	0.128	4.15
S-9.5-14	9.54	0.810	0.080	0.074	0.185	2.020	1.963	2.573	2.898	0.443	0.338	0.328	0.90
S-9.5-15	9.57	0.403	0.077	0.069	0.191	1.872	1.832	2.410	2.751	0.415	0.313	0.306	1.00

UNLESS OTHERWISE INDICATED, ALL DATA ARE FOR:

1. SUPERCAVITATING PLOW.
2. BOTH STATIC PRESSURE TAPS OPEN.

**LEGEND**

- \* ONLY UPSTREAM STATIC PRESSURE TAP UTILIZED
- ONLY DOWNSTREAM STATIC PRESSURE TAP UTILIZED
- PC (TB) PARTIALLY CAVITATING (TAP WETTED)
- PW FULLY WETTED
- AT (ALPHAT) (TRUE) ANGLE OF ATTACK, CORRECTED FOR EFFECTS OF IMAGES OF TRAILING VORTICES
- AT2 ALPHAT+0.2
- SIGC CAVITATION NUMBER COMPUTED WITH MEASURED CAVITY PRESSURE
- SIGV CAVITATION NUMBER COMPUTED WITH CALCULATED VAPOR PRESSURE
- CD DRAG COEFFICIENT, CORRECTED FOR EFFECTS OF IMAGES OF TRAILING VORTICES
- (D/L) CORRECTED DRAG-TO-LIFT RATIO = CD/CL
- CAVLTN CAVITY LENGTH MEASURED FROM MIDCHORD AT CENTROID POSITION, NORMALIZED ON CHORD (OBTAINED FROM PHOTOGRAPHS)

SUPER IONES OF GALL EFFECTS ON SUPERCAVITATING HYDROPOLES OF FINITE SPAN

HYDROPOLE INPUT DATA

TR	TT	AREA	SPAN	BAC
75	89	10.0	5.0	2.01

ZERO READINGS AND TUNNEL TRAP BEFORE AND AFTER  
 MAN 1-8      1-8      2-8      2-8      3-8      3-8  
 0.    0.0    0.0    0.0    100.0    0.0    100.0    0.0    87.0  
 0.    0.0    0.0    0.0    110.5    0.0    104.0    0.0    90.0  
 CELL KGS/CF (BONDAK/ART) 81-0.16000 P2=0.02690 03=0.04030  
 TWIST= 7260.0 SHARP DIA.= 1.5018  
 OUTPUT DATA AS RECORDED<sup>ee</sup>

RUN NO.	MAN 0	S	A1	S	82	S	83	PIPP	PCAV
S-11.-01*	1330.	-350.0	R	120.2	R	260.0	R	201.	39.
S-11.-02*	1340.	-380.0	R	127.9	R	260.0	R	204.	39.
S-11.-03*	1332.	-330.0	R	127.0	R	260.0	R	197.	38.
S-11.-04*	1335.	-336.0	R	126.6	R	260.0	R	197.	39.
S-11.-05	1326.	-319.0	R	125.1	R	258.0	R	185.	39.
S-11.-06*	1330.	-312.0	R	125.0	R	257.0	R	185.	39.
S-11.-07	1327.	-290.0	R	128.0	R	250.0	R	170.	36.
S-11.-08*	1326.	-284.0	R	123.5	R	250.0	R	171.	36.
S-11.-09*	1325.	-252.0	R	122.5	R	240.0	R	155.	36.
S-11.-10	1328.	-258.0	R	122.5	R	241.0	R	155.	36.
S-11.-11*	1323.	-218.0	R	121.2	R	222.0	R	136.	36.
S-11.-12	1323.	-212.0	R	120.9	R	226.0	R	137.	37.
S-11.-13*	1323.	-182.0	R	120.2	R	213.0	R	120.	36.
S-11.-14	1319.	-176.0	R	119.6	R	210.0	R	119.	36.
S-11.-15*	1323.	-160.0	R	119.0	R	200.0	R	110.	37.
S-11.-16	1318.	-154.0	R	118.7	R	198.0	R	110.	36.
S-11.-17*	1320.	-166.0	R	118.4	R	192.0	R	100.	36.
S-11.-18	1323.	-139.0	R	118.0	R	187.0	R	101.	36.
S-11.-19*	1320.	-182.0	R	118.0	R	188.0	R	100.	37.
S-11.-20	1323.	-132.0	R	117.8	R	184.0	R	90.	37.
S-11.-21*	1333.	-126.0	R	117.5	R	180.0	R	90.	36.
S-11.-22	1370.	-116.0	R	116.5	R	174.0	R	84.	37.
S-11.-23*	1365.	-110.0	R	116.1	R	175.0	R	85.	40.

LEGEND      TR ROOM TEMPER (DEG FAHR)  
 TT TUNNEL " ( " )  
 AREA HALF-SPAN MODEL PLATFORM AREA (SQ IN)  
 SPAN FOIL HALF-SPAN (IN)  
 BAC HEAD CHORD, ALSO, A MODEL CHORD (IN)  
 MAN VELOCITY MEASUREMENT READING (IN)  
 TWIST SHARP TWIST (DEGREES/IN-LB)  
 S LOAD CELL POLARITY (R-NORMAL, R-REVERSE)

LOAD CELL #1 LIFT (COUNTS)  
 #2 BOREST ABOUT MIDCHORD (COUNTS)

DRAG (COUNTS)

STATIC PRESSURE (MM HG)

PIPP CAVITY PRESSURE (MM HG)

RUN NO Q-III-IV: Q-POIL TESTED (S-SMALL, R-LARGE)  
 KIN-GOMMETRIC ATTACK ANGLE (DEGREES)  
 TT-POIL NUMBER, THIS POIL = THIS ANGLE

RIPER INVES OF WALL EFFECTS ON SUPERCAVITATING HYDROFOILS OF FLUTTE SPAN

INPUT DATA CORRECTED FOR 1880 READINGS, SIGNS, AND BAROMETRIC PRESSURE

SUB NO	NAUTON	61	62	63	PINR	PCAV
S-11,-01	1336.	-350.0	-28.2	-160.0	189.	39.
S-11,-02	1340.	-348.0	-27.4	-159.8	189.	39.
S-11,-03	1333.	-338.0	-26.9	-159.6	182.	38.
S-11,-04	1335.	-336.0	-25.2	-159.5	182.	39.
S-11,-05	1328.	-318.0	-23.2	-157.3	170.	39.
S-11,-06	1330.	-312.0	-22.6	-156.1	170.	39.
S-11,-07	1327.	-290.0	-21.1	-148.9	155.	36.
S-11,-08	1324.	-288.0	-20.2	-148.7	156.	36.
S-11,-09	1325.	-252.0	-18.7	-138.5	180.	36.
S-11,-10	1328.	-258.0	-18.2	-139.4	180.	36.
S-11,-11	1322.	-218.0	-16.4	-127.2	121.	36.
S-11,-12	1323.	-212.0	-15.6	-124.0	122.	37.
S-11,-13	1322.	-182.0	-14.5	-110.8	105.	36.
S-11,-14	1319.	-176.0	-13.4	-107.6	104.	36.
S-11,-15	1323.	-160.0	-12.3	-97.5	95.	37.
S-11,-16	1318.	-154.0	-11.5	-95.3	95.	36.
S-11,-17	1320.	-146.0	-10.8	-89.1	85.	36.
S-11,-18	1323.	-138.0	-9.9	-83.9	86.	36.
S-11,-19	1320.	-142.0	-9.4	-84.7	85.	37.
S-11,-20	1323.	-132.0	-8.7	-80.5	75.	37.
S-11,-21	1333.	-126.0	-8.0	-76.4	75.	36.
S-11,-22	1370.	-116.0	-6.5	-70.2	69.	37.
S-11,-23	1365.	-114.0	-5.6	-71.0	70.	40.

SUPER LAVES OF WALL EFFECTS ON SUPERCAVITATING HYDROFOILS OF FINITE SPAN

\*\*HYDROFOIL DATA SUBSECTION\*\*

RUN NO	ALPHA	LIFT-LB	DRAIG-LB	HOE-IMLB VEL-FPS
S-11.-01	11.00	35.59	6.45	10.61 27.13
S-11.-02	11.00	35.37	6.44	10.32 27.15
S-11.-03	11.00	36.34	6.43	9.80 27.08
S-11.-04	11.00	36.13	6.43	9.47 27.10
S-11.-05	11.00	32.28	6.34	8.72 27.03
S-11.-06	11.00	31.67	6.29	8.51 27.05
S-11.-07	11.00	29.34	6.00	7.95 27.02
S-11.-08	11.00	28.82	5.99	7.58 27.00
S-11.-09	11.00	25.59	5.58	7.03 27.01
S-11.-10	11.00	26.18	5.62	6.85 27.00
S-11.-11	11.00	22.14	5.13	6.18 26.99
S-11.-12	11.00	21.53	5.00	5.89 26.99
S-11.-13	11.00	18.50	4.47	5.44 26.99
S-11.-14	11.00	17.88	4.34	5.04 26.95
S-11.-15	11.00	16.26	3.93	4.63 26.99
S-11.-16	11.00	15.63	3.84	4.34 26.94
S-11.-17	11.00	18.82	3.59	4.05 26.96
S-11.-18	11.00	14.01	3.38	3.72 26.99
S-11.-19	11.00	14.40	3.41	3.54 26.96
S-11.-20	11.00	13.38	3.25	3.28 26.99
S-11.-21	11.00	12.77	3.08	2.99 27.08
S-11.-22	11.00	11.74	2.83	2.44 27.03
S-11.-23	11.00	11.52	2.86	2.11 27.38

LNGRAD

VEL UPSTREAM VELOCITY (ft)

**UPPER INVISOR WALL EFFECTS ON SUPERCAVITATING HYDROPOILS OF FINITE SPAN**

**\*\*HYDROPOIL DATA IN NONDIMENSIONAL FORM (NO CORRECTIONS APPLIED) \*\***

BUS NO	ALPHA	CL	CDUNC	CH	L/D	Re*10 <sup>6</sup> *6
S-11.-01	11.00	0.7207	0.1202	0.1069	5.9966	0.1668
S-11.-02	11.00	0.7153	0.1193	0.1038	5.9882	0.1676
S-11.-03	11.00	0.6979	0.1203	0.0991	5.7995	0.1726
S-11.-04	11.00	0.6925	0.1200	0.0956	5.7705	0.1733
S-11.-05	11.00	0.6586	0.1189	0.0885	5.5193	0.1805
S-11.-06	11.00	0.6550	0.1177	0.0862	5.4197	0.1823
S-11.-07	11.00	0.6038	0.1121	0.0807	5.6112	0.1865
S-11.-08	11.00	0.5896	0.1122	0.0772	5.2583	0.1903
S-11.-09	11.00	0.5229	0.1037	0.0715	5.9428	0.1983
S-11.-10	11.00	0.5154	0.1045	0.0697	5.1255	0.1951
S-11.-11	11.00	0.4331	0.0945	0.0629	4.7957	0.2085
S-11.-12	11.00	0.4005	0.0919	0.0599	4.7954	0.2085
S-11.-13	11.00	0.3196	0.0810	0.0554	4.6149	0.2139
S-11.-14	11.00	0.3669	0.0766	0.0515	4.6672	0.2143
S-11.-15	11.00	0.3227	0.0700	0.0472	4.7546	0.2103
S-11.-16	11.00	0.3212	0.0684	0.0444	4.6928	0.2131
S-11.-17	11.00	0.3040	0.0632	0.0413	4.6082	0.2080
S-11.-18	11.00	0.2566	0.0588	0.0379	4.8745	0.2051
S-11.-19	11.00	0.2952	0.0596	0.0361	4.7517	0.2019
S-11.-20	11.00	0.2139	0.0560	0.0334	4.6879	0.2016
S-11.-21	11.00	0.2594	0.0521	0.0303	4.9751	0.2010
S-11.-22	11.00	0.2225	0.0457	0.0280	5.0920	0.1964
S-11.-23	11.00	0.2289	0.0465	0.0208	4.9233	0.2031

**LEGEND**

ALPHA GEOMETRIC ANGLE OF ATTACK CORRECTED FOR SHAFT TWIST  
 CL LIFT COEFFICIENT, NONDIMENSIONALIZED ON UPSTREAM VELOCITY AND MODEL PLANFORM AREA,  
 CDUNC CD (UNCORRECTED). THE UNCORRECTED DRAG COEFFICIENT AS COMPUTED FROM MEASURED DRAG,  
 ON UPSTREAM VELOCITY AND MODEL PLANFORM AREA  
 CH BONNET COEFFICIENT, NONDIMENSIONALIZED ON UPSTREAM VELOCITY, MODEL PLANFORM AREA, AND BEAM CHORD  
 L/D LIFT-TO-DRAG RATIO = CL/CDUNC  
 D/L DRAG-TO-LIFT RATIO = CDUNC/CL  
 RN REYNOLDS NUMBER, BASED ON BEAM CHORD

**EFFECTS OF WALL EFFECTS ON SUPERCAVITATING HYDROPOOLS OF PLATE SPAN**

**APPENDIX DATA CORRECTED FOR EFFECTS OF IMAGES OF TRAILING VORTICES SYSTEMS\***

Run No	Alpha <sup>†</sup>	Cl <sup>‡</sup>	Cd <sup>§</sup>	(D/L)	SIGC/AT <sup>¶</sup>	SIGC/AT <sup>  </sup>	CD/AT <sup>  </sup>	CH/AT <sup>  </sup>	SIGC	CAVTH <sup>  </sup>	CAVTH <sup>¶</sup>
S-11-0-1	11.13	0.721	0.122	0.107	0.169	3.155	3.031	3.710	0.613	0.589	0.73
S-11-0-2*	11.13	0.715	0.121	0.108	0.170	3.189	3.027	3.682	0.538	0.612	0.588
S-11-0-3	11.13	0.698	0.122	0.099	0.175	3.020	2.921	3.599	0.510	0.586	0.567
S-11-0-4*	11.13	0.693	0.122	0.096	0.175	3.013	2.897	3.566	0.492	0.585	0.563
S-11-0-5	11.12	0.658	0.120	0.089	0.185	2.783	2.669	3.392	3.192	0.456	0.540
S-11-0-6*	11.12	0.685	0.119	0.086	0.185	2.776	2.666	3.325	3.161	0.444	0.539
S-11-0-7	11.11	0.601	0.113	0.081	0.188	2.976	2.829	3.099	3.011	0.416	0.480
S-11-0-8*	11.11	0.589	0.113	0.077	0.192	2.499	2.455	3.080	3.014	0.398	0.484
S-11-0-9*	11.10	0.523	0.105	0.071	0.200	2.170	2.129	2.700	2.788	0.369	0.420
S-11-1-0	11.10	0.535	0.105	0.070	0.197	2.169	2.131	2.764	2.808	0.360	0.420
S-11-1-1*	11.08	0.453	0.095	0.063	0.210	1.781	1.746	2.383	2.583	0.325	0.345
S-11-1-2	11.08	0.441	0.092	0.060	0.210	1.799	1.747	2.278	2.473	0.319	0.348
S-11-1-3*	11.07	0.379	0.081	0.055	0.215	1.450	1.421	1.960	2.182	0.287	0.338
S-11-1-4*	11.07	0.367	0.079	0.051	0.215	1.430	1.404	1.900	2.119	0.266	0.274
S-11-1-5*	11.06	0.333	0.070	0.047	0.211	1.240	1.196	1.723	1.887	0.239	0.231
S-11-1-6	11.06	0.322*	0.069	0.048	0.216	1.241	1.221	1.664	1.846	0.230	0.236
S-11-1-7*	11.06	0.304	0.064	0.041	0.209	1.031	1.014	1.576	1.706	0.214	0.196
S-11-1-8	11.05	0.287	0.059	0.038	0.207	1.047	1.033	1.486	1.587	0.196	0.202
S-11-1-9*	11.05	0.295	0.060	0.036	0.203	1.025	0.994	1.530	1.609	0.187	0.192
S-11-1-10	11.05	0.274	0.056	0.033	0.205	0.815	0.787	1.420	1.513	0.173	0.152
S-11-1-11*	11.05	0.259	0.052	0.030	0.202	0.806	0.802	1.385	1.408	0.157	0.155
S-11-1-12	11.04	0.232	0.046	0.024	0.197	0.664	0.643	1.206	1.234	0.125	0.128
S-11-1-13*	11.04	0.229	0.037	0.021	0.204	0.683	0.605	1.168	1.257	0.108	0.132

**QUESTIONABLE**

UNLESS OTHERWISE INDICATED, ALL DATA ARE FOR:

1. SUPERCAVITATING FLOW.
2. BOTH STATIC PRESSURE TAPS OPEN.

**LEGEND**

- \* CM1 UPSTREAM STATIC PRESSURE TAP UTILIZED
- o ONLY DNSTREAM STATIC PRESSURE TAP UTILIZED
- PC PARTIALLY CAVITATING
- PC(TW) PARTIALLY CAVITATING (TAP WETTED)
- PW PULL WETTED
- AT (Alpha)<sup>†</sup> (TRB) ANGLE OF ATTACK, CORRECTED FOR EFFECTS OF IMAGES OF TRAILING VORTICES
- AT2 AT2 AT2 AT2 AT2
- SIGC CAVITATION NUMBER COMPUTED WITH MEASURED CAVITY PRESSURE
- SIGV CAVITATION NUMBER COMPUTED WITH CALCULATED VAPOR PRESSURE
- CD Drag Coefficient, CORRECTED FOR EFFECTS OF IMAGES OF TRAILING VORTICES
- (D/L) CORRECTED DRAG-TO-LIFT RATIO = CD/CL
- CAVTH CAVITY LENGTH MEASURED FROM MIDCHORD AT CENTROID POSITION, nondimensionalized on mean chord (OBTAINED PROB PHOTOPHGRPHS)

BIPHA LINES OF WALL EFFECTS ON SUPERCAVITATING HYDROPOILS OF FINITE SPAN

HYDROPOIL INPUT DATA

TR	TT	AREA	SPAN	BAC
77	69	10.0	5.0	2.01

ZERO READINGS AND TUNNEL TEMP BEFORE AND AFTER

SEASON	1-A	2-B	3-C	4-D
0. - 0.0	0.0	0.0	100.0	17.
0. - 10.0	0.0	0.0	99.3	98.9
CBLL LBS/CR (NORMAL/BAR)	0.1-0.10000	0.2-0.02090	0.3-0.04030	
TWIST= 7200.0	SHARP DIA.= 1.50IN	INPUT DATA AS RECEIVED		

RUN NO	BARO	S	81	S	82	S	83	PW	PW	PCAV
S-12.-0.1	1284.	-354.0		122.0		282.0		199.		66.
S-12.-0.2+	1281.	-356.0		121.5		282.0		199.		45.
S-12.-0.3	1286.	-332.0		120.6		279.0		187.		44.
S-12.-0.4	1287.	-312.0		119.8		275.0		178.		44.
S-12.-0.5	1286.	-286.0		119.0		266.0		165.		43.
S-12.-0.6	1286.	-260.0		118.4		257.0		158.		42.
S-12.-0.7	1289.	-230.0		117.6		242.0		141.		39.
S-12.-0.8	1288.	-206.0		116.9		232.0		130.		36.
S-12.-0.9	1289.	-192.0		115.9		223.0		119.		36.
S-12.-1.0	1279.	-170.0		115.3		211.0		110.		36.
S-12.-1.1	1287.	-158.0		114.4		203.0		103.		36.
S-12.-1.2+	1286.	-152.0		116.3		200.0		103.		36.
S-12.-1.3	1289.	-144.0		114.1		194.0		96.		37.
S-12.-1.4	1297.	-138.0		113.5		188.0		90.		39.
S-12.-1.5	1317.	-130.0		112.9		184.0		83.		39.
S-12.-1.6	1288.	-130.0		138.0		250.0		662.		—
S-12.-1.7	1281.	-182.0		115.9		219.0		118.		38.
S-12.-1.8	839.	-140.0		111.2		188.0		102.		38.
S-12.-1.9	420.	-78.0		106.2		148.0		91.		48.
S-12.-2.0	419.	-130.0		110.0		155.0		769.		—

LEGEND TR ROOM TEMPER (DEG FARN)

TT TUNNEL " ( " "

AREA HALF-SPAN MODEL PLATEAU AREA (SQ IN)

SPAN FOIL HALF-SPAN (IN)

BAC MEAN CHORD, MEAS. @ MODEL CENTROID (IN)

MANON VELOCITY MAJORANT BEARING (IN)

TWIST SHARP TWIST (DEGREES/IN-LB)

3 LOAD CELL POLARITY (N-NORMAL, P-REVERSE)

LOAD CELL

P1 LIPT (COUNTS)

P2 MOMENT (COUNTS)

PW DRAG (COUNTS)

PW STATIC PRESSURE (IN HG)

PCAV CAVITY PRESSURE (IN HG)

RUN NO Q-XXX-IV: Q-FOIL TESTED(S-SHALL, R-NMED,L-LARG)

III-GRADIENT ATTACK ANGLE (DEGREES)

IV-RUG BURDEN, THIS FOIL @ THIS ANGLE

**INPUT DATA CONCERNING FOR ZERO READINGS, SIGGS, AND DIROSTATIC PRESSURE**

INPUT DATA	RAISON	91	92	93	PIPE	PCAV
S-12--01	1286.	-346.0	-22.0	-182.0	186.	46.
S-12--02	1281.	-197.9	-21.5	-181.7	186.	45.
S-12--03	1286.	-323.8	-20.7	-178.4	172.	44.
S-12--04	1287.	-303.7	-19.9	-178.1	163.	44.
S-12--05	1286.	-275.6	-19.1	-164.7	150.	43.
S-12--06	1286.	-251.5	-18.6	-155.4	139.	42.
S-12--07	1289.	-221.4	-17.8	-160.1	126.	39.
S-12--08	1288.	-197.3	-17.2	-129.8	115.	36.
S-12--09	1283.	-163.2	-16.2	-120.5	108.	36.
S-12--10	1279.	-161.1	-15.6	-108.2	95.	36.
S-12--11	1287.	-148.9	-14.8	-99.8	88.	36.
S-12--12	1286.	-142.8	-14.7	-96.5	88.	36.
S-12--13	1289.	-138.7	-14.5	-90.2	81.	37.
S-12--14	1297.	-128.6	-14.0	-83.9	75.	39.
S-12--15	1317.	-120.5	-13.8	-79.6	66.	39.
S-12--16	1288.	-330.4	-34.6	-165.3	64.7.	—
S-12--17	1281.	-172.3	-16.5	-113.9	103.	38.
S-12--18	839.	-130.2	-11.8	-82.6	87.	38.
S-12--19	820.	-68.1	-6.9	-42.3	76.	40.
S-12--20	419.	-120.0	-10.7	-49.0	75.	—

SUPER JAWS OF HALL EFFECTS ON SUPERCAVITATING HYDROPOILS OF FINITE SPAN

••HYDROPOIL DATA SECTION••

TEST NO	ALPHA	LIFT-LB	BEND-LB	BOW-TAIL	VEL-PPS
S-12--01	12.00	35.06	7.33	8.28	26.60
S-12--02	12.00	35.24	7.32	8.10	26.57
S-12--03	12.00	32.81	7.19	7.78	26.62
S-12--04	12.00	30.78	7.01	7.89	26.63
S-12--05	12.00	27.96	6.64	7.20	26.62
S-12--06	12.00	25.54	6.26	6.99	26.62
S-12--07	12.00	22.51	5.65	6.70	26.65
S-12--08	12.00	20.00	5.23	6.85	26.64
S-12--09	12.00	18.65	4.86	6.69	26.59
S-12--10	12.00	16.43	4.36	5.88	26.55
S-12--11	12.00	15.20	4.02	5.56	26.63
S-12--12	12.00	14.59	3.89	5.53	26.62
S-12--13	12.00	13.78	3.64	5.87	26.65
S-12--14	12.00	13.16	3.38	5.26	26.73
S-12--15	12.00	12.33	3.21	5.05	26.92
S-12--16	12.00	33.76	5.85	13.00	26.68
S-12--17	12.00	17.58	4.59	6.20	26.57
S-12--18	12.00	13.27	3.33	4.45	21.82
S-12--19	12.00	6.95	1.71	2.58	15.82
S-12--20	12.00	12.22	1.97	4.03	15.80

LEGEND

V2L UPSTREAM VELOCITY (0)

**UPPER LIVES OF WALL EFFECTS ON SUPERCRITICAL WIND TUNNELS OF FINITE SPAN**

**\*\*TURBOPROP DATA IN NONDIMENSIONAL FORM (NO CORRECTIONS APPLIED) \*\***

SUB NO	ALPHA	CL	CDUNC	CL	CD	L/D	D/L	Bu* 1000-6
S-12--01	12.00	0.7380	0.1941	0.0667	5.1250	0.1951	0.3241	
S-12--02	12.00	0.7330	0.1941	0.0651	5.1609	0.1938	0.3235	
S-12--03	12.00	0.6901	0.1908	0.0614	4.9024	0.2040	0.3245	
S-12--04	12.00	0.6470	0.1370	0.0763	4.7226	0.2117	0.3267	
S-12--05	12.00	0.5880	0.1292	0.0754	4.5508	0.2197	0.3240	
S-12--06	12.00	0.5371	0.1213	0.0732	4.4271	0.2259	0.3245	
S-12--07	12.00	0.4724	0.1081	0.0700	4.3708	0.2288	0.3250	
S-12--08	12.00	0.4218	0.0974	0.0674	4.2423	0.2157	0.3249	
S-12--09	12.00	0.3932	0.0919	0.0639	4.2778	0.2138	0.3239	
S-12--10	12.00	0.3473	0.0817	0.0618	4.2507	0.2353	0.3231	
S-12--11	12.00	0.3195	0.0741	0.0581	4.3094	0.2320	0.3267	
S-12--12	12.00	0.3069	0.0714	0.0579	4.2984	0.2326	0.3245	
S-12--13	12.00	0.2891	0.0659	0.0571	4.3890	0.2276	0.3250	
S-12--14	12.00	0.2795	0.0601	0.0566	4.5648	0.2191	0.3266	
S-12--15	12.00	0.2537	0.0556	0.0517	4.5655	0.2190	0.3203	
S-12--16	12.00	0.2591	0.1125	0.1158	6.3016	0.1587	0.5249	
S-12--17	12.00	0.3710	0.0865	0.0651	4.2886	0.2332	0.5235	
S-12--18	12.00	0.4152	0.0935	0.0993	4.4412	0.2252	0.5100	
S-12--19	12.00	0.8141	0.0904	0.0765	4.5882	0.2181	0.3116	
S-12--20	12.00	0.7299	0.1067	0.1196	6.8414	0.1462	0.3113	

**LEGEND**

ALPHA GEOMETRIC ANGLE OF ATTACK CORRECTED FOR SHARP TRAIL  
 CL LIPT COEFFICIENT, nondimensionalized on upstream velocity and model planform area  
 CDUNC CD (uncorrected). THE UNCORRECTED DRAG COEFFICIENT AS COMPUTED FROM MEASURED DRAG,  
 ON UPSTREAM VELOCITY AND MODEL PLANFORM AREA  
 CR NONDIM COEFFICIENT, nondimensionalized on upstream velocity, model planform area, and chord  
 L/D LIPT-TO-DRAG RATIO = CL/CDUNC  
 D/L DRAG-TO-LIPT RATIO = CDUNC/CL  
 Bu AIRFOIL NUMBER, BASED ON REYNOLDS NUMBER, BASED ON REYNOLDS CHORD

**RIPPLE INLET OF WALL EFFECTS ON SUPERCAVITATING HYDROFOILS OF FINITE SPAN**

**APPENDIX DATA CORRECTED FOR EFFECTS OF IMAGES OF TRAILING VORTEX SYSTEM\***

RUN NO.	ALPHAT	CL	CD	CH	(D/L)		SIGC/AT	SIGC	CL/AT	CD/AT	CH/AT	SIGC	CAVLT	COMMENTS/REMARKS
					0.087	0.197	2.894	2.661						
S-12-0-1	12.13	0.738	0.146	0.087	0.197	2.894	2.661	3.250	0.409	0.613	0.564	0.82	---	
S-12-0-2*	12.13	0.738	0.146	0.085	0.196	2.897	2.666	3.512	3.252	0.402	0.614	0.569	---	
S-12-0-3	12.13	0.690	0.142	0.081	0.206	2.657	2.467	3.261	3.176	0.395	0.562	0.522	0.91	
S-12-0-4	12.12	0.687	0.138	0.078	0.210	2.481	2.293	3.059	3.092	0.370	0.525	0.495	0.92	
S-12-0-5	12.11	0.588	0.130	0.075	0.222	2.233	2.066	2.783	2.918	0.357	0.672	0.437	1.00	
S-12-0-6	12.10	0.537	0.122	0.073	0.228	2.020	1.875	2.283	2.781	0.346	0.927	0.396	1.10	
S-12-0-7	12.09	0.472	0.109	0.070	0.230	1.766	1.680	2.239	2.845	0.322	0.372	0.354	1.30	
S-12-0-8	12.08	0.422	0.100	0.067	0.237	1.554	1.529	2.001	2.251	0.220	0.228	0.322	1.47	
S-12-0-9	12.07	0.393	0.092	0.064	0.235	1.385	1.322	1.866	2.081	0.191	0.281	0.279	1.80	
S-12-1-0	12.06	0.347	0.082	0.062	0.236	1.173	1.152	1.650	1.852	0.194	0.247	0.243	2.40	
S-12-1-1	12.06	0.320	0.078	0.058	0.233	1.029	1.011	1.518	1.681	0.276	0.217	0.213	2.50	
S-12-1-2*	12.06	0.307	0.072	0.058	0.234	1.028	1.012	1.458	1.619	0.275	0.216	0.213	2.50	
S-12-1-3	12.05	0.289	0.066	0.057	0.229	0.889	0.855	1.370	1.895	0.272	0.187	0.180	3.87	
S-12-1-4	12.05	0.278	0.060	0.055	0.220	0.767	0.697	1.305	1.365	0.260	0.161	0.147	4.30	
S-12-1-5	12.05	0.254	0.056	0.052	0.210	0.621	0.555	1.207	1.262	0.246	0.131	0.117	6.30	
S-12-1-6	12.13	0.709	0.114	0.136	0.161	----	----	3.389	2.586	0.682	----	----	----	
S-12-1-7	12.07	0.371	0.087	0.065	0.234	1.310	1.266	1.761	1.960	0.369	0.276	0.267	----	
S-12-1-8	12.08	0.415	0.094	0.069	0.226	1.478	1.417	1.970	2.117	0.329	0.312	0.299	1.50	
S-12-1-9	12.08	0.414	0.091	0.077	0.219	2.207	1.549	1.966	2.047	0.363	0.465	0.327	1.65	
S-12-1-20	12.13	0.730	0.108	0.120	0.148	----	----	3.467	2.417	0.565	----	----	----	

UNLESS OTHERWISE INDICATED, ALL DATA ARE FOR:

1. SUPERCAVITATING FLOW.
2. BOTH STATIC PRESSURE TAPS OPEN.

**LEGEND**

- \* ONLY UPSTREAM STATIC PRESSURE TAP UTILIZED
- ONLY DOWNTREAM STATIC PRESSURE TAP UTILIZED
- PC PARTIALLY CAVITATING
- PC(?) PARTIALLY CAVITATING (TAP WETTED)
- PW PULLY WETTED

AT (ALPHAT) (TRUE) ANGLE OF ATTACK, CORRECTED FOR EFFECTS OF IMAGES OF TRAILING VORTICES

AT2 ALPHAT+0.2

SIGC CAVITATION NUMBER COMPUTED WITH MEASURED CAVITY PRESSURE

SIGV CAVITATION NUMBER COMPUTED WITH CALCULATED VAPOR PRESSURE

CD DRAG COEFFICIENT, CORRECTED FOR EFFECTS OF IMAGES OF TRAILING VORTICES

(D/L) CORRECTED DRAG-TO-LIFT RATIO = CD/CL

CAVLT CAVITY LENGTH MEASURED FROM MIDCHORD AT CENTROID POSITION, NORMALIZED ON REAR CHORD  
(OBTAINED FROM PHOTOGRAPHS)

EXPERIMENTS OF WALL EFFECTS ON SUPERCAVITATING HYDROFOILS OF FINITE SPAN

HYDROFOIL INPUT DATA

TT	TT AREA	SPAN	BAC
77	92	10.0	5.0

ZERO STABILITIES AND TUNNEL TESTS BEFORE AND AFTER  
 BARON 1-8 1-8 2-8 2-8 3-8 3-8 TT  
 0. 0.0 0.0 0.0 100.0 0.0 100.0 20.0  
 0. -2.0 0.0 0.0 100.0 0.0 100.0 93.0  
 CAV. LOSS/ACT.(NORMAL/NET) 8=0.10000 82=0.02000 83=0.04000  
 THISP-7200.0 SWIFT DIA.= 1.50 IN  
 OUTPUT DATA AS RECORDINGS

NUM	BARON	S	81	S	82	S	83	PINPI	PCAV
S-18,-01	016.	-158.0	R	116.0	R	173.0	R	762.	---
S-18,-02	093.	-262.0	R	131.0	R	235.0	R	707.	---
S-18,-03	1376.	-418.0	R	148.0	R	300.0	R	655.	---
S-18,-04	1361.	-484.0	R	149.0	R	300.0	R	325.	---
S-18,-05	1351.	-660.0	R	142.0	R	325.0	R	297.	---
S-18,-06	1368.	-460.0	R	132.0	R	350.0	R	265.	73.
S-18,-07	1357.	-432.0	R	127.6	R	349.0	R	242.	61.
S-18,-08	1328.	-400.0	R	125.2	R	343.0	R	224.	56.
S-18,-09	1322.	-358.0	R	123.5	R	332.0	R	204.	52.
S-18,-10	1322.	-324.0	R	122.3	R	319.0	R	188.	50.
S-18,-11	1319.	-290.0	R	121.2	R	300.0	R	172.	48.
S-18,-12*	1316.	-288.0	R	121.2	R	300.0	R	172.	48.
S-18,-13	1313.	-262.0	R	120.4	R	287.0	R	159.	45.
S-18,-14	1312.	-230.0	R	119.5	R	216.0	R	163.	41.
S-18,-15	1309.	-208.0	R	118.2	R	256.0	R	130.	40.
S-18,-16	1309.	-190.0	R	117.9	R	248.0	R	121.	40.
S-18,-17	1304.	-172.0	R	117.0	R	231.0	R	109.	40.
S-18,-18*	1302.	-164.0	R	116.0	R	223.0	R	109.	40.
S-18,-19	1301.	-158.0	R	116.0	R	217.0	R	101.	40.
S-18,-20	1308.	-146.0	R	115.5	R	207.0	R	94.	30.
S-18,-21	1316.	-138.0	R	115.0	R	200.0	R	87.	40.
S-18,-22	1300.	-266.0	R	120.1	R	276.0	R	151.	44.
S-18,-23	070.	-176.0	R	116.1	R	223.0	R	126.	47.
S-18,-24	694.	-130.0	R	111.1	R	188.0	R	105.	42.
S-18,-25	450.	-82.0	R	107.6	R	155.0	R	89.	42.
LEGEND	TT ROOM TEMPS (DEG FARS)	"	"	"	"	"	"	"	"
	TT TUNNEL "	"	"	"	"	"	"	"	"
	AREA HALF-SPAN MODEL PLATEFORM AREA (50 IN)								
	SPAN FOIL HALF-SPAN (IN)								
	BAC BACH CHORD, FEET. A MODEL CHORD (IN)								
	BARON VELOCITY BAROMETER READING (INH)								
	TWIST SPUR TWIST (DEGREES/IN-LB)								
	S LOAD CELL POLARITIES (+-FORWARD, -+REVVERSE)								

LOAD CELL #1 LIFT (COUNTS)  
 #2 MOUNT ABOUT MIDCHORD (COUNTS)  
 #3 DRAG (COUNTS)  
 PUMP STATIC PRESSURE (MM HG)  
 PUMP CAVITY PRESSURE (MM HG)  
 RUN NO Q-III-II: Q=FOIL TESTED(S-SHALL, H-MED, L-LARGE)  
 III-COORDINATE ATTACK ANGLE (DEGREES)  
 II-BUS NUMBERS, THIS POLE @ THIS ANGLE

**INPUT LINES OF WALL SUPPORTS OR SUPERCAVITATING HYDROPOLES OF FINITE SPAN**

INPUT DATA CONNECTED FOR ZERO BRANCHES, SIZES, AND HYDROSTATIC PRESSURE					
RUN NO	SIZE	01	02	03	PINP
S-10--01	076.	-350.0	-16.0	-73.0	787.
S-10--02	093.	-261.9	-31.9	-135.0	692.
S-10--03	1376.	-617.8	-16.0	-200.0	310.
S-10--04	1361.	-653.7	-46.9	-200.0	310.
S-10--05	1351.	-659.7	-41.9	-225.0	282.
S-10--06	1360.	-659.6	-31.9	-250.0	250.
S-10--07	1337.	-631.5	-27.5	-248.0	227.
S-10--08	1326.	-399.8	-25.1	-243.0	209.
S-10--09	1323.	-357.3	-23.4	-232.0	189.
S-10--10	1326.	-323.2	-22.1	-219.0	173.
S-10--11	1319.	-289.2	-21.0	-200.0	157.
S-10--12	1316.	-285.1	-21.0	-200.0	157.
S-10--13	1313.	-261.0	-20.2	-187.0	144.
S-10--14	1312.	-228.9	-19.3	-170.0	128.
S-10--15	1309.	-202.6	-18.0	-156.0	115.
S-10--16	1309.	-186.7	-17.6	-144.0	106.
S-10--17	1308.	-170.7	-16.5	-131.0	94.
S-10--18	1302.	-162.6	-16.5	-123.0	90.
S-10--19	1301.	-156.5	-15.7	-117.0	86.
S-10--20	1308.	-164.4	-15.2	-107.0	79.
S-10--21	1334.	-136.3	-14.7	-100.0	72.
S-10--22	1300.	-244.2	-19.8	-176.0	136.
S-10--23	070.	-172.2	-13.7	-123.0	111.
S-10--24	694.	-126.1	-10.7	-88.0	90.
S-10--25	450.	-80.0	-7.2	-55.0	74.

SUPER INLES OF WALL EFFECTS ON SUPERCAVITATING HYDROFOILS OF FINITE SPAN

**HYDROFOIL DATA SECTION**

SUB NO.	ALPHA	LIFT-LB	DRAG-LB	HOB-INLES	VBL-PPS
S-18--01	18.00	16.13	2.98	6.02	16.77
S-18--02	18.00	28.44	5.44	11.66	22.67
S-18--03	18.00	32.79	8.06	18.05	27.58
S-18--04	18.00	45.40	8.06	18.41	27.34
S-18--05	18.00	96.84	9.07	15.78	27.28
S-18--06	18.00	86.63	10.07	12.01	27.21
S-18--07	18.00	63.72	9.99	10.35	27.11
S-18--08	18.00	80.47	9.79	9.44	27.03
S-18--09	18.00	36.22	9.35	6.79	26.98
S-18--10	18.00	32.79	8.83	8.33	26.99
S-18--11	18.00	29.36	8.06	7.91	26.94
S-18--12	18.00	28.95	8.06	7.91	26.91
S-18--13	18.00	26.52	7.54	7.60	26.88
S-18--14	18.00	23.29	6.85	7.25	26.87
S-18--15	18.00	20.66	6.29	6.76	26.85
S-18--16	18.00	19.24	5.80	6.64	26.85
S-18--17	18.00	17.42	5.28	6.30	26.80
S-18--18	18.00	16.60	4.96	6.21	26.78
S-18--19	18.00	15.38	4.72	5.91	26.77
S-18--20	18.00	18.76	6.31	5.71	26.88
S-18--21	18.00	13.94	4.03	5.52	27.08
S-18--22	18.00	26.84	7.09	7.43	26.76
S-18--23	18.00	17.50	4.96	5.17	22.20
S-18--24	18.00	13.03	3.55	3.03	19.98
S-18--25	18.00	8.15	2.22	2.71	16.34

LEGEND

VBL UPSTREAM VELOCITY (ft)

**LIFTER LINES OF HULL EFFECTS ON SUPERCAVITATING HISTOPOILS OF FINITE SPAN**

**HISTOPOIL DATA IN HOMOGENEOUS FLUID (NO CORRECTIONS APPLIED)**

BLN NO	ALPHA	CL	CD0BC	CH	L/D	D/L	Re=1000-6
S-14,-01	14.00	0.4556	0.1449	0.1588	5.7000	0.1690	0.387
S-14,-02	14.00	0.4516	0.1500	0.1712	5.6766	0.1762	0.4530
S-14,-03	14.00	0.4459	0.1480	0.1773	5.6779	0.1761	0.5549
S-14,-04	14.00	0.4058	0.1505	0.1828	6.0197	0.1661	0.5521
S-14,-05	14.00	0.39410	0.1718	0.1977	5.4772	0.1826	0.5502
S-14,-06	14.00	0.39386	0.1925	0.1203	6.8767	0.2051	0.5497
S-14,-07	14.00	0.38869	0.1924	0.104	6.6104	0.2169	0.5476
S-14,-08	14.00	0.38260	0.1895	0.0958	6.3580	0.2295	0.5459
S-14,-09	14.00	0.37420	0.1812	0.0896	6.0957	0.2442	0.5449
S-14,-10	14.00	0.37412	0.1703	0.0849	3.9411	0.2537	0.5451
S-14,-11	14.00	0.36030	0.1552	0.0809	3.8854	0.2578	0.5481
S-14,-12	14.00	0.35959	0.1556	0.0610	3.8308	0.2610	0.5436
S-14,-13	14.00	0.35871	0.1951	0.0780	3.7708	0.2652	0.5430
S-14,-14	14.00	0.4809	0.1311	0.0745	3.6691	0.2725	0.5428
S-14,-15	14.00	0.4274	0.1197	0.0696	3.5707	0.2801	0.5422
S-14,-16	14.00	0.3981	0.1097	0.0683	3.6296	0.2755	0.5422
S-14,-17	14.00	0.3616	0.0992	0.0650	3.6838	0.2744	0.5412
S-14,-18	14.00	0.3452	0.0927	0.0643	3.7244	0.2685	0.5409
S-14,-19	14.00	0.3324	0.0877	0.0611	3.7894	0.2639	0.5407
S-14,-20	14.00	0.3056	0.0789	0.0588	3.8725	0.2582	0.5420
S-14,-21	14.00	0.2834	0.0716	0.0558	3.9596	0.2526	0.5470
S-14,-22	14.00	0.5172	0.1373	0.0770	3.7664	0.2655	0.5405
S-14,-23	14.00	0.5296	0.1393	0.0778	3.8012	0.2631	0.4884
S-14,-24	14.00	0.4866	0.1216	0.0749	4.0017	0.2499	0.4036
S-14,-25	14.00	0.4554	0.1127	0.0753	4.0403	0.2475	0.3299

**LEGEND**

ALPHA GEOMETRIC ANGLE OF ATTACK CORRECTED FOR SEAPLANE TWIST  
 CL LIFT COEFFICIENT, HOMOGENEIZED ON UPSTREAM VELOCITY AND MODEL PLATEFORM AREA  
 CD0BC CD (UNCORRECTED), THE UNCORRECTED DRAG COEFFICIENT AS COMPUTED FROM MEASURED DRAG,  
 ON UPSTREAM VELOCITY AND MODEL PLATEFORM AREA  
 CH HORNET COEFFICIENT, HOMOGENEIZED ON UPSTREAM VELOCITY, MODEL PLATEFORM AREA, AND REYNOLDS NUMBER  
 L/D LIFT-TO-DRAG RATIO = CL/CD0BC  
 D/L DRAG-TO-LIFT RATIO = CD0BC/CL  
 BL REYNOLDS NUMBER, BASED ON REYNOLDS CHORD

BIGE LINES OF WALL EFFECTS ON SUPERCAVITATING HYDROFOILS OF FINITE SPAN

**\*\*PRIOR DATA CORRECTED FOR EFFECTS OF TRAILING VORTEX SYSTEM\***

RUN NO.	ALPHAT	CL	CD	CH	(D/L)		SIGV/AT	SIGC/AT	CD/AT2	CH/AT	SIGV	SIGC	CAVLT	COMENTS/MARKS
					CL/AT	CH/AT	SIGV/AT	SIGC/AT	CD/AT2	CH/AT	SIGV	SIGC	CAVLT	COMENTS/MARKS
S-14,-01	14.-16	0.856	0.167	0.159	0.172	-----	3.463	2.012	0.683	-----	-----	-----	-----	-----
S-14,-02	14.-16	0.852	0.152	0.171	0.179	-----	3.467	2.095	0.693	-----	-----	-----	-----	-----
S-14,-03	14.-16	0.865	0.151	0.177	0.179	-----	3.420	2.876	0.718	-----	-----	-----	-----	-----
S-14,-04	14.-17	0.906	0.153	0.183	0.169	-----	3.663	2.504	0.739	-----	-----	-----	-----	PC (TV)
S-14,-05	14.-17	0.941	0.175	0.158	0.186	-----	3.804	2.654	0.637	-----	-----	-----	-----	PC (TV)
S-14,-06	14.-17	0.939	0.195	0.120	0.208	3.161	2.792	3.795	3.192	0.486	0.811	0.690	0.72	
S-14,-07	14.-16	0.837	0.195	0.104	0.220	3.022	2.640	3.588	0.422	0.747	0.653	0.78		
S-14,-08	14.-15	0.526	0.192	0.096	0.232	2.753	2.851	3.385	3.183	0.380	0.680	0.605	0.88	
S-14,-09	14.-14	0.782	0.183	0.090	0.246	2.442	2.205	3.005	0.163	0.003	0.584	0.91		
S-14,-10	14.-12	0.671	0.172	0.085	0.256	2.184	1.981	2.723	2.827	0.248	0.318	0.488	1.03	
S-14,-11	14.-11	0.603	0.156	0.081	0.259	1.933	1.764	2.449	2.578	0.228	0.376	0.434	1.30	
S-14,-12*	14.-11	0.596	0.157	0.081	0.263	1.935	1.768	2.420	2.584	0.329	0.476	0.435	1.30	
S-14,-13	14.-10	0.547	0.146	0.078	0.267	1.727	1.611	2.223	2.412	0.317	0.425	0.396	1.40	
S-14,-14	14.-09	0.481	0.142	0.075	0.274	1.467	1.418	1.956	2.180	0.303	0.361	0.349	1.65	
S-14,-15	14.-08	0.427	0.120	0.070	0.281	1.257	1.227	1.739	1.992	0.283	0.309	0.301	1.80	
S-14,-16	14.-07	0.398	0.110	0.068	0.277	1.109	1.081	1.621	1.826	0.278	0.272	0.265	2.18	
S-14,-17	14.-07	0.362	0.106	0.065	0.276	0.915	0.889	1.473	1.653	0.265	0.225	0.218	2.60	
S-14,-18*	14.-06	0.345	0.093	0.064	0.270	0.914	0.890	1.406	1.545	0.262	0.224	0.219	2.60	
S-14,-19	14.-06	0.332	0.088	0.061	0.265	0.781	0.760	1.355	1.463	0.192	0.186	0.186	4.10	
S-14,-20	14.-06	0.306	0.079	0.059	0.259	0.660	0.642	1.246	1.316	0.240	0.162	0.158	4.80	
S-14,-21	14.-05	0.283	0.072	0.056	0.253	0.534	0.518	1.155	1.198	0.228	0.131	0.127	6.40	
S-14,-22	14.-09	0.517	0.138	0.077	0.267	1.591	1.512	2.102	2.283	0.313	0.391	0.372	-----	
S-14,-23	14.-10	0.530	0.140	0.078	0.265	1.713	1.602	2.153	2.316	0.316	0.421	0.398	1.40	
S-14,-24	14.-09	0.487	0.122	0.075	0.251	1.494	1.420	1.979	2.028	0.305	0.367	0.349	1.55	
S-14,-25	14.-08	0.455	0.113	0.075	0.249	1.526	1.422	1.853	1.877	0.306	0.375	0.349	1.50	

UNLESS OTHERWISE INDICATED, ALL DATA ARE FOR:

1. SUPERCAVITATING FLOW.
2. BOTH STATIC PRESSURE TAPS OPEN.

LEGEND

- \* ONLY UPSTREAM STATIC PRESSURE TAP UTILIZED
- o ONLY DOWNSTREAM STATIC PRESSURE TAP UTILIZED
- PC PARTIALLY CAVITATING
- PC(TV) PARTIALLY CAVITATING (TAP BOTTED)
- PW FULLY BOTTED
- AT (ALPHAT) (TRUE) ANGLE OF ATTACK, CORRECTED FOR EFFECTS OF IMAGES OF TRAILING VORTICES
- AT2 ALPHAT\*\*2
- SIGC CAVITATION NUMBER COMPUTED WITH MEASURED CAVITY PRESSURE
- SIGV CAVITATION NUMBER COMPUTED WITH CALCULATED VAPOR PRESSURE
- CD DRAG COEFFICIENT, CORRECTED FOR EFFECTS OF IMAGES OF TRAILING VORTICES
- (D/L) CORRECTED DRAG-TO-LIFT RATIO = CD/CL
- CAVLT CAVITY LENGTH MEASURED FROM MIDCHORD AT CENTROID POSITION. NONDIMENSIONALIZED ON MEAN CHORD  
(OBTAINED FROM PHOTOGRAPHS)

**INPUT DATA OF WALL EFFECTS ON SURFACEVITATING HYDROPOLES OF PLATE SPAN**

HYDROPOLE INPUT DATA  
 TT AREA SPAN MAC  
 77 9.3 10.0 5.0 2.01

**ZERO BRAIDINGS AND TUBEUL TRSF BEFORE AND AFTER**

RABON 1-8 1-8 2-8 2-8 3-8 3-8 TT  
 0. 0.0 0.0 0.0 100.0 0.0 100.0 92.8  
 0. 0.0 0.0 0.0 99.4 0.0 106.0 94.0  
 CELL LBS/CF (NORMAL/REV) 01=0.10000 02=0.02090 03=0.04030  
 TWIST= 7200.0 SHAFT DIA.= 1.5018

**OUTPUT DATA AS RECORDED\***

RUN NO	RABON	S	61	62	63	PCAV	PINP
S-16.-01	1193.	-400.0	R 128.2	R 128.2	R 376.0	236.	72.
S-16.-02	1189.	-370.0	R 122.6	R 122.6	R 372.0	217.	64.
S-16.-03*	1190.	-362.0	R 122.4	R 122.4	R 368.0	216.	62.
S-16.-04	1189.	-360.0	R 121.8	R 121.8	R 357.0	201.	60.
S-16.-05	1188.	-318.0	R 121.1	R 121.1	R 348.0	192.	57.
S-16.-06	1186.	-300.0	R 120.6	R 120.6	R 337.0	182.	55.
S-16.-07	1188.	-284.0	R 119.7	R 119.7	R 330.0	174.	53.
S-16.-08	1183.	-262.0	R 119.5	R 119.5	R 318.0	163.	50.
S-16.-09	1184.	-242.0	R 118.9	R 118.9	R 307.0	153.	46.
S-16.-10	1180.	-224.0	R 117.9	R 117.9	R 294.0	143.	44.
S-16.-11*	1181.	-220.0	R 118.0	R 118.0	R 291.0	143.	44.
S-16.-12	1178.	-202.0	R 117.1	R 117.1	R 278.0	131.	43.
S-16.-13	1179.	-184.0	R 116.4	R 116.4	R 261.0	119.	42.
S-16.-14	1176.	-168.0	R 115.9	R 115.9	R 248.0	109.	42.
S-16.-15	1172.	-158.0	R 115.2	R 115.2	R 237.0	102.	42.
S-16.-16	1181.	-146.0	R 114.6	R 114.6	R 225.0	92.	42.
S-16.-17	1195.	-138.0	R 113.9	R 113.9	R 219.0	88.	42.
S-16.-18	721.	-130.0	R 110.9	R 110.9	R 212.0	105.	42.
S-16.-19	485.	-110.0	R 108.4	R 108.4	R 188.0	100.	43.

LEGEND TR BOOM TAPER (DEG PAHR)

TT TUBEUL " ( " " )

AREA HALF-SPAN MODEL PLATFORM AREA (SQ IN)

SPAN FOIL HALF-SPAN (IN)

BAC BEAM CHORD, MEAS. A MODEL CENTROID (IN)

RABON VELOCITY METER/TER RADING (MM)

TWIST SHAFT TWIST (DEGREES/IN-LB)

S LOAD CELL POLARITY (R-NORMAL, R-VERSE)

LOAD CELL 61 LIFT (COUNTS)

62 ROTAT ABOUT HICHOORD (COUNTS)

63 DRAG (COUNTS)

PUMP STATIC PRESSURE (MM HG)

PCAV CAVITY PRESSURE (MM HG)

RUN NO Q-III-KIV: Q=FOIL TESTED (S=SMALL, R=MD,L=LARGE)  
 KIV=GEOMETRIC ATTACK ANGLE (DEGREES)  
 IV=RUN NUMBER, THIS FOIL A THIS ANGLE

INPUT DATA CONNECTED FOR ZERO DRAWINGS, SIGNS, AND HYDROSTATIC PRESSURE

BURN NO	MANOM	61	62	63	PINP	PCAV
S-16.-01	1193.	-400.0	-25.2	-276.0	221.	72.
S-16.-02	1195.	-370.0	-21.6	-271.8	202.	64.
S-16.-03	1199.	-362.0	-22.5	-267.6	201.	62.
S-16.-04	1199.	-360.0	-21.9	-255.3	166.	60.
S-16.-05	1198.	-318.0	-21.2	-287.1	177.	57.
S-16.-06	1196.	-300.0	-20.8	-235.9	167.	55.
S-16.-07	1196.	-284.0	-19.9	-228.7	159.	53.
S-16.-08	1183.	-262.0	-19.7	-216.4	148.	50.
S-16.-09	1184.	-242.0	-19.2	-205.2	138.	46.
S-16.-10	1180.	-228.0	-18.2	-192.0	128.	46.
S-16.-11	1181.	-220.0	-16.3	-188.6	128.	44.
S-16.-12	1178.	-202.0	-17.5	-175.6	116.	43.
S-16.-13	1179.	-184.0	-16.8	-158.3	104.	42.
S-16.-14	1176.	-168.0	-16.3	-145.1	94.	42.
S-16.-15	1172.	-158.0	-15.7	-133.9	87.	42.
S-16.-16	1181.	-146.0	-15.1	-121.7	77.	42.
S-16.-17	1195.	-138.0	-14.4	-115.4	73.	42.
S-16.-18	721.	-130.0	-11.5	-108.2	90.	42.
S-16.-19	485.	-110.0	-9.0	-86.0	85.	43.

## EFFECTS OF WALL EFFECTS ON SUPERCAVITATING HYDROPOILS OF FINITE SPAN

## HYDROPOIL DATA REDUCTION

BUS NO	ALPHA	LIFT-LB	DRAG-LB	NON-THLB VEL-PPS
S-16-01	16.00	90.51	11.12	9.10
S-16-02	16.00	37.67	10.95	6.51
S-16-03	16.00	36.67	10.78	6.95
S-16-04	16.00	34.46	10.33	6.24
S-16-05	16.00	32.28	9.96	7.99
S-16-06	16.00	30.43	9.51	7.81
S-16-07	16.00	28.62	9.22	7.49
S-16-08	16.00	26.61	8.72	7.42
S-16-09	16.00	24.60	8.27	7.21
S-16-10	16.00	22.78	7.74	6.85
S-16-11	16.00	22.38	7.61	6.90
S-16-12	16.00	20.57	7.07	6.57
S-16-13	16.00	18.75	6.38	6.32
S-16-14	16.00	17.19	5.85	6.14
S-16-15	16.00	16.13	5.40	5.89
S-16-16	16.00	14.92	4.90	5.68
S-16-17	16.00	14.10	4.65	5.43
S-16-18	16.00	13.24	4.35	4.31
S-16-19	16.00	11.19	3.39	3.39

## LEGEND

VEL UPSTREAM VELOCITY (U)

SUPER INLES OF WALL EFFECTS ON SUPERCAVITATING HYDROFOILS OF FINITE SPAN

HYDROFOIL DATA IN NONDIMENSIONAL FORM (NO CORRECTIONS APPLIED)

RUN NO.	ALPHA	CL	CD <sub>UC</sub>	CH	L/D	D/L	R <sub>IN</sub> (10 <sup>6</sup> )
S-16-01	16.00	0.9136	0.2404	0.1022	3.7995	0.2632	0.5235
S-16-02	16.00	0.8478	0.2374	0.0958	3.5716	0.2900	0.5226
S-16-03	16.00	0.8220	0.2333	0.0951	3.5528	0.2615	0.5228
S-16-04	16.00	0.7796	0.2233	0.0927	3.4913	0.2864	0.5226
S-16-05	16.00	0.7301	0.2151	0.0900	3.3967	0.2946	0.5224
S-16-06	16.00	0.6902	0.2052	0.0881	3.3681	0.2373	0.5220
S-16-07	16.00	0.6525	0.1982	0.0843	3.2914	0.3338	0.5224
S-16-08	16.00	0.6019	0.1879	0.0840	3.2203	0.3105	0.5219
S-16-09	16.00	0.5588	0.1774	0.0815	3.1493	0.3175	0.5216
S-16-10	16.00	0.5191	0.1659	0.0776	3.1292	0.3196	0.5208
S-16-11	16.00	0.5096	0.1628	0.0781	3.1306	0.3198	0.5210
S-16-12	16.00	0.4693	0.1510	0.0746	3.1075	0.3218	0.5204
S-16-13	15.00	0.4276	0.1351	0.0717	3.1656	0.3159	0.5206
S-16-14	15.00	0.3918	0.1232	0.0699	3.1793	0.3145	0.5200
S-16-15	15.00	0.3698	0.1133	0.0672	3.2662	0.3064	0.5192
S-16-16	15.00	0.3396	0.1012	0.0683	3.3555	0.2980	0.5210
S-16-17	15.00	0.3176	0.0943	0.0608	3.3658	0.2971	0.5239
S-16-18	15.00	0.4771	0.1454	0.0773	3.2591	0.3068	0.5191
S-16-19	15.00	0.5831	0.1654	0.0878	3.5261	0.2836	0.3444

LEGEND

ALPHA GEOMETRIC ANGLE OF ATTACK CORRECTED FOR SNAPT TWIST  
 CL LIFT COEFFICIENT, NONDIMENSIONALIZED ON UPSTREAM VELOCITY AND MODEL PLANFORM AREA  
 CD<sub>UC</sub> CE (UNCORRECTED). THE UNCORRECTED DRAG COEFFICIENT AS COMPUTED FROM MEASURED DRAG, AND NONDIMENSIONALIZED  
 ON UPSTREAM VELOCITY AND MODEL PLANFORM AREA  
 CH COEFFICIENT, NONDIMENSIONALIZED ON UPSTREAM VELOCITY, MODEL PLANFORM AREA, AND STEM CHORD  
 L/D LIFT-TO-DRAG RATIO = CL/CD<sub>UC</sub>  
 D/L DRAG-TO-LIFT RATIO = CD<sub>UC</sub>/CL  
 R<sub>IN</sub> REYNOLDS NUMBER, BASED ON STEM CHORD

**RISER LEVES OF WALL EFFECTS ON SUPERCAVITATING HYDROPOOLS OF PINTLE SPAN**

**SECTION DATA CORRECTED FOR EFFECTS OF IMAGES OF TRAILING VORTEX SYSTEM\***

RUN NO	ALPHAT	CL	CD	CN	(D/L)	SIGC/AT	SIGV/AT	CL/AT	CD/AT2	CH/AT	SIGV	SIGC	CAVITH	COMMENTS/REMARKS
S-16--01	16.17	0.918	0.243	0.162	0.266	2.813	2.309	3.238	3.053	0.362	0.798	0.651	0.88	
S-16--02	16.15	0.968	0.280	0.096	0.281	2.520	2.187	3.007	3.015	0.340	0.713	0.605	0.90	
S-16--03*	16.15	0.929	0.225	0.095	0.284	2.509	2.161	2.941	2.964	0.337	0.707	0.609	---	
S-16--04	16.14	0.760	0.225	0.093	0.289	2.279	1.962	2.767	2.837	0.329	0.682	0.553	1.02	
S-16--05	16.13	0.730	0.217	0.090	0.297	2.140	1.872	2.593	2.734	0.320	0.603	0.527	1.09	
S-16--06	16.13	0.950	0.207	0.088	0.299	1.998	1.751	2.452	2.609	0.313	0.559	0.493	1.10	
S-16--07	16.12	0.952	0.200	0.088	0.306	1.655	2.319	2.522	0.300	0.523	0.466	1.30		
S-16--08	16.11	0.905	0.189	0.084	0.312	1.695	1.538	2.151	2.391	0.299	0.476	0.432	1.35	
S-16--09	16.10	0.559	0.178	0.081	0.319	1.536	1.463	1.968	2.259	0.290	0.432	0.406	1.58	
S-16--10	16.09	0.519	0.167	0.078	0.321	1.384	1.323	1.848	2.113	0.276	0.389	0.372	1.70	
S-16--11*	16.09	0.570	0.168	0.078	0.321	1.382	1.322	1.818	2.074	0.278	0.388	0.371	---	
S-16--12	16.09	0.969	0.152	0.075	0.323	1.196	1.153	1.672	1.925	0.266	0.336	0.329	2.10	
S-16--13	16.08	0.928	0.136	0.072	0.317	1.005	0.980	1.524	1.723	0.256	0.282	0.275	2.80	
S-16--14	16.07	0.392	0.128	0.070	0.316	0.869	0.825	1.397	1.572	0.249	0.238	0.231	3.20	
S-16--15	16.07	0.370	0.114	0.067	0.308	0.740	0.717	1.319	1.446	0.240	0.208	0.201	4.30	
S-16--16	16.06	0.340	0.102	0.064	0.299	0.577	0.555	1.211	1.292	0.230	0.162	0.156	6.00	
S-16--17	16.06	0.318	0.095	0.061	0.298	0.487	0.433	1.205	1.217	0.182	0.136	0.137	7.00	
S-16--18	16.09	0.677	0.147	0.077	0.308	1.230	1.200	1.699	1.866	0.275	0.345	0.337	2.10	
S-16--19	16.11	0.583	0.166	0.088	0.285	1.596	1.510	2.074	2.106	0.312	0.468	0.427	1.22	

UNLESS OTHERWISE INDICATED, ALL DATA ARE FOR:

1. SUPERCAVITATING FLOW.
2. BOTH STATIC PRESSURE TAPS OPEN.

- LEGEND
- + ONLY UPSTREAM STATIC PRESSURE TAP UTILIZED
  - ONLY DOWNSTREAM STATIC PRESSURE TAP UTILIZED
  - PC PARTIALLY CAVITATING (TAP WETTED)
  - PC(TW) PARTIALLY CAVITATING (TAP DRYED)
  - PW FULLY WETTED
- AT (ALPHAT) (TRUE) ANGLE OF ATTACK, CORRECTED FOR EFFECTS OF IMAGES OF TRAILING VORTEXES
- AT2 ALPHAT\*2
- SIGC CAVITATION NUMBER COMPUTED WITH MEASURED CAVITY PRESSURE
- SIGV CAVITATION NUMBER COMPUTED WITH CALCULATED VAPOR PRESSURE
- CD DRAG COEFFICIENT, CORRECTED FOR EFFECTS OF IMAGES OF TRAILING VORTEXES
- (D/L) CORRECTED DRAG-TO-LIFT RATIO = CD/CL
- CAVITH CAVITY LENGTH MEASURED FROM MIDCHORD AT CENTROID POSITION, NONDIMENSIONALIZED ON REAR CHORD  
(OBTAINED FROM PHOTOGRAPHS)

RESULTS OF WALL EFFECTS ON SUPERERUPTING HYDROFOILS OF FINITE SPAN

HYDROFOIL INPUT DATA

TR	TT	AREA	SPAN	HAC
78	92	10.0	5.0	2.01

ZERO READINGS AND TUNNEL TEST BEFORE AND AFTER

	TR	TT	AREA	SPAN	HAC	
AERON	1-1	1-1	2-8	2-8	3-1	3-1
0-	0.0	0.0	0.0	100.0	0.0	100.0
0.	0.0	0.0	0.0	100.0	0.0	91.0
CELL LEG/CT (BORNAL/BEV)	0-0	0.0	0.0	10000.0	0-0	93.0
TRUST- 7200.0	SHAPT DIA.-	1.5018				

INPUT DATA AS RECORDED

RUN NO	AERON	S	A1	S	A2	S	A3	PINN'	PCAV
5-18.-01	1455.	-562.0		R	131.9	R	508.0	310.	91.
5-18.-02*	1654.	-530.0		R	131.9	R	503.0	310.	89.
5-18.-03	1454.	-520.0		R	132.4	R	500.0	297.	86.
5-18.-04	1654.	-500.0		R	131.2	R	493.0	283.	79.
5-18.-05	1666.	-471.0		R	130.1	R	486.0	268.	75.
5-18.-06	1644.	-452.0		R	129.1	R	474.0	255.	71.
5-18.-07	1666.	-420.0		R	128.4	R	463.0	241.	67.
5-18.-08	1453.	-400.0		R	128.0	R	442.0	226.	
5-18.-09	1937.	-370.0		R	127.2	R	436.0	217.	59.
5-18.-10*	1638.	-322.0		R	127.1	R	420.0	217.	58.
5-18.-11	1435.	-351.0		R	126.7	R	418.0	204.	
5-18.-12	1630.	-336.0		R	126.0	R	406.0	193.	52.
5-18.-13	1427.	-316.0		R	125.3	R	392.0	183.	47.
5-18.-14	1625.	-290.0		R	124.9	R	377.0	170.	46.
5-18.-15	1421.	-276.0		R	124.0	R	362.0	158.	43.
5-18.-16	1617.	-256.0		R	123.1	R	348.0	146.	
5-18.-17*	1618.	-250.0		R	123.0	R	337.0	195.	40.
5-18.-18	1415.	-249.0		R	122.5	R	331.0	139.	40.
5-18.-19	1610.	-226.0		R	122.0	R	313.0	129.	
5-18.-20	1404.	-214.0		R	121.1	R	300.0	120.	40.
5-18.-21*	1401.	-209.0		R	121.0	R	297.0	119.	
5-18.-22	1399.	-200.0		R	120.5	R	285.0	110.	40.
5-18.-23	1406.	-184.0		R	119.2	R	269.0	98.	40.
5-18.-24	1606.	-178.0		R	118.9	R	263.0	96.	40.
5-18.-25	1423.	-172.0		R	118.4	R	257.0	87.	
5-18.-26	1408.	-166.0		R	117.9	R	250.0	79.	40.
5-18.-27	845.	-212.0		R	117.0	R	286.0	148.	46.
5-18.-28	643.	-186.0		R	113.9	R	252.0	137.	

LEGEND TR ROOM TRAPPER (DEG PARM)

TT TUNNEL " "

AREA HALF-SPAN BODY PLATFORM AREA (SQ IN)

SPAN FOIL HALF-SPAN (IN)

HAC REAL CHORD, MEAS. A MODEL CENTROID (IN)

BIGON VELOCITY MACHINERY READING (MM)

TRUST SHAPT 100% (DEGREES/IN-LB)

S LOAD CELL POLARITY (N-NORMAL, P-REVERSE)

LOAD CELL 1 LIFT (COUNTS)  
LOAD CELL 2 BOWING ABOUT MIDCHORD (COUNTS)

03 DRAG (COUNTS)

PINP STATIC PRESSURE (MM HG)

PCAV CAVITY PRESSURE (MM HG)

RUN NO Q-XXX-Y: Q=FOIL TESTED(S-SHALL, B-BUD, L-LARGE)  
XXX=GEOMETRIC ATTACK ANGLE (DEGREES)  
YY=RUN NUMBER, THIS FOIL # THIS ANGLE

INPUT DATA CONNECTED FOR ZERO IMBALANCES, SIGNS, AND HYDROSTATIC PRESSURE

BUZ NO	MANO	01	02	03	PRBP
S-18.-01	1455.	-542.0	-33.9	-406.0	295.
S-18.-02	1454.	-531.0	-33.9	-403.3	295.
S-18.-03	1458.	-520.0	-32.3	-400.7	282.
S-18.-04	1453.	-500.0	-31.1	-399.0	268.
S-18.-05	1456.	-875.0	-30.0	-387.3	253.
S-18.-06	1460.	-692.0	-29.0	-375.7	240.
S-18.-07	1466.	-928.0	-28.2	-365.0	226.
S-18.-08	1443.	-400.0	-27.6	-355.3	211.
S-18.-09	1437.	-378.0	-27.0	-3318.7	202.
S-18.-10	1438.	-372.0	-26.8	-3313.0	202.
S-18.-11	1435.	-354.0	-26.4	-321.3	55.
S-18.-12	1430.	-316.0	-25.7	-309.7	189.
S-18.-13	1427.	-316.0	-24.9	-296.0	178.
S-18.-14	1425.	-296.0	-24.5	-281.3	168.
S-18.-15	1421.	-226.0	-23.6	-267.7	155.
S-18.-16	1417.	-256.0	-22.7	-249.0	143.
S-18.-17	1418.	-250.0	-22.5	-242.3	131.
S-18.-18	1415.	-244.0	-22.0	-236.7	130.
S-18.-19	1410.	-226.0	-21.5	-219.0	124.
S-18.-20	1408.	-218.0	-20.5	-206.3	114.
S-18.-21	1401.	-208.0	-20.4	-203.7	40.
S-18.-22	1399.	-200.0	-19.9	-191.0	41.
S-18.-23	1406.	-184.0	-18.5	-176.3	40.
S-18.-24	1406.	-178.0	-18.2	-170.7	40.
S-18.-25	1423.	-172.0	-17.7	-165.0	40.
S-18.-26	1408.	-166.0	-17.2	-158.3	40.
S-18.-27	845.	-212.0	-16.2	-194.7	46.
S-18.-28	643.	-186.0	-13.1	-161.0	46.

## EFFECTS OF WALL EFFECTS ON SUPERACCELERATING HYDROPOILS OR PINTLE SPAN

## \*HYDROPOIL DATA REDUCTION\*

Run No	Alpha	LIPPI-LB	BORG-LB	BORG-ILB	VBL-PPS
S-18--01	18.00	58.91	16.36	12.75	28.19
S-18--02	18.00	58.11	16.25	12.74	28.18
S-18--03	18.00	52.68	16.15	12.17	28.18
S-18--04	18.00	50.65	15.88	11.70	28.18
S-18--05	18.00	48.03	15.61	11.28	28.11
S-18--06	18.00	45.81	15.14	10.69	28.09
S-18--07	18.00	43.39	14.71	10.62	28.11
S-18--08	18.00	40.58	13.92	10.46	28.08
S-18--09	18.00	38.36	13.65	10.14	28.03
S-18--10	18.00	37.76	13.42	10.09	28.04
S-18--11	18.00	35.95	12.95	9.93	28.01
S-18--12	18.00	34.14	12.48	9.66	27.97
S-18--13	18.00	32.12	11.93	9.38	27.94
S-18--14	18.00	30.11	11.38	9.22	27.92
S-18--15	18.00	28.09	10.79	8.87	27.88
S-18--16	18.00	26.07	10.03	8.52	27.85
S-18--17	18.00	25.47	9.77	8.47	27.82
S-18--18	18.00	24.86	9.54	8.29	27.83
S-18--19	18.00	23.05	8.83	8.08	27.78
S-18--20	18.00	21.83	8.32	7.73	27.73
S-18--21	18.00	21.23	8.21	7.68	27.70
S-18--22	18.00	20.42	7.70	7.48	27.68
S-18--23	18.00	18.79	7.11	6.98	27.75
S-18--24	18.00	18.18	6.88	6.85	27.75
S-18--25	18.00	17.57	6.65	6.65	27.90
S-18--26	18.00	16.96	6.38	6.46	27.77
S-18--27	18.00	21.54	7.85	6.11	21.69
S-18--28	18.00	18.87	6.49	6.93	19.28

LEGEND

VBL UPSTREAM VELOCITY (U)

ZIPPER INLES OF HALL EFFECTS ON SUPERACCELERATING HYDROPOILS OF FINITE SPAN

\*\*HYDROPOIL DATA IN BIODIMENSIONAL FORM (NO CORRECTIONS APPLIED)\*\*

SUB NO	ALPHA	CL	CDUNC	CH	L/D	D/L	BH10**-6
S-18.-01	18.00	1.0300	0.2966	0.1190	1.4728	0.2880	0.5694
S-18.-02	18.00	1.0156	0.2948	0.1190	1.4451	0.2903	0.5692
S-18.-03	18.00	0.9887	0.2928	0.1190	1.3770	0.2961	0.5692
S-18.-04	18.00	0.9507	0.2877	0.1093	1.3041	0.3027	0.5692
S-18.-05	18.00	0.9061	0.2862	0.1059	1.0883	0.3137	0.5678
S-18.-06	18.00	0.8653	0.2757	0.1024	1.1386	0.3186	0.5674
S-18.-07	18.00	0.8186	0.2672	0.0997	1.0635	0.3264	0.5678
S-18.-08	18.00	0.7671	0.2528	0.0983	1.0348	0.3295	0.5672
S-18.-09	18.00	0.7280	0.2467	0.0958	1.0273	0.3416	0.5663
S-18.-10	18.00	0.7161	0.2442	0.0952	2.9125	0.3410	0.5663
S-18.-11	18.00	0.6831	0.2358	0.0939	2.8976	0.3451	0.5658
S-18.-12	18.00	0.6508	0.2276	0.0916	2.6593	0.3497	0.5648
S-18.-13	18.00	0.6135	0.2175	0.0892	2.8204	0.3546	0.5643
S-18.-14	18.00	0.5759	0.2065	0.0878	2.7885	0.3586	0.5639
S-18.-15	18.00	0.5387	0.1965	0.0846	2.7410	0.3648	0.5632
S-18.-16	18.00	0.5013	0.1826	0.0815	2.7451	0.3643	0.5624
S-18.-17	18.00	0.4907	0.1778	0.0812	2.7594	0.3624	0.5619
S-18.-18	18.00	0.4786	0.1711	0.0793	2.7616	0.3621	0.5621
S-18.-19	18.00	0.4452	0.1601	0.0776	2.7798	0.3597	0.5612
S-18.-20	18.00	0.4233	0.1509	0.0745	2.8047	0.3565	0.5600
S-18.-21	18.00	0.4124	0.1492	0.0742	2.7651	0.3616	0.5595
S-18.-22	18.00	0.3972	0.1395	0.0724	2.8487	0.3510	0.5591
S-18.-23	18.00	0.3638	0.1273	0.0672	2.8582	0.3499	0.5604
S-18.-24	18.00	0.3521	0.1229	0.0660	2.8654	0.3490	0.5604
S-18.-25	18.00	0.3165	0.1170	0.0634	2.8751	0.3478	0.5636
S-18.-26	18.00	0.3280	0.1131	0.0621	2.9003	0.3448	0.5608
S-18.-27	18.00	0.6699	0.2331	0.0945	2.8712	0.3483	0.4422
S-18.-26	18.00	0.7569	0.2493	0.0983	3.0357	0.3294	0.3894

LEGEND

CL ALPHABETIC ANGLE OF ATTACK CORRECTED FOR SHAFT TWIST  
 CDUNC CL (UNCORRECTED), TWO UNCORRECTED DRAG COEFFICIENT AS COMPUTED FROM MEASURED DRAG, AND NONDIMENSIONALIZED  
 ON UPSTREAM VELOCITY AND MODEL PLATEFORM AREA  
 CH BIOMENT COEFFICIENT, NONDIMENSIONALIZED ON UPSTREAM VELOCITY, MODEL PLATEFORM AREA, AND MEAN CHORD  
 L/D LIFT-TO-DRAG RATIO = CL/CDUNC  
 D/L DRAG-TO-LIFT RATIO = CDUNC/CL  
 BH BIOMENTS NUMBER, BASED ON MEAN CHORD

**UPPER TOWERS OF WALL EFFECTS ON SUPERCAVITATING HYDROPOLES OF FINITE SPAN**

**OPTION DATA CORRECTED FOR EFFECTS OF IMAGES OF TRAILING VORTEX SYSTEMS**

TEST NO.	ALPHAT	CL	CD	CH	(D/L)	SIGC/AT	SIGC/AT	CL/AT	CD/AT2	CH/AT	SIGC	CAVITY	CAVITY
S-18.-01	18.19	1.330	0.300	0.119	0.291	2.963	2.335	3.245	2.977	0.940	0.781	0.98	
S-18.-02*	18.19	1.016	0.299	0.119	0.293	2.965	2.360	3.200	2.959	0.941	0.789	---	
S-18.-03	18.18	0.939	0.296	0.118	0.299	2.810	2.246	3.116	2.939	0.893	0.713	0.89	
S-18.-04	18.17	0.951	0.291	0.109	0.306	2.650	2.167	2.997	2.888	0.845	0.842	0.687	0.91
S-18.-05	18.17	0.906	0.287	0.106	0.317	2.499	2.053	2.858	2.853	0.730	0.791	0.651	0.92
S-18.-06	18.16	0.865	0.278	0.102	0.321	2.347	1.952	2.730	2.769	0.744	0.619	0.595	
S-18.-07	18.15	0.819	0.269	0.100	0.329	2.183	1.815	2.594	2.604	0.715	0.581	0.597	
S-18.-08	18.14	0.767	0.255	0.098	0.332	2.013	1.736	2.423	2.580	0.611	0.637	0.550	1.15
S-18.-09	18.13	0.728	0.250	0.096	0.348	1.916	1.662	2.300	2.500	0.503	0.606	0.526	1.20
S-18.-10*	18.13	0.716	0.246	0.095	0.343	1.916	1.673	2.263	2.455	0.301	0.606	0.529	---
S-18.-11	18.12	0.683	0.237	0.094	0.347	1.765	1.561	2.160	2.371	0.297	0.558	0.494	1.30
S-18.-12	18.12	0.651	0.229	0.092	0.352	1.662	1.873	2.058	2.289	0.290	0.519	0.466	1.35
S-18.-13	18.11	0.614	0.219	0.089	0.356	1.556	1.418	1.981	2.189	0.282	0.483	0.448	1.60
S-18.-14	18.11	0.576	0.208	0.088	0.360	1.376	1.303	1.823	2.079	0.278	0.435	0.412	1.60
S-18.-15	18.10	0.539	0.197	0.085	0.367	1.238	1.178	1.705	1.979	0.268	0.391	0.372	2.00
S-18.-16	18.09	0.501	0.183	0.082	0.366	1.099	1.064	1.588	1.839	0.258	0.347	0.336	2.05
S-18.-17*	18.09	0.491	0.179	0.081	0.364	1.008	1.066	1.554	1.791	0.257	0.383	0.337	---
S-18.-18	18.09	0.479	0.174	0.079	0.364	1.015	0.995	1.516	1.746	0.251	0.320	0.314	2.20
S-18.-19	18.08	0.445	0.161	0.078	0.361	0.899	0.880	1.411	1.618	0.246	0.288	0.278	
S-18.-20	18.08	0.423	0.151	0.075	0.358	0.794	0.777	1.342	1.522	0.236	0.250	0.245	3.20
S-18.-21*	18.09	0.412	0.150	0.074	0.363	0.782	0.766	1.307	1.504	0.235	0.247	0.242	---
S-18.-22	18.07	0.397	0.180	0.072	0.352	0.670	0.660	1.259	1.406	0.229	0.213	0.208	5.10
S-18.-23	18.07	0.368	0.128	0.067	0.351	0.527	0.515	1.154	1.285	0.213	0.166	0.162	5.00
S-18.-24	18.06	0.352	0.123	0.066	0.350	0.502	0.491	1.117	1.280	0.209	0.158	0.155	7.20
S-18.-25	18.06	0.336	0.117	0.063	0.349	0.389	0.380	1.067	1.181	0.201	0.123	0.120	---
S-18.-26	18.06	0.328	0.113	0.062	0.346	0.296	0.289	1.041	1.142	0.197	0.093	0.091	---
S-18.-27	18.12	0.670	0.235	0.094	0.350	1.785	1.661	2.118	2.347	0.298	0.564	0.525	1.37
S-18.-28	18.14	0.757	0.251	0.098	0.332	2.027	1.871	2.391	2.506	0.311	0.642	0.592	0.98

UNLESS OTHERWISE INDICATED, ALL DATA ARE FOR:

1. SUPERCAVITATING FLOW.
2. BOTH STATIC PRESSURE TAPS OPEN.

**LEGEND**

- \* ONLY UPSTREAM STATIC PRESSURE TAP UTILIZED
- + ONLY DOWNTREAM STATIC PRESSURE TAP UTILIZED
- PC PARTIALLY CAVITATING
- PC(TV) PARTIALLY CAVITATING (TAP RETTED)
- F2 FULLY WETTED

**AT (ALPHAT)**

(TRUE) ANGLE OF ATTACK, CORRECTED FOR EFFECTS OF IMAGES OF TRAILING VORTEXES

AT2 ALPHAT+0.2

SIGC CAVITATION NUMBER COMPUTED WITH MEASURED CAVITY PRESSURE

SIGV CAVITATION NUMBER COMPUTED WITH CALCULATED VAPOR PRESSURE

CD DRAG COEFFICIENT, CORRECTED FOR EFFECTS OF IMAGES OF TRAILING VORTEXES

(D/L) CORRECTED DRAG-TO-LIFT RATIO = CD/CL

CAVITY LENGTH MEASURED FROM MIDCHORD AT CENTROID POSITION, nondimensionalized on mean chord (obtained from photographs)

## EFFECTS OF WALL EFFECTS ON SUPERCAVITATING HYDROFOILS OF FLIGHT SPAN

## HYDROFOIL INPUT DATA

TR	TZ	AREA	SPAN	AAC
76	94	10.0	5.0	2.01

ZERO READINGS AND INICIAL TEMP BEFORE AND AFTER  
 BAND 1-A 1-A 2-A 2-A 3-A 3-A FT  
 0. 0.0 0.0 0.0 100.0 0.0 93.0  
 0. 0.0 0.0 0.0 100.7 0.0 95.0  
 CALL 1AS/CR (NORMAL/REV) 01-0.10000 02-0.02090 03-0.04030  
 S1313-7200.0 SHAPT DIA = 1.50IN \*INPUT DATA AS RECORDED\*

BUS NO	MACH	S	A1	S	42	S	83	PIMP
S-21-01	1.653.	-560.0		137.2		605.0		375.
S-21-02*	1.653.	-560.0		136.8		602.0		375.
S-21-03*	1.652.	-560.0		135.2		598.0		359.
S-21-04*	1.652.	-532.0		133.4		593.0		362.
S-21-05*	1.659.	-512.0		131.4		584.0		324.
S-21-06*	1.626.	-488.0		130.1		573.0		304.
S-21-07*	1.636.	-466.0		128.9		568.0		284.
S-21-08*	1.629.	-448.0		126.9		559.0		270.
S-21-09	1.622.	-452.0		128.7		557.0		270.
S-21-10	1.616.	-432.0		126.1		543.0		256.
S-21-11	1.616.	-432.0		126.1		543.0		255.
S-21-12	1.611.	-412.0		127.6		528.0		241.
S-21-13	1.610.	-389.0		127.1		515.0		226.
S-21-14	1.612.	-364.0		126.6		495.0		211.
S-21-15*	1.608.	-358.0		126.4		493.0		211.
S-21-16	1.608.	-342.0		126.0		477.0		198.
S-21-17	1.605.	-316.0		125.5		459.0		181.
S-21-18	1.600.	-290.0		127.3		449.0		170.
S-21-19	1.599.	-282.0		123.6		420.0		160.
S-21-20	1.597.	-266.0		123.1		400.0		145.
S-21-21	1.595.	-258.0		122.9		385.0		139.
S-21-22	1.594.	-240.0		122.4		372.0		133.
S-21-23*	1.589.	-236.0		121.3		365.0		130.
S-21-24	1.588.	-230.0		122.0		360.0		122.
S-21-25	1.590.	-220.0		121.2		366.0		116.
S-21-26	1.590.	-208.0		120.6		331.0		106.
S-21-27	1.594.	-198.0		119.6		326.0		100.
S-21-28	1.596.	-194.0		119.1		315.0		93.
S-21-29	1.590.	-126.0		112.2		237.0		83.
S-21-30	1.602.	-155.0		113.1		265.0		124.

LEGEND TR ROOM TEMPER (DEG FAH)  
 TT TUNNEL " "  
 AREA HALF-SPAN MODEL PLATFORM AREA (SQ IN)

SPAN FOIL HALF-SPAN (IN)

AAC

AREA CHORD, MM.

A MODEL CANTEROID (IN)

BAND VELOCITY MEASUREMENT (MM)

SHAPT TEST (DEGREES/IN-LD)

S LOAD CELL POLARITY (P=FORWARD, S=REVERSE)

LOAD CELL 01 LIFT (COUNTS)  
 02 BOREST ABOUT MIDCROWN (COUNTS)  
 03 DIAIG (COUNTS)

PIMP SPATIC PRESSURE (MM HG)

PCAV CAVITY PRESSURE (MM HG)

ACU NO Q-TICK-V: Q=FOIL TESTED (S=SMALL, N=MED, L=LARGE)

EXC=CHROMATRIC ATTACK ANGLE (DEGREES)

FT-BUS NUMBER. THIS POLL @ THIS ANGLE

EFFECTS OF WALL EFFECTS ON SUPERCAVITATING HYDROFOILS OF FINITE SPAN

INPUT DATA CORRECTED FOR ZERO READING, SIGNALS, AND HYDROSTATIC PRESSURE

BU#	SO	RABON	01	02	03	PIBP	PCAV
S-21.-01	1457.	-564.0	-37.2	-505.0	360.	151.	
S-21.-02	1453.	-560.0	-16.8	-502.1	360.	151.	
S-21.-03	1452.	-568.0	-35.2	-498.1	344.	148.	
S-21.-04	1442.	-532.0	-33.3	-493.2	327.	122.	
S-21.-05	1439.	-512.0	-31.3	-484.3	309.	109.	
S-21.-06	1436.	-488.0	-30.0	-477.3	289.	99.	
S-21.-07	1434.	-466.0	-28.8	-468.8	269.	89.	
S-21.-08	1429.	-448.0	-28.7	-459.5	255.	61.	
S-21.-09	1422.	-452.0	-28.5	-457.6	255.	60.	
S-21.-10	1418.	-432.0	-27.9	-443.6	241.	75.	
S-21.-11	1416.	-432.0	-27.9	-443.7	240.	75.	
S-21.-12	1411.	-412.0	-27.5	-428.8	226.	71.	
S-21.-13	1410.	-388.0	-26.8	-415.8	211.	64.	
S-21.-14	1412.	-364.0	-26.3	-395.9	196.	58.	
S-21.-15	1408.	-358.0	-26.1	-394.0	196.	56.	
S-21.-16	1408.	-342.0	-25.6	-378.0	183.	53.	
S-21.-17	1405.	-316.0	-25.1	-360.1	168.	49.	
S-21.-18	1400.	-298.0	-24.2	-341.2	155.	47.	
S-21.-19	1399.	-282.0	-23.2	-321.2	145.	45.	
S-21.-20	1397.	-266.0	-22.6	-301.3	130.	44.	
S-21.-21	1395.	-254.0	-22.4	-286.4	124.	43.	
S-21.-22	1394.	-240.0	-21.9	-273.4	115.	43.	
S-21.-23	1389.	-236.0	-26.8	-266.5	115.	43.	
S-21.-24	1388.	-230.0	-21.4	-261.6	107.	43.	
S-21.-25	1390.	-220.0	-20.6	-247.7	101.	43.	
S-21.-26	1390.	-208.0	-19.8	-232.7	91.	43.	
S-21.-27	1394.	-198.0	-19.0	-225.8	85.	43.	
S-21.-28	1396.	-194.0	-18.4	-216.9	79.	43.	
S-21.-29	780.	-126.0	-11.5	-138.9	79.	43.	
S-21.-30	602.	-156.0	-12.4	-167.0	109.	41.	

TIPPER TUBES OF WALL EFFECTS ON SUPERCAVITATING HYDROPOILS OF PIVOT SPAN

CONTROPOIL DATA REDUCTION

BUS NO	ALPHA	LJPP-L8	DJAC-L8	MOS-11BLB	VEL-PPS
S-21--01	21.00	57.18	20.35	13.99	28.21
S-21--02	21.00	56.77	20.23	13.84	28.18
S-21--03	21.00	55.53	20.07	13.22	28.17
S-21--04	21.00	53.90	19.88	12.54	28.06
S-21--05	21.00	51.85	19.52	11.78	28.05
S-21--06	21.00	49.43	19.08	11.28	28.02
S-21--07	21.00	47.20	18.72	10.82	28.01
S-21--08	21.00	45.40	16.52	10.81	27.96
S-21--09	21.00	45.80	18.44	10.72	27.90
S-21--10	21.00	43.78	17.68	10.49	27.86
S-21--11	21.00	43.78	17.88	10.48	27.84
S-21--12	21.00	41.78	17.28	10.36	27.80
S-21--13	21.00	39.36	16.76	10.09	27.79
S-21--14	21.00	36.95	15.95	9.89	27.81
S-21--15	21.00	36.34	15.88	9.80	27.77
S-21--16	21.00	38.74	15.23	9.64	27.77
S-21--17	21.00	32.12	16.51	9.45	27.74
S-21--18	21.00	30.31	13.75	9.10	27.70
S-21--19	21.00	28.68	12.95	8.71	27.69
S-21--20	21.00	27.07	12.14	8.52	27.67
S-21--21	21.00	25.87	11.54	8.43	27.65
S-21--22	21.00	24.46	11.02	8.24	27.64
S-21--23	21.00	24.16	10.74	10.07	27.59
S-21--24	21.00	23.45	10.54	8.07	27.58
S-21--25	21.00	22.83	9.98	7.76	27.60
S-21--26	21.00	21.21	9.38	7.95	27.60
S-21--27	21.00	20.20	9.10	7.18	27.64
S-21--28	21.00	19.79	8.78	6.98	27.66
S-21--29	21.00	12.84	5.60	4.34	21.10
S-21--30	21.00	15.86	6.73	4.66	18.70

LEGEND

VEL UPSTREAM VELOCITY (0)

**EFFECTS OF WALL EFFECTS ON SUPERCRITICAL WINGFOLDS OF FINITE SPAN**

**\*\*WINGFOLD DATA IS NONDIMENSIONAL FORM (NO CONNECTIONS APPLIED)\*\***

BLW NO.	ALPHA	CL	CDUWC	CH	L/D	D/L	Rn=1044-6
S-21,-0.1	21.00	1.0712	0.3710	0.1308	2.8873	0.3963	0.5788
S-21,-0.2	21.00	1.0663	0.3698	0.1293	2.8837	0.3968	0.5781
S-21,-0.3	21.00	1.0639	0.3670	0.1237	2.8836	0.3516	0.5779
S-21,-0.4	21.00	1.0195	0.3657	0.1180	2.7876	0.3587	0.5761
S-21,-0.5	21.00	0.9828	0.3596	0.1110	2.7329	0.3659	0.5755
S-21,-0.6	21.00	0.9386	0.3520	0.1066	2.6668	0.3750	0.5750
S-21,-0.7	21.00	0.8975	0.3456	0.1023	2.5970	0.3851	0.5746
S-21,-0.8	21.00	0.8661	0.3429	0.1026	2.5253	0.3960	0.5736
S-21,-0.9	21.00	0.8776	0.3451	0.1022	2.5581	0.3909	0.5723
S-21,-1.0	21.00	0.8412	0.3332	0.1003	2.5286	0.3961	0.5716
S-21,-1.1	21.00	0.8423	0.3337	0.1003	2.5281	0.3962	0.5712
S-21,-1.2	21.00	0.8064	0.3232	0.0995	2.4947	0.4008	0.5703
S-21,-1.3	21.00	0.7603	0.3138	0.0969	2.4259	0.4122	0.5701
S-21,-1.4	21.00	0.7127	0.2975	0.0949	2.3960	0.4174	0.5705
S-21,-1.5	21.00	0.7029	0.2968	0.0943	2.3686	0.4222	0.5697
S-21,-1.6	21.00	0.6710	0.2884	0.0926	2.3626	0.4233	0.5697
S-21,-1.7	21.00	0.6226	0.2709	0.0911	2.2978	0.4352	0.5691
S-21,-1.8	21.00	0.5892	0.2570	0.0880	2.2925	0.4362	0.5682
S-21,-1.9	21.00	0.5581	0.2416	0.0846	2.3101	0.4329	0.5680
S-21,-2.0	21.00	0.5274	0.2263	0.0826	2.3311	0.4290	0.5676
S-21,-2.1	21.00	0.5037	0.2153	0.0819	2.3489	0.4257	0.5673
S-21,-2.2	21.00	0.4774	0.2048	0.0800	2.3310	0.4290	0.5671
S-21,-2.3	21.00	0.4732	0.2001	0.0861	2.3652	0.4228	0.5661
S-21,-2.4	21.00	0.4596	0.1963	0.0787	2.3410	0.4272	0.5659
S-21,-2.5	21.00	0.4391	0.1850	0.0755	2.3726	0.4215	0.5663
S-21,-2.6	21.00	0.4152	0.1733	0.0725	2.3964	0.4173	0.5663
S-21,-2.7	21.00	0.3983	0.1673	0.0693	2.3562	0.4244	0.5671
S-21,-2.8	21.00	0.3857	0.1601	0.0673	2.4096	0.4150	0.5674
S-21,-2.9	21.00	0.4303	0.1769	0.0723	2.4323	0.4111	0.5328
S-21,-3.0	21.00	0.6763	0.2761	0.0990	2.4494	0.4083	0.3837

**LEGEND**

CL LIFT COEFFICIENT, NONDIMENSIONALIZED ON UPSTREAM VELOCITY AND MODEL PLATFORM AREA  
 CDUWC CL (UNCORRECTED). THE UNCORRECTED DRAG COEFFICIENT AS COMPUTED FROM MEASURED DRAG  
 ON UPSTREAM VELOCITY AND MODEL PLATFORM AREA  
 CH DOWNSTREAM COEFFICIENT, NONDIMENSIONALIZED ON UPSTREAM VELOCITY, MODEL PLATFORM AREA, AND BEAM CHORD  
 L/D LIFT-TO-DRAG RATIO = CL/CDUWC  
 D/L DRAG-TO-LIFT RATIO = CDUWC/CL  
 Rn RETROD NUMBER, BASED ON BEAM CHORD

**EFFECTS OF WALL EFFECTS ON SUPERCAVITATING WINGFOILS OF FINITE SPAN**

**SECTION DATA CORRECTED FOR EFFECTS OF IMAGES OF TRAILING VORTICES SYSTEM\***

TEST NO.	ALPHAT	CL	CN	(D/L)	SIGC/AT	SIGC/AT CL/AT	CD/AT2	CH/AT	SIGC	SIGC	CAVLTN
S-21-0-1	21.20	1.071	0.375	0.120	0.350	3.181	2.031	2.738	0.353	1.162	0.751
S-21-0-2*	21.19	1.066	0.373	0.120	0.350	3.189	2.056	2.726	0.353	1.165	0.760
S-21-0-3*	21.19	1.044	0.370	0.124	0.355	2.993	2.028	2.822	0.334	1.107	0.750
S-21-0-4*	21.19	1.020	0.369	0.118	0.362	2.884	2.032	2.757	0.319	1.052	0.751
S-21-0-5*	21.18	0.983	0.363	0.111	0.369	2.671	1.987	2.659	0.300	0.987	0.734
S-21-0-6*	21.17	0.939	0.355	0.107	0.378	2.478	2.040	2.598	0.288	0.916	0.699
S-21-0-7*	21.16	0.897	0.348	0.102	0.388	2.282	1.795	2.430	0.255	0.883	0.663
S-21-0-8*	21.16	0.866	0.345	0.103	0.399	2.149	1.742	2.385	0.278	0.794	0.643
S-21-0-9	21.16	0.878	0.345	0.102	0.398	2.158	1.760	2.376	0.253	0.277	0.797
S-21-1-0	21.15	0.841	0.335	0.100	0.399	2.022	1.674	2.279	0.241	0.222	0.747
S-21-1-1	21.15	0.842	0.336	0.100	0.399	2.014	1.666	2.282	0.245	0.272	0.746
S-21-1-2	21.15	0.806	0.325	0.099	0.403	1.979	1.571	2.185	0.238	0.693	0.615
S-21-1-3	21.14	0.760	0.315	0.097	0.415	1.728	1.492	2.061	0.236	0.538	0.540
S-21-1-4	21.13	0.713	0.299	0.095	0.420	1.578	1.399	1.933	0.257	0.580	0.516
S-21-1-5*	21.13	0.703	0.298	0.094	0.424	1.577	1.424	1.906	0.256	0.562	0.525
S-21-1-6	21.12	0.672	0.286	0.093	0.425	1.485	1.322	1.822	0.252	0.533	0.488
S-21-1-7	21.11	0.623	0.272	0.091	0.437	1.295	1.214	1.689	0.204	0.247	0.477
S-21-1-8	21.11	0.589	0.258	0.089	0.438	1.166	1.106	1.599	0.239	0.430	0.407
S-21-1-9	21.10	0.558	0.243	0.084	0.435	1.064	1.025	1.515	0.229	0.392	0.378
S-21-1-10	21.10	0.527	0.227	0.083	0.431	0.911	0.884	1.433	0.175	0.224	0.325
S-21-1-11	21.09	0.505	0.216	0.082	0.427	0.850	0.834	1.371	0.151	0.222	0.313
S-21-1-12	21.09	0.477	0.206	0.080	0.430	0.758	0.742	1.297	0.151	0.217	0.273
S-21-1-13*	21.09	0.473	0.201	0.098	0.428	0.760	0.745	1.286	0.162	0.280	0.274
S-21-1-14	21.08	0.460	0.197	0.079	0.429	0.677	0.663	1.249	0.155	0.214	0.249
S-21-1-15	21.08	0.439	0.186	0.076	0.423	0.614	0.600	1.193	0.172	0.205	0.221
S-21-1-16	21.08	0.415	0.174	0.073	0.419	0.510	0.497	1.129	0.125	0.197	0.183
S-21-1-17	21.07	0.394	0.168	0.069	0.426	0.446	0.435	1.072	0.145	0.188	0.164
S-21-1-18	21.07	0.386	0.161	0.067	0.416	0.363	0.373	1.049	1.187	0.183	0.141
S-21-1-19	21.06	0.430	0.177	0.072	0.412	0.657	0.640	1.170	1.311	0.196	0.242
S-21-1-20	21.06	0.676	0.278	0.099	0.410	1.503	1.529	2.012	0.266	0.554	0.564

UNLESS OTHERWISE INDICATED, ALL DATA ARE FOR:

1. SUPERCAVITATING FLOW.
2. BOTH STATIC PRESSURE TAPS OPEN.

**LEGEND**

- \* CHTL UPSTREAM STATIC PRESSURE TAP UTILIZED
- o ONLY DISTANT STATIC PRESSURE TAP UTILIZED
- PC (TU) PARTIALLY CAVITATING (TAP SETTED)
- PW PULLY METED
- AT (ALPHAT) (TRUE) ANGLE OF ATTACK, CORRECTED FOR EFFECTS OF IMAGES OF TRAILING VORTICES
- AT2 SEPARATE
- SIGC CAVITATION NUMBER COMPUTED WITH MEASURED CAVITY PRESSURE
- SIGV CAVITATION NUMBER COMPUTED WITH CALCULATED VAPOR PRESSURE
- CD FRAG COEFFICIENT, CORRECTED FOR EFFECTS OF IMAGES OF TRAILING VORTICES
- (D/L) CORRECTED DRAG-TO-LIFT RATIO = CD/CCL
- CAVLTN CAVITY LENGTH ASSESSED FROM MIDCHORD AT CENTROID POSITION, NONDIMENSIONALIZED ON MID CHORD (OBTAINED FROM PHOTOGRAPHS)

**EFERRED EFFECTS OF WALL EFFECTS ON SUPERCAVITATING HYDROFOILS OF FINITE SPAN**

**HYDROFOIL INPUT DATA**

TA TT AREA SPAN RAC

73 81 40.0 10.0 0.02

**ZERO READING AND TUNNEL TRAP BEFORE AND AFTER**

RAON	1-N	1-N	2-N	2-N	3-N	3-N	TT
0.	0.0	0.0	100.0	0.0	0.0	100.0	80.0
0.	0.0	0.0	99.0	0.0	0.0	100.0	82.0
CELL LSS/CR1(GORNAL/LST)	01=0.20000	02=0.20000	03=0.04030				
TWIST= 7200.0	SHAFT DIA.= 1.50IN						

\*INPUT DATA AS RECORDED\*

RUN NO	RAON	S	81	S	82	S	83	PISF	PCAV
B-8-0-01	1417.		-566.0		86.5		543.0		
B-8-0-02	1396.		-500.0		87.5		530.0	172.	28.
B-8-0-03	1376.		-430.0		88.0		505.0	157.	28.
B-8-0-04	1370.		-362.0		88.5		467.0	141.	28.
B-8-0-05	1367.		-301.0		89.0		423.0	126.	28.
B-8-0-06	1373.		-236.0		90.0		370.0	109.	28.
B-8-0-07	1385.		-212.0		90.5		367.0	90.	29.
								81.	29.

LEGEND  
TA TUNNEL " ( " )  
AREA HALF-SPAN MODEL PLATEFORM AREA (SQ IN)  
SPAN FOIL HALF-SPAN (IN)  
RAC MEAN CHORD AREAS. A MODEL CENTROID (IN)  
RAON VELOCITY BAROMETRIC HEADING (RAD)  
TWIST SHAFT TWIST (DEGREES/IN-LB)  
S LOAD CELL POLARITY (S=NORMAL, R=REVERSE)

LOAD CELL #1 LIPT (COUNTS)

#2 MOMENT ABOUT MIDCHORD (COUNTS)

#3 DRAG (COUNTS)

PISF STATIC PRESSURE (IN HG)

PCAV CAVITY PRESSURE (IN HG)

SUB NO Q-KIN-IV: Q-FOIL TESTED(S-SMALL, R-MOD,L-LARGE)

XXI=G203 METRIC ATTACK ANGLE (DEGREES)

YY-BUS NUMBER, THIS FOIL # THIS ANGLE

BIPER LINES OF WALL EFFECTS ON SUPERCAVITATING HYDROPOILS OF PRINTS SPAN

INPUT DATA CORRECTED FOR ZERO FRAGMENTS, SIGNS, AND HYDROSTATIC PRESSURE

BUN NO	MANG	01	02	03	PINP	PCAV
A-8-0-01	1417.	-566.0	-13.5	-46.0	161.	28.
A-8-0-02	1396.	-500.0	-12.3	-810.0	146.	28.
A-8-0-03	1376.	-430.0	-11.7	-405.0	130.	28.
A-8-0-04	1376.	-365.0	-11.0	-367.0	113.	28.
A-8-0-05	1367.	-303.0	-10.3	-323.0	98.	28.
A-8-0-06	1373.	-235.0	-9.2	-270.0	79.	29.
A-8-0-07	1385.	-212.0	-8.5	-267.0	70.	29.

EFFECTS OF WALL EFFECTS ON SUPERCAVITATING HYDROFOILS OF FINITE SPAN

\*\*HYDROFOIL DATA REDUCTION\*\*

TEST NO	ALPHA	LIFT-LB	DRAG-LB	MOM-IMLB	VEL-FPS
A-8-0-01	8.01	115.90	17.85	48.60	27.86
A-8-0-02	8.01	102.47	17.33	44.40	27.67
A-8-0-03	8.01	88.33	16.32	42.00	27.48
A-8-0-04	8.01	78.60	14.79	39.60	27.43
A-8-0-05	8.01	62.67	13.02	37.20	27.40
A-8-0-06	8.00	49.03	10.88	33.88	27.45
A-8-0-07	8.00	44.10	9.95	30.60	27.57

LEGEND VEL UPSTREAM VELOCITY (ft)

UPPER INLES OF WALL EFFECTS ON SUPERCAVITATING HYDROPOOLS OF FINITE SPAN

CHORDWISE DATA IN NONDIMENSIONAL FORM (NO CORRECTIONS APPLIED)  $\infty$

RUN NO	ALPHA	CL	CD <sub>DUC</sub>	CH	L/D	Re <sup>10<sup>6</sup></sup>
E-8-0-01	8.01	0.5557	0.0801	0.6580	6.933	0.1141
E-8-0-02	8.01	0.4981	0.0787	0.0537	6.3279	0.1580
E-8-0-03	8.01	0.4352	0.0749	0.0615	5.8117	0.1721
E-8-0-04	8.01	0.3691	0.0676	0.0487	5.4563	0.1833
E-8-0-05	8.01	0.3107	0.0590	0.0859	5.2556	0.1899
E-8-0-06	8.00	0.2421	0.0482	0.0405	5.0236	0.1991
E-8-0-07	8.00	0.2160	0.0432	0.0373	4.9960	0.2001

LEGEND

ALPHA GEOMETRIC ANGLE OF ATTACK CORRECTED FOR SHAFT TWIST  
CL LIFT COEFFICIENT, NONDIMENSIONALIZED ON UPSTREAM VELOCITY AND MODEL PLATEFORM AREA  
CD<sub>DUC</sub> CD (UNCORRECTED). THE UNCORRECTED DRAG COEFFICIENT AS COMPUTED FROM MEASURED DRAG, AND NONDIMENSIONALIZED  
ON UPSTREAM VELOCITY AND MODEL PLATEFORM AREA  
CH BODILY COEFFICIENT, NONDIMENSIONALIZED ON UPSTREAM VELOCITY, MODEL PLATEFORM AREA, AND REAP CHORD  
L/D LIFT-TO-DRAG RATIO = CL/CD<sub>DUC</sub>  
D/L DRAG-TO-LIFT RATIO = CD<sub>DUC</sub>/CL  
Re REYNOLDS NUMBER, BASED ON REAP CHORD

RIBBERS AND EFFECTS ON SUPERCAVITATING HYDROFOILS OF VARIOUS SPANS

APPENDIX DATA CONNECTED FOR EFFECTS OF IMAGES OF TRAILING VORTICES SYSTEMS.

RIB NO	ALPHAT	CL	CD	CB	(D/L)	SIGC/AT	SIGC/AT	CB/AT	CB/AT2	SIGC	SIGC	CAVLEN	CAVLEN
R-0-0-01	8.38	0.556	0.083	0.058	0.150	3.463	3.397	3.619	3.933	0.398	0.501	0.494	0.60
R-0-0-02	8.39	0.558	0.081	0.058	0.150	3.463	3.109	3.070	3.438	0.371	0.451	0.485	0.62
R-0-0-03	8.27	0.435	0.077	0.051	0.177	2.735	2.703	3.017	3.698	0.357	0.395	0.390	0.75
R-0-0-04	8.23	0.369	0.069	0.049	0.187	2.298	2.274	2.571	3.351	0.339	0.330	0.326	0.95
R-0-0-05	8.19	0.311	0.060	0.056	0.193	1.903	1.886	2.173	2.936	0.321	0.272	0.270	1.18
R-0-0-06	8.15	0.242	0.049	0.041	0.202	1.386	1.351	1.702	2.413	0.285	0.197	0.192	1.75
R-0-0-07	8.13	0.216	0.044	0.037	0.202	1.130	1.102	1.522	2.169	0.263	0.160	0.156	2.55

UNLESS OTHERWISE INDICATED, ALL DATA ARE FOR:

1. SUPERCAVITATING FLOW.
2. BOTH STATIC PRESSURE TAPS OPEN.

LEGEND

- CAVITY UPSTREAM STATIC PRESSURE TAP UTILIZED
- \* ONLY DISTREAM STATIC PRESSURE TAP UTILIZED
- PC (TAP) PARTIALLY CAVITATING
- PC (TAP) PARTIALLY CAVITATING (TAP BENTED)
- PW FULLY WETTED
- AT (ALPHAT) (TRC2) ANGLE OF ATTACK, CORRECTED FOR EFFECTS OF IMAGES OF TRAILING VORTICES
- AT2 ALPHAT\*2
- SIGC CAVITATION NUMBER COMPUTED WITH MEASURED CAVITY PRESSURE
- SIGV CAVITATION NUMBER COMPUTED WITH CALCULATED VAPOR PRESSURE
- CD DRAG COEFFICIENT, CORRECTED FOR EFFECTS OF IMAGES OF TRAILING VORTICES
- (D/L) CORRECTED DRAG-TO-LIFT RATIO = CD/CL
- CAVLEN CAVITY LENGTH MEASURED FROM MIDCHORD AT CHORDOID POSITION, NORMALEMENTIZED ON MEAN CHORD  
(OBTAINED FROM PHOTOGRAHS)

LIPPS STUDIES OF WALL EFFECTS ON SUPERCAVITATING HYDROFOILS OF FINITE SPAN

**HYDROFOIL INPUT DATA**

IN	TT	DATA	SPAN	HAC
72	78	40.0	10.0	0.02

**ZERO BRAKING AND TUNNEL TRAP SPACING AND ANGLES**

WACOS	1-8	2-8	3-8	3-8
0.	0.0	0.0	100.0	0.0
0.	0.0	0.0	99.0	0.0
CELL LBS/CF (NORMAL/ARM)	01-0.20000	02-0.20000	03-0.00030	
18157-7200.0	SHRAFT DIA.=	1.50IN		

\*OUTPUT DATA AS RECORDED\*

RUN NO	WACOS	S	A1	S	A2	S	A3	P1UP	P2AV
B-9-5-01	1363.		-715.0		117.0		660.0	193.	36.
B-9-5-02	1360.		-640.0		115.0		645.0	177.	38.
B-9-5-03	1357.		-580.0		116.5		625.0	163.	38.
B-9-5-04	1359.		-505.0		116.0		590.0	195.	38.
B-9-5-05	1352.		-440.0		113.0		551.0	132.	32.
B-9-5-06	1346.		-370.0		112.0		500.0	116.	30.
B-9-5-07	1346.		-322.0		111.0		460.0	103.	30.
B-9-5-08	1353.		-265.0		110.0		412.0	87.	30.
B-9-5-09	1355.		-250.0		109.5		398.0	80.	30.

**LEGEND** IN ROOM TEMPER (DEG FAREN)

TT TUNNEL - ( " )

AREA HALF-SPAN MODEL PLATFORM AREA (50 LB)  
 SPAN FOIL HALF-SPAN (LB)  
 HAC AREA CROWN, AREA, A MODEL CENTROID (LB)  
 MAJOR VELOCITY MACHINERY READING (RM)  
 THRUST SHRAFT THRUST (DEGREES/10-LB)

3 LOAD CELL POLARITY (B=HORIZONTAL, R=VERTICAL)

**LOAD CELL #1 LIIFT (COUNTS)**

02 HORNET ABOUT MIDCROSS (COUNTS)

03 DRAG (COUNTS)

P1UP STATIC PRESSURE (MM HG)

P2AV CAVITY PRESSURE (MM HG)

ANG NO Q-III-PI: Q-FOIL TESTED(S-SHALL, B-BRD-L-LANG)

XIX-CROMETIC ATTACK ANGLE (DEGREES)

II-RUN NUMBER, THIS FOIL & THIS ANGLE

RIPPLE TUNES OF WALL EFFECTS ON SUPERCAVITATING HYDROFOILS OF VARIOUS SPAN

INPUT DATA CORRECTED FOR ZERO MARKINGS, SIGNS, AND HYDROSTATIC PRESSURE

SUB NO	SPAN	61	62	63	PWFP	PCAV
E-9-5-01	1363.	-715.0	-17.0	-560.0	182.	34.
E-9-5-02	1360.	-640.0	-15.1	-544.1	166.	34.
E-9-5-03	1357.	-580.0	-14.8	-523.7	152.	34.
E-9-5-04	1359.	-505.0	-16.4	-488.1	138.	34.
E-9-5-05	1353.	-480.0	-13.5	-468.5	121.	32.
E-9-5-06	1346.	-370.0	-12.6	-396.9	105.	30.
E-9-5-07	1346.	-322.0	-11.8	-356.2	92.	30.
E-9-5-08	1353.	-265.0	-10.9	-308.6	76.	30.
E-9-5-09	1355.	-250.0	-10.5	-293.0	69.	30.

PIPER LINES OF WALL EFFECTS ON SUPERELEVATING HYDROPOOLS OF PINTLE SPAN

\*\*HYDROPOOL DATA REDUCTION\*\*

BUS NO	ALPHA	LIFT-LB	DRAG-LB	BOR-IPLB	VBL-PPS
E-9-5-01	9.51	146.40	22.57	61.20	27.36
E-9-5-02	9.51	131.02	21.98	54.45	27.33
E-9-5-03	9.51	118.95	21.11	53.10	27.31
E-9-5-04	9.51	103.87	19.67	51.75	27.32
E-9-5-05	9.51	90.70	16.07	48.60	27.27
E-9-5-06	9.51	76.52	15.99	45.45	27.20
E-9-5-07	9.51	66.75	14.36	42.30	27.20
E-9-5-08	9.51	55.17	12.84	39.15	27.27
E-9-5-09	9.51	52.10	11.81	37.80	27.29

LEGEND      VBL UPSTREAM VELOCITY (V)

EFFECTS OF WALL EFFECTS ON SUPERACCELERATING HYDROFOILS OF FINITE SPAN

\*\*HYDROFOIL DATA IN NONDIMENSIONAL FORM (NO CORRECTIONS APPLIED)\*\*

TEST NO	ALPHA	CL	CD <sub>0.0C</sub>	CH	L/D	D/L	$R = 10^{6.6}$
8-9-5-01	9.51	0.7274	0.1066	0.0756	6.8254	0.1465	0.9686
8-9-5-02	9.51	0.6523	0.1037	0.0674	6.2927	0.1589	0.9676
8-9-5-03	9.51	0.5934	0.0997	0.0659	5.9497	0.1581	0.9666
8-9-5-04	9.51	0.5175	0.0924	0.0641	5.5980	0.1786	0.9672
8-9-5-05	9.51	0.4537	0.0849	0.0605	5.3869	0.1870	0.9652
8-9-5-06	9.51	0.3887	0.0748	0.0568	5.1802	0.1975	0.9629
8-9-5-07	9.51	0.3355	0.0666	0.0529	5.0376	0.1985	0.9629
8-9-5-08	9.51	0.2760	0.0567	0.0487	4.8715	0.2753	0.9652
8-9-5-09	9.51	0.2603	0.0534	0.0470	4.8715	0.2753	0.9659

LEGEND

ALPHA GEOMETRIC ANGLE OF ATTACK CORRECTED FOR SHAW'S TWIST  
 CL LIFT COEFFICIENT, NONDIMENSIONALIZED ON UPSTREAM VELOCITY AND MODEL PLATEFORM AREA  
 CD<sub>0.0C</sub> CD (UNCORRECTED). THE UNCORRECTED DRAG COEFFICIENT AS COMPUTED FROM MEASURED DRAG, AND nondimensionalized  
 ON UPSTREAM VELOCITY AND MODEL PLATEFORM AREA  
 CH BOREN'S COEFFICIENT, nondimensionalized on upstream velocity, model plateform area, and mean chord  
 L/D LIFT-TO-DRAG RATIO = CL/CD<sub>0.0C</sub>  
 D/L DRAG-TO-LIFT RATIO = CD<sub>0.0C</sub>/CL  
 R REYNOLDS NUMBER, BASED ON MEAN CHORD

SUPER INLES OF WALL EFFECTS ON SUPERCAVITATING HYDROFOILS OF FINITE SPAN

APPENDIX DATA CONNECTED FOR EFFECTS OF IMAGES OF TRAILING VORTICES SYSTEM

TEST NO.	ALPHAT	CL	CD	(D/L)	STICK/AT	SIGC/AT	CL/AT	CD/AT	SIGV	SIGC	CAVLTB	COMMENTS/REMARKS
A-9-5-01	9.94	0.727	0.112	0.076	0.154	3.529	3.285	0.192	3.722	0.316	0.612	0.570
A-9-5-02	9.90	0.652	0.100	0.067	0.166	3.187	2.950	0.177	3.623	0.300	0.551	0.510
A-9-5-03	9.46	0.593	0.103	0.065	0.174	2.883	2.653	0.448	3.491	0.383	0.496	0.457
A-9-5-04	9.82	0.518	0.095	0.068	0.188	2.478	2.256	0.021	3.245	0.378	0.425	0.387
A-9-5-05	9.78	0.454	0.087	0.060	0.192	2.194	2.025	0.659	2.989	0.350	0.379	0.346
A-9-5-06	9.74	0.385	0.076	0.057	0.199	1.839	1.723	2.268	2.685	0.338	0.312	0.293
A-9-5-07	9.71	0.336	0.066	0.053	0.202	1.536	1.430	1.981	2.362	0.312	0.260	0.242
A-9-5-08	9.67	0.276	0.057	0.059	0.208	1.158	1.061	1.635	2.017	0.269	0.195	0.179
A-9-5-09	9.66	0.260	0.054	0.047	0.208	0.987	0.901	1.594	1.904	0.279	0.166	0.152

UNLESS OTHERWISE INDICATED, ALL DATA ARE FOR:

1. SUPERCAVITATING FLOW.
2. BOTH STATIC PRESSURE TAPS OPEN.

LEGEND

- ONLY UPSTREAM STATIC PRESSURE TAP UTILIZED
- ONLY DOWNSTREAM STATIC PRESSURE TAP UTILIZED
- PC (P<sub>C</sub>) PARTIALLY CAVITATING
- PC (P<sub>C'</sub>) PARTIALLY CAVITATING (TAP WETTED)
- PW (P<sub>PW</sub>) FULLY WETTED
- AT (ALPHAT) (TURB) ANGLE OF ATTACK, CORRECTED FOR EFFECTS OF IMAGES OF TRAILING VORTICES
- AT2 ALPHAT-0.02
- SIGC CAVITATION NUMBER COMPUTED WITH MEASURED CAVITY PRESSURE
- SIGV CAVITATION NUMBER COMPUTED WITH CALCULATED VAPOR PRESSURE
- CD DRAG COEFFICIENT, CORRECTED FOR EFFECTS OF IMAGES OF TRAILING VORTICES
- (D/L) CORRECTED DRAG-TO-LIFT RATIO = CD/CL
- CAVLTB CAVITY LENGTH MEASURED FROM MIDCHORD AT CENTROID POSITION, NONDIMENSIONALIZED ON REAS CHORD  
(OBTAINED FROM PHOTOGRAPHS)

HYPHER TESTS OF HALL EFFECTS ON SUPERCAVITATING HYDROPOILS OF FINITE SPAN

HYDROPOIL INPUT DATA

TH	TT	AREA	SPAN	SAC
74	65	40.0	10.0	4.02

ZERO READINGS AND TUNNEL TEMP BEFORE AND AFTER

TEST NO	NAUTON	TT	2-B	3-B	3-B	TT
0.	0.0	0.0	0.0	100.0	0.0	100.0
0.	0.0	0.0	0.0	101.0	0.0	103.0
CENTER LBS/CF (NORMAL/ABOVE)	61-0.20000	62-0.20000	63-0.20000			
TEST NO	NAUTON	TT	2-B	3-B	3-B	TT
1417.	-810.0	R	134.3	R	728.0	
1439.	-856.0	R	129.0	R	775.0	
1438.	-886.0	R	123.5	R	826.0	
1425.	-886.0	R	121.0	R	833.0	
1416.	-790.0	R	119.5	R	825.0	
1407.	-728.0	R	118.5	R	803.0	
1400.	-654.0	R	118.0	R	767.0	
1397.	-576.0	R	117.0	R	723.0	
1390.	-512.0	R	116.0	R	677.0	
1388.	-446.0	R	115.5	R	617.0	
1383.	-396.0	R	114.5	R	568.0	
1377.	-346.0	R	114.0	R	525.0	
1377.	-306.0	R	113.0	R	482.0	
1380.	-290.0	R	112.8	R	466.0	
1377.	-746.0	R	135.5	R	298.0	
1378.	-726.0	R	135.5	R	692.0	
1373.	-698.0	R	132.0	R	680.0	
692.	-366.0	R	117.0	R	410.0	
360.	-194.0	R	110.0	R	265.0	

LEGEND  
TT TUNNEL " ( " )  
SPAN FOIL HALF-SPAN AREA (SQ IN)

TEST NO	NAUTON	TT	2-B	3-B	3-B	TT
B-11-01	1447.	R	134.3	R	728.0	
B-11-02	1439.	R	129.0	R	775.0	
B-11-03	1438.	R	123.5	R	826.0	
B-11-04	1425.	R	121.0	R	833.0	
B-11-05	1416.	R	119.5	R	825.0	
B-11-06	1407.	R	118.5	R	803.0	
B-11-07	1400.	R	118.0	R	767.0	
B-11-08	1397.	R	117.0	R	723.0	
B-11-09	1390.	R	116.0	R	677.0	
B-11-10	1388.	R	115.5	R	617.0	
B-11-11	1383.	R	114.5	R	568.0	
B-11-12	1377.	R	114.0	R	525.0	
B-11-13	1377.	R	113.0	R	482.0	
B-11-14	1380.	R	112.8	R	466.0	
B-11-15	1377.	R	135.5	R	298.0	
B-11-16	1378.	R	135.5	R	692.0	
B-11-17	1373.	R	132.0	R	680.0	
B-11-18	692.	R	117.0	R	410.0	
B-11-19	360.	R	110.0	R	265.0	

LEGEND  
TT TUNNEL " ( " )  
SPAN FOIL HALF-SPAN AREA (SQ IN)

TEST NO	NAUTON	TT	2-B	3-B	3-B	TT
B-11-01	1447.	R	134.3	R	728.0	
B-11-02	1439.	R	129.0	R	775.0	
B-11-03	1438.	R	123.5	R	826.0	
B-11-04	1425.	R	121.0	R	833.0	
B-11-05	1416.	R	119.5	R	825.0	
B-11-06	1407.	R	118.5	R	803.0	
B-11-07	1400.	R	118.0	R	767.0	
B-11-08	1397.	R	117.0	R	723.0	
B-11-09	1390.	R	116.0	R	677.0	
B-11-10	1388.	R	115.5	R	617.0	
B-11-11	1383.	R	114.5	R	568.0	
B-11-12	1377.	R	114.0	R	525.0	
B-11-13	1377.	R	113.0	R	482.0	
B-11-14	1380.	R	112.8	R	466.0	
B-11-15	1377.	R	135.5	R	298.0	
B-11-16	1378.	R	135.5	R	692.0	
B-11-17	1373.	R	132.0	R	680.0	
B-11-18	692.	R	117.0	R	410.0	
B-11-19	360.	R	110.0	R	265.0	

LEGEND  
TT TUNNEL " ( " )  
SPAN FOIL HALF-SPAN AREA (SQ IN)

TEST NO	NAUTON	TT	2-B	3-B	3-B	TT
B-11-01	1447.	R	134.3	R	728.0	
B-11-02	1439.	R	129.0	R	775.0	
B-11-03	1438.	R	123.5	R	826.0	
B-11-04	1425.	R	121.0	R	833.0	
B-11-05	1416.	R	119.5	R	825.0	
B-11-06	1407.	R	118.5	R	803.0	
B-11-07	1400.	R	118.0	R	767.0	
B-11-08	1397.	R	117.0	R	723.0	
B-11-09	1390.	R	116.0	R	677.0	
B-11-10	1388.	R	115.5	R	617.0	
B-11-11	1383.	R	114.5	R	568.0	
B-11-12	1377.	R	114.0	R	525.0	
B-11-13	1377.	R	113.0	R	482.0	
B-11-14	1380.	R	112.8	R	466.0	
B-11-15	1377.	R	135.5	R	298.0	
B-11-16	1378.	R	135.5	R	692.0	
B-11-17	1373.	R	132.0	R	680.0	
B-11-18	692.	R	117.0	R	410.0	
B-11-19	360.	R	110.0	R	265.0	

LEGEND  
TT TUNNEL " ( " )  
SPAN FOIL HALF-SPAN AREA (SQ IN)

TEST NO	NAUTON	TT	2-B	3-B	3-B	TT
B-11-01	1447.	R	134.3	R	728.0	
B-11-02	1439.	R	129.0	R	775.0	
B-11-03	1438.	R	123.5	R	826.0	
B-11-04	1425.	R	121.0	R	833.0	
B-11-05	1416.	R	119.5	R	825.0	
B-11-06	1407.	R	118.5	R	803.0	
B-11-07	1400.	R	118.0	R	767.0	
B-11-08	1397.	R	117.0	R	723.0	
B-11-09	1390.	R	116.0	R	677.0	
B-11-10	1388.	R	115.5	R	617.0	
B-11-11	1383.	R	114.5	R	568.0	
B-11-12	1377.	R	114.0	R	525.0	
B-11-13	1377.	R	113.0	R	482.0	
B-11-14	1380.	R	112.8	R	466.0	
B-11-15	1377.	R	135.5	R	298.0	
B-11-16	1378.	R	135.5	R	692.0	
B-11-17	1373.	R	132.0	R	680.0	
B-11-18	692.	R	117.0	R	410.0	
B-11-19	360.	R	110.0	R	265.0	

LEGEND  
TT TUNNEL " ( " )  
SPAN FOIL HALF-SPAN AREA (SQ IN)

TEST NO	NAUTON	TT	2-B	3-B	3-B	TT
B-11-01	1447.	R	134.3	R	728.0	
B-11-02	1439.	R	129.0	R	775.0	
B-11-03	1438.	R	123.5	R	826.0	
B-11-04	1425.	R	121.0	R	833.0	
B-11-05	1416.	R	119.5	R	825.0	
B-11-06	1407.	R	118.5	R	803.0	
B-11-07	1400.	R	118.0	R	767.0	
B-11-08	1397.	R	117.0	R	723.0	
B-11-09	1390.	R	116.0	R	677.0	
B-11-10	1388.	R	115.5	R	617.0	
B-11-11	1383.	R	114.5	R	568.0	
B-11-12	1377.	R	114.0	R	525.0	
B-11-13	1377.	R	113.0	R	482.0	
B-11-14	1380.	R	112.8	R	466.0	
B-11-15	1377.	R	135.5	R	298.0	
B-11-16	1378.	R	135.5	R	692.0	
B-11-17	1373.	R	132.0	R	680.0	
B-11-18	692.	R	117.0	R	410.0	
B-11-19	360.	R	110.0	R	265.0	

LEGEND  
TT TUNNEL " ( " )  
SPAN FOIL HALF-SPAN AREA (SQ IN)

TEST NO	NAUTON	TT	2-B	3-B	3-B	TT
B-11-01	1447.	R	134.3	R	728.0	
B-11-02	1439.	R	129.0	R	775.0	
B-11-03	1438.	R	123.5	R	826.0	
B-11-04	1425.	R	121.0	R	833.0	
B-11-05	1416.	R	119.5	R	825.0	
B-11-06	1407.	R	118.5	R	803.0	
B-11-07	1400.	R	118.0	R	767.0	
B-11-08	1397.	R	117.0	R	723.0	
B-11-09	1390.	R	116.0	R	677.0	
B-11-10	1388.	R	115.5	R	617.0	
B-11-11	1383.	R	114.5	R	568.0	
B-11-12	1377.	R	114.0	R	525.0	
B-11-13	1377.	R	113.0	R	482.0	
B-11-14	1380.	R	112.8	R	466.0	
B-11-15	1377.	R	135.5	R	298.0	
B-11-16	1378.	R	135.5	R	692.0	
B-11-17	1373.	R	132.0	R	680.0	
B-11-18	692.	R	117.0	R	410.0	
B-11-19	360.	R	110.0	R	265.0	

LEGEND  
TT TUNNEL " ( " )  
SPAN FOIL HALF-SPAN AREA (SQ IN)

TEST NO	NAUTON	TT	2-B	3-B	3-B	TT
B-11-01	1447.	R	134.3	R	728.0	
B-11-02	1439.	R	129.0	R	775.0	
B-11-03	1438.	R	123.5	R	826.0	
B-11-04	1425.	R	121.0	R	833.0	
B-11-05	1416.	R	119.5	R	825.0	
B-11-06	1407.	R	118.5	R	803.0	
B-11-07	1400.	R	118.0	R	767.0	
B-11-08	1397.	R	117.0	R	723.0	
B-11-09	1390.	R	116.0	R	677.0	
B-11-10	1388.	R	115.5	R	617.0	
B-11-11	1383.	R	114.5	R	568.0	
B-11-12	1377.	R	114.0	R	525.0	
B-11-13	1377.	R	113.0	R	482.0	
B-11-14	1380.	R	112.8	R	466.0	
B-11-15	1377.	R	135.5	R	298.0	
B-11-16	1378.	R	135.5	R	692.0	
B-11-17	1373.	R	132.0	R	680.0	
B-11-18	692.	R	117.0	R	410.0	
B-11-19	360.	R	110.0	R	265.0	

LEGEND  
TT TUNNEL " ( " )  
SPAN FOIL HALF-SPAN AREA (SQ IN)

TEST NO	NAUTON	TT	2-B	3-B	3-B	TT
B-11-01	1447.	R	134.3	R	728.0	
B-11-02	1439.	R	129.0	R	775.0	
B-11-03	1438.	R	123.5	R	826.0	
B-11-04	1425.	R	121.0	R	833.0	
B-11-05	1416.	R	119.5	R	825.0	
B-11-06	1407.	R	118.5	R	803.0	
B-11-07	1400.	R	118.0	R	767.0	
B-11-08	1397.	R	117.0	R	723.0	
B-11-09	1390.	R	116.0	R	677.0	

KIPIER THERES OF WALL EFFECTS ON SUPERCAPITATING HYDROPOILS OF PIBBLE SPAN

INPUT DATA CORRECTED FOR ZERO BEARINGS, SIGNS, AND HYDROSTATIC PRESSURE

BUN NO.	BAH03	61	62	63	PINP	PCAV
R-11,-01	1447.	-810.0	-36.3	-628.0	261.	191.
R-11,-02	1439.	-856.1	-26.9	-676.8	246.	82.
R-11,-03	1438.	-886.2	-23.4	-725.7	232.	52.
R-11,-04	1425.	-386.3	-20.8	-732.5	217.	68.
R-11,-05	1416.	-790.4	-19.3	-726.3	203.	55.
R-11,-06	1407.	-728.6	-18.2	-702.2	188.	44.
R-11,-07	1400.	-659.7	-17.7	-666.0	172.	63.
R-11,-08	1397.	-576.8	-16.6	-621.8	155.	41.
R-11,-09	1390.	-512.9	-15.6	-575.7	139.	39.
R-11,-10	1388.	-447.0	-15.0	-515.5	126.	33.
R-11,-11	1383.	-397.1	-11.9	-466.3	113.	33.
R-11,-12	1377.	-387.2	-11.4	-423.2	101.	32.
R-11,-13	1377.	-307.3	-12.3	-380.0	86.	22.
R-11,-14	1360.	-291.4	-10.1	-36.8	80.	32.
R-11,-15	1377.	-747.6	-36.2	-572.7	277.	—
R-11,-16	1378.	-727.7	-21.7	-579.5	306.	—
R-11,-17	1373.	-699.8	-31.1	-577.3	647.	—
R-11,-18	692.	-367.9	-16.1	-307.2	734.	—
R-11,-19	360.	-196.0	-9.0	-162.0	774.	—

BIPER INVES OF WALL EFFECTS ON SUPERCAVITATING HYDROPOILS OF PISITH SPAN

\*\*HYDROPOIL DATA REDUCTION\*\*

BUS NO	ALPHA	LIFT-LB	BRAG-LB	HOR-TENS	VRL-PBS
8-11-01	11.02	168.86	25.31	123.98	20.13
8-11-02	11.01	177.01	27.20	164.20	20.06
8-11-03	11.01	181.92	29.29	89.20	20.05
8-11-04	11.01	173.83	29.52	75.00	21.93
8-11-05	11.01	161.94	29.19	69.90	21.85
8-11-06	11.01	168.56	28.30	65.60	21.77
8-11-07	11.01	134.47	26.84	63.60	21.71
8-11-08	11.01	118.68	25.06	59.80	21.68
8-11-09	11.01	105.69	23.20	56.00	21.61
8-11-10	11.01	92.80	20.77	59.00	21.59
8-11-11	11.01	82.21	18.79	50.20	21.55
8-11-12	11.01	72.12	17.05	48.20	21.49
8-11-13	11.01	63.93	15.31	44.90	21.49
8-11-14	11.01	60.70	14.66	43.48	21.52
8-11-15	11.02	156.36	23.08	123.20	21.49
8-11-16	11.02	152.27	23.35	121.20	21.50
8-11-17	11.02	146.18	23.27	112.00	21.46
8-11-18	11.01	76.79	12.38	57.80	19.96
8-11-19	11.00	41.00	6.53	32.40	16.73

LEGEND

VEL. OF STREAM VELOCITY (ft)

SUPER INVIS OF WALL EFFECTS ON SUPERCAVITATING HYDROPOILS OF FINITE SPAN

••• HYDROPOIL DATA IN NONDIMENSIONAL FORM (NO CORRECTIONS APPLIED) •••

FIN NO	ALPHA	CL	CDUNC	CH	L/D	D/L
E-11.-01	11.02	0.796	0.1136	0.1445	6.9940	0.1820
E-11.-02	11.01	0.8170	0.1221	0.1226	6.7986	0.1471
E-11.-03	11.01	0.8668	0.1329	0.0991	6.5776	0.1584
E-11.-04	11.01	0.8216	0.1354	0.0890	6.1132	0.1636
E-11.-05	11.01	0.7774	0.1346	0.0829	5.7740	0.1732
E-11.-06	11.01	0.7173	0.1311	0.0788	5.4696	0.1828
E-11.-07	11.01	0.6523	0.1267	0.0767	5.2306	0.1912
E-11.-08	11.01	0.5769	0.1163	0.0723	4.9598	0.2016
E-11.-09	11.01	0.5161	0.1078	0.0680	4.7879	0.2089
E-11.-10	11.01	0.4519	0.0961	0.0657	4.7021	0.2127
E-11.-11	11.01	0.4038	0.0867	0.0613	4.6518	0.2150
E-11.-12	11.01	0.3553	0.0785	0.0591	4.5253	0.2210
E-11.-13	11.01	0.3150	0.0699	0.0588	4.3910	0.2221
E-11.-14	11.01	0.2985	0.0666	0.0532	4.4819	0.2231
E-11.-15	11.02	0.2703	0.1082	0.1510	7.1192	0.1405
E-11.-16	11.02	0.2796	0.1095	0.1488	6.8874	0.1460
E-11.-17	11.02	0.2721	0.1094	0.1376	6.5585	0.1516
E-11.-18	11.01	0.2776	0.1099	0.1348	6.5280	0.1532
E-11.-19	11.00	0.3038	0.1061	0.1384	6.5360	0.1507

LEGEND

ALPHA GEOMETRIC ANGLE OF ATTACK CORRECTED FOR SHAFT TWIST  
 CL LIFT COEFFICIENT, NONDIMENSIONALIZED ON UPSTREAM VELOCITY AND MODEL PLATEFORM AREA  
 CDUNC CL (UNCORRECTED), THE UNCORRECTED DRAG COEFFICIENT AS COMPUTED FROM MEASURED DRAG, AND NONDIMENSIONALIZED  
 ON UPSTREAM VELOCITY AND MODEL PLATEFORM AREA  
 CH MOMENT COEFFICIENT, NONDIMENSIONALIZED ON UPSTREAM VELOCITY, MODEL PLATEFORM AREA, AND Mean CHORD  
 L/D LIFT-TO-DRAG RATIO = CL/CDUNC  
 D/L DRAG-TO-LIFT RATIO = CDUNC/CL  
 RE REYNOLDS NUMBER, BASED ON Mean CHORD

EFFECTS OF WALL EFFECTS ON SUPERCAVITATING HYDROPOILS OF FINITE SPAN

\*\*PRIORITY DATA CORRECTED FOR EFFECTS OF IMAGES OF TRAILING VORTEX SYSTEM\*\*

BUN NO	ALPHAT	CL	CD	CN	(D/L)	SIGC/AT	CL/AT	CD/AT2	CH/AT	SIGV	SIGC	CAVLTH	COMMENTS/REMARKS
R-11-01	11.49	0.759	0.120	0.145	0.151	4.217	1.276	3.961	2.987	0.721	0.846	0.256	PC
R-11-02	11.51	0.837	0.130	0.123	0.156	3.954	2.991	4.166	3.230	0.610	0.795	0.601	0.65
R-11-03	11.52	0.661	0.141	0.099	0.163	3.694	3.281	4.280	3.475	0.493	0.743	0.660	0.63
R-11-04	11.50	0.828	0.143	0.069	0.172	3.452	3.113	4.122	3.535	0.443	0.693	0.625	0.64
R-11-05	11.47	0.777	0.141	0.083	0.181	3.219	2.935	3.882	3.514	0.414	0.644	0.588	0.66
R-11-06	11.44	0.717	0.137	0.079	0.190	2.963	2.700	3.594	3.426	0.395	0.591	0.539	0.66
R-11-07	11.40	0.652	0.129	0.077	0.198	2.681	2.439	3.279	3.263	0.386	0.533	0.485	0.72
R-11-08	11.35	0.577	0.120	0.072	0.208	2.371	2.169	3.051	3.165	0.470	0.430	0.79	
R-11-09	11.32	0.516	0.111	0.068	0.214	2.079	1.919	2.895	3.054	0.411	0.379	0.73	
R-11-10	11.28	0.452	0.098	0.066	0.217	1.835	1.793	2.596	2.536	0.334	0.361	0.353	1.10
R-11-11	11.25	0.403	0.088	0.061	0.219	1.591	1.553	2.055	2.294	0.312	0.312	0.305	1.40
R-11-12	11.22	0.355	0.080	0.059	0.225	1.363	1.349	1.815	2.082	0.302	0.267	0.264	1.75
R-11-13	11.19	0.315	0.071	0.054	0.225	1.069	1.059	1.612	1.860	0.279	0.209	0.207	2.80
R-11-14	11.18	0.296	0.066	0.053	0.226	0.947	0.941	1.529	1.772	0.212	0.185	0.184	3.25
R-11-15	11.43	0.770	0.114	0.151	0.146	-----	-----	3.846	2.851	0.754	-----	-----	PC(TV)
R-11-16	11.46	0.750	0.115	0.148	0.154	-----	-----	3.747	2.881	0.742	-----	-----	PC(TV)
R-11-17	11.45	0.722	0.115	0.138	0.159	-----	-----	3.615	2.878	0.689	-----	-----	PW
R-11-18	11.44	0.718	0.115	0.134	0.161	-----	-----	3.596	2.894	0.673	-----	-----	PW
R-11-19	11.42	0.704	0.111	0.138	0.158	-----	-----	3.530	2.798	0.694	-----	-----	PW

UNLESS OTHERWISE INDICATED, ALL DATA ARE FOR:

1. SUPERCAVITATING FLOW.
2. BOTH STATIC PRESSURE TAPS OPEN.

LEGEND

- \* ONLY UPSTREAM STATIC PRESSURE TAP UTILIZED
- \* ONLY DNSTREAM STATIC PRESSURE TAP UTILIZED
- PC PARTIALLY CAVITATING
- PC(TV) PARTIALLY CAVITATING (TAP WETTED)
- PW FULLY WETTED

AT (ALPHAT) (TRUE) ANGLE OF ATTACK, CORRECTED FOR EFFECTS OF IMAGES OF TRAILING VORTICES  
AT2 ALPHAT\*2

SIGC CAVITATION NUMBER COMPUTED WITH MEASURED CAVITY PRESSURE  
SIGV CAVITATION NUMBER COMPUTED WITH CALCULATED VAPOR PRESSURE  
CD DRAG COEFFICIENT, CORRECTED FOR EFFECTS OF IMAGES OF TRAILING VORTICES  
(D/L) CORRECTED DRAG-TO-LIFT RATIO = CD/CL  
CAVLTH CAVITY LENGTH MEASURED FROM MIDCHORD AT CENTROID POSITION, NONDIMENSIONALIZED ON MEAN CHORD  
(OBTAINED FROM PHOTOGRAPHS)

## EXPERIMENTAL WALL EFFECTS ON SUPERCAVITATING HYDROFOILS OF FINITE SPAN

HIDROFOIL INPUT DATA  
 TB TT AREA SPAN MAC  
 78 95 40.0 10.0 4.02

## ZERO READINGS AND TUNNEL TEMP SUPPORT AND AFTER

RUN NO. 1-N 1-R 2-N 2-R 3-N 3-R TT  
 U. 0.0 0.0 100.0 0.0 100.0 94.0  
 0. 0.0 0.0 100.5 0.0 100.0 96.0  
 CELL LBS/CT (NOSEAL/REV) 01=0.20000 02=0.20000 03=0.04030  
 TWIST= 7200.0 SHFT DIA.= 1.50IN

\*\*INPUT DATA AS RECORDED\*\*

RUN NO.	MANO	S	#1	S	#2	S	#3	PINP	PCAV
R-12-01	1297.	-830.0	R	121.0	R	890.0	R	245.	63.
R-12-02	1267.	-746.0	R	119.0	R	870.0	R	220.	59.
R-12-03	1282.	-682.0	R	118.0	R	832.0	R	203.	55.
R-12-04	1277.	-590.0	R	117.0	R	770.0	R	181.	53.
R-12-05	1276.	-508.0	R	116.0	R	708.0	R	161.	49.
R-12-06	1271.	-434.0	R	115.0	R	638.0	R	146.	44.
R-12-07	1270.	-402.0	R	114.5	R	598.0	R	133.	43.
R-12-08	1272.	-348.0	R	113.8	R	547.0	R	119.	43.
R-12-09	1272.	-312.0	R	113.0	R	507.0	R	109.	43.
R-12-10*	1274.	-296.0	R	112.5	R	487.0	R	109.	44.
R-12-11*	1257.	-326.0	R	113.2	R	523.0	R	103.	44.
R-12-12	1275.	-292.0	C	112.5	R	483.0	R	101.	44.
R-12-13	1278.	-282.0	C	112.3	R	470.0	R	90.	44.
R-12-14*	1273.	-292.0	R	112.5	R	480.0	R	89.	44.

## LEGEND TB BOOM TEMPER (DEG FAHR)

TT TUNNEL ( " )

APEA HALF-SPAN MODEL PLANFORM AREA (SQ IN)

SPAN POIL HALF-SPAN (IN)

MAC MEAN CHORD, MEAS. @ MODEL CENTROID (IN)

MANO VELOCITY MANOMETER READING (MM)

TWIST SHAFT TWIST (DEGREES/N-LB)

S LOAD CELL POLARITY (N=NORMAL, R=REVERSE)

LOAD CELL #1 LIFT (COUNTS)

#2 MOMENT ABOUT MIDCHORD (COUNTS)

PINP STATIC PRESSURE (MM HG)

PCAV CAVITY PRESSURE (MM HG)

RUN NO Q-XXX-YY: Q=POIL TESTED(S=SMALL, N=MED, I=LARGE)

III=GEOMETRIC ATTACK ANGLE (DEGREES)

YY=RUN NUMBER, THIS POIL @ THIS ANGLE

EFFECTS OF WALL EFFECTS ON SUPERCAVITATING HYDROPOOLS OF FINITE SPAN

INPUT DATA CORRECTED FOR ZERO READINGS, SIGNS, AND HYDROSTATIC PRESSURE

RUN NO	RAW DATA	01	02	03	PINP	PCAV
R-12--01	1297.	-830.0	-21.0	-790.0	229.	63.
R-12--02	1287.	-748.0	-19.0	-770.0	209.	59.
R-12--03	1282.	-682.0	-17.9	-732.0	192.	55.
R-12--04	1277.	-590.0	-16.9	-670.0	170.	53.
R-12--05	1276.	-508.0	-15.8	-608.0	150.	49.
R-12--06	1271.	-434.0	-14.8	-538.0	135.	44.
R-12--07	1270.	-402.0	-14.3	-498.0	122.	43.
R-12--08	1272.	-348.0	-13.5	-447.0	109.	42.
R-12--09	1272.	-312.0	-12.7	-407.0	98.	43.
R-12--10	1274.	-296.0	-12.2	-387.0	44.	44.
R-12--11	1267.	-326.0	-12.8	-423.0	97.	44.
R-12--12	1275.	-292.0	-12.1	-383.0	90.	44.
R-12--13	1278.	-282.0	-11.8	-370.0	79.	44.
R-12--14	1273.	-292.0	-12.0	-380.0	76.	44.

RIPER 100% OF WALL EFFECTS ON SUPERCAVITATING HYDROFOILS OF FINITE SPAN

\*\*HYDROFOIL DATA REDUCTIONS\*\*

BLW NO	ALPHA	LIFT-LB	DRAG-LB	BON-IMLBS	VEL-PPS
8-12-01	12.31	170.20	31.84	75.60	26.73
8-12-02	12.01	153.39	31.03	68.26	26.63
8-12-03	12.01	139.98	29.50	64.52	26.59
8-12-04	12.01	121.38	27.00	60.78	26.54
8-12-05	12.01	104.77	28.50	57.05	26.53
8-12-06	12.01	89.76	21.68	53.31	26.48
8-12-07	12.01	63.25	20.07	51.37	26.47
8-12-08	12.01	72.31	18.01	46.71	26.49
8-12-09	12.01	64.94	16.40	45.69	26.49
8-12-10	12.01	61.63	15.60	43.75	26.51
8-12-11	12.01	67.76	17.05	46.14	26.44
8-12-12	12.01	60.02	15.43	43.48	26.52
8-12-13	12.01	58.77	14.91	42.62	26.55
8-12-14	12.01	60.80	15.31	43.20	26.50

LEGEND VEL UPSTREAM VELOCITY (U)

**PIPER INLES OF WALL EFFECTS ON SUPERCAVITATING HYDROFOILS OF FINITE SPAN**

**\*\*HYDROFOIL DATA IN NONDIMENSIONAL FORM (NO CORRECTIONS APPLIED)\*\*\***

RUN NO.	ALPHA	CL	CDUNC	CH	L/D	D/L	Re <sup>10<sup>6</sup></sup>
B-12--01	12.01	0.6863	0.1607	0.0982	5.5274	0.1809	1.1051
B-12--02	12.01	0.8064	0.1577	0.0893	5.1143	0.1955	1.1011
B-12--03	12.01	0.7386	0.1502	0.0887	4.9178	0.2033	1.0992
B-12--04	12.01	0.6427	0.1375	0.0801	4.6738	0.2140	1.0972
B-12--05	12.01	0.5552	0.1289	0.0752	4.4636	0.2240	1.0966
B-12--06	12.01	0.4774	0.1098	0.0705	4.3459	0.2301	1.0968
B-12--07	12.01	0.4431	0.1014	0.0680	4.3719	0.2287	1.0966
B-12--08	12.01	0.3843	0.0903	0.0644	4.2567	0.2389	1.0952
B-12--09	12.01	0.3451	0.0817	0.0609	4.2238	0.2368	1.0952
B-12--10	12.01	0.3271	0.0773	0.0578	4.2308	0.2364	1.0960
B-12--11	12.01	0.3615	0.0855	0.0612	4.2292	0.2365	1.0932
B-12--12	12.01	0.3225	0.0764	0.0574	4.2218	0.2369	1.0964
B-12--13	12.01	0.3110	0.0734	0.0561	4.2342	0.2362	1.0976
B-12--14	12.01	0.3229	0.0759	0.0571	4.2560	0.2350	1.0956

**LEGEND**

ALPHA GEOMETRIC ANGLE OF ATTACK CORRECTED FOR SHAFT TWIST  
 CL LIFT COEFFICIENT, NONDIMENSIONALIZED ON UPSTREAM VELOCITY AND MODEL PLANFORM AREA  
 CDUNC CD (UNCORRECTED). THE UNCORRECTED DRAG COEFFICIENT AS COMPUTED FROM MEASURED DRAG, AND NONDIMENSIONALIZED  
 ON UPSTREAM VELOCITY AND MODEL PLANFORM AREA  
 CH DOWNTWIST COEFFICIENT, NONDIMENSIONALIZED ON UPSTREAM VELOCITY, MODEL PLANFORM AREA, AND MEAN CHORD  
 L/D LIFT-TO-DRAG RATIO = CL/CD<sub>TCRC</sub>  
 D/L DRAG-TO-LIFT RATIO = CD<sub>TCRC</sub>/CL  
 RE REYNOLDS NUMBER, BASED ON MEAN CHORD

**EFFECTS OF HALL EFFECTS ON SUPERCAVITATING HYDROPOOLS OF FINITE SPAN**

**••• PATOR DATA CORRECTED FOR EFFECTS OF TRAILING VORTEX SYSTEM •••**

RUN NO	ALPHAT	CL	CD	CH	(D/L)	SIGV/AT	SIGC/AT	CL/AT	CD/AT2	CH/AT	SIGV	SIGC	CAVTH	COMMENTS/REMARKS
B-12--0 1	12.54	0.880	0.169	0.098	0.190	2.975	0.059	3.326	0.448	0.741	0.651	0.65		
B-12--0 2	12.49	0.806	0.168	0.089	0.208	3.138	2.800	3.699	0.460	0.688	0.619	0.69		
B-12--0 3	12.45	0.739	0.156	0.085	0.111	2.837	2.579	3.399	0.301	0.390	0.616	0.560	0.71	
B-12--0 4	12.39	0.683	0.182	0.080	0.221	2.460	2.222	2.972	0.312	0.370	0.528	0.480	0.82	
B-12--0 5	12.34	0.555	0.128	0.075	0.230	2.068	1.928	2.578	0.349	0.445	0.415	0.98		
B-12--0 6	12.29	0.477	0.112	0.071	0.235	1.792	1.751	2.225	0.338	0.329	0.384	0.376	1.12	
B-12--0 7	12.27	0.483	0.103	0.068	0.233	1.542	1.522	2.069	0.354	0.318	0.330	0.326	1.55	
B-12--0 8	12.24	0.384	0.092	0.064	0.239	1.271	1.257	1.799	0.302	0.271	0.268	0.268		
B-12--0 9	12.21	0.385	0.083	0.060	0.240	1.077	1.067	1.619	1.826	0.283	0.230	0.227	2.69	
B-12--10*	12.20	0.327	0.078	0.058	0.240	1.073	1.047	1.536	1.729	0.271	0.228	0.223	3.57	
B-12--11*	12.22	0.361	0.087	0.061	0.240	1.053	1.031	1.694	1.908	0.287	0.225	0.220	---	
B-12--12	12.20	0.322	0.077	0.057	0.240	0.910	0.892	1.515	1.709	0.269	0.194	0.190	---	
B-12--13	12.19	0.311	0.074	0.056	0.239	0.693	0.679	1.461	1.644	0.264	0.147	0.144	4.65	
B-12--14*	12.20	0.323	0.077	0.057	0.238	0.672	0.662	1.517	1.698	0.268	0.143	0.141	---	

UNLESS OTHERWISE INDICATED, ALL DATA ARE FOR:

1. SUPERCAVITATING FLOW.
2. BOTH STATIC PRESSURE TAPS OPEN.

**LEGEND**

- ONLY UPSTREAM STATIC PRESSURE TAP UTILIZED
- ONLY DOWNTAP STATIC PRESSURE TAP UTILIZED
- PC PARTIALLY CAVITATING
- PC(TU) PARTIALLY CAVITATING (TAP BOTTED)
- PW PARTIALLY BRETTED
- AT (ALPHAT) (TRUE) ANGLE OF ATTACK, CORRECTED FOR EFFECTS OF IMAGES OF TRAILING VORTICES
- AT2 ALPHAT\*\*2
- SIGC CAVITATION NUMBER COMPUTED WITH MEASURED CAVITY PRESSURE
- SIGV CAVITATION NUMBER COMPUTED WITH CALCULATED VAPOR PRESSURE
- CD DRAG COEFFICIENT, CORRECTED FOR EFFECTS OF IMAGES OF TRAILING VORTICES
- (D/L) CORRECTED DRAG-TO-LIFT RATIO = CD/CL
- CAVTH CAVITY LENGTH MEASURED FROM MIDCHORD AT CENTROID POSITION, NONDIMENSIONALIZED ON NEAR CHORD  
(OBTAINED FROM PHOTOGRAPHS)

ZIPPER TUNNEL EFFECTS ON SUPERCAVITATING HYDROPOOLS OF FINITE SPAN

HYDROPOOL INPUT DATA

TT	AREA	SPAN	HAC
77	90	40.0	4.02

ZERO BEATINGS AND TUNNEL TRAP REPORT AND AFTER

DATA	1-A	2-A	2-B	3-A	3-B	TT
0.	0.0	0.0	0.0	100.0	0.0	100.0
0.	0.0	0.0	0.0	99.5	0.0	110.0
CBL LBS/CT(NORMAL/REV)	01-0.20000	02-0.20000	03-0.04030			
TUNST- 7200.0 SHARP DIA.- 1.5013						

OUTPUT DATA AS RECORDED\*

RUN NO	HAC/H	S	01	S	02	S	03	PIMP	PCAV
B-14--01	802.		-550.0		127.0		617.0	722.	722.
B-14--02	1183.		-790.0		139.0		886.0	676.	722.
B-14--03	1526.		-996.0		149.5		1045.0	638.	722.
B-14--04	1630.		-956.0		187.5		988.0	449.	722.
B-14--05	1613.		-968.0		146.5		986.0	395.	722.
B-14--06	1409.		-1000.0		143.0		1045.0	357.	722.
B-14--07	1397.		-1022.0		133.4		1175.0	318.	136.
B-14--08	1380.		-1042.0		127.4		1204.0	293.	87.
B-14--09	1381.		-1004.0		125.0		1209.0	279.	77.
B-14--10	1375.		-950.0		123.0		1195.0	264.	69.
B-14--11	1372.		-890.0		122.0		1170.0	248.	64.
B-14--12	1366.		-828.0		121.0		1135.0	234.	62.
B-14--13	1361.		-754.0		120.0		1075.0	216.	55.
B-14--14	1362.		-696.0		119.5		1025.0	203.	53.
B-14--15	1358.		-660.0		118.6		973.0	189.	50.
B-14--16	1359.		-578.0		118.0		912.0	173.	46.
B-14--17	1357.		-534.0		117.5		860.0	160.	41.
B-14--18	1353.		-452.0		116.0		762.0	136.	39.
B-14--19	1352.		-196.0		115.0		688.0	118.	39.
B-14--20	1353.		-366.0		114.5		650.0	109.	39.
B-14--21	455.		-260.0		107.0		643.0	110.	45.
B-14--22	988.		-600.0		115.6		659.0	105.	55.
B-14--23	992.		-664.0		132.6		735.0	706.	722.

LEGEND

TR ROOM TEMPER (DEG FAREN)

TT TUNNEL ( " )

AREA HALF-SPAN MODEL PLATEFORM AREA (SQ IN)

SPAN POIL HALF-SPAN (IN)

HAC ROLL CHORD, MEAS. A MODEL CENTROID (IN)

RANS VELOCITY MACHINERIE READING (IN)

SHARP TWIST (DEGREES/IN-LB)

TWIST TWIST (DEGREES/IN-LB)

LOAD CELL POLARITY (+-NORMAL, -REVERSE)

LOAD CELL 0 LIFT (COUNTERS)  
02 HORNET ABOUT RIOCHORD (COUNTERS)

PIMP STATIC PRESSURE (IN HG)

PCAV CAVITY PRESSURE (IN HG)

RUN NO Q-XII-VI: Q=POLE TESTED(S=SHALL, H=RED, L=LARGE)  
XIX-GEOSTATIC ATTACK ANGLE (DEGREES)

WT=RUN NUMBER, THIS POLE & THIS ANGLE

INPUT DATA OF WALL EFFECTS ON SUPERCHARGING HYDROPOOLS OF PISITE SPAN

INPUT DATA CORRECTED FOR ZONE READINGS, SIGNS, AND HYDROSTATIC PRESSURE

ROW NO	BARON	01	02	03	PIWP	PCAV
-10,-01	802.	-550.0	-27.0	-517.0	711.	---
-10,-02	1083.	-790.0	-39.0	-745.5	665.	---
-10,-03	1526.	-996.0	-99.5	-996.1	627.	---
-10,-04	1430.	-956.0	-74.6	-956.6	438.	---
-10,-05	1613.	-968.0	-76.6	-982.2	380.	---
-10,-06	1609.	-1000.0	-73.1	-1042.7	346.	---
-10,-07	1397.	-1062.0	-72.5	-1072.3	136.	---
-10,-08	1380.	-1042.0	-727.6	-1100.8	307.	---
-10,-09	1381.	-1004.0	-725.2	-1055.4	282.	---
-10,-10	1375.	-950.0	-723.2	-1010.9	268.	---
-10,-11	1372.	-900.0	-722.2	-1065.5	251.	---
-10,-12	1366.	-828.0	-721.2	-1030.0	237.	66
-10,-13	1361.	-754.0	-720.3	-969.5	223.	62
-10,-14	1362.	-696.0	-719.8	-919.1	205.	55
-10,-15	1358.	-640.0	-718.9	-866.6	192.	53
-10,-16	1359.	-578.0	-718.3	-805.2	178.	50
-10,-17	1357.	-534.0	-717.2	-752.7	162.	46
-10,-18	1352.	-452.0	-716.7	-654.3	149.	41
-10,-19	1352.	-396.0	-715.7	-579.8	125.	35
-10,-20	1353.	-266.0	-714.9	-501.4	107.	35
-10,-21	635.	-260.0	-713.5	-333.9	98.	35
-10,-22	966.	-660.0	-716.1	-749.5	78.	35
-10,-23	922.	-656.0	-731.1	-625.0	693.	---

INPUT VALUES OF WALL EFFECTS ON SUPERELEVATING HYDROPOLES OF PIVOT SPAN

CONTINUOUS DATA SELECTIONS

SEG NO	LIFT-LB	DRAG-LB	SEG-THD VEL-PPS
S-10,-01	115.40	20.84	97.26
S-10,-02	165.60	30.05	100.48
S-10,-03	10.02	20.11	25.61
S-10,-04	10.02	20.71	28.63
S-10,-05	10.02	20.92	25.55
S-10,-06	10.02	20.62	37.99
S-10,-07	10.02	21.19	155.21
S-10,-08	10.02	21.91	120.73
S-10,-09	10.01	20.5.68	46.36
S-10,-10	10.01	19.64	99.21
S-10,-11	10.01	182.45	43.96
S-10,-12	10.01	169.85	42.94
S-10,-13	10.01	150.85	41.51
S-10,-14	10.01	183.16	39.07
S-10,-15	10.01	121.78	37.05
S-10,-16	10.01	121.78	71.26
S-10,-17	10.01	119.27	34.93
S-10,-18	10.01	110.37	32.95
S-10,-19	10.01	62.28	30.33
S-10,-20	10.01	76.19	26.37
S-10,-21	10.00	62.28	23.37
S-10,-22	10.01	76.19	55.47
S-10,-23	10.02	139.82	21.82
			53.75
			27.26
			60.11
			27.30
			60.31
			27.30
			58.99
			27.36
			27.25
			55.47
			27.25
			26.68
			16.42
			23.55
			57.88
			23.59
			119.16
			23.59

SEGNO      VEL. OPERATOR VELOCITY (ft)

UPPER LIPSTICK EFFECTS ON SUPERCAVITATING HYDROFOILS OF FINITE SPAN

\*\*HYDROFOIL DATA IN NONDIMENSIONAL FORM (NO CORRECTIONS APPLIED)\*\*

2000 SD	ALPHA	CL	CD <sub>HC</sub>	CL <sub>HC</sub>	D/D	D/L	B <sup>0.10446</sup>
8-10.-01	10.01	0.9815	0.1603	0.1973	5.7296	0.1785	0.8493
8-10.-02	10.02	0.9222	0.1652	0.1986	5.7028	0.1754	0.0176
8-10.-03	10.02	0.9376	0.1652	0.1989	5.6767	0.1762	1.1456
8-10.-04	10.02	0.9561	0.1648	0.2029	5.6031	0.1723	1.1115
8-10.-05	10.02	0.9778	0.1658	0.2010	5.5954	0.1696	1.1053
8-10.-06	10.02	1.0075	0.1780	0.1865	5.5595	0.1777	1.1039
8-10.-07	10.02	1.0666	0.2069	0.1462	5.3055	0.1921	1.0995
8-10.-08	10.01	1.0533	0.2130	0.1215	8.9555	0.2022	1.0932
8-10.-09	10.01	1.0228	0.2137	0.1110	8.7388	0.2110	1.0936
8-10.-10	10.01	0.9616	0.2117	0.1027	8.5616	0.2202	1.0914
8-10.-11	10.01	0.9332	0.2071	0.0935	4.3612	0.2293	1.0903
8-10.-12	10.01	0.8643	0.2009	0.0946	4.0332	0.2379	1.0881
8-10.-13	10.01	0.7724	0.1894	0.0906	8.0776	0.2152	1.0862
8-10.-14	10.01	0.7336	0.1792	0.0884	3.9330	0.2511	1.0866
8-10.-15	10.01	0.6587	0.1591	0.0847	3.0953	0.2567	1.0851
8-10.-16	10.01	0.5557	0.1566	0.0820	3.0039	0.2629	1.0855
8-10.-17	10.01	0.3520	0.1462	0.0800	3.7745	0.2689	1.0847
8-10.-18	10.01	0.4698	0.1268	0.0736	3.7061	0.2698	1.0832
8-10.-19	10.01	0.4129	0.1118	0.0693	3.9336	0.2707	1.0829
8-10.-20	10.01	0.3821	0.1039	0.0671	3.6756	0.2720	1.0832
8-10.-21	10.00	0.7396	0.1802	0.0923	8.1048	0.2136	0.6524
8-10.-22	10.01	0.9280	0.1975	0.0967	8.9350	0.2386	0.9358
8-10.-23	10.02	0.3533	0.1630	0.1984	5.7249	0.1747	0.9376

LAWSON

ALPHA GEOMETRIC ANGLE OF ATTACK CORRECTED FOR SMART TWIST  
 CL LIFT COEFFICIENT. nondimensionalized on upstream velocity and model planform area.  
 CD<sub>HC</sub> CD (uncorrected). THE UNCORRECTED DRAG COEFFICIENT AS COMPUTED FROM ASSURED DRAG, AND nondimensionalized  
 ON UPSTREAM VELOCITY AND MODEL PLANFORM AREA  
 CL AERODYNAMIC COEFFICIENT. nondimensionalized on upstream velocity. MODEL PLANFORM AREA, AND REYNOLD CHORD  
 D/D LIFT-TO-DRAG RATIO = CL/CD<sub>HC</sub>  
 D/L BRAD-TO-LIFT RATIO = CD<sub>HC</sub>/CL  
 B ARTHOLES NUMBER. BASED ON AREA CHORD

**REPORT ISSUES OF WALL EFFECTS ON SUPERCAVITATING HYDROFOILS OF PIVOT SPAN**

**\*APPENDIX DATA CORRECTED FOR EFFECTS OF IMAGES OF TRAILING VORTEX SYSTEM\***

TEST NO	ALPHAT	CL	CD	CA	(D/L)	SIGM/AT	SIGG/AT	CL/AT	CD/AT	SIGT	SIGC	CAVLT	COMMENTS/REMARKS	
													PW	PW
B-10,-01	10.57	0.942	0.174	0.197	0.189	---	---	3.701	2.692	0.776	---	---	---	---
B-10,-02	10.59	0.942	0.174	0.199	0.185	---	---	3.702	2.694	0.780	---	---	---	---
B-10,-03	10.59	0.938	0.174	0.199	0.185	---	---	3.684	2.691	0.782	---	---	---	---
B-10,-04	10.59	0.956	0.174	0.198	0.203	---	---	3.754	2.686	0.797	---	---	---	PC (PW)
B-10,-05	10.61	0.977	0.176	0.201	0.180	---	---	3.634	2.704	0.788	---	---	---	PC (PW)
B-10,-06	10.62	1.008	0.189	0.186	0.187	---	---	3.918	2.896	0.731	---	---	---	PC (PW)
B-10,-07	10.65	1.067	0.217	0.146	0.203	0.020	2.522	6.171	3.314	0.572	0.628	0.685	0.65	---
B-10,-08	10.66	1.053	0.225	0.122	0.213	0.693	2.911	6.122	3.438	0.616	0.744	0.662	0.62	---
B-10,-09	10.62	1.013	0.224	0.111	0.222	1.886	2.854	3.970	3.488	0.689	0.728	0.63	0.62	---
B-10,-10	10.58	0.962	0.221	0.103	0.230	3.277	2.767	3.778	3.416	0.603	0.824	0.604	0.64	---
B-10,-11	10.55	0.903	0.216	0.099	0.239	3.007	2.614	3.557	3.343	0.388	0.778	0.664	0.68	---
B-10,-12	10.51	0.864	0.208	0.095	0.247	2.850	2.440	3.333	3.246	0.323	0.722	0.620	0.70	---
B-10,-13	10.47	0.772	0.196	0.091	0.259	2.590	2.296	3.359	3.259	0.654	0.580	0.90	0.90	---
B-10,-14	10.46	0.719	0.194	0.088	0.258	2.391	2.132	2.906	2.951	0.602	0.517	0.88	0.88	---
B-10,-15	10.40	0.659	0.174	0.085	0.264	2.186	1.973	2.620	2.748	0.337	0.589	0.916	0.90	---
B-10,-16	10.36	0.596	0.160	0.082	0.269	1.938	1.792	2.376	2.550	0.327	0.486	0.849	1.15	---
B-10,-17	10.34	0.552	0.149	0.080	0.271	1.719	1.674	2.206	2.386	0.320	0.415	0.819	1.30	---
B-10,-18	10.29	0.570	0.129	0.074	0.275	1.712	1.342	1.884	2.075	0.295	0.362	0.335	1.75	---
B-10,-19	10.25	0.613	0.114	0.069	0.275	1.092	1.066	1.660	1.835	0.218	0.272	0.265	2.65	---
B-10,-20	10.20	0.382	0.105	0.067	0.276	0.967	0.926	1.709	1.709	0.270	0.235	0.230	3.50	---
B-10,-21	10.16	0.740	0.186	0.092	0.251	2.005	2.303	2.934	2.924	0.366	0.657	0.581	0.75	---
B-10,-22	10.10	0.828	0.204	0.097	0.247	2.796	2.450	3.271	3.192	0.382	0.708	0.620	0.75	---
B-10,-23	10.07	0.933	0.172	0.198	0.184	---	---	3.670	3.660	0.700	---	---	---	---

UNLESS OTHERWISE INDICATED, ALL DATA ARE FOR:

1. SUPERCAVITATING FLOW.
2. BOTH STATIC PRESSURE TAPS OPEN.

**LEGEND**

- ONLY UPSTREAM STATIC PRESSURE TAP UTILISED
- ONLY DOWNTREAM STATIC PRESSURE TAP UTILISED
- PC PARTIALLY CAVITATING
- PC (PW) PARTIALLY CAVITATING (TAP RETTED)
- PW FULLY WETTED

**AT**

(ALPHAT)

AT2

ALPHA2=0.2

- SIGC CAVITATION NUMBER COMPUTED WITH MEASURED CAVITY PRESSURE  
 SIGG CAVITATION NUMBER COMPUTED WITH CALCULATED TURBINE PRESSURE  
 CD DRAG COEFFICIENT, CORRECTED FOR EFFECTS OF IMAGES OF TRAILING VORTICES  
 (D/L) CORRECTED DRAG-TO-LIFT RATIO = CD/CL  
 CAVLT CAVITY LENGTH MEASURED FROM MIDCHORD AT CENTRODE POSITION, NORMALIZED ON MEAN CHORD  
 (OBTAINED FROM PHOTOGRAPHS)

INPUT VALUES OF WALL EFFECTS ON SUPERERUPTING HYDROPOOLS OF PLATE SPAN

HYPOTHETICAL INPUT DATA  
 TS TT AREA SPAN HAC  
 75 92 40.0 10.0 0.02

TSPO READINGS AND THERM. TEMP BEFORE AND AFTER

BARO 1-8 1-8 2-8 2-8 3-8 3-8  
 0. 0.0 0.0 100.0 0.0 100.0 89.5  
 0. 0.0 0.0 101.0 0.0 100.0 95.0  
 CELL LAS/CR (NORMAL/REV) 0-1=0.20000 0-2=0.20000 0-3=0.00030  
 TWIST= 7200.0 SWIFT DIA.= 1.5018

DISPOT DATA AS RECORDED\*

RUN NO	BARO	S	61	5	92	5	63	PIWP	PCAV
B-16-01	1451.	-1042.0	128.2	126.5	125.5	126.5	1516.0	293.	89.
B-16-02	1451.	-1042.0	128.2	126.5	125.5	126.5	1516.0	293.	79.
B-16-03	1451.	-1042.0	128.2	126.5	125.5	126.5	1516.0	293.	79.
B-16-04	1452.	-1042.0	128.2	126.5	125.5	126.5	1516.0	293.	79.
B-16-05	1452.	-1042.0	128.2	126.5	125.5	126.5	1516.0	293.	79.
B-16-06	1452.	-1042.0	128.2	126.5	125.5	126.5	1516.0	293.	79.
B-16-07	1452.	-1042.0	128.2	126.5	125.5	126.5	1516.0	293.	79.
B-16-08	1452.	-1042.0	128.2	126.5	125.5	126.5	1516.0	293.	79.
B-16-09	1385.	-678.0	122.0	121.0	121.0	121.0	1159.0	195.	49.
B-16-10	1379.	-612.0	122.0	121.0	121.0	121.0	1074.0	179.	45.
B-16-11	1377.	-552.0	120.0	120.0	120.0	120.0	983.0	161.	42.
B-16-12	1377.	-522.0	119.0	119.0	119.0	119.0	941.0	152.	41.
B-16-13	1369.	-484.0	118.5	118.5	118.5	118.5	891.0	141.	40.
B-16-14	1369.	-450.0	118.0	118.0	118.0	118.0	837.0	129.	40.
B-16-15	1367.	-410.0	117.0	117.0	117.0	117.0	775.0	111.	42.
B-16-16	1396.	-672.0	121.3	121.3	121.3	121.3	1156.0	198.	42.
B-16-17	1395.	-630.0	122.8	122.8	122.8	122.8	1329.0	237.	63.
B-16-18	1395.	-610.0	122.9	122.9	122.9	122.9	1308.0	238.	62.
B-16-19	1391.	-550.0	123.4	123.4	123.4	123.4	1353.0	238.	62.
B-16-20	619.	-222.0	109.3	109.3	109.3	109.3	470.0	93.	44.
B-16-21	279.	-178.0	106.0	106.0	106.0	106.0	358.0	96.	44.
B-16-22	550.	-180.0	111.0	111.0	111.0	111.0	635.0	137.	55.
B-16-23	722.	-488.0	113.9	113.9	113.9	113.9	795.0	159.	57.
B-16-24	966.	-1330.0	117.5	117.5	117.5	117.5	1007.0	190.	61.
B-16-25	1181.	-752.0	121.0	121.0	121.0	121.0	1193.0	218.	62.
B-16-26	1423.	-912.0	125.0	125.0	125.0	125.0	1922.0	253.	65.
B-16-27	1429.	-1058.0	125.2	125.2	125.2	125.2	1224.0	642.	—
B-16-28	722.	-560.0	127.0	127.0	127.0	127.0	698.0	726.	—
LOAD CELL	TS	LOAD TEMP (DEG FAREN)	1	LIFT (COUNTS)	1	DRAG (COUNTS)	1	NOSE R ABOUT HYDROPOD (COUNTS)	
LOAD CELL	TT	TEMP (°F)	(°F)	PIWP (COUNTS)	(°F)	PCAV (COUNTS)	(°F)	STATIC PRESSURE (IN HG)	
AREA HALF-SPAN NOBEL PLANTON AREA (50 IN)				PIWP CAVITY PRESSURE (IN HG)					
SPAN FOIL HALF-SPAN (IN)				PCAV CAVITY PRESSURE (IN HG)					
HAC AREA CHORD, MAS, & NORMAL CHORD (IN)				RUN NO Q-XIII-11: Q-POLE TESTED (S-SHALL, H-NUED, L-LARGE)					
BARON VELOCITY, MAJOR/SECOND SPACING (IN)				X-XI-GRAVITIC ATTACK ANGLE (DEGREES)					
ZWIST SWIFT TWIST (FORCES/IN-LB)				Y-XI-GRAVITIC ATTITUDE ANGLE (DEGREES)					
S LOAD CELL POLARITY (N-NORMAL, P-REVERSE)				Z-XI-RUN NUMBER, THIS POLE @ THIS ANGLE					

AREA HALF-SPAN NOBEL PLANTON AREA (50 IN)  
 SPAN FOIL HALF-SPAN (IN)  
 HAC AREA CHORD, MAS, & NORMAL CHORD (IN)  
 BARON VELOCITY, MAJOR/SECOND SPACING (IN)  
 ZWIST SWIFT TWIST (FORCES/IN-LB)  
 S LOAD CELL POLARITY (N-NORMAL, P-REVERSE)

## PIPER INVS OF WALL EFFECTS ON SUPERCAVITATING HYDROPOOLS OF FINITE SPAN

## INPUT DATA CORRECTED FOR ZERO READINGS, SIGNS, AND HYDROSTATIC PRESSURE

RUN NO	RAN008	01	02	03	PINP	PCAV
R-16--01	1450.	-1106.0	-28.2	-1436.0	298.	89.
R-16--02	1451.	-1042.0	-26.5	-1414.0	282.	79.
R-16--03	1458.	-994.0	-25.4	-1386.0	264.	73.
R-16--04	1452.	-928.0	-24.6	-1336.0	250.	67.
R-16--05	1422.	-876.0	-23.9	-1286.0	236.	61.
R-16--06	1413.	-814.0	-23.3	-1210.0	220.	57.
R-16--07	1408.	-756.0	-22.7	-1157.0	207.	54.
R-16--08	1391.	-706.0	-21.7	-1092.0	192.	46.
R-16--09	1385.	-678.0	-21.7	-1059.0	189.	49.
R-16--10	1379.	-612.0	-20.7	-974.0	168.	95.
R-16--11	1373.	-552.0	-19.6	-883.0	150.	42.
R-16--12	1371.	-522.0	-18.6	-841.0	141.	41.
R-16--13	1369.	-484.0	-16.1	-791.0	130.	40.
R-16--14	1369.	-450.0	-17.5	-737.0	118.	41.
R-16--15	1367.	-410.0	-16.5	-675.0	100.	42.
R-16--16	1396.	-672.0	-20.7	-1056.0	183.	42.
R-16--17	1395.	-830.0	-22.2	-1229.0	226.	63.
R-16--18	1396.	-810.0	-22.3	-1208.0	227.	62.
R-16--19	1391.	-850.0	-22.7	-1253.0	227.	62.
R-16--20	619.	-222.0	-8.6	-370.0	82.	44.
R-16--21	279.	-178.0	-5.3	-254.0	83.	44.
R-16--22	550.	-380.0	-10.2	-535.0	126.	55.
R-16--23	723.	-488.0	-13.1	-695.0	148.	57.
R-16--24	966.	-630.0	-16.6	-907.0	179.	61.
R-16--25	1181.	-752.0	-20.1	-1093.0	207.	63.
R-16--26	1433.	-912.0	-24.2	-1322.0	242.	65.
R-16--27	1429.	-1058.0	-24.2	-1124.0	631.	---
R-16--28	722.	-560.0	-26.8	-598.0	715.	---

EFFECTS OF WALL EFFECTS ON SUPERCAPITATING HYDROFOILS OF FINITE SPAN

CONTINUOUS DATA REDUCTION

REH 35	ALPHA	LIFT-LB	DRAG-LB	WIND-IBLS VEL-FPS
R-16.-01	16.01	226.84	57.07	101.52 28.17
R-16.-02	16.01	213.69	56.98	95.27 28.18
R-16.-03	16.01	203.89	55.86	91.53 28.15
R-16.-04	16.01	190.52	53.88	88.52 28.00
R-16.-05	16.01	179.97	51.83	85.87 27.31
R-16.-06	16.01	167.86	49.09	81.93 27.03
R-16.-07	16.01	155.74	46.63	81.64 27.79
R-16.-08	16.01	145.55	44.01	78.27 27.63
R-16.-09	16.01	138.98	42.68	78.13 27.57
R-16.-10	16.01	126.53	39.25	78.40 27.52
R-16.-11	16.01	116.33	35.58	70.67 27.46
R-16.-12	16.01	108.12	33.89	66.93 27.44
R-16.-13	16.01	100.81	31.88	65.00 27.42
R-16.-14	16.01	93.50	29.70	63.07 27.42
R-16.-15	16.01	85.30	27.20	59.33 27.41
R-16.-16	16.01	78.55	22.56	78.68 27.67
R-16.-17	16.01	70.44	19.53	79.95 27.67
R-16.-18	16.01	66.85	18.68	80.17 27.67
R-16.-19	16.01	62.55	16.30	81.84 27.63
R-16.-20	16.00	46.12	16.91	30.95 18.96
R-16.-21	16.00	36.65	10.24	18.93 13.08
R-16.-22	16.01	78.04	21.56	36.80 17.94
R-16.-23	16.01	100.22	28.01	47.11 20.38
R-16.-24	16.01	129.33	36.55	59.93 23.12
R-16.-25	16.01	159.82	46.05	72.40 25.60
R-16.-26	16.01	187.21	53.28	86.67 28.01
R-16.-27	16.01	216.45	45.30	87.25 27.98
R-16.-28	16.01	217.36	24.10	96.48 20.36

LEGEND

VEL. UPSTREAM VELOCITY (ft)

RIPPER TAMES OF WALL EFFECTS ON SUPERCAVITATING HYDROFOILS OF FINITE SPAN

CONT'D. DATA IS NONDIMENSIONAL FORM (NO CORRECTIONS APPLIED)

BUS NO	ALPHA	CL	CDIBC	CH	L/D	D/L	$\alpha_{\text{L}} \cdot 10^{+6}$
8-16.-01	16.01	1.0657	0.2668	0.1186	3.9997	0.2500	1.1378
8-16.-02	16.01	1.0033	0.2621	0.1113	3.8277	0.2613	1.1382
8-16.-03	16.01	0.9591	0.2573	0.1071	3.7273	0.2683	1.1371
8-16.-04	16.01	0.9055	0.2505	0.1087	3.6153	0.2766	1.1312
8-16.-05	16.01	0.8610	0.2425	0.1022	3.5505	0.2817	1.1275
8-16.-06	16.01	0.8059	0.2308	0.1005	3.4921	0.2868	1.1282
8-16.-07	16.01	0.7519	0.2197	0.0981	3.4228	0.2922	1.1224
8-16.-08	16.01	0.7107	0.2094	0.0951	3.3934	0.2947	1.1160
8-16.-09	16.01	0.6861	0.2038	0.0953	3.3667	0.2970	1.1138
8-16.-10	16.01	0.6229	0.1878	0.0911	3.3172	0.3015	1.1116
8-16.-11	16.01	0.5651	0.1708	0.0869	3.3155	0.3016	1.1093
8-16.-12	16.01	0.5351	0.1623	0.0824	3.2972	0.3033	1.1086
8-16.-13	16.01	0.4976	0.1525	0.0801	3.2625	0.3065	1.1078
8-16.-14	16.01	0.4638	0.1417	0.0778	3.2693	0.3059	1.1078
8-16.-15	16.01	0.4233	0.1295	0.0732	3.2676	0.3060	1.1070
8-16.-16	16.01	0.6743	0.2017	0.0908	3.3435	0.2991	1.1179
8-16.-17	16.01	0.8301	0.2358	0.0969	3.5208	0.2840	1.1175
8-16.-18	16.01	0.8101	0.2315	0.0971	3.4996	0.2857	1.1179
8-16.-19	16.01	0.8523	0.2411	0.0994	3.5347	0.2829	1.1160
8-16.-20	16.00	0.4784	0.1489	0.0799	3.2123	0.3113	0.7657
8-16.-21	16.00	0.7791	0.2168	0.1025	3.6807	0.2717	0.5295
8-16.-22	16.01	0.9036	0.2438	0.1060	3.7058	0.2698	0.7248
8-16.-23	16.01	0.8997	0.2457	0.1052	3.6609	0.2732	0.8231
8-16.-24	16.01	0.8863	0.2450	0.1022	3.6188	0.2763	0.9419
8-16.-25	16.01	0.8781	0.2450	0.1024	3.5846	0.2790	1.0362
8-16.-26	16.01	0.8892	0.2476	0.1024	3.5912	0.2785	1.1316
8-16.-27	16.01	1.0307	0.2103	0.1034	4.9019	0.2040	1.3301
8-16.-28	16.01	1.0549	0.2109	0.2157	5.0012	0.2000	0.8226

LEGEND

ALPHA GEOMETRIC ANGLE OF ATTACK CORRECTED FOR SHAFT TWIST

CL LIFT COEFFICIENT, nondimensionalized on upstream velocity and model planform area  
CDIBC CD (uncorrected), the uncorrected drag coefficient as computed from measured drag, and nondimensionalized  
on upstream velocity and model planform area

CH nondrag coefficient, nondimensionalized on upstream velocity, model planform area, and mean chord

L/D LIFT-TO-DRAG RATIO = CL/CDIBC

D/L DRAG-TO-LIFT RATIO = CDIBC/CL

Re REYNOLDS NUMBER, based on mean chord

**RIPPLE LINES OF BULK EFFECTS ON SUPERCAVITATING HYDROFOILS OF FINITE SPAN**

**\*SOPHORUS DATA CORRECTED FOR EFFECTS OF IMAGES OF TRAILING VORTEX SYSTEM\***

TEST NO.	ALPHAT	CL	CD	CH	(D/L)	SIGC/AT	SIGC/AT CL/AT	CD/AT2	CH/AT	SIGN	SIGC	CAVLTN	COMMENTS/REMARKS
R-16--01	16.65	1.666	0.278	0.119	0.261	2.618	3.667	3.295	0.400	0.955	0.761	0.69	
R-16--02	16.61	1.603	0.273	0.111	0.272	3.086	2.567	3.461	3.243	0.384	0.895	0.738	
R-16--03	16.58	0.959	0.267	0.107	0.278	2.920	2.455	3.313	3.185	0.370	0.845	0.711	0.72
R-16--04	16.55	0.965	0.259	0.105	0.286	2.725	2.333	3.134	3.103	0.362	0.787	0.674	0.82
R-16--05	16.52	0.861	0.250	0.102	0.291	2.564	2.249	2.985	3.008	0.354	0.740	0.649	0.98
R-16--06	16.49	0.806	0.238	0.100	0.295	2.375	2.112	2.800	2.867	0.349	0.688	0.608	0.96
R-16--07	16.46	0.752	0.226	0.098	0.300	2.215	1.993	2.617	2.733	0.381	0.636	0.573	1.00
R-16--08	16.43	0.711	0.215	0.095	0.302	2.043	1.927	2.478	2.610	0.331	0.586	0.553	1.10
R-16--09	16.42	0.666	0.209	0.095	0.305	1.984	1.791	2.394	2.541	0.333	0.557	0.513	1.15
R-16--10	16.38	0.623	0.192	0.091	0.308	1.780	1.682	2.179	2.346	0.319	0.498	0.469	1.17
R-16--11	16.35	0.565	0.174	0.087	0.307	1.507	1.461	1.981	2.135	0.305	0.430	0.414	1.62
R-16--12	16.33	0.535	0.165	0.082	0.309	1.386	1.347	1.878	2.035	0.289	0.395	0.384	1.89
R-16--13	16.31	0.498	0.155	0.080	0.312	1.239	1.216	1.749	1.915	0.282	0.352	0.346	2.17
R-16--14	16.28	0.463	0.144	0.078	0.311	1.075	1.043	1.630	1.782	0.274	0.306	0.296	2.75
R-16--15	16.26	0.423	0.131	0.073	0.310	0.831	0.789	1.492	1.632	0.258	0.236	0.224	4.35
R-16--16	16.21	0.678	0.206	0.090	0.306	1.095	1.057	2.354	2.515	0.316	0.543	0.532	1.10
R-16--17	16.21	0.830	0.243	0.097	0.293	2.445	2.135	2.881	2.927	0.336	0.704	0.615	----
R-16--18*	16.19	0.810	0.238	0.097	0.294	2.155	2.014	2.876	2.917	0.337	0.707	0.622	----
R-16--19*	16.52	0.852	0.249	0.099	0.292	2.056	2.166	2.956	2.992	0.345	0.708	0.624	----
R-16--20	16.29	0.478	0.151	0.080	0.316	1.191	1.081	1.872	1.981	0.319	0.307	0.307	----
R-16--21	16.48	0.798	0.223	0.103	0.280	2.515	2.301	2.775	2.701	0.357	0.723	0.662	----
R-16--22	16.54	0.504	0.252	0.106	0.279	2.658	2.412	3.130	3.027	0.367	0.768	0.639	----
R-16--23	16.54	0.900	0.254	0.105	0.283	2.594	2.196	3.116	3.049	0.364	0.746	0.639	----
R-16--24	16.58	0.887	0.253	0.102	0.286	2.539	2.174	3.072	3.039	0.354	0.733	0.627	----
R-16--25	16.53	0.878	0.253	0.102	0.288	2.529	2.200	3.043	3.038	0.355	0.730	0.635	----
R-16--26	16.58	0.889	0.256	0.102	0.288	2.554	2.256	3.080	3.069	0.355	0.727	0.651	----
R-16--27	16.63	1.031	0.221	0.103	0.215	-----	-----	3.552	2.628	0.356	-----	-----	----
R-16--28	16.64	1.055	0.223	0.216	0.211	-----	-----	3.632	2.637	0.783	-----	-----	----

UNLESS OTHERWISE INDICATED, ALL DATA ARE FOR:

1. SUPERCAVITATING FLOW.
2. BOTH STATIC PRESSURE TAPS OPEN.

**LEGEND**

- \* ONLY UPSTREAM STATIC PRESSURE TAP UTILIZED
- + ONLY DOWNSTREAM STATIC PRESSURE TAP UTILIZED
- PC PARTIALLY CAVITATING
- PC(TW) PARTIALLY CAVITATING (TAP WETTED)

TW FULLY WETTED

AT (ALPHAT) (TRUE) ANGLE OF ATTACK, CORRECTED FOR EFFECTS OF IMAGES OF TRAILING VORTEXES  
 AT2 ALPHAT=0.2

SIGC CAVITATION NUMBER COMPUTED WITH MEASURED CAVITY PRESSURE  
 SIGN CAVITATION NUMBER COMPUTED WITH CALCULATED VAPOR PRESSURE  
 CP DRAG COEFFICIENT, CORRECTED FOR EFFECTS OF IMAGES OF TRAILING VORTEXES

(D/L) CORRECTED DRAG-TO-LIFT RATIO = CD/CL  
 CAVLTN CAVITY LENGTH MEASURED FROM MIDCHORD  
 (OBTAINED FROM PHOTOGRAPHS)

HIPER TUNES OF WALL EFFECTS ON SUPERCAVITATING HYDROPOILS OF FINITE SPAN

HYDROPOIL INPUT DATA  
 TS TT AREA SPAN HAC  
 78 94 40.0 10.0 4.02

ZERO READINGS AND TUNNEL TEMP BEFORE AND AFTER

MANON 1-N 1-A 2-N 2-B 3-N 3-B TT  
 0- 0.0 0.0 0.0 100.0 0.0 100.0 92.0  
 0- 0.0 0.0 0.0 100.6 0.0 101.0 95.0  
 CELL LBS/CF (NORMAL/REVERSE) S1=0.20000 S2=0.20000 S3=0.00030  
 TWIST= 7200.0 SHARP DIA.= 1.50IN

\*INPUT DATA AS RECORDED\*

RUN NO	MANON	S	01	S	02	S	03	PIMP	PCAV
R-18--01	1521.	-1230.0	B	135.5	R	1820.0	R	383.	170.
R-18--02	1522.	-1212.0	B	133.7	R	1818.0	R	368.	153.
R-18--03	1512.	-1186.0	B	131.5	R	1818.0	R	352.	133.
R-18--04	1509.	-1140.0	B	129.0	R	1809.0	R	331.	114.
R-18--05	1499.	-1106.0	B	128.0	R	1790.0	R	315.	101.
R-18--06	1491.	-1060.0	R	126.8	R	1770.0	R	295.	82.
R-18--07	1484.	-1004.0	R	126.0	R	1715.0	R	276.	74.
R-18--08	1478.	-930.0	B	125.2	R	1694.0	R	254.	65.
R-18--09	1468.	-852.0	C	124.2	R	1569.0	R	234.	61.
R-18--10	1459.	-790.0	B	123.4	R	1473.0	R	216.	56.
R-18--11	1462.	-730.0	R	122.6	R	1392.0	R	198.	47.
R-18--12	1456.	-666.0	R	122.0	R	1290.0	R	180.	47.
R-18--13	1449.	-618.0	B	121.2	R	1206.0	R	164.	44.
R-18--14	1448.	-568.0	R	120.6	R	1118.0	R	148.	43.
R-18--15	1439.	-520.0	R	120.0	R	1042.0	R	131.	43.
R-18--16	1439.	-492.0	B	119.5	R	1002.0	R	121.	43.
R-18--17	1437.	-476.0	R	119.0	R	969.0	R	113.	43.
R-18--18	1137.	-394.0	R	115.5	R	812.0	R	113.	43.
R-18--19+	1127.	-366.0	R	115.1	R	788.0	R	113.	43.
R-18--20*	1154.	-402.0	R	116.0	R	836.0	R	113.	43.

LEGEND TS ROOM TEMPER (DEG FAHR)

TT TUNNEL ( " )

AREA HALF-SPAN MODEL PLANFORM AREA (SQ IN)

SPAN FOIL HALF-SPAN (IN)

HAC MEAN CHORD, MEAS. @ MODEL CENTROID (IN)

MANON VELOCITY MOMENTUM HEADING (IN)

TWIST SHARP TWIST (DEGREES/IN-LB)

S LOAD CELL POLARITY (R=NORMAL, P=REVERSE)

LOAD CELL #1 LIPT (COUNTS)

#2 MOMENT ABOUT MIDCHORD (COUNTS)

PIPE DRAG (COUNTS)

PIPE STATIC PRESSURE (MM HG)

PCAV CAVITY PRESSURE (MM HG)

RUN NO Q-KKK-YY: Q=FOIL TESTED (S=SMALL, P=LARGE)  
 KKK=GROMMETIC ATTACK ANGLE (DEGREES)  
 YY=RUN NUMBER, THIS FOIL @ THIS ANGLE

## EFFECTS OF WALL EFFECTS ON SUPERCAPITATING HYDROPOOLS OF PLATE SPAN

## INPUT DATA CORRECTED FOR ZERO READINGS, SIGNS, AND HYDROSTATIC PRESSURE

BIN NO	NABON	#1	#2	#3	PINP	PCAV
B-18--01	1521.	-1230.0	-35.5	-1720.0	372.	170.
B-18--02	1522.	-1212.0	-33.7	-1717.8	357.	153.
B-18--03	1512.	-1186.0	-31.9	-1717.7	341.	133.
B-18--04	1509.	-1140.0	-28.9	-1708.5	320.	118.
B-18--05	1499.	-1106.0	-27.9	-1689.4	308.	101.
B-18--06	1491.	-1060.0	-26.6	-1669.2	284.	82.
B-18--07	1488.	-1004.0	-25.8	-1614.1	265.	74.
B-18--08	1478.	-930.0	-25.0	-1542.9	243.	65.
B-18--09	1468.	-862.0	-23.9	-1467.7	223.	61.
B-18--10	1459.	-790.0	-23.1	-1371.6	205.	56.
B-18--11	1462.	-730.0	-22.3	-1290.4	187.	47.
B-18--12	1456.	-666.0	-21.7	-1188.3	169.	47.
B-18--13	1449.	-618.0	-20.8	-1104.1	153.	44.
B-18--14	1448.	-568.0	-20.2	-1015.9	137.	43.
B-18--15	1439.	-520.0	-19.6	-939.8	120.	43.
B-18--16	1439.	-492.0	-19.0	-899.6	110.	43.
B-18--17	1437.	-476.0	-18.5	-866.5	102.	43.
B-18--18	1137.	-394.0	-15.0	-709.3	102.	43.
B-18--19	1127.	-366.0	-14.5	-685.2	102.	43.
B-18--20	1154.	-402.0	-15.4	-733.0	43.	

**EXPERIMENTS OF WALL EFFECTS ON SUPERERODATING HYDROPOOLS OF FINITE SPAN**

**CONTINUOUS DATA REDUCTION**

BUS NO	ALPHA	LIFT-LB	DRAG-LB	MOR-TIME	VFL-TPS
S-18.-01	18.02	251.10	69.32	127.80	28.78
S-18.-02	18.02	249.13	69.23	121.21	28.79
S-18.-03	18.02	263.99	69.22	113.17	28.71
S-18.-04	18.01	233.78	68.85	104.06	28.68
S-18.-05	18.01	226.77	68.08	100.35	28.59
S-18.-06	18.01	217.33	67.27	95.91	28.52
S-18.-07	18.01	205.96	65.05	92.92	28.46
S-18.-08	18.01	191.00	62.18	89.92	28.40
S-18.-09	18.01	177.19	59.15	86.21	28.31
S-18.-10	18.01	162.62	55.27	81.22	28.23
S-18.-11	18.01	150.46	52.00	80.22	28.26
S-18.-12	18.01	137.53	47.89	77.95	28.21
S-18.-13	18.01	127.76	44.50	74.96	28.14
S-18.-14	18.01	117.64	40.94	72.68	28.13
S-18.-15	18.01	107.91	37.87	70.61	28.05
S-18.-16	18.01	102.21	36.26	68.49	28.05
S-18.-17	18.01	98.90	34.92	66.58	28.03
S-18.-18	18.01	91.79	28.59	53.87	25.14
S-18.-19	18.01	76.11	27.61	52.31	25.04
S-18.-20	18.01	63.46	29.54	55.44	25.31

LEGEND      VFL UPSTREAM VELOCITY (U)

UPPER TURBULENCE OF HULL EFFECTS ON SUPERCAVITATING HYDROFOILS OF FINITE SPAN

• HYDROFOIL DATA IN NONDIMENSIONAL FORM (NO CORRECTIONS APPLIED) •

BLW NO	ALPHA	CL	CD0BC	CH	L/D	D/L	$\text{Re} \times 10^{6}$
R-18--01	18.-02	1.-1390	0.-1065	0.-1031	3.-7150	0.-2691	1.-1811
R-18--02	18.-02	1.-1204	0.-1059	0.-1356	3.-6622	0.-2731	1.-1814
R-18--03	18.-02	1.-1018	0.-3078	0.-1274	3.-5792	0.-2794	1.-1778
R-18--04	18.-01	1.-0598	0.-0567	0.-1173	3.-4552	0.-2894	1.-1767
R-18--05	18.-01	1.-0348	0.-1051	0.-1119	3.-3900	0.-2950	1.-1731
R-18--06	18.-01	0.-9963	0.-3030	0.-1094	3.-2884	0.-3041	1.-1702
R-18--07	18.-01	0.-9883	0.-2981	0.-1068	3.-2247	0.-3101	1.-1676
R-18--08	18.-01	0.-8827	0.-2820	0.-1034	3.-1307	0.-3194	1.-1654
R-18--09	18.-01	0.-8241	0.-2697	0.-0997	3.-0558	0.-3273	1.-1618
R-18--10	18.-01	0.-7607	0.-2531	0.-0968	3.-0051	0.-3228	1.-1584
R-18--11	18.-01	0.-7024	0.-2374	0.-0332	2.-9592	0.-3379	1.-1595
R-18--12	18.-01	0.-6446	0.-2190	0.-009	2.-9430	0.-3398	1.-1573
R-18--13	18.-01	0.-6015	0.-2041	0.-0018	2.-9477	0.-3393	1.-1547
R-18--14	18.-01	0.-5502	0.-1875	0.-0052	2.-9563	0.-3383	1.-1544
R-18--15	18.-01	0.-5113	0.-1740	0.-0830	2.-9380	0.-3404	1.-1510
R-18--16	18.-01	0.-4863	0.-1664	0.-0007	2.-9109	0.-3435	1.-1510
R-18--17	18.-01	0.-4692	0.-1602	0.-0786	2.-9281	0.-3615	1.-1503
R-18--18	18.-01	0.-4925	0.-1611	0.-0191	2.-9580	0.-3381	1.-0315
R-18--19	18.-01	0.-4527	0.-1587	0.-0774	2.-8520	0.-3506	1.-0273
R-18--20	18.-01	0.-4857	0.-1664	0.-0802	2.-9195	0.-3425	1.-0387

LEGEND

ALPHA GEOMETRIC ANGLE OF ATTACK CORRECTED FOR SHARP TWIST

CL LIFT COEFFICIENT, NONDIMENSIONALIZED ON UPSTREAM VELOCITY AND MODEL PLATFROM AREA  
CD0BC CD (UNCORRECTED). THE UNCORRECTED DRAG COEFFICIENT AS COMPUTED FROM MEASURED DRAG,  
ON UPSTREAM VELOCITY AND MODEL PLATFROM AREA

CH MOMENT COEFFICIENT, NONDIMENSIONALIZED ON UPSTREAM VELOCITY. MODEL PLATFROM AREA, AND MEAN CHORD

L/D LIFT-TO-DRAG RATIO = CL/CD0BC

D/L DRAG-TO-LIFT RATIO = CD0BC/CL

RE REYNOLDS NUMBER, BASED ON MEAN CHORD

## EFFECTS OF WALL EFFECTS ON SUPERCAVITATING HYDROFOILS OF FINITE SPAN

## \*EXPLANATION DATA CORRECTED FOR EFFECTS OF IMAGES OF TRAILING VORTEX SYSTEM\*

TEST NO	ALPHAT	CL	CD	CN	(D/L)	SIGC/AT	CL/AT	CD/AT	SIGC	CAVLT	COMMENTS/REMARKS
E-18--01	18.70	1.139	0.320	0.183	0.562	2.158	3.490	3.005	0.438	1.162	0.708
E-18--02	18.68	1.120	0.319	0.136	0.285	2.179	3.400	3.000	0.416	1.109	0.711
E-18--03	18.67	1.102	0.320	0.127	0.291	2.237	3.381	3.017	0.391	1.059	0.729
E-18--04	18.65	1.060	0.318	0.117	0.300	3.031	2.223	3.257	3.007	0.361	0.987
E-18--05	18.63	1.034	0.316	0.114	0.306	2.877	2.206	3.181	2.991	0.350	0.935
E-18--06	18.61	0.996	0.313	0.109	0.314	2.678	2.209	3.068	2.971	0.337	0.869
E-18--07	18.58	0.948	0.303	0.106	0.320	2.680	2.101	2.925	2.886	0.328	0.804
E-18--08	18.56	0.883	0.290	0.103	0.329	2.249	1.970	2.728	2.771	0.320	0.728
E-18--09	18.50	0.820	0.277	0.100	0.336	2.013	1.808	2.552	2.654	0.309	0.660
E-18--10	18.46	0.761	0.259	0.097	0.381	1.854	1.676	2.360	2.495	0.300	0.598
E-18--11	18.43	0.702	0.283	0.093	0.385	1.650	1.575	2.188	2.384	0.290	0.531
E-18--12	18.39	0.645	0.223	0.091	0.346	1.454	1.381	2.008	2.167	0.283	0.467
E-18--13	18.37	0.601	0.208	0.088	0.386	1.276	1.282	1.876	2.022	0.274	0.410
E-18--14	18.34	0.554	0.191	0.085	0.384	1.097	1.073	1.731	1.861	0.266	0.351
E-18--15	18.31	0.511	0.177	0.083	0.346	0.908	0.886	1.600	1.730	0.260	0.290
E-18--16	18.30	0.488	0.169	0.081	0.349	0.791	0.772	1.516	1.655	0.251	0.253
E-18--17	18.29	0.469	0.163	0.079	0.346	0.698	0.682	1.470	1.595	0.246	0.223
E-18--18	18.29	0.483	0.166	0.079	0.343	0.865	0.847	1.511	1.624	0.248	0.276
E-18--19	18.28	0.453	0.161	0.077	0.355	0.870	0.855	1.419	1.581	0.243	0.278
E-18--20*	18.30	0.486	0.169	0.060	0.348	0.848	0.836	1.521	1.655	0.251	0.271

UNLESS OTHERWISE INDICATED, ALL DATA ARE FOR:

1. SUPERCAVITATING PLATE.
2. BOTH STATIC PRESSURE TAPS OPEN.

## LEGEND

- \* ONLY UPSTREAM STATIC PRESSURE TAP UTILIZED
- \* ONLY DOWNSTREAM STATIC PRESSURE TAP UTILIZED
- PC PARTIALLY CAVITATING
- PC(TV) PARTIALLY CAVITATING (TAP WETTED)
- PW FULLY WETTED

AT

(ALPHAT) (TAN) ANGLE OF ATTACK, CORRECTED FOR EFFECTS OF IMAGES OF TRAILING VORTICES

AT2 ALPHAT\*2

SIGC CAVITATION NUMBER COMPUTED WITH MEASURED CAVITY PRESSURE

SIGV CAVITATION NUMBER COMPUTED WITH CALCULATED VAPOR PRESSURE

CD DRAG COEFFICIENT, CORRECTED FOR EFFECTS OF IMAGES OF TRAILING VORTICES

(D/L) CORRECTED DRAG-TO-LIFT RATIO = CD/CL

CAVLT CAVITY LENGTH AS MEASURED FROM MIDCHORD AT CENTROID POSITION. NONDIMENSIONALIZED ON MID CHORD  
(OBTAINED FROM PHOTOGRAPHS)

THREE INCHES OF WALL EFFECTS ON SUPERCAVITATING HYDROPOILS OF FINITE SPAN

HYDROPOIL INPUT DATA

TR	TT	AREA	SPAN	RAC
78	96	80.0	10.0	4.02

ZERO READINGS AND TUNNEL TEMP BEFORE AND AFTER  
 MARCH 1-8 1-8 2-8 2-8 3-8 3-8 °F  
 0. 0.0 0.0 0.0 100.0 0.0 100.0 94.5  
 0. 0.0 0.0 0.0 100.5 0.0 110.0 97.0  
 CBL LBS/CF (NORMAL/REV) 01=0.20000 02=0.20000 03=0.04030  
 TWIST= 7200.0 SWIFT DIA.= 1.5000  
 \*\*INPUT DATA AS RECORDED\*\*

RUN #	RAON	S	01	S	02	S	03	PIMP	PCAV
8-21-01	1436.	-1102.0	R	129.5	R	210.0	R	396.	177.
8-21-02	1439.	-1076.0	R	127.8	R	207.5	R	373.	154.
8-21-03	1434.	-1042.0	R	126.6	R	205.0	R	350.	133.
8-21-04	1439.	-1020.0	R	123.8	R	202.0	R	327.	115.
8-21-05	1424.	-978.0	R	125.1	R	198.0	R	308.	99.
8-21-06*	1412.	-967.0	R	128.8	R	196.0	R	305.	93.
8-21-07*	1420.	-990.0	R	125.2	R	199.5	R	306.	93.
8-21-08	1422.	-920.0	R	124.2	R	191.0	R	282.	85.
8-21-09	1415.	-866.0	R	123.6	R	185.0	R	258.	75.
8-21-10	1420.	-820.0	R	123.3	R	179.0	R	280.	65.
8-21-11	1423.	-768.0	R	122.9	R	171.2	R	222.	59.
8-21-12	1420.	-718.0	R	122.5	R	163.0	R	204.	58.
8-21-13	1423.	-666.0	R	122.0	R	150.0	R	184.	50.
8-21-14	1423.	-634.0	R	121.9	R	143.0	R	172.	47.
8-21-15	1415.	-608.0	R	121.5	R	137.0	R	163.	47.
8-21-16	1411.	-576.0	R	121.0	R	132.0	R	151.	47.
8-21-17	1405.	-550.0	R	120.6	R	126.0	R	143.	47.
8-21-18	1401.	-500.0	R	120.5	R	124.0	R	138.	47.

LEGEND TR ROOM TEMPER (DEG FAREN)

TT TUNNEL " "

AREA HALF-SPAN MODEL PLATFORM AREA (SQ IN)

SPAN POIL HALF-SPAN (IN)

RAC RAIL CHORD, MM

RAON VELOCITY MANOMETER READING (MM)

TWIST SWIFT TWIST (DEGREES/IN-LB)

; LOAD CELL POLARITY (R=FORWARD, B=REVERSE)

LOAD CELL 01 LIFT (COUNTS)

02 ROTATION ABOUT MIDCHORD (COUNTS)

03 DRAG (COUNTS)

PIMP STATIC PRESSURE (MM HG)

PCAV CAVITY PRESSURE (MM HG)

RUN NO Q-XXX-YY: Q=POIL TESTED (S=SMALL, M=MED, L=LARGE)

YY=GEOMETRIC ATTACK ANGLE (DEGREES)

YY=RUN NUMBER. THIS POIL @ THIS ANGLE

EFFECTS OF WALL EFFECTS ON SUPERCAVITATING HYDROPOOLS OF FINITE SPAN

INPUT DATA CONTACTED FOR ZERO BEADING, SIGNS, AND HYDROSTATIC PRESSURE

JOH NO	BARON	$\theta_1$	$\theta_2$	$\theta_3$	PINP	PCAV
B-21,-01	1455.	-1102.0	-29.5	-200.0	385.	177.
B-21,-02	1439.	-1076.0	-27.6	-1974.8	362.	156.
B-21,-03	1424.	-1042.0	-26.5	-1950.8	339.	133.
B-21,-04	1423.	-1020.0	-25.7	-1910.2	316.	115.
B-21,-05	1425.	-971.0	-25.0	-1877.6	297.	99.
B-21,-06	1412.	-960.0	-26.7	-1862.1	294.	93.
B-21,-07	1420.	-990.0	-25.0	-1891.5	295.	93.
B-21,-08	1422.	-920.0	-26.0	-1805.9	271.	85.
B-21,-09	1419.	-866.0	-23.4	-1745.3	287.	75.
B-21,-10	1420.	-821.0	-23.0	-1687.7	229.	65.
B-21,-11	1423.	-768.0	-22.6	-1606.1	211.	59.
B-21,-12	1420.	-718.0	-22.2	-1496.5	193.	54.
B-21,-13	1423.	-666.0	-21.6	-1390.9	173.	50.
B-21,-14	1423.	-616.0	-21.5	-1326.4	161.	47.
B-21,-15	1415.	-600.0	-21.1	-1267.8	152.	47.
B-21,-16	1411.	-576.0	-20.6	-1211.2	140.	47.
B-21,-17	1405.	-550.0	-20.1	-1150.6	132.	47.
B-21,-18	1401.	-580.0	-20.0	-1137.0	127.	47.

EFFECTS OF WALL EFFECTS ON SUPERCAVITATING HYDROPOOLS OF FINITE SPAN

\*\*HYDROPOOL DATA REDUCTION\*\*

BON NO	ALPHA	LIFT-LB	DRAG-LB	BOR-TUBS	VEL-PPS
8-21,-01	21.01	226.30	80.96	106.20	26.21
8-21,-02	21.01	220.75	79.57	99.97	26.06
8-21,-03	21.01	213.71	78.62	95.55	26.01
8-21,-04	21.01	209.18	77.30	92.56	27.96
8-21,-05	21.01	199.80	75.67	85.94	27.92
8-21,-06	21.01	196.93	75.04	88.75	27.81
8-21,-07	21.01	203.00	76.23	90.08	27.88
8-21,-08	21.01	168.80	72.78	86.38	27.90
8-21,-09	21.01	177.87	70.34	88.11	27.87
8-21,-10	21.01	169.81	68.01	82.93	27.88
8-21,-11	21.01	158.12	68.73	81.38	27.91
8-21,-12	21.01	148.06	60.31	79.84	27.88
8-21,-13	21.01	137.51	56.22	77.93	27.91
8-21,-14	21.01	131.10	53.45	77.46	27.91
8-21,-15	21.01	125.82	51.17	75.92	27.84
8-21,-16	21.01	119.31	48.81	76.01	27.80
8-21,-17	21.01	114.03	46.69	72.47	27.75
8-21,-18	21.01	112.09	45.82	72.00	27.71

LEGEND

VEL UPSTREAM VELOCITY (U)

**UPPER INFLUX OF WALL EFFECTS ON SUPERCAVITATING HYDROPOOLS OF PIKE SPAD**

**HYDROPOOL DATA IN NONDIMENSIONAL FORM (NO CORRECTIONS APPLIED)**

BUB NO	ALPHA	CL	CDUNC	CH	L/D	D/L	Re=100e-6
R-21-01	21.01	1.0606	0.3740	0.1230	2.8355	0.3527	1.1750
R-21-02	21.01	1.0460	0.3716	0.1170	2.0180	0.3553	1.1686
R-21-03	21.01	1.0159	0.3683	0.1130	2.7582	0.3625	1.1667
R-21-04	21.01	0.9974	0.3633	0.1095	2.7457	0.3682	1.1688
R-21-05	21.01	0.9560	0.3566	0.1070	2.6805	0.3771	1.1629
R-21-06	21.01	0.9497	0.3565	0.1065	2.6682	0.3753	1.1583
R-21-07	21.01	0.9739	0.3603	0.1075	2.7032	0.3699	1.1614
R-21-08	21.01	0.9045	0.3433	0.1029	2.6351	0.3795	1.1621
R-21-09	21.01	0.8539	0.3322	0.1004	2.5702	0.3991	1.1610
R-21-10	21.01	0.8127	0.3209	0.0990	2.5328	0.3948	1.1614
R-21-11	21.01	0.7571	0.3045	0.0969	2.4864	0.4022	1.1625
R-21-12	21.01	0.7102	0.2839	0.0953	2.5014	0.3998	1.1614
R-21-13	21.01	0.6585	0.2637	0.0926	2.4967	0.4005	1.1625
R-21-14	21.01	0.6277	0.2505	0.0923	2.5058	0.3391	1.1625
R-21-15	21.01	0.6056	0.2449	0.0909	2.5140	0.3978	1.1595
R-21-16	21.01	0.5758	0.2301	0.0889	2.5019	0.3997	1.1579
R-21-17	21.01	0.5524	0.2208	0.0873	2.5021	0.3997	1.1556
R-21-18	21.01	0.5341	0.2172	0.0870	2.5053	0.3992	1.1541

**LEGEND**

ALPHA = CHORDWISE ANGLE OF ATTACK CORRECTED FOR SHARP TWIST  
 CL = LIFT COEFFICIENT, NONDIMENSIONALIZED ON UPSTREAM VELOCITY AND MODEL PLATEFORM AREA  
 CDUNC = UNCORRECTED DRAG COEFFICIENT AS COMPUTED FROM MEASURED DRAG, AND nondimensionalized  
 ON UPSTREAM VELOCITY AND MODEL PLATEFORM AREA  
 CH = DRAG COEFFICIENT, nondimensionalized on upstream velocity, model plateform area, and mean chord  
 L/D = LIFT-TO-DRAG RATIO = CL/CDUNC  
 D/L = DRAG-TO-LIFT RATIO = CDUNC/CL  
 Re = REYNOLDS NUMBER, BASED ON MEAN CHORD

EFFECTS OF WALL EFFECTS ON SUPERCAVITATING HYDROFOILS OF FINITE SPAN

\*OPINION DATA CORRECTED FOR EFFECTS OF IMAGES OF TRAILING VORTEX SYSTEM\*

RUN NO	ALPHAT	CL	CD	(D/L)	SIGC	SIGV	CD/AT2	CM/AT	SIGN	SIGC	CAVLTN	COMMENTS/REMARKS
A-21,-01	21.65	1.061	0.386	0.124	3.299	1.999	2.807	2.702	0.328	1.246	0.755	0.80
B-21,-02	21.68	1.086	0.381	0.118	3.166	3.112	2.022	2.770	2.686	3.312	1.175	0.85
B-21,-03	21.62	1.016	0.379	0.113	3.173	2.699	2.011	2.692	2.662	2.299	1.094	0.759
B-21,-04	21.61	0.997	0.376	0.110	0.375	0.110	0.375	0.683	1.969	2.645	2.627	0.291
B-21,-05	21.58	0.956	0.366	0.107	0.383	2.506	1.949	2.538	2.581	0.268	0.944	0.96
B-21,-06*	21.59	0.950	0.366	0.106	0.385	2.495	1.994	2.522	2.579	0.283	0.939	1.03
B-21,-07*	21.59	0.574	0.370	0.108	0.380	2.488	1.992	2.584	2.606	0.285	0.918	0.751
B-21,-08	21.55	0.905	0.352	0.103	0.389	2.251	1.836	2.405	2.486	0.274	0.887	1.10
B-21,-09	21.52	0.854	0.380	0.100	0.398	2.019	1.703	2.273	2.409	0.267	0.759	0.640
B-21,-10	21.50	0.613	0.328	0.099	0.403	1.840	1.625	2.166	2.328	0.264	0.690	1.40
B-21,-11	21.46	0.757	0.310	0.097	0.410	1.660	1.506	2.021	2.212	0.259	0.622	0.564
B-21,-12	21.43	0.710	0.289	0.095	0.407	1.585	1.382	1.898	2.066	0.255	0.555	1.42
B-21,-13	21.40	0.658	0.268	0.093	0.407	1.298	1.222	1.763	1.922	0.248	0.480	1.75
B-21,-14	21.38	0.628	0.255	0.092	0.406	1.164	1.134	1.682	1.828	0.247	0.414	0.423
B-21,-15	21.37	0.606	0.245	0.091	0.404	1.079	1.051	1.623	1.759	0.244	0.402	2.80
B-21,-16	21.35	0.576	0.239	0.089	0.406	0.960	0.934	1.545	1.682	0.238	0.358	3.55
B-21,-17	21.34	0.552	0.229	0.087	0.405	0.882	0.858	1.483	1.615	0.234	0.329	0.320
B-21,-18	21.33	0.544	0.220	0.087	0.405	0.832	0.810	1.461	1.589	0.234	0.310	0.302

UNLESS OTHERWISE INDICATED, ALL DATA ARE FOR:

1. SUPERCAVITATING FLOW.
2. BOTH STATIC PRESSURE TAPS OPEN.

LEGEND

- \* ONLY UPSTREAM STATIC PRESSURE TAP UTILIZED
- PC PARTIALLY CAVITATING
- PC(TB) PARTIALLY CAVITATING (FAP WETTED)
- F\* FULLY WETTED
- AT (ALPHAT) (TRUE) ANGLE OF ATTACK, CORRECTED FOR EFFECTS OF IMAGES OF TRAILING VORTICES
- AT2 ALPHAT\*\*2
- SIGC CAVITATION NUMBER COMPUTED WITH MEASURED CAVITY PRESSURE
- SIGV CAVITATION NUMBER COMPUTED WITH CALCULATED VAPOR PRESSURE
- CD DRAG COEFFICIENT, CORRECTED FOR EFFECTS OF IMAGES OF TRAILING VORTICES
- (D/L) CORRECTED DIAG-TO-LIFT RATIO = CD/CL
- CAVLTN CAVITY LENGTH MEASURED FROM MIDCHORD AT CENTROID POSITION, NONDIMENSIONALIZED ON MEAN CHORD  
(OBTAINED FROM PHOTOGRAPHS)

EXPERIMENTS OF WALL EFFECTS ON SUPERCRITICATING HYDROPOILS OF PIVOT SPAN

HYDROPOIL INPUT DATA

TR	TT	AREA	SPAN	HAC
79	96	90.0	15.0	6.03

ZERO READINGS AND TUNNEL TEMP BEFORE AND AFTER

MANOM 1-N	1-N	2-N	2-R	3-N	3-R
0.	0.0	0.0	100.0	0.0	100.0
0.	0.0	0.0	9.0 C 100.0	0.0	104.0
CELL LBS/IN <sup>2</sup> (NORMAL/REV)	0.1=0.20000	0.2=0.20000	0.3=0.06030		
TWIST=	7260.0	SWEEP DIA.=	1.50IN		

\*INPUT DATA AS RECORDED\*

RUN NO	MANOM	S	81	S	82	S	83	PIMP	PCAV
1-8-0-01	1213.	-1218.0	R	141.0	R	980.0	R	172.	48.
1-8-0-02	1204.	-1022.0	R	137.5	R	914.0	R	154.	47.
1-8-0-03*	1204.	-968.0	R	137.0	R	892.0	R	153.	48.
1-8-0-04*	1201.	-1062.0	R	138.0	R	932.0	R	153.	48.
1-8-0-05	1205.	-818.0	R	135.0	R	812.0	R	134.	46.
1-8-0-06	1207.	-648.0	R	132.0	R	705.0	R	117.	46.
1-8-0-07	1207.	-548.0	R	128.8	R	619.0	R	104.	46.
1-8-0-08*	1165.	-488.0	R	126.9	R	576.0	R	103.	46.
1-8-0-09*	1207.	-566.0	R	129.5	R	639.0	R	102.	47.
1-8-0-10	1200.	-498.0	R	127.9	R	583.0	R	93.	47.
1-8-0-11*	1080.	-452.0	R	124.0	R	545.0	R	102.	47.
1-8-0-12*	1193.	-522.0	R	128.4	R	606.0	R	90.	53.

LEGEND TR BOOR TEMPS (DEG FAHR) LOAD CELL 81 LIFT (COUNTS)

TT TUNNEL " 82 MOMENT ABOUT MIDCROSS (COUNTS)

AREA HALF-SPAN MODEL PLATEFORM AREA (SQ IN)

SPAN POIL HALF-SPAN (IN)

HAC BEAM CHORD, BEAMS A MODEL CENTROID (IN)

MANOM VELOCITY MANOMETER 3 FEADING (IN)

TWIST SHAFT TWIST (DEGREES/IN-LB)

S LOAD CELL POLARITY (N=NORMAL, R=REVERSE)

01 DRAG (COUNTS)

PIMP STATIC PRESSURE (IN HG)

PCAV CAVITY PRESSURE (IN HG)

RUN NO Q-XXX-YI: Q=POIL TESTED(S=SMALL,M=MED,L=LARGE)

YI=GEOMETRIC ATTACK ANGLE (DEGREES)

YI=RUN NUMBER. THIS POIL @ THIS ANGLE

RIPPER TUNES OF WALL EFFECTS ON SUPERCAVITATING HYDROPOILS OF FIFTY SPAN

INPUT DATA CORRECTED FOR ZERO READINGS, SIGHTS, AND BAROMETRIC PRESSURE

RUN NO	MANO	81	82	83	P1P	P2AV
L-8-0-01	1213.	-1218.0	-41.0	-880.0	165.	48.
L-8-0-02	1206.	-1022.0	-37.5	-813.6	187.	47.
L-8-0-03	1204.	-968.0	-37.0	-791.3	166.	48.
L-8-0-04	1201.	-1062.0	-38.0	-830.9	186.	48.
L-8-0-05	1205.	-818.0	-35.0	-710.5	127.	46.
L-8-0-06	1207.	-648.0	-32.0	-603.2	110.	46.
L-8-0-07	1207.	-548.0	-28.8	-516.8	97.	46.
L-8-0-08	1185.	-488.0	-26.9	-473.5	96.	46.
L-8-0-09	1207.	-566.0	-29.5	-536.1	95.	47.
L-8-0-10	1200.	-698.0	-27.8	-479.7	86.	47.
L-8-0-11	1080.	-852.0	-26.0	-641.8	95.	47.
L-8-0-12	1193.	-522.0	-28.4	-502.0	83.	53.

**EFFECTS OF WALL EFFECTS ON SUPERERODATING HYDROPOOLS OF FINITE SPAN**

**\*\*HYDROPOOL DATA REDUCTIONS\*\***

RUN NO	ALPHA	LIFT-LB	DRAG-LB	MOM-IN-LB	VFL-FPS
L-8.0-01	8.02	251.80	35.46	147.60	25.91
L-8.0-02	8.02	211.90	32.79	135.00	25.82
L-8.0-03	8.02	201.00	31.89	131.20	25.82
L-8.0-04	8.02	220.00	33.49	136.80	25.79
L-8.0-05	8.02	170.60	28.63	126.00	25.83
L-8.0-06	8.02	136.00	24.31	115.20	25.85
L-8.0-07	8.01	115.36	20.63	103.68	25.85
L-8.0-08	8.01	102.98	19.08	96.84	25.63
L-8.0-09	8.01	119.10	21.60	106.20	25.85
L-8.0-10	8.01	105.16	19.33	100.08	25.78
L-8.0-11	8.01	95.20	17.79	66.40	24.54
L-8.0-12	8.01	110.08	20.23	102.24	25.71

LEGEND

VEL OBSERVEAN VELOCITY (U)

RIPPER LINES OF WALL EFFECTS ON SUPERCavitating HYDROFOILS OF FINITE SPAN

\*\*HYDROFOIL DATA IN NONDIMENSIONAL FORM (NO CORRECTIONS APPLIED)\*\*

RUN NO	ALPHA	CL	CDUHC	CH	L/D	D/L	$Re^{10^{6.6}}$
L-8-0-01	8.02	0.6219	0.0031	0.0605	7.4828	0.1336	1.6185
L-8-0-02	8.02	0.5270	0.0771	0.0557	6.8382	0.1862	1.6129
L-8-0-03	8.02	0.4999	0.0748	0.0549	6.6807	0.1897	1.6129
L-8-0-04	8.02	0.5484	0.0790	0.0566	6.9828	0.1840	1.6111
L-8-0-05	8.02	0.4240	0.0667	0.0519	6.3581	0.1573	1.6136
L-8-0-06	8.02	0.3375	0.0558	0.0474	6.0438	0.1655	1.6148
L-8-0-07	8.01	0.2863	0.0472	0.0427	6.0645	0.1689	1.6148
L-8-0-08	8.01	0.2599	0.0437	0.0405	5.9516	0.1680	1.6010
L-8-0-09	8.01	0.2955	0.0491	0.0437	6.0155	0.1662	1.6148
L-8-0-10	8.01	0.2628	0.0538	0.0414	5.9967	0.1668	1.6104
L-8-0-11	8.01	0.2620	0.0484	0.0394	5.8960	0.1696	1.5334
L-8-0-12	8.01	0.2761	0.0463	0.0425	5.9686	0.1675	1.6061

LEGEND

ALPHA GEOMETRIC ANGLE OF ATTACK CORRECTED FOR SHARP TWIST

CL LIFT COEFFICIENT, NONDIMENSIONALIZED ON UPSTREAM VELOCITY AND MODEL PLANFORM AREA  
CDUHC CL (UNCORRECTED), THE UNCORRECTED DRAG COEFFICIENT AS COMPUTED FROM MEASURED DRAG, AND NONDIMENSIONALIZED  
ON UPSTREAM VELOCITY AND MODEL PLANFORM AREA

CH MOMENT COEFFICIENT, NONDIMENSIONALIZED ON UPSTREAM VELOCITY, MODEL PLANFORM AREA, AND REYNOLD CHORD

L/D LIFT-TO-DRAG RATIO = CL/CDUHC

D/L DRAG-TO-LIFT RATIO = CDUHC/CL

Re REYNOLDS NUMBER, BASED ON REYN CHORD

EFFECTS OF WALL EFFECTS ON SUPERCAVITATING HYDROFOILS OF FINITE SPAN

APPENDIX DATA CORRECTED FOR EFFECTS OF IMAGES OF TRAILING VORTEX SYSTEM\*

TEST NO.	ALPHAT	CL	CD	CN	(D/L)		SIGC/AT CL/AT	CD/T2	CM/AT	SIGV	SIGC	CAVLTH	
					D	L	SIGV/AT						
1-8-0-01	8.76	0.622	0.091	0.060	0.147	3.297	4.069	3.900	0.526	0.504	0.68		
1-8-0-02	8.69	0.527	0.083	0.056	0.157	2.992	2.876	3.493	0.369	0.451	0.338		
1-8-0-03*	8.61	0.500	0.080	0.055	0.160	2.969	2.830	3.326	0.366	0.446	0.425	----	
1-8-0-04*	8.67	0.548	0.085	0.057	0.155	2.951	2.817	3.625	3.722	0.378	0.446	0.426	----
1-8-0-05	8.52	0.424	0.070	0.052	0.166	2.915	2.363	2.851	3.184	0.369	0.362	0.351	0.96
1-8-0-06	8.42	0.337	0.053	0.067	0.172	1.956	1.889	2.297	2.697	0.323	0.287	0.277	1.38
1-8-0-07	8.35	0.286	0.049	0.063	0.171	1.580	1.518	1.963	2.300	0.293	0.230	0.221	2.15
1-8-0-08*	8.32	0.260	0.045	0.061	0.173	1.578	1.520	1.790	2.137	0.279	0.229	0.221	2.65
1-8-0-09*	8.37	0.296	0.051	0.049	0.172	1.508	1.427	2.024	2.390	0.299	0.220	0.208	
1-8-0-10	8.33	0.262	0.045	0.041	0.172	1.249	1.173	1.806	2.140	0.285	0.182	0.170	----
1-8-0-11*	8.32	0.262	0.046	0.039	0.175	1.669	1.591	1.809	2.173	0.271	0.242	0.231	----
1-8-0-12*	8.34	0.276	0.048	0.043	0.173	1.152	0.907	2.257	2.492	0.168	0.132	0.132	----

UNLESS OTHERWISE INDICATED, ALL DATA ARE FOR:

1. SUPERCAVITATING FLOW.
2. BOTH STATIC PRESSURE TAPS OPEN.

LEGEND

- \* CNLT MEASUREMENT STATIC PRESSURE TAP UTILIZED
- ONLY DOWNTREAM STATIC PRESSURE TAP UTILIZED
- PC PARTIALLY CAVITATING
- PC (TW) PARTIALLY CAVITATING (TAP WETTED)
- PW FULLY WETTED

AT (ALPHAT) (TRUP) ANGLE OF ATTACK, CORRECTED FOR EFFECTS OF IMAGES OF TRAILING VORTICES

AT2 ALPHAT\*<sup>2</sup>

SIGC CAVITATION NUMBER COMPUTED WITH MEASURED CAVITY PRESSURE  
 SIGV CAVITATION NUMBER COMPUTED WITH CALCULATED VAPOR PRESSURE  
 CD DRAG COEFFICIENT, CORRECTED FOR EFFECTS OF IMAGES OF TRAILING VORTICES  
 (D/L) CORRECTED DRAG-TO-LIFT RATIO = CD/CL  
 CAVLTH CAVITY LENGTH MEASURED FROM MIDCHORD AT CENTROID POSITION, NONDIMENSIONALIZED ON MEAN CHORD  
 (OBTAINED FROM PHOTOGRAPHS)

HIGHER LAVES OF WALL EFFECTS ON SUPERCAVITATING HYDROPOILS OF FINITE SPAN

**HYDROPOIL INPUT DATA**

TR	TT	AREA	SPAN	HAC
77	85	90.0	15.0	6.03

**ZERO READINGS AND TUNNEL TEMP BEFORE AND AFTER**  
 HACON 1-B 1-B 2-B 2-B 3-B 3-B TT  
 0. 0.0 0.0 0.0 0.0 0.0 0.0 0.0  
 0. 0.0 0.0 0.0 0.0 0.0 0.0 0.0  
 CELL LBS/CTR (BONAVENTURE) 01=0.20000 02=0.20000 03=0.04030  
 TWIST= 7200.0 SMART DIA.= 1.50IN

\*INPUT DATA AS RECORDED\*

RUN NO	HACON	S	01	S	02	S	03	PINP	PCAV
L-9-5-01	383.		-942.0		130.0		435.0	742.	---
L-9-5-02	991.		-1100.0		174.5		941.0	695.	---
L-9-5-03	1252.		-1368.0		192.2		1140.0	665.	---
L-9-5-04	1254.		-1392.0		197.2		1113.0	281.	PC (TP)
L-9-5-05	1252.		-1440.0		198.5		1082.0	246.	PC (TP)
L-9-5-06	1245.		-1550.0		185.9		1150.0	225.	PC (TP)
L-9-5-07	1240.		-1650.0		161.8		1288.0	208.	40.
L-9-5-08	1230.		-1530.0		153.3		1295.0	190.	39.
L-9-5-09*	1227.		-1454.0		152.0		1288.0	190.	38.
L-9-5-10	1226.		-1368.0		189.5		1255.0	172.	37.
L-9-5-11*	1233.		-1320.0		149.0		1237.0	172.	37.
L-9-5-12	1243.		-1182.0		147.6		1181.0	156.	37.
L-9-5-13*	1248.		-1180.0		147.0		1157.0	156.	37.
L-9-5-14	1255.		-1019.0		145.1		1080.0	140.	36.
L-9-5-15*	1255.		-966.0		148.6		1047.0	140.	34.
L-9-5-16	1256.		-886.0		143.0		1085.0	126.	33.
L-9-5-17*	1256.		-846.0		141.5		950.0	127.	33.
L-9-5-18	1257.		-808.0		140.7		922.0	116.	33.
L-9-5-19*	1258.		-752.0		140.3		887.0	116.	33.
L-9-5-20	1257.		-682.0		138.1		824.0	104.	33.
L-9-5-21*	1255.		-644.0		137.2		792.0	104.	32.
L-9-5-22	1242.		-622.0		136.4		768.0	94.	32.
L-9-5-23*	1182.		-578.0		134.5		721.0	96.	32.
L-9-5-24	1253.		-1658.0		161.5		1284.0	210.	42.
L-9-5-25	905.		-1216.0		151.6		948.0	169.	41.
L-9-5-26	680.		-900.0		134.2		767.0	133.	38.
L-9-5-27	589.		-750.0		127.1		686.0	114.	37.

**LEGEND**

TR ROOM TEMPER (DEG FAHR)

TT TUNNEL " "

AREA HALF-SPAN MODEL PLATEFORM AREA (SQ IN)

SPAN POIL HALF-SPAN (IN)

HAC REAS. & MODEL CANTHOID (IN)

MANON VELOCITY MANOMETER READING (IN)

TWIST SHAPT TWIST (DEGREES/IN-LB)

S LOAD CPLL POLARITY (B=NORMAL, R=REVERSE)

LOAD CELL 01 LIPT (COUNTS)

02 HORNET ABOUT MIDCHORD (COUNTS)

03 DRAG (COUNTS)

PINP STATIC PRESSURE (MM HG)

PCAV CAVITY PRESSURE (MM HG)

RUN NO Q-XXX-YY: Q=POIL TESTED (S=SMALL, M=MED, L=LARGE)

XIX=GEOMETRIC ATTACK ANGLE (DEGREES)

YY=RUN NUMBER. THIS FOIL # THIS ANGLE

## EFFECTS OF WALL EFFECTS ON SUPERCAVITATING HYDROPOILS OF PIVITE SPAN

## INPUT DATA CONNECTED FOR ZERO READINGS, SIGNS, AND HYDROSTATIC PRESSURE

RUB NO	RUB NO	01	02	03	P1BP	PCAV
L-9-5-01	183.	-442.0	-30.0	-335.0	735.	----
L-9-5-02	991.	-1100.0	-74.8	-811.0	688.	----
L-9-5-03	1252.	-1368.0	-92.0	-1000.0	658.	----
L-9-5-04	1259.	-1392.0	-97.0	-1013.0	278.	----
L-9-5-05	1252.	-1400.0	-98.2	-992.0	241.	----
L-9-5-06	1285.	-1550.0	-85.5	-1050.0	218.	----
L-9-5-07	1280.	-1650.0	-61.3	-1188.0	201.	40.
L-9-5-08	1230.	-1510.0	-52.8	-1195.0	183.	39.
L-9-5-09	1227.	-1668.0	-51.4	-1188.0	183.	38.
L-9-5-10	1226.	-1368.0	-48.8	-1155.0	165.	37.
L-9-5-11	1233.	-1320.0	-48.2	-1117.0	165.	37.
L-9-5-12	1243.	-1182.0	-46.8	-1081.0	149.	37.
L-9-5-13	1268.	-1190.0	-46.1	-1057.0	149.	37.
L-9-5-14	1255.	-1014.0	-44.1	-990.0	133.	36.
L-9-5-15	1255.	-966.0	-43.5	-947.0	133.	34.
L-9-5-16	1256.	-886.0	-41.8	-985.0	119.	33.
L-9-5-17	1256.	-886.0	-40.3	-950.0	120.	33.
L-9-5-18	1257.	-808.0	-39.4	-922.0	109.	33.
L-9-5-19	1258.	-752.0	-38.9	-787.0	109.	33.
L-9-5-20	1257.	-682.0	-36.6	-724.0	97.	33.
L-9-5-21	1255.	-644.0	-35.7	-692.0	97.	32.
L-9-5-22	1242.	-622.0	-34.8	-668.0	87.	32.
L-9-5-23	1182.	-578.0	-32.8	-621.0	89.	32.
L-9-5-24	1253.	-1658.0	-59.7	-1384.0	203.	42.
L-9-5-25	905.	-1216.0	-49.8	-848.0	162.	41.
L-9-5-26	680.	-900.0	-32.3	-667.0	126.	38.
L-9-5-27	589.	-750.0	-25.1	-586.0	107.	37.

## NUPH LINES OF WALL EFFECTS ON SUPERACCELERATING HYDROOILS OF PINTLE SPAN

## \*\*\*HYDROOIL DATA REDUCTION\*\*\*

RUN NO	ALPHA	LIFT-LB	DRAG-LB	BUD-JNLB	VEL-FPS
L-9.5-01	9.51	94.80	13.50	108.00	15.15
L-9.5-02	9.58	238.00	31.89	267.92	23.57
L-9.5-03	9.55	292.01	41.91	331.37	26.28
L-9.5-04	9.55	257.79	60.82	349.09	26.30
L-9.5-05	9.55	367.66	39.57	353.49	26.28
L-9.5-06	9.54	327.10	42.31	307.45	26.21
L-9.5-07	9.53	392.27	67.88	220.82	26.17
L-9.5-08	9.53	316.55	48.16	189.34	26.07
L-9.5-09	9.53	307.08	47.88	184.98	26.04
L-9.5-10	9.52	283.36	46.55	175.71	26.03
L-9.5-11	9.52	273.65	65.82	173.63	26.10
L-9.5-12	9.52	245.75	63.56	168.31	26.19
L-9.5-13	9.52	237.22	42.60	165.88	26.24
L-9.5-14	9.52	211.62	39.49	158.76	26.31
L-9.5-15	9.52	201.90	38.16	156.68	26.31
L-9.5-16	9.52	165.57	39.70	150.65	26.32
L-9.5-17	9.52	177.25	36.25	144.97	26.32
L-9.5-18	9.52	169.89	33.13	141.81	26.33
L-9.5-19	9.52	158.18	31.72	140.10	26.34
L-9.5-20	9.52	143.73	29.18	131.50	26.33
L-9.5-21	9.52	135.93	27.89	128.38	26.31
L-9.5-22	9.52	131.16	26.92	125.22	26.19
L-9.5-23	9.52	122.16	25.03	118.11	25.59
L-9.5-24	9.53	343.55	67.72	215.03	26.29
L-9.5-25	9.52	253.15	34.17	179.11	22.60
L-9.5-26	9.52	186.96	26.88	116.20	19.78
L-9.5-27	9.51	155.02	23.62	90.36	18.51

## LEGEND

VEL UPSTREAM VELOCITY (U)

RIPER INLES OF WALL EFFECTS ON SUPERCAVITATING HYDROFOILS OF FINITE SPAN

• HYDROFOIL DATA IN NONDIMENSIONAL FORM (NO CORRECTIONS APPLIED) •

RUN NO	ALPHA	CL	CDUNC	CH	L/D	D/L	BH10**-6
L-9-5-01	9.51	0.6809	0.0925	0.1292	7.3628	0.1358	0.8639
L-9-5-02	9.54	0.6995	0.0963	0.1323	7.2612	0.1377	1.3844
L-9-5-03	9.55	0.6996	0.0959	0.1317	7.2963	0.1371	1.4989
L-9-5-04	9.55	0.7124	0.0931	0.1385	7.6493	0.1307	1.5000
L-9-5-05	9.55	0.7370	0.0903	0.1804	8.1635	0.1225	1.4989
L-9-5-06	9.54	0.7877	0.0974	0.1230	6.0898	0.1236	1.4950
L-9-5-07	9.53	0.8274	0.1112	0.0885	7.4803	0.1344	1.4922
L-9-5-08	9.53	0.7710	0.1128	0.0767	6.8374	0.1463	1.4866
L-9-5-09	9.53	0.7496	0.1123	0.0789	6.6729	0.1499	1.4849
L-9-5-10	9.52	0.6922	0.1092	0.0712	6.3406	0.1577	1.4883
L-9-5-11	9.52	0.6650	0.1068	0.0700	6.2255	0.1606	1.4883
L-9-5-12	9.52	0.5927	0.1005	0.0673	5.8953	0.1696	1.4939
L-9-5-13	9.52	0.5700	0.0978	0.0661	5.8267	0.1716	1.4967
L-9-5-14	9.52	0.5059	0.0899	0.0629	5.6282	0.1777	1.5006
L-9-5-15	9.52	0.4826	0.0867	0.0621	5.5667	0.1796	1.5006
L-9-5-16	9.52	0.4433	0.0903	0.0597	4.9092	0.2037	1.5011
L-9-5-17	9.52	0.4234	0.0773	0.0574	5.8776	0.1826	1.5011
L-9-5-18	9.52	0.4045	0.0745	0.0561	5.4268	0.1843	1.5017
L-9-5-19	9.52	0.3773	0.0711	0.0554	5.3049	0.1885	1.5022
L-9-5-20	9.52	0.3431	0.0651	0.0522	5.2685	0.1898	1.5017
L-9-5-21	9.52	0.3249	0.0621	0.0509	5.2295	0.1912	1.5006
L-9-5-22	9.52	0.3171	0.0604	0.0501	5.2452	0.1907	1.4933
L-9-5-23	9.52	0.3088	0.0587	0.0495	5.2593	0.1901	1.4593
L-9-5-24	9.53	0.8224	0.1097	0.0854	7.4971	0.1334	1.4995
L-9-5-25	9.52	0.8203	0.1061	0.0983	7.7306	0.1294	1.2888
L-9-5-26	9.52	0.7883	0.1089	0.0815	7.2369	0.1382	1.1283
L-9-5-27	9.51	0.7891	0.1094	0.0774	6.8500	0.1460	1.0554

LEGEND

ALPHA GEOMETRIC ANGLE OF ATTACK CORRECTED FOR SHAFT TWIST

CL LIFT COEFFICIENT, nondimensionalized on upstream velocity and model planform area  
 CDUNC CD (uncorrected). THE UNCORRECTED DRAG COEFFICIENT AS COMPUTED FROM MEASURED DRAG, AND nondimensionalized  
 ON UPSTREAM VELOCITY AND MODEL PLANFORM AREA

CH MOMENT COEFFICIENT, nondimensionalized on upstream velocity, model planform area, and mean chord  
 L/D LIFT-TO-DRAG RATIO = CL/CDUNC  
 D/L DRAG-TO-LIFT RATIO = CDUNC/CL  
 BN BETHEOLD'S NUMBER, BASED ON AREA CHORD

## PIPELINES OF WALL EFFECTS ON SUPERCAVITATING HYDROPOOLS OF FINITE SPAN

## \*OPINION DATA CORRECTED FOR EFFECTS OF IMAGES OF TRAILING VORTEX SYSTEM\*

RUN NO	ALPHAT	CL	CD	CAV	(D/L)	SIGT	SIGC	CD/AT	CM/AT	SIGN	CAVLTN	COMENTS/REMARKS
L-9-5-01	10.32	0.681	0.102	0.129	0.150	-----	-----	3.779	3.185	0.717	-----	PW
L-9-5-02	10.37	0.699	0.106	0.132	0.152	-----	-----	3.866	3.252	0.731	-----	PW
L-9-5-03	10.38	0.700	0.106	0.132	0.152	-----	-----	3.863	3.233	0.721	-----	PW
L-9-5-04	10.39	0.712	0.106	0.138	0.145	-----	-----	3.927	3.189	0.763	-----	PC (PW)
L-9-5-05	10.42	0.732	0.102	0.140	0.138	-----	-----	4.051	3.068	0.772	-----	PC (PW)
L-9-5-06	10.48	0.788	0.110	0.123	0.140	-----	-----	4.308	3.296	0.672	-----	PC (PW)
L-9-5-07	10.51	0.827	0.125	0.089	0.152	3.918	3.698	3.725	0.882	0.722	0.678	-----
L-9-5-08	10.84	0.771	0.125	0.077	0.162	3.573	3.510	3.766	0.421	0.651	0.611	-----
L-9-5-09*	10.91	0.750	0.124	0.075	0.165	3.568	3.395	4.124	3.752	0.412	0.652	0.617
L-9-5-10	10.35	0.692	0.119	0.071	0.172	3.188	3.020	3.834	3.653	0.394	0.576	0.545
L-9-5-11*	10.31	0.665	0.116	0.070	0.178	3.178	3.018	3.694	3.580	0.389	0.572	0.74
L-9-5-12	10.23	0.593	0.108	0.067	0.182	2.802	2.690	3.321	3.384	0.377	0.500	0.471
L-9-5-13*	10.20	0.570	0.105	0.066	0.183	2.797	2.637	3.300	3.371	0.498	0.469	0.82
L-9-5-14	10.12	0.506	0.095	0.063	0.188	2.828	2.290	2.863	3.050	0.428	0.405	-----
L-9-5-15*	10.09	0.483	0.092	0.062	0.190	2.428	2.344	2.739	2.949	0.353	0.428	0.413
L-9-5-16	10.05	0.483	0.098	0.060	0.213	2.103	2.045	2.528	3.069	0.380	0.369	0.359
L-9-5-17*	10.02	0.423	0.081	0.057	0.191	2.129	2.078	2.420	2.647	0.328	0.372	0.363
L-9-5-18	10.00	0.405	0.078	0.056	0.193	1.868	1.815	2.318	2.559	0.322	0.326	0.317
L-9-5-19*	9.97	0.377	0.074	0.055	0.196	1.870	1.619	2.169	2.448	0.319	0.325	0.317
L-9-5-20	9.93	0.343	0.068	0.052	0.197	1.589	1.541	2.251	2.301	0.275	0.267	-----
L-9-5-21*	9.90	0.325	0.068	0.051	0.198	1.592	1.570	1.880	2.153	0.294	0.275	0.271
L-9-5-22	9.89	0.317	0.063	0.050	0.197	1.363	1.348	1.836	2.097	0.290	0.235	0.232
L-9-5-23*	9.88	0.309	0.061	0.050	0.197	1.477	1.460	1.790	2.040	0.287	0.255	0.252
L-9-5-24	10.51	0.822	0.124	0.085	0.150	3.904	3.668	3.680	0.866	0.716	0.672	-----
L-9-5-25	10.50	0.820	0.120	0.096	0.146	6.022	3.732	4.477	3.576	0.525	0.737	0.684
L-9-5-26	10.45	0.788	0.122	0.081	0.159	3.818	3.560	3.322	3.660	0.587	0.696	0.689
L-9-5-27	10.40	0.749	0.121	0.072	0.161	3.495	3.255	4.127	3.671	0.399	0.634	0.591

UNLESS OTHERWISE INDICATED, ALL DATA ARE FOR:

1. SUPERCAVITATING FLOW.
2. BOTH STATIC PRESSURE TAPS OPEN.

## LEGEND

- \* ONLY UPSTREAM STATIC PRESSURE TAP UTILIZED
- \* CAVLTN STATIC PRESSURE TAP UTILIZED
- PC PARTIALLY CAVITATING
- PC (PW) PARTIALLY CAVITATING (TAP WETTED)
- PW FULLY WETTED

AT (ALPHAT) (TDEU) ANGLE OF ATTACK, CORRECTED FOR EFFECTS OF IMAGES OF TRAILING VORTICES  
 AT2 ALPHAT+0.2

SIGC CAVITATION NUMBER COMPUTED WITH MEASURED CAVITY PRESSURE  
 SIGN CAVITATION NUMBER COMPUTED WITH CALCULATED VAPOR PRESSURE  
 CD DRAG COEFFICIENT, CORRECTED FOR EFFECTS OF IMAGES OF TRAILING VORTICES  
 (D/L) CORRECTED DRAG-TO-LIFT RATIO = CD/CL  
 CAVLTN CAVITY LENGTH MEASURED FROM MIDCHORD AT CENTROID POSITION, NONDIMENSIONALIZED ON MEAN CHORD  
 (OBTAINED FROM PHOTOGRAPHS)

HIPER TESTS OF WALL EFFECTS ON SUPERCAVITATING HYDROPOOLS OF FINITE SPAN

HYDROPOOL INPUT DATA

TR TT AREA SPAN RAC

75 82 90.0 15.0 6.03

ZERO READINGS AND TUNNEL TEMP BEFORE AND AFTER

BARO 1-N 1-N 2-N 2-N 3-N 3-N  
 BARO 1-N 1-N 2-N 2-N 3-N 3-N  
 0- 0-0 0-0 0-0 100.0 0-0 100.0 0-0 100.0 0-0 100.0  
 0- 0-0 0-0 0-0 101.5 0-0 95.0 0-0 92.5  
 CBL LES/CT (NORMAL/REV) 41=0.20000 42=0.20000 43=0.04030  
 TWIST= 7200.0 SHARP DI= 1.50IN

INPUT DATA AS RECORDED\*\*

RUN NO	BARO	S	01	S	02	S	03	PIMP	PCAV
L-11-01	1227.	-1796.0	R	163.0	R	1665.0	R	219.	41.
L-11-02	1227.	-1620.0	R	157.0	R	1634.0	R	198.	39.
L-11-03	1225.	-1466.0	R	154.2	R	1565.0	R	181.	37.
L-11-04	1231.	-1316.0	R	151.8	R	1870.0	R	165.	35.
L-11-05*	1229.	-1256.0	R	151.2	R	1434.0	R	165.	35.
L-11-06*	1229.	-1358.0	R	152.6	R	1506.0	R	165.	35.
L-11-07	1238.	-1196.0	R	150.5	R	1388.0	R	150.	35.
L-11-08*	1237.	-1140.0	R	149.5	R	1346.0	R	154.	34.
L-11-09	1237.	-1048.0	R	148.0	R	1272.0	R	140.	30.
L-11-10*	1240.	-1008.0	R	147.5	R	1234.0	R	139.	29.
L-11-11	1240.	-916.0	R	144.8	R	1140.0	R	122.	29.
L-11-12*	1243.	-858.0	R	144.5	R	1103.0	R	122.	29.
L-11-13	1241.	-830.0	R	143.8	R	1074.0	R	113.	29.
L-11-14*	1243.	-778.0	R	142.7	R	1018.0	R	113.	29.
L-11-15	1246.	-748.0	R	141.9	R	987.0	R	103.	29.
L-11-16*	1239.	-696.0	R	180.0	R	933.0	R	102.	29.
L-11-17	1238.	-710.0	R	141.0	R	950.0	R	94.	29.
L-11-18*	1105.	-638.0	R	136.2	R	862.0	R	97.	29.
L-11-19	1026.	-892.0	R	140.9	R	1085.0	R	123.	31.
L-11-20*	1028.	-860.0	R	140.6	R	1059.0	R	124.	30.

LEGEND TR ROOM TEMPER (DEG FAHRS)

TT TUNNEL " ( " )

AREA HALF-SPAN MODEL PLANE AREA (SQ IN)

SPAN POOL HALF-SPAN (IN)

RAC MEAN CHORD, MEAS. A MODEL CENTROID (IN)

MANON VELOCITY MANOMETER READING (IN)

TWIST SHARP TWIST (DEGREES/IN-LB)

S LOAD CELL POLARITY (N=NORMAL, R=REVERSE)

LOAD CELL #1 LIPT (COUNTS)

#2 BOWENT ABOUT CHORD (COUNTS)

03 DRAG (COUNTS)

PIMP STATIC PRESSURE (MM HG)

PCAV CAVITY PRESSURE (MM HG)

RUN NO Q-KKK-KY: Q=POOL TESTED(S=SMALL, N=MED, L=LARGE)

KK=GEOMETRIC ATTACK ANGLE (DEGREES)

YY=RUN NUMBER, THIS POOL @ THIS ANGLE

## EFFECTS OF WALL EFFECTS ON SUPERCAVITATING HYDROPOILS OF PIVOT SPAN

## INPUT DATA CORRECTED FOR ZERO READINGS, SIGNS, AND HYDROSTATIC PRESSURE

RUN NO.	MASS	81	82	83	PMBP	PCAV
L-11.-01	1227.	-1796.0	-63.0	-1565.0	212.	41.
L-11.-02	1227.	-1620.0	-56.9	-1534.3	191.	39.
L-11.-03	1225.	-1466.0	-54.0	-1465.5	178.	37.
L-11.-04	1231.	-1316.0	-51.6	-1370.8	158.	35.
L-11.-05	1229.	-1256.0	-50.9	-1335.1	158.	35.
L-11.-06	1229.	-1358.0	-52.2	-1807.3	158.	35.
L-11.-07	1238.	-1196.0	-50.0	-1289.6	187.	35.
L-11.-08	1237.	-1140.0	-48.9	-1247.8	187.	34.
L-11.-09	1237.	-1048.0	-47.4	-1174.1	133.	30.
L-11.-10	1240.	-1008.0	-46.8	-1136.4	112.	29.
L-11.-11	1240.	-916.0	-44.0	-1042.6	115.	29.
L-11.-12	1243.	-858.0	-43.6	-1005.9	115.	29.
L-11.-13	1241.	-830.0	-42.9	-977.2	106.	29.
L-11.-14	1243.	-774.0	-41.7	-921.4	106.	29.
L-11.-15	1246.	-788.0	-40.8	-890.7	96.	29.
L-11.-16	1239.	-696.0	-38.8	-836.9	95.	29.
L-11.-17	1238.	-710.0	-39.7	-854.2	87.	29.
L-11.-18	1105.	-638.0	-34.9	-766.5	90.	29.
L-11.-19	1026.	-882.0	-39.5	-989.7	116.	31.
L-11.-20	1028.	-860.0	-39.1	-964.0	117.	30.

REPORT ON WALL EFFECTS ON SUPERFACILITATING HYDROPOOLS OF PINEY SPAR

\*\*HYDROPOOL DATA REDUCTION\*\*

RUN NO	ALPHA	LIFT-LB	DRAG-LB	BON-IBLS	VEL-PPS
L-11--01	11.03	371.80	63.07	226.80	26.04
L-11--02	11.03	335.38	61.83	204.92	26.04
L-11--03	11.03	304.01	59.06	194.55	26.02
L-11--04	11.03	271.51	55.26	185.63	26.00
L-11--05	11.03	261.38	53.80	183.18	26.06
L-11--06	11.03	262.04	56.71	187.94	26.06
L-11--07	11.03	249.21	51.97	180.09	26.15
L-11--08	11.02	237.79	50.29	176.21	26.14
L-11--09	11.02	219.07	47.32	170.53	26.14
L-11--10	11.02	210.96	45.80	168.44	26.17
L-11--11	11.02	192.00	42.02	158.44	26.17
L-11--12	11.02	180.33	40.54	157.07	26.20
L-11--13	11.02	179.57	39.38	154.27	26.18
L-11--14	11.02	162.13	37.13	150.03	26.20
L-11--15	11.02	157.76	35.89	146.86	26.23
L-11--16	11.02	186.96	33.73	139.74	26.16
L-11--17	11.02	189.95	34.42	143.05	26.15
L-11--18	11.02	134.57	30.89	125.49	24.81
L-11--19	11.02	168.30	39.89	142.12	23.96
L-11--20	11.02	179.82	38.85	140.76	23.99

LEGEND

VEL UPSTREAM VELOCITY (D)

**UPPER LIVES OF WALL EFFECTS ON SUPERACCELERATING HYDROPOILS OF FINITE SPAN**

**HYDROPOIL DATA IN NONDIMENSIONAL FORM (NO CORRECTIONS APPLIED) ::**

BUS NO	ALPHA	CL	CDUNC	CA	L/D	D/L
L-11.-01	11.03	0.3067	0.1493	0.0917	6.0749	8.8E10***-6
L-11.-02	11.03	0.8179	0.1462	0.0829	5.5931	0.1646
L-11.-03	11.03	0.7125	0.1397	0.0788	5.3152	1.4427
L-11.-04	11.03	0.6650	0.1298	0.0768	5.1248	1.7880
L-11.-05	11.03	0.6365	0.1265	0.0780	5.0310	0.1881
L-11.-06	11.03	0.6668	0.1335	0.0759	5.1825	0.1951
L-11.-07	11.03	0.6027	0.1211	0.0722	6.9753	0.1987
L-11.-08	11.02	0.5155	0.1172	0.0707	6.9122	0.2010
L-11.-09	11.02	0.5102	0.1100	0.0684	6.8216	1.4481
L-11.-10	11.02	0.5098	0.1060	0.0675	4.8082	0.2074
L-11.-11	11.02	0.6637	0.0969	0.0635	6.7880	0.2082
L-11.-12	11.02	0.4345	0.0931	0.0628	6.6657	1.4498
L-11.-13	11.02	0.4213	0.0905	0.0617	6.6550	0.2143
L-11.-14	11.02	0.3931	0.0849	0.0599	6.6286	1.4514
L-11.-15	11.02	0.3193	0.0817	0.0586	6.3936	0.2155
L-11.-16	11.02	0.3552	0.0770	0.0560	6.6186	1.4530
L-11.-17	11.02	0.3627	0.0787	0.0574	6.6077	0.2167
L-11.-18	11.02	0.3618	0.0785	0.0559	6.6112	1.4492
L-11.-19	11.02	0.5109	0.1101	0.0679	6.8136	0.2170
L-11.-20	11.02	0.5170	0.1071	0.0671	6.3278	1.3287

**LEGEND**

ALPHA GEOMETRIC ANGLE OF ATTACK CORRECTED FOR SHARP TWIST  
 CL LIFT COEFFICIENT, NONDIMENSIONALIZED ON UPSTREAM VELOCITY AND MODEL PLANFORM AREA  
 CDUNC CD (UNCORRECTED). THE UNCORRECTED DRAG COEFFICIENT AS COMPUTED FROM MEASURED DRAG, AND NONDIMENSIONALIZED  
 ON UPSTREAM VELOCITY AND MODEL PLANFORM AREA  
 CA MOMENT COEFFICIENT, NONDIMENSIONALIZED ON UPSTREAM VELOCITY, MODEL PLANFORM AREA, AND MEAN CHORD  
 L/D LIFT-TO-DRAG RATIO = CL/CDUNC  
 D/L DRAG-TO-LIFT RATIO = CDUNC/CL  
 RE REYNOLDS NUMBER, BASED ON MEAN CHORD

## EFFECTS OF WALL EFFECTS ON SUPERCAVITATING HYDROFOILS OF FINITE SPAN

## APPENDIX DATA CORRECTED FOR EFFECTS OF IMAGES OF TRAILING VORTEX SYSTEM\*

BUN NO	ALPHAT	CL	CD	CH	(D/L)	SIGC/AT	CL/AT	CD/AT2	CH/AT	SIGV	SIGC	CAVTH	COMMENTS/REMARKS
L-11.-01	12.11	0.967	0.166	0.092	0.183	3.720	0.291	3.728	0.484	0.786	0.727	0.72	
L-11.-02	12.00	0.818	0.160	0.083	0.196	3.326	0.3086	3.906	1.650	0.396	0.697	0.646	0.82
L-11.-03	11.91	0.784	0.151	0.079	0.204	3.007	2.807	3.573	3.493	0.379	0.625	0.583	0.92
L-11.-04	11.81	0.665	0.139	0.075	0.209	2.668	2.529	3.225	3.267	0.363	0.554	0.522	0.95
L-11.-05*	11.78	0.636	0.135	0.078	0.212	2.698	2.540	3.096	3.190	0.360	0.555	0.522	---
L-11.-06*	11.84	0.687	0.143	0.076	0.209	2.683	2.528	3.323	3.356	0.357	0.554	0.522	---
L-11.-07	11.74	0.693	0.129	0.072	0.213	2.460	2.306	2.982	3.065	0.353	0.504	0.472	1.03
L-11.-08*	11.71	0.576	0.124	0.071	0.215	2.467	2.335	2.817	2.971	0.346	0.504	0.477	1.08
L-11.-09	11.65	0.530	0.116	0.068	0.218	2.187	2.139	2.607	2.800	0.337	0.445	0.435	---
L-11.-10*	11.63	0.509	0.111	0.067	0.219	2.165	2.138	2.510	2.705	0.332	0.439	0.434	1.30
L-11.-11	11.57	0.464	0.101	0.063	0.219	1.820	1.795	2.296	2.885	0.318	0.368	0.363	---
L-11.-12*	11.54	0.438	0.097	0.063	0.223	1.820	1.796	2.158	2.393	0.312	0.366	0.362	1.68
L-11.-13	11.52	0.421	0.094	0.062	0.223	1.636	2.095	2.329	2.477	0.307	0.329	0.329	---
L-11.-14*	11.49	0.393	0.088	0.060	0.224	1.637	1.616	1.961	2.192	0.299	0.328	0.328	2.05
L-11.-15	11.47	0.379	0.085	0.059	0.223	1.495	1.405	1.895	2.118	0.292	0.285	0.281	---
L-11.-16*	11.44	0.355	0.080	0.056	0.224	1.414	1.395	1.779	1.996	0.282	0.279	0.279	3.20
L-11.-17	11.45	0.363	0.081	0.057	0.225	1.243	1.227	1.815	2.039	0.287	0.248	0.245	3.12
L-11.-18*	11.45	0.362	0.081	0.056	0.224	1.451	1.434	1.811	2.034	0.280	0.290	0.287	4.12
L-11.-19	11.65	0.531	0.116	0.068	0.219	2.167	2.102	2.611	2.809	0.334	0.461	0.427	---
L-11.-20*	11.63	0.517	0.113	0.067	0.218	2.189	2.150	2.547	2.732	0.331	0.444	0.437	---

UNLESS OTHERWISE INDICATED, ALL DATA ARE FOR:

1. SUPERCAVITATING FLOW.
2. BOTH STATIC PRESSURE TAPS OPEN.

## LEGEND

- \* ONLY UPSTREAM STATIC PRESSURE TAP UTILIZED
- PC PARTIALLY CAVITATING
- PC(TW) PARTIALLY CAVITATING (TAP WETTED)
- PW FULLY WETTED

AT (ALPHAT) (TRUE) ANGLE OF ATTACK, CORRECTED FOR EFFECTS OF IMAGES OF TRAILING VORTICES

AT2 ALPHAT\*\*2

SIGC CAVITATION NUMBER COMPUTED WITH MEASURED CAVITY PRESSURE

SIGV CAVITATION NUMBER COMPUTED WITH CALCULATED VAPOR PRESSURE

CD DRAG COEFFICIENT, CORRECTED FOR EFFECTS OF IMAGES OF TRAILING VORTICES

(D/L) CORRECTED DRAG-TO-LIFT RATIO = CD/CL

CAVTH CAVITY LENGTH MEASURED FROM MIDCHORD AT CENTROID POSITION, NONDIMENSIONALIZED ON MEAN CHORD  
(OBTAINED FROM PHOTOGRAPHS)

HYPHER ILLUSTRATION OF WALL EFFECTS ON SUPERACCELERATING HYDROPOILS OF PIVOT SPAN

HYDROPOIL INPUT DATA

TR	TT	AREA	SPAN	HAC
76	86	90.0	15.0	6.03

ZERO BEATINGS AND TUNNEL TEMP BEFORE AND AFTER

BAIRON	1-8	2-8	3-8	3-8	FT
0-	0.0	0.0	100.0	0.0	85.5
0.	0.0	0.0	99.5	0.0	86.0
CELL LBS/CF (NORMAL/REV)	0=0.20000	02=0.20000	03=0.04030		
TWIST= 7200.0	SHARP DIA.= 1.50IN				

\*INPUT DATA AS RECORDED\*

RUN NO	BAIRON	S	A1	S	#2	S	#3	PIMP	PCAV
L-12--01	476.		-698.0	R	151.6	R	665.0	760.	-----
L-12--02	778.		-1110.0	R	181.8	R	1004.0	722.	-----
L-12--03	1160.		-1620.0	R	219.6	R	1420.0	675.	-----
L-12--04	1165.		-1706.0	R	215.0	R	1518.0	298.	-----
L-12--05	1165.		-1884.0	R	197.5	R	1670.0	272.	-----
L-12--06	1167.		-1944.0	R	180.5	R	1797.0	255.	-----
L-12--07	1166.		-1870.0	R	167.5	R	1880.0	236.	52.
L-12--08+	1167.		-1830.0	R	164.1	R	1839.0	236.	52.
L-12--09	1166.		-1730.0	R	159.7	R	1819.0	218.	0.
L-12--10+	1166.		-1680.0	R	158.2	R	1807.0	218.	0.
L-12--11	1166.		-1594.0	R	156.0	R	1770.0	202.	47.
L-12--12+	1166.		-1582.0	R	155.0	R	1755.0	202.	66.
L-12--13	1165.		-1414.0	R	153.0	R	1610.0	184.	44.
L-12--14+	1167.		-1364.0	R	152.1	R	1630.0	186.	44.
L-12--15	1168.		-1276.0	R	150.8	R	1560.0	168.	43.
L-12--16+	1169.		-1220.0	R	149.9	R	1518.0	168.	42.
L-12--17	1169.		-1150.0	R	148.6	R	1457.0	154.	41.
L-12--18+	1169.		-1100.0	R	147.8	R	1413.0	154.	39.
L-12--19	1169.		-1022.0	R	146.2	R	1335.0	141.	36.
L-12--20+	1170.		-980.0	R	145.5	R	1285.0	141.	36.
L-12--21	1171.		-94.0	R	146.0	R	1031.0	112.	36.
L-12--22+	1169.		-874.0	R	143.4	R	1198.0	129.	36.
L-12--23	1171.		-850.0	R	142.9	R	1170.0	121.	36.
L-12--24+	1170.		-810.0	R	142.0	R	1127.0	121.	36.
L-12--25	1171.		-780.0	R	140.9	R	1084.0	111.	36.
L-12--26+	1171.		-728.0	R	139.5	R	1031.0	112.	36.
L-12--27	1171.		-728.0	R	139.5	R	1032.0	101.	36.
L-12--28+	1160.		-662.0	R	136.0	R	950.0	36.	36.
L-12--29	1164.		-1810.0	R	152.4	R	1657.0	184.	45.
L-12--30	900.		-1086.0	R	180.9	R	1320.0	151.	02.
L-12--31	612.		-708.0	R	127.5	R	905.0	113.	40.
L-12--32	388.		-498.0	R	118.2	R	643.0	93.	40.
LEGEND	TR ROOM TAPER (DEG FAHR)							LOAD CELL #1 LIFT (COUNTS)	
TT TUNNEL "	"							#2 MOMENT ABOUT MIDCHORD (COUNTS)	
AREA HALF-SPAN MODEL PLATEFORM AREA (SQ IN)								#3 DRAG (COUNTS)	
SPAN POIL HALF-SPAN (IN)								PIMP STATIC PRESSURE (MM HG)	
HAC MEAN CHORD, MEAS. @ MODEL CENTROID (IN)								PCAV CAVITY PRESSURE (MM HG)	
MANOM VELOCITY MANOMETER READING (MM)								RUN NO Q-KKI-II: Q-POIL TESTED(S-SMALL, M-MED, L-LARGE)	
TWIST SHARP TWIST (DEGREES/IN-1D)								X-X-GEAR METRIC ATTACK ANGLE (DEGREES)	
S LOAD CELL POLARITY (N-NORMAL, R-REVERSE)								YY-ROW NUMBER, THIS POIL @ THIS ANGLZ	

## EFFECTS OF WALL EFFECTS ON SUPERCAVITATING HYDROFOILS OF FINITE SPAN

## INPUT DATA CORRECTED FOR ZERO READINGS, SIGNS, AND HYDROSTATIC PRESSURES

PIN#	RHO	01	02	03	PIN#	PCAV
L-12--01	976.	-698.0	-51.6	-565.0	753.	----
L-12--02	778.	-1110.0	-81.8	-903.8	715.	----
L-12--03	1160.	-1628.0	-119.6	-1319.5	668.	----
L-12--04	1165.	-1786.0	-115.0	-1617.3	287.	----
L-12--05	1163.	-1863.0	-97.6	-1569.1	265.	----
L-12--06	1167.	-1934.0	-80.6	-1695.9	248.	----
L-12--07	1166.	-1870.0	-67.6	-1718.6	229.	52.
L-12--08	1167.	-1830.0	-64.2	-1737.4	229.	52.
L-12--09	1166.	-1710.0	-59.8	-1717.2	211.	69.
L-12--10	1166.	-1680.0	-58.3	-1705.0	211.	48.
L-12--11	1166.	-1594.0	-56.2	-1667.7	195.	47.
L-12--12	1166.	-1522.0	-55.2	-1682.5	195.	86.
L-12--13	1165.	-1418.0	-53.2	-1567.3	177.	44.
L-12--14	1167.	-1364.0	-52.3	-1527.1	177.	48.
L-12--15	1168.	-1276.0	-51.0	-1656.8	161.	43.
L-12--16	1169.	-1220.0	-50.1	-1444.6	161.	42.
L-12--17	1169.	-1150.0	-48.9	-1353.4	147.	41.
L-12--18	1169.	-1100.0	-48.1	-1309.2	147.	39.
L-12--19	1169.	-1022.0	-46.5	-1230.9	134.	36.
L-12--20	1170.	-960.0	-45.8	-1180.7	134.	36.
L-12--21	1171.	-934.0	-44.3	-1136.5	123.	36.
L-12--22	1169.	-874.0	-43.7	-1093.3	122.	36.
L-12--23	1171.	-850.0	-43.3	-1065.0	114.	36..
L-12--24	1170.	-810.0	-42.4	-1021.8	114.	36..
L-12--25	1171.	-780.0	-41.3	-978.6	104.	36..
L-12--26	1171.	-728.0	-19.9	-925.4	105.	36..
L-12--27	1171.	-728.0	-19.9	-926.1	94.	36..
L-12--28	1160.	-662.0	-36.4	-863.9	97.	36..
L-12--29	1164.	-1410.0	-52.9	-1550.7	177.	45.
L-12--30	900.	-1096.0	-41.4	-1213.5	144.	42.
L-12--31	612.	-708.0	-28.0	-798.2	106.	40.
L-12--32	386.	-498.0	-18.7	-536.0	86.	40.

EXPERIMENTS OF WALL EFFECTS ON SUPERCAVITATING HYDROFOILS OF FINITE SPAN

\*\*\*HYDROFOIL DATA REDUCTIONS\*\*\*

SUP NO	ALPHA	LIFT-LB	DRAG-LB	MOM-INLB	VEL-FPS
L-12.-.01	12.03	149.92	22.77	185.76	16.76
L-12.-.02	12.04	236.36	36.42	294.54	21.02
L-12.-.03	12.06	369.53	53.18	430.68	25.37
L-12.-.04	12.06	369.53	53.12	418.17	25.92
L-12.-.05	12.05	380.21	57.12	351.23	25.40
L-12.-.06	12.04	356.31	63.23	290.09	25.44
L-12.-.07	12.03	387.52	70.07	243.35	25.43
L-12.-.08	12.03	378.84	70.02	231.17	25.44
L-12.-.09	12.03	351.97	69.20	215.38	25.63
L-12.-.10	12.03	387.67	68.71	210.04	25.43
L-12.-.11	12.03	330.03	67.21	202.18	25.43
L-12.-.12	12.03	319.48	66.19	198.64	25.43
L-12.-.13	12.03	293.44	63.16	191.50	25.42
L-12.-.14	12.03	283.26	61.54	188.31	25.44
L-12.-.15	12.03	265.81	58.71	183.69	25.46
L-12.-.16	12.03	250.03	57.01	180.51	25.47
L-12.-.17	12.02	239.77	54.54	175.89	25.47
L-12.-.18	12.02	229.61	52.76	173.07	25.47
L-12.-.19	12.02	213.70	49.61	167.37	25.47
L-12.-.20	12.02	205.16	47.58	164.90	25.48
L-12.-.21	12.02	195.66	45.80	159.56	25.49
L-12.-.22	12.02	183.55	44.06	157.46	25.47
L-12.-.23	12.02	178.65	42.92	155.72	25.49
L-12.-.24	12.02	170.47	41.18	152.54	25.48
L-12.-.25	12.02	168.26	39.44	148.63	25.49
L-12.-.26	12.02	153.58	37.29	143.65	25.49
L-12.-.27	12.02	153.58	37.32	143.71	25.49
L-12.-.28	12.02	139.69	34.01	131.17	25.47
L-12.-.29	12.03	292.57	62.49	190.27	25.91
L-12.-.30	12.02	227.47	48.90	148.92	22.55
L-12.-.31	12.01	197.20	32.17	100.74	18.84
L-12.-.32	12.01	103.34	21.60	67.32	15.24

LEGEND

VEL UPSTREAM VELOCITY (0)

AD-A056 090

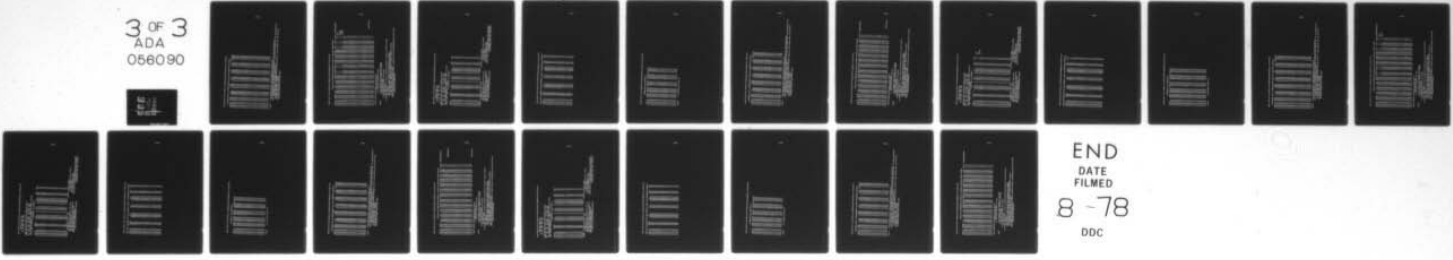
MASSACHUSETTS INST OF TECH CAMBRIDGE DEPT OF OCEAN E--ETC F/G 20/4  
AN EXPERIMENTAL INVESTIGATION OF WALL EFFECTS ON SUPERCAVITATION--ETC(U)  
AUG 77 M R MAIXNER

N00014-76-C-0358

NL

UNCLASSIFIED

3 OF 3  
ADA  
056090



END  
DATE  
FILMED  
8-78  
DDC

SUPER INLES OF WALL EFFECTS ON SUPERCAVITATING HYDROFOILS OF FINITE SPAN

CONT'D

RUN NO.	ALPHA	CL	CDUNC	CB	L/D	D/L	BRe10 <sup>6</sup> -6
L-12--01	12.03	0.8829	0.1293	0.1814	6.8299	0.1464	0.9650
L-12--02	12.04	0.8929	0.1316	0.1830	6.7164	0.1476	1.2099
L-12--03	12.06	0.8996	0.1322	0.1836	6.7988	0.1471	1.4605
L-12--04	12.06	0.9736	0.1417	0.1759	6.8700	0.1456	1.4634
L-12--05	12.05	1.0166	0.1576	0.1494	6.4880	0.1551	1.4623
L-12--06	12.04	1.0301	0.1702	0.1230	6.0528	0.1652	1.4646
L-12--07	12.03	0.9915	0.1747	0.1033	6.6795	0.1762	1.4640
L-12--08	12.03	0.9685	0.1745	0.0980	5.5516	0.1801	1.4646
L-12--09	12.03	0.9159	0.1725	0.0914	5.3089	0.1884	1.4640
L-12--10	12.03	0.8895	0.1713	0.0891	5.1982	0.1925	1.4640
L-12--11	12.03	0.8844	0.1674	0.0858	5.0437	0.1983	1.4640
L-12--12	12.03	0.8173	0.1648	0.0843	4.9588	0.2017	1.4640
L-12--13	12.03	0.7518	0.1572	0.0813	4.7801	0.2092	1.4634
L-12--14	12.03	0.7242	0.1528	0.0798	4.7397	0.2110	1.4646
L-12--15	12.03	0.6780	0.1454	0.0778	4.6618	0.2145	1.4652
L-12--16	12.33	0.6464	0.1410	0.0764	4.5995	0.2174	1.4658
L-12--17	12.02	0.6120	0.1397	0.0745	4.5844	0.2200	1.4658
L-12--18	12.02	0.5851	0.1301	0.0733	4.5041	0.2220	1.4658
L-12--19	12.02	0.5655	0.1221	0.0708	4.4682	0.2238	1.4658
L-12--20	12.02	0.5232	0.1168	0.0697	4.4794	0.2232	1.4668
L-12--21	12.02	0.4986	0.1122	0.0674	4.4451	0.2250	1.4669
L-12--22	12.02	0.4685	0.1079	0.0667	4.3444	0.2303	1.4658
L-12--23	12.02	0.4553	0.1048	0.0658	4.3427	0.2303	1.4669
L-12--24	12.02	0.4313	0.1005	0.0645	4.3270	0.2311	1.4664
L-12--25	12.02	0.4186	0.0960	0.0628	4.3622	0.2292	1.4669
L-12--26	12.02	0.3914	0.0905	0.0607	4.3251	0.2312	1.4669
L-12--27	12.32	0.3914	0.0936	0.0607	4.3249	0.2314	1.4669
L-12--28	12.02	0.3591	0.0829	0.0559	4.3346	0.2348	1.4605
L-12--29	12.03	0.2897	0.1556	0.0809	4.8184	0.2075	1.4629
L-12--30	12.02	0.2906	0.1546	0.0804	4.7907	0.2087	1.2979
L-12--31	12.01	0.6861	0.1452	0.0779	4.7553	0.2116	1.0847
L-12--32	12.01	0.7361	0.1490	0.0795	4.9411	0.2324	0.8774

LEGEND

ALPHA GEOMETRIC ANGLE OF ATTACK CORRECTED FOR SHAFT TWIST

CL LIFT COEFFICIENT, NONDIMENSIONALIZED ON UPSTREAM VELOCITY AND MODEL PLANTFORM AREA  
 CDUNC CD (UNCORRECTED). THE UNCORRECTED DRAG COEFFICIENT AS COMPUTED FROM MEASURED DRAG, AND NONDIMENSIONALIZED  
 ON UPSTREAM VELOCITY AND MODEL PLANTFORM AREA

CB NONDIMENSIONALIZED DRAG COEFFICIENT, NONDIMENSIONALIZED ON UPSTREAM VELOCITY. MODEL PLANTFORM AREA, AND REYNOLD CHORD  
 L/D LIFT-TO-DRAG RATIO = CL/CDUNC  
 D/L DRAG-TO-LIFT RATIO = CDUNC/CL  
 RN REYNOLDS NUMBER, BASED ON ARAM CHORD

EXPERIMENTS ON SUPERCAVITATING HYDROFOILS OF FINITE SPAN

\*OPERATOR DATA CORRECTED FOR EFFECTS OF IMAGES OF TRAILING VORTEX SYSTEM\*

RUN NO.	ALPHAT	CL	CD	CH	(D/L)	SIGV	AT SIGV/AT	CL/AT	CD/AT2	CH/AT	SIGC	SIGV	CAVTH	COMMENTS/REMARKS
L-12.-0.1	13.07	0.883	0.185	0.181	0.165	-----	-----	3.870	2.793	0.795	-----	-----	PW	
L-12.-0.2	13.10	0.893	0.148	0.183	0.166	-----	-----	3.906	2.837	0.800	-----	-----	PW	
L-12.-0.3	13.13	0.893	0.149	0.184	0.166	-----	-----	3.922	2.837	0.802	-----	-----	PW	
L-12.-0.4	13.21	0.974	0.161	0.176	0.166	-----	-----	4.222	3.034	0.763	-----	-----	PC (PW)	
L-12.-0.5	13.25	1.016	0.179	0.189	0.176	-----	-----	4.394	3.385	0.646	-----	-----	PC (PW)	
L-12.-0.6	13.26	1.030	0.192	0.123	0.187	-----	-----	4.450	3.586	0.531	-----	-----	PC (PW)	
L-12.-0.7	13.21	0.991	0.195	0.103	0.197	3.814	3.424	4.210	3.663	0.426	0.879	0.789	0.61	
L-12.-0.8*	13.18	0.969	0.194	0.098	0.200	3.818	3.428	4.210	3.663	0.426	0.879	0.789	0.61	
L-12.-0.9	13.12	0.916	0.190	0.091	0.207	3.468	3.156	4.001	3.623	0.399	0.798	0.723	-----	
L-12.-10*	13.08	0.690	0.188	0.089	0.211	3.495	3.183	3.995	3.598	0.390	0.798	0.727	0.64	
L-12.-11	13.03	0.884	0.182	0.086	0.216	3.194	2.903	3.711	3.523	0.377	0.726	0.660	-----	
L-12.-12*	13.00	0.817	0.179	0.084	0.219	3.201	2.930	3.603	3.472	0.372	0.726	0.665	0.74	
L-12.-13	12.92	0.751	0.169	0.081	0.225	2.866	2.639	3.333	3.322	0.361	0.636	0.594	-----	
L-12.-14*	12.89	0.728	0.164	0.084	0.226	2.636	2.420	3.236	3.236	0.355	0.645	0.593	1.00	
L-12.-15	12.83	0.678	0.155	0.078	0.229	2.557	2.389	3.028	3.090	0.348	0.573	0.526	-----	
L-12.-16*	12.79	0.648	0.150	0.076	0.231	2.561	2.372	2.904	3.002	0.342	0.572	0.530	1.05	
L-12.-17	12.75	0.612	0.142	0.074	0.233	2.288	2.121	2.750	2.876	0.335	0.509	0.472	-----	
L-12.-18*	12.72	0.586	0.137	0.073	0.235	2.292	2.166	2.640	2.785	0.330	0.509	0.481	1.18	
L-12.-19	12.67	0.585	0.128	0.071	0.235	2.038	1.974	2.467	2.622	0.320	0.451	0.436	-----	
L-12.-20*	12.64	0.523	0.122	0.070	0.234	2.039	1.976	2.371	2.515	0.316	0.450	0.436	1.20	
L-12.-21	12.61	0.498	0.117	0.067	0.235	1.819	1.758	2.265	2.421	0.306	0.400	0.387	-----	
L-12.-22*	12.58	0.468	0.112	0.067	0.240	1.805	1.785	2.134	2.334	0.304	0.396	0.383	1.73	
L-12.-23	12.56	0.455	0.109	0.066	0.240	1.641	1.581	2.077	2.270	0.300	0.360	0.347	-----	
L-12.-24*	12.54	0.435	0.104	0.065	0.240	1.644	1.587	1.987	2.180	0.295	0.360	0.347	2.10	
L-12.-25	12.52	0.419	0.100	0.063	0.238	1.440	1.386	1.916	2.087	0.288	0.315	0.303	-----	
L-12.-26*	12.48	0.391	0.094	0.061	0.239	1.463	1.410	1.796	1.973	0.279	0.319	0.307	3.55	
L-12.-27	12.46	0.391	0.094	0.061	0.240	1.237	1.186	1.796	2.279	0.270	0.258	0.258	-----	
L-12.-28*	12.44	0.359	0.086	0.056	0.238	1.312	1.262	1.653	1.814	0.257	0.285	0.274	4.10	
L-12.-29	12.92	0.750	0.167	0.081	0.223	2.842	2.617	3.226	3.291	0.359	0.641	0.590	-----	
L-12.-30	12.90	0.741	0.166	0.080	0.224	2.782	2.573	3.290	3.274	0.357	0.626	0.579	-----	
L-12.-31	12.83	0.686	0.155	0.078	0.226	2.625	2.400	3.065	3.091	0.348	0.588	0.537	-----	
L-12.-32	12.88	0.726	0.160	0.080	0.218	2.886	2.550	3.274	3.169	0.354	0.649	0.573	-----	

UNLESS OTHERWISE INDICATED, ALL DATA ARE FOR:

1. SUPERCAVITATING PLATE.
2. BOTH STATIC PRESSURE TAPS OPEN.

LEGEND

- ONLY UPSTREAM STATIC PRESSURE TAP UTILIZED
- ONLY DOWNSTREAM STATIC PRESSURE TAP UTILIZED
- PC (PARTIALLY) CAVITATING (TAP WETTED)
- PW (PARTIALLY) CAVITATING (TAP DRIED)
- AT (ALPHAT) (TRUE) ANGLE OF ATTACK, CORRECTED FOR EFFECTS OF IMAGES OF TRAILING VORTICES
  - AT2 ALPHAT=2
  - SIGC CAVITATION NUMBER COMPUTED WITH MEASURED CAVITY PRESSURE.
  - SIGV CAVITATION NUMBER COMPUTED WITH CALCULATED VAPOR PRESSURE
  - CD DRAG COEFFICIENT, CORRECTED FOR EFFECTS OF IMAGES OF TRAILING VORTICES
  - (D/L) CORRECTED DRAG-TO-LIFT RATIO = CD/CL
  - CAVTH CAVITY LENGTH MEASURED FROM MIDCHORD AT CENTROID POSITION, NONDIMENSIONALIZED ON MEAN CHORD (OBTAINED FROM PHOTOGRAPHS)

THE SPANISH INFLUENCE ON THE LITERATURE OF SPAIN

卷之三

BRUNSWICK, 1975-76  
SARAS  
BAC  
6-03

ZERO READINGS AND JEWEL TRAP BEFORE AND AFTER  
 HOURS 1-3 1-3 2-3 3-3 FT  
 0.0 0.0 0.0 100.0 0.0 100.0 82.5  
 0.0 0.0 0.0 100.0 0.0 100.0 84.0  
 CELL LS/CT (HORNBL. & SIV) 81=0.20000 82=0.20000 83=0.04030  
 TUST=7200.0 SMART DIA= 1.507

ESTATE PLANNING

SUPER INVES OF WALL EFFECTS ON SUPERCAVITATING HYDROPOOLS OF FINITE SPAN

INPUT DATA CORRECTED FOR ZERO BRADING, SIGNS, AND HYDROSTATIC PRESSURE

BUS NO.	RADIAL	01	02	03	PINP	PCAV
L-10.-01	1034.	-1816.0	-64.5	-2025.0	222.	53.
L-10.-02	1034.	-1750.0	-61.8	-2000.0	222.	51.
L-10.-03	1033.	-1700.0	-59.7	-1985.0	207.	89.
L-10.-04	1034.	-1640.0	-50.1	-1967.0	207.	48.
L-10.-05	1034.	-1582.0	-56.6	-1938.0	193.	45.
L-10.-06	1034.	-1528.0	-55.3	-1895.0	193.	44.
L-10.-07	1035.	-1426.0	-53.9	-1825.0	175.	81.
L-10.-08	1036.	-1372.0	-52.7	-1780.0	174.	40.
L-10.-09	1039.	-1301.0	-51.7	-1717.0	162.	39.
L-10.-10	1040.	-1258.0	-50.8	-1678.0	162.	38.
L-10.-11	1041.	-1196.0	-49.6	-1605.0	149.	37.
L-10.-12	1042.	-1140.0	-48.6	-1555.0	149.	36.
L-10.-13	1043.	-1062.0	-47.1	-1465.0	134.	32.
L-10.-14	1043.	-1018.0	-46.8	-1406.0	134.	31.
L-10.-15	1044.	-922.0	-46.1	-1336.0	120.	31.
L-10.-16	1044.	-908.0	-44.9	-1294.0	120.	30.
L-10.-17	1045.	-892.0	-44.9	-1275.0	114.	31.
L-10.-18	1044.	-826.0	-37.8	-1206.0	114.	30.
L-10.-19	1047.	-839.0	-43.7	-1193.0	107.	30.
L-10.-20	1043.	-776.0	-42.2	-1121.0	107.	30.
L-10.-21	1044.	-792.0	-42.2	-1115.0	99.	30.
L-10.-22	1034.	-718.0	-39.5	-1085.0	99.	30.
L-10.-23	697.	-732.0	-32.1	-1000.0	103.	32.
L-10.-24	697.	-694.0	-31.5	-954.0	103.	32.

RIBBED TUBES OF WALL EFFECTS ON SUPERFACILITATING HYDROPOOLS OF PINTLE SPAN

**CONTRAPORTFOL MESH REDUCTIONS\***

BUK NO	ALPHA	LIFT-LB	DRAG-LB	MOR-INLB	VEL-PPS
L-18.-01	18.-03	376.-10	81.-61	233.-20	28.-05
L-18.-02	18.-03	363.-95	80.-60	222.-34	28.-05
L-18.-03	18.-03	351.-94	80.-00	215.-00	28.-04
L-18.-04	18.-03	341.-22	79.-27	209.-10	28.-05
L-18.-05	18.-03	322.-73	77.-94	203.-92	28.-05
L-18.-06	18.-03	316.-66	76.-37	199.-10	28.-05
L-18.-07	18.-03	295.-67	73.-55	192.-11	24.-06
L-18.-08	18.-03	289.-35	71.-73	189.-81	24.-07
L-18.-09	18.-03	271.-18	69.-20	186.-07	24.-11
L-18.-10	18.-03	261.-77	67.-46	181.-05	24.-12
L-18.-11	18.-02	248.-72	68.-68	178.-59	24.-13
L-18.-12	18.-02	237.-71	62.-67	174.-85	24.-14
L-18.-13	18.-02	221.-83	59.-04	169.-67	24.-15
L-18.-14	18.-02	212.-96	56.-66	168.-85	24.-15
L-18.-15	18.-02	201.-61	53.-84	165.-79	24.-16
L-18.-16	18.-02	190.-58	52.-15	161.-69	24.-16
L-18.-17	18.-02	187.-37	51.-38	161.-55	24.-17
L-18.-18	18.-02	175.-77	48.-52	157.-81	24.-16
L-18.-19	18.-02	175.-56	48.-08	157.-30	24.-19
L-18.-20	18.-02	163.-63	45.-18	151.-76	24.-15
L-18.-21	18.-02	166.-84	45.-74	151.-98	24.-16
L-18.-22	18.-02	152.-70	42.-11	142.-12	24.-05
L-18.-23	18.-02	152.-83	40.-30	115.-70	19.-89
L-18.-24	18.-02	105.-10	38.-85	113.-40	19.-89

LEGEND

VEL UPSTREAM VELOCITY (U)

**REFINED LAVES OF SAIL EFFECTS ON SUPERCAVITATING RIBTOPS OF FISHER SPAN**

**•UNDIMENSIONAL DATA IN NONDIMENSIONAL FORM (NO CORRECTIONS APPLIED)•**

BUS NO	ALPHA	CL	CDUWC	CR	L/D	D/L	RE*10**-6
L-14.-01	18.-03	1.0755	0.2288	0.1101	8.7013	0.2127	1.3457
L-14.-02	18.-03	1.0408	0.2259	0.1059	8.6075	0.2170	1.3457
L-14.-03	18.-03	1.0074	0.2244	0.1021	8.5897	0.2227	1.3451
L-14.-04	18.-03	0.9758	0.2221	0.0992	8.52936	0.2276	1.3457
L-14.-05	18.-03	0.9372	0.2183	0.0967	8.42935	0.2329	1.3457
L-14.-06	18.-03	0.9056	0.2138	0.0946	8.32357	0.2361	1.3457
L-14.-07	18.-03	0.8854	0.2055	0.0910	8.11129	0.2431	1.3463
L-14.-08	18.-03	0.8138	0.2002	0.0899	8.06315	0.2461	1.3469
L-14.-09	18.-03	0.7719	0.1924	0.0878	8.01021	0.2492	1.3467
L-14.-10	18.-03	0.7446	0.1873	0.0863	7.97755	0.2515	1.3493
L-14.-11	18.-02	0.7068	0.1792	0.0842	7.94840	0.2536	1.3499
L-14.-12	18.-02	0.6749	0.1733	0.0823	7.89339	0.2568	1.3505
L-14.-13	18.-02	0.6293	0.1629	0.0798	7.86333	0.2588	1.3511
L-14.-14	18.-02	0.6041	0.1561	0.0792	7.86690	0.2585	1.3511
L-14.-15	18.-02	0.5714	0.1480	0.0779	7.86068	0.2590	1.3517
L-14.-16	18.-02	0.5402	0.1432	0.0760	7.77119	0.2651	1.3517
L-14.-17	18.-02	0.5306	0.1409	0.0759	7.7656	0.2656	1.3523
L-14.-18	18.-02	0.4987	0.1329	0.0762	7.7520	0.2665	1.3517
L-14.-19	18.-02	0.4962	0.1313	0.0737	7.7789	0.2646	1.3535
L-14.-20	18.-02	0.4642	0.1236	0.0714	7.7568	0.2662	1.3511
L-14.-21	18.-02	0.4729	0.1250	0.0710	7.7817	0.2644	1.3517
L-14.-22	18.-02	0.4367	0.1158	0.0678	7.7698	0.2653	1.3467
L-14.-23	18.-02	0.6398	0.1639	0.0803	7.9016	0.2563	1.1126
L-14.-24	18.-02	0.6070	0.1561	0.0787	7.8883	0.2572	1.1126

**LEGEND**

ALPHA GEOMETRIC ANGLE OF ATTACK CORRECTED FOR SHAPT TWIST

CL LIFT COEFFICIENT, nondimensionalized on upstream velocity and model planform area  
CDUWC CD (uncorrected), the uncorrected drag coefficient as computed from measured drag, and nondimensionalized  
on upstream velocity and model planform area

CR ROBERT COEFFICIENT, nondimensionalized on upstream velocity, model planform area, and mean chord

L/D LIFT-TO-DRAG RATIO = CL/CDUWC

D/L DRAG-TO-LIFT RATIO = CDUWC/CL

REYNOLDS NUMBERS, BASED ON REAR CHORD

**DATA TAKES OF WALL EFFECTS ON SUPERCAVITATING HYDROFOILS OF FINITE SPAN**

**APPENDIX DATA CORRECTED FOR EFFECTS OF IMAGES OF TRAILING VORTICES\***

BUS NO.	ALPHAT	C1	CD	CH	(D/L)	SIGC/AT	SIGC/AT	CL/AT	CD/AT2	CH/AT	SIGC	SIGC	CAVITY LENGTH	COMMENTS/REMARKS
L-14,-01	15.31	1.076	0.253	0.110	0.235	3.611	3.153	0.026	3.540	0.412	0.965	0.862	---	
L-14,-02*	15.27	1.061	0.248	0.105	0.239	3.620	3.199	3.906	3.898	0.396	0.964	0.852	0.70	
L-14,-03	15.22	1.007	0.245	0.102	0.244	3.567	3.155	3.791	3.475	0.384	0.890	0.788	---	
L-14,-04*	15.19	0.976	0.242	0.099	0.248	3.355	2.991	3.681	3.442	0.374	0.889	0.793	0.80	
L-14,-05	15.18	0.937	0.236	0.097	0.252	3.100	2.792	3.547	3.387	0.366	0.819	0.738	---	
L-14,-06*	15.10	0.906	0.231	0.094	0.255	3.107	2.816	3.322	3.358	0.819	0.783	0.83	---	
L-14,-07	15.03	0.845	0.220	0.091	0.261	2.777	2.545	3.223	3.202	0.347	0.728	0.668	---	
L-14,-08*	14.99	0.813	0.214	0.090	0.263	2.761	2.549	3.109	3.124	0.343	0.722	0.667	0.92	
L-14,-09	14.94	0.772	0.205	0.088	0.265	2.531	2.392	2.960	3.011	0.337	0.661	0.611	---	
L-14,-10*	14.91	0.745	0.199	0.086	0.267	2.536	2.364	2.862	2.936	0.332	0.660	0.615	0.95	
L-14,-11	14.86	0.707	0.190	0.084	0.268	2.292	2.140	2.725	2.817	0.324	0.595	0.555	---	
L-14,-12*	14.82	0.675	0.183	0.082	0.271	2.295	2.163	2.609	2.730	0.318	0.598	0.560	1.10	
L-14,-13	14.77	0.629	0.171	0.080	0.272	2.013	1.958	2.441	2.575	0.310	0.519	0.505	---	
L-14,-14*	14.79	0.608	0.168	0.079	0.271	2.016	1.982	2.388	2.473	0.308	0.519	0.510	1.43	
L-14,-15	14.70	0.571	0.155	0.078	0.271	1.789	1.716	2.227	2.351	0.304	0.449	0.460	---	
L-14,-16*	14.66	0.580	0.189	0.076	0.276	1.752	1.740	2.111	2.279	0.297	0.448	0.465	1.80	
L-14,-17	14.65	0.531	0.147	0.076	0.277	1.635	1.604	2.075	2.244	0.297	0.418	0.410	1.68	
L-14,-18*	14.61	0.499	0.138	0.074	0.277	1.659	1.629	1.955	2.123	0.291	0.419	0.416	2.20	
L-14,-19	14.61	0.496	0.136	0.074	0.275	1.699	1.690	1.946	2.098	0.289	0.382	0.380	---	
L-14,-20*	14.57	0.464	0.128	0.071	0.276	1.504	1.500	1.825	1.979	0.281	0.381	0.381	2.95	
L-14,-21	14.58	0.473	0.130	0.071	0.274	1.349	1.342	1.858	2.002	0.281	0.343	0.382	---	
L-14,-22*	14.54	0.437	0.120	0.067	0.274	1.364	1.358	1.721	1.861	0.266	0.346	0.345	4.50	
L-14,-23	14.77	0.639	0.172	0.080	0.270	2.075	2.012	2.480	2.592	0.311	0.535	0.519	---	
L-14,-24*	14.74	0.607	0.168	0.079	0.270	2.076	2.017	2.360	2.476	0.306	0.535	0.519	---	

UNLESS OTHERWISE INDICATED, ALL DATA ARE FOR:

1. SUPERCAVITATING FLOW.
2. BOTH STATIC PRESSURE TAPS OPEN.

**LEGEND**

\* ONLY UPSTREAM STATIC PRESSURE TAP UTILIZED  
+ ONLY DISTREAN STATIC PRESSURE TAP UTILIZED

PC PARTIALLY CAVITATING

PC (TP) PARTIALLY CAVITATING (TAP SETTED)

PW FULLY WETTED

AT (ALPHAT) (TRUE) ANGLE OF ATTACK, CORRECTED FOR EFFECTS OF IMAGES OF TRAILING VORTICES

AT2 ALPHAT=0.2

SIGC CAVITATION NUMBER COMPUTED WITH MEASURED CAVITY PRESSURE  
SIGC CAVITATION NUMBER COMPUTED WITH CALCULATED VAPOR PRESSURE

CD DRAG COEFFICIENT,

(D/L) CORRECTED DRAG-TO-LIFT RATIO = CD/CL

CAVITY LENGTH MEASURED FROM MIDCHORD AT CENTROID POSITION, NONDIMENSIONALIZED ON MEAN CHORD  
(OBTAINED FROM PHOTOGRAPIES)

HIPPLE TESTS OF BALL EFFECTS ON SUPERCAVITATING HYDROFOILS OF FINITE SPAN

HYDROFOIL INPUT DATA  
TE TT AREA SPAN RAC  
75 89 90.0 15.0 6.03

TEST READINGS AND TUNNEL TEMP BEFORE AND AFTER

RAC 1-S 1-S 2-S 2-S 3-H 3-S TT  
RAC 0. 0. 0. 0. 0. 0. 0. 0. 0.  
0. 0. 0. 0. 0. 0. 0. 0. 0.  
CILL LUS/CTI (NORMAL/BREV) 91=0.20000 82=0.20000 83=0.04030  
TWIST- 7200.0 SHAFT DIA.- 1.50IN

\*INPUT DATA AS RECORDED\*

RUN NO	RAC/R	S	SI	S	SI	S	SI	PIMP	PCAV
L-16--01	463.		-888.0	B	154.0	B	1103.0	764.	---
L-16--02	696.		-1316.0	B	179.0	B	1598.0	733.	---
L-16--03	972.		-1790.0	B	208.0	B	2150.0	700.	---
L-16--04	964.		-1936.0	B	198.0	B	2335.0	311.	PC (TV)
L-16--05	967.		-1930.0	B	189.5	B	2395.0	296.	PC
L-16--06	966.		-1900.0	B	179.0	B	215.0	277.	90.
L-16--07*	963.		-1870.0	B	177.5	B	2020.0	277.	90.
L-16--08	961.		-1830.0	B	170.8	B	2445.0	255.	81.
L-16--09*	962.		-1794.0	B	167.8	B	2425.0	255.	75.
L-16--10	963.		-1710.0	B	163.0	B	2385.0	233.	68.
L-16--11*	962.		-1672.0	B	160.0	B	2165.0	233.	64.
L-16--12	963.		-1602.0	B	158.0	B	2110.0	214.	60.
L-16--13*	964.		-1550.0	B	156.0	B	2290.0	214.	57.
L-16--14	968.		-1478.0	B	154.0	B	2233.0	197.	52.
L-16--15*	970.		-1418.0	B	153.0	B	2190.0	197.	50.
L-16--16	971.		-1314.0	B	151.8	B	2075.0	176.	47.
L-16--17*	971.		-1260.0	B	150.9	B	2015.0	176.	46.
L-16--18	973.		-1180.0	B	149.2	B	1930.0	161.	44.
L-16--19*	976.		-1124.0	B	148.3	B	1855.0	161.	42.
L-16--20	978.		-1062.0	B	147.9	B	1772.0	147.	40.
L-16--21*	973.		-1012.0	B	147.4	B	1708.0	147.	39.
L-16--22	976.		-976.0	B	146.5	B	1655.0	135.	38.
L-16--23*	977.		-926.0	B	146.5	B	1597.0	135.	38.
L-16--24	981.		-900.0	B	145.6	B	1555.0	126.	38.
L-16--25*	979.		-850.0	B	145.5	B	1480.0	125.	38.
L-16--26	976.		-842.0	B	146.1	B	1471.0	118.	36.
L-16--27*	977.		-842.0	B	144.5	B	1476.0	114.	36.
L-16--28	977.		-1350.0	B	152.5	B	2115.0	182.	48.
L-16--29	708.		-954.0	B	137.5	B	1538.0	139.	45.
L-16--30	363.		-554.0	B	121.5	B	925.0	102.	42.

LEGEND TT ROOM TEMPER (DEG FAHR)

TT TUNNEL " (")

AREA HALF-SPAN MODEL PLATE AREA (SQ IN)

SPAN FOIL HALF-SPAN (IN)

RAC MEAN CHORD, AREAS, A MODEL CENTROID (IN)

RAC VELOCITY MONITOR SPADING (IN)

TISSUE TWIST (DEGREES/IN-LB)

S LOAD CELL POLARITY (B=NORMAL, B=REVERSE)

LOAD CELL 1 LIPT (COUNTS)

LOAD CELL 2 BOREHOLE ABOUT MIDCHORD (COUNTS)

PIMP STATIC PRESSURE (IN HG)

PCAV CAVITY PRESSURE (IN HG)

RUN NO Q-XXX-TV: Q=FOIL TESTED (S=SMALL, B=LARGE)  
XIX=GEOMETRIC ATTACK ANGLE (DEGREES)  
TV=RUN NUMBER, THIS FOIL # THIS ANGLE

UPPER LIVES OF WALL EFFECTS OR SUPERCHARGING HYDROPOOLS OF FINITE SPAN

INPUT DATA CONCERNING FOR ZERO PRIMING, SIGNS, AND HYDROSTATIC PRESSURE

PIPE NO.	SEGNO	S1	S2	S3	P1SP	P2AV
L-16--01	863-	-888.0	-56.0	-1003.0	757.	-----
L-16--02	864-	-1316.0	-79.0	-1697.0	726.	-----
L-16--03	865-	-1790.0	-108.0	-2049.5	693.	-----
L-16--04	866-	-1936.0	-98.0	-2235.3	308.	-----
L-16--05	867-	-1910.0	-89.5	-2298.0	289.	117.
L-16--06	868-	-1900.0	-79.0	-2313.8	270.	90.
L-16--07	869-	-1870.0	-77.5	-2318.6	270.	90.
L-16--08	870-	-1830.0	-70.8	-2343.3	248.	81.
L-16--09	871-	-1798.0	-67.8	-2323.1	248.	75.
L-16--10	872-	-1710.0	-63.0	-2282.8	226.	68.
L-16--11	873-	-1672.0	-60.0	-2262.6	226.	64.
L-16--12	874-	-1602.0	-58.0	-2207.3	207.	60.
L-16--13	875-	-1550.0	-56.0	-2187.1	207.	57.
L-16--14	876-	-1478.0	-54.0	-2129.9	190.	52.
L-16--15	877-	-1418.0	-53.0	-2086.6	190.	50.
L-16--16	878-	-1316.0	-51.8	-1971.8	171.	47.
L-16--17	879-	-1260.0	-50.9	-1911.1	171.	46.
L-16--18	880-	-1187.0	-49.2	-1825.9	154.	44.
L-16--19	881-	-1128.0	-48.3	-1750.7	154.	42.
L-16--20	882-	-1062.0	-47.9	-1667.4	140.	40.
L-16--21	883-	-1012.0	-47.4	-1603.2	140.	39.
L-16--22	884-	-978.0	-46.5	-1549.9	128.	38.
L-16--23	885-	-926.0	-46.0	-1491.7	128.	38.
L-16--24	886-	-900.0	-45.6	-1449.4	119.	38.
L-16--25	887-	-850.0	-44.5	-1376.2	118.	38.
L-16--26	888-	-812.0	-44.1	-1365.0	107.	38.
L-16--27	889-	-842.0	-44.5	-1369.7	107.	38.
L-16--28	890-	-1350.0	-52.5	-2008.5	175.	48.
L-16--29	891-	-954.0	-37.5	-1431.2	132.	45.
L-16--30	892-	-556.0	-21.5	-818.0	95.	42.

**RIFLE LINES OF HALL EFFECTS ON SUPERCAPITATING HYDROFOILS OF PINTLE SPAN**

**HYDROFOIL DATA REDUCTION\*\***

BUS NO	ALPHA	LIFT-LB	DRAG-LB	BOR-1LB	VEL-PPS
L-16-01	16.03	188.80	60.42	194.10	16.56
L-16-02	16.03	219.00	60.36	284.40	20.02
L-16-03	16.05	375.60	82.60	386.80	23.38
L-16-04	16.05	406.80	90.04	352.80	21.29
L-16-05	16.04	403.90	92.45	322.20	23.32
L-16-06	16.04	395.80	93.25	284.80	23.31
L-16-07	16.04	389.50	93.44	279.00	23.28
L-16-08	16.08	380.16	98.44	254.89	23.26
L-16-09	16.03	372.36	92.62	294.08	23.27
L-16-10	16.03	358.60	92.00	226.80	23.28
L-16-11	16.03	386.80	91.18	216.00	23.27
L-16-12	16.03	332.00	88.96	208.80	23.28
L-16-13	16.03	321.20	88.18	201.60	23.29
L-16-14	16.03	306.40	85.83	194.40	23.29
L-16-15	16.03	298.20	88.09	190.80	23.36
L-16-16	16.03	273.16	79.45	186.48	23.37
L-16-17	16.03	262.18	77.02	183.24	23.37
L-16-18	16.02	245.89	73.58	177.12	23.39
L-16-19	16.02	234.46	70.55	173.88	23.42
L-16-20	16.02	221.98	67.20	172.44	23.40
L-16-21	16.02	211.88	64.61	170.64	23.39
L-16-22	16.02	204.90	62.46	167.40	23.42
L-16-23	16.02	194.40	60.12	165.60	23.44
L-16-24	16.02	189.12	58.41	164.16	23.46
L-16-25	16.02	178.90	55.38	160.20	23.46
L-16-26	16.02	177.22	55.01	158.76	23.42
L-16-27	16.02	177.30	55.20	160.20	23.44
L-16-28	16.03	280.50	80.94	189.00	23.44
L-16-29	16.02	198.30	57.68	135.00	20.17
L-16-30	16.01	115.10	32.97	77.80	14.79

LEGEND VEL UPSTREAM VELOCITY (0)

PIPES INFLUENCE ON SURFACE VIBRATIONS AND WORLDS OF FINITE SPAN

CONTROFOIL DATA IN NONDIMENSIONAL FORM (NO CORFRACTIONS APPLIED)

BUS NO	ALPHA	CL	CDUNC	CH	L/D	D/L	Rho1000-6
L-16--01	16.03	1.1380	0.2393	0.1947	0.7587	0.2103	0.9787
L-16--02	16.04	1.1532	0.2448	0.1950	0.7107	0.2123	1.1831
L-16--03	16.05	1.1499	0.2456	0.1953	0.6816	0.2136	1.3820
L-16--04	16.05	1.2618	0.2703	0.1786	0.5945	0.2176	1.3766
L-16--05	16.04	1.2239	0.2768	0.1626	0.4412	0.2252	1.3786
L-16--06	16.04	1.2059	0.2795	0.1437	0.3143	0.2318	1.3780
L-16--07	16.04	1.1902	0.2809	0.1414	0.2366	0.2360	1.3760
L-16--08	16.04	1.1639	0.2845	0.1294	0.0905	0.2445	1.3747
L-16--09	16.03	1.1389	0.2818	0.1238	0.0421	0.2474	1.3753
L-16--10	16.03	1.0835	0.2765	0.1149	0.9183	0.2552	1.3760
L-16--11	16.03	1.0595	0.2743	0.1096	3.8625	0.2589	1.3753
L-16--12	16.03	1.0195	0.2672	0.1058	3.7962	0.2634	1.3760
L-16--13	16.03	0.9805	0.2645	0.1021	3.7073	0.2697	1.3766
L-16--14	16.03	0.9353	0.2574	0.0984	3.6333	0.2752	1.3766
L-16--15	16.03	0.8929	0.2506	0.0960	3.5626	0.2807	1.3806
L-16--16	16.03	0.8283	0.2363	0.0938	3.5049	0.2853	1.3813
L-16--17	16.03	0.7930	0.2290	0.0921	3.4722	0.2980	1.3813
L-16--18	16.02	0.7480	0.2181	0.0889	3.4111	0.2932	1.3826
L-16--19	16.02	0.7075	0.2083	0.0970	3.3963	0.2344	1.3846
L-16--20	16.02	0.6712	0.1986	0.0865	3.3796	0.2959	1.3833
L-16--21	16.02	0.6412	0.1909	0.0856	3.3562	0.2978	1.3826
L-16--22	16.02	0.6183	0.1839	0.0838	3.3621	0.2974	1.3846
L-16--23	16.02	0.5861	0.1767	0.0828	3.3176	0.3014	1.3853
L-16--24	16.02	0.5680	0.1709	0.0818	3.3244	0.3008	1.3879
L-16--25	16.02	0.5383	0.1621	0.0799	3.3217	0.3111	1.3866
L-16--26	16.02	0.5148	0.1614	0.0795	3.3111	0.3018	1.3846
L-16--27	16.02	0.5345	0.1618	0.0801	3.3029	0.3028	1.3853
L-16--28	16.03	0.8057	0.2394	0.0945	3.5317	0.2831	1.3853
L-16--29	16.02	0.8067	0.2300	0.0911	3.5079	0.2851	1.1925
L-16--30	16.01	0.8719	0.2448	0.0972	3.5613	0.2808	0.8739

LEGEND

ALPHA GEOMETRIC ANGLE OF ATTACK CORRECTED FOR SHAFT TWIST

CL LIFT COEFFICIENT, NONDIMENSIONALIZED ON UPSTREAM VELOCITY AND MODEL PLATFORN AREA

CDUNC CL (UNCORRECTED), THE UNCORRECTED DRAG COEFFICIENT AS COMPUTED FROM MEASURED DRAG, AND NONDIMENSIONALIZED

ON UPSTREAM VELOCITY AND MODEL PLATFORN AREA

CH BIOMENT COEFFICIENT, NONDIMENSIONALIZED ON UPSTREAM VELOCITY, MODEL PLATFORN AREA, AND UPST CHORD

L/D LIFT-TO-DRAG RATIO = CL/CDUNC

D/L DRAG-TO-LIFT RATIO = CDUNC/CL

RE REYNOLDS NUMBER, BASED ON AREA CHORD

## EFFECTS OF WALL EFFECTS ON SUPERCAVITATING HYDROFOILS OF FINITE SPAN

## APPENDIX DATA CONNECTED FOR EFFECTS OF IMAGES OF TRAILING VORTICES

RUN NO	ALPHAT	CL	CD	CB	(D/L)	SIGC	SIGV	CM/AT	CM/AT2	SIGC	SIGV	CAVTH	COMMENTS/REMARKS
L-16--01	17.38	1.138	0.266	0.195	0.234	-----	-----	2.094	0.642	-----	-----	-----	PW
L-16--02	17.41	1.153	0.272	0.195	0.236	-----	-----	2.796	0.642	-----	-----	-----	PW
L-16--03	17.42	1.150	0.273	0.195	0.237	-----	-----	2.954	0.643	-----	-----	-----	PW
L-16--04	17.52	1.282	0.302	0.179	0.243	-----	-----	0.061	2.331	0.584	-----	-----	PC (PW)
L-16--05	17.50	1.229	0.308	0.163	0.251	0.423	2.987	4.024	0.532	1.351	0.913	-----	PC
L-16--06	17.67	1.206	0.310	0.144	0.257	0.104	3.135	3.55	3.330	0.471	1.251	0.916	-----
L-16--07*	17.45	1.190	0.310	0.141	0.261	0.120	3.188	3.908	3.345	0.464	1.255	0.959	0.60
L-16--08	17.42	1.164	0.313	0.129	0.269	0.132	3.129	3.83	0.826	1.139	0.891	-----	-----
L-16--09*	17.38	1.139	0.309	0.128	0.271	0.750	3.080	3.758	3.352	0.408	1.138	0.922	0.69
L-16--10	17.32	1.088	0.301	0.115	0.278	3.373	2.785	3.505	3.293	0.380	1.019	0.842	-----
L-16--11*	17.29	1.059	0.298	0.110	0.281	3.381	2.863	3.512	3.269	0.363	1.020	0.864	0.85
L-16--12	17.23	1.014	0.289	0.106	0.284	3.051	2.604	3.371	3.190	0.352	0.918	0.783	-----
L-16--13*	17.19	0.981	0.284	0.102	0.290	3.054	2.661	3.268	3.159	0.340	0.916	0.798	0.86
L-16--14	17.14	0.935	0.276	0.098	0.295	2.760	2.856	3.127	3.080	0.329	0.826	0.735	-----
L-16--15*	17.09	0.893	0.267	0.096	0.299	2.751	2.484	2.994	3.004	0.322	0.820	0.741	0.82
L-16--16	17.01	0.829	0.251	0.094	0.302	2.422	2.422	2.209	2.863	0.316	0.719	0.656	-----
L-16--17*	16.97	0.795	0.242	0.092	0.304	2.426	2.232	2.684	2.760	0.311	0.719	0.661	0.92
L-16--18	16.91	0.794	0.230	0.089	0.309	2.124	1.968	2.521	2.636	0.301	0.627	0.581	-----
L-16--19*	16.86	0.768	0.219	0.087	0.309	2.124	2.001	2.404	2.525	0.296	0.625	0.590	1.40
L-16--20	16.82	0.671	0.208	0.086	0.310	1.881	1.797	2.286	2.413	0.295	0.552	0.528	-----
L-16--21*	16.78	0.641	0.199	0.086	0.311	1.885	1.821	2.189	2.324	0.292	0.552	0.533	1.71
L-16--22	16.76	0.618	0.192	0.084	0.310	1.666	1.621	2.114	2.243	0.286	0.487	0.474	-----
L-16--23*	16.72	0.586	0.184	0.083	0.314	1.667	1.623	2.009	2.158	0.284	0.486	0.474	2.17
L-16--24	16.70	0.568	0.178	0.082	0.313	1.500	1.457	1.949	2.091	0.281	0.437	0.425	-----
L-16--25*	16.66	0.538	0.168	0.080	0.312	1.487	1.485	1.851	1.988	0.273	0.432	0.420	2.94
L-16--26	16.66	0.515	0.167	0.079	0.313	1.291	1.251	1.880	1.980	0.273	0.375	0.364	-----
L-16--27*	16.66	0.535	0.168	0.080	0.314	1.288	1.250	1.839	1.985	0.276	0.375	0.363	2.98
L-16--28	17.03	0.896	0.254	0.094	0.301	2.287	2.845	2.878	3.318	0.731	0.668	-----	-----
L-16--29	16.98	0.607	0.283	0.091	0.302	2.300	2.005	2.723	2.773	0.307	0.681	0.618	-----
L-16--30	17.04	0.872	0.261	0.097	0.299	2.621	2.360	2.931	2.944	0.327	0.780	0.702	-----

UNLESS OTHERWISE INDICATED, ALL DATA AND FOR:

1. SUPERCAVITATING FLOW.
2. BOTH STATIC PRESSURE TAPS OPEN.

## LEGEND

- \* ONLY UPSTREAM STATIC PRESSURE TAP UTILIZED
- \* ONLY DOWNSTREAM STATIC PRESSURE TAP UTILIZED
- PC PARTIALLY CAVITATING
- PC (PW) PARTIALLY CAVITATING (TAP WETTED)
- PW FULLY WETTED
- AT (ALPHAT) ANGLE OF ATTACK, CORRECTED FOR EFFECTS OF IMAGES OF TRAILING VORTICES
- AT2 ALPHAT=0.2
- SIGC CAVITATION NUMBER COMPUTED WITH MEASURED CAVITY PRESSURE
- SIGV CAVITATION NUMBER COMPUTED WITH CALCULATED VAPOR PRESSURE
- CD DRAG COEFFICIENT, CORRECTED FOR EFFECTS OF IMAGES OF TRAILING VORTICES
- (D/L) CORRECTED DRAG-TO-LIFT RATIO = CD/CL
- CAVTH CAVITY LENGTH MEASURED FROM MIDCHORD AT CAVITOID POSITION, BOUNDARIES LOCALIZED ON REAR CHORD (OBTAINED FROM PHOTOGRAPIES)

EXPERIMENTS OF WALL EFFECTS ON SUPERCAVITATING HYDROFOILS OF FINITE SPAN

HYDROFOIL INPUT DATA

TA	TT	AREA	SPAN	HAC
76	80	90.0	15.0	6.03

SEED RATINGS AND TUNNEL TEST SPOTS AND APPROX

WALL 1-8	1-8	2-8	2-8	3-8	3-8
0.	0.0	0.0	100.0	0.0	100.0
0.	0.0	0.0	100.5	0.0	109.0
C2L LAS/CR (NORMAL/REV)	81-0.20000	92-0.20000	83-0.00030		
1W1ST- 7200.0	SUPER DIA.= 1.5013				

\*INPUT DATA AS RECORDED\*

RUN NO	RAMON	S	81	S	82	S	83
L-18.-01	1150.	-2054.0	R	177.3	R	32275.0	PICP
L-18.-02*	1150.	-2020.0	R	176.5	R	3240.0	PCAV
L-18.-03	1152.	-1990.0	R	174.2	R	3210.0	
L-18.-04*	1151.	-1942.0	R	172.0	R	3175.0	
L-18.-05	1150.	-1916.0	R	171.2	R	3150.0	
L-18.-06*	1148.	-1870.0	R	169.4	R	3130.0	
L-18.-07	1143.	-1825.0	R	167.5	R	3070.0	
L-18.-08*	1139.	-1790.0	R	167.2	R	3030.0	
L-18.-09	971.	-1585.0	R	158.5	R	2680.0	
L-18.-10*	971.	-1536.0	R	158.0	R	2625.0	
L-18.-11	971.	-1504.0	R	156.3	R	2605.0	
L-18.-12*	971.	-1464.0	R	155.8	R	2540.0	
L-18.-13	969.	-1376.0	R	155.3	R	2450.0	
L-18.-14*	972.	-1328.0	R	153.6	R	2390.0	
L-18.-15	969.	-1288.0	R	152.5	R	2330.0	
L-18.-16*	972.	-1220.0	R	151.5	R	2255.0	
L-18.-17	972.	-1200.0	R	151.3	R	2225.0	
L-18.-18*	973.	-1182.0	R	151.0	R	2135.0	
L-18.-19	973.	-1122.0	R	150.8	R	2112.0	
L-18.-20*	972.	-1084.0	R	150.3	R	2035.0	
L-18.-21	972.	-1080.0	R	150.2	R	2027.0	
L-18.-22*	973.	-1036.0	R	150.2	R	1960.0	
L-18.-23	972.	-1016.0	R	150.0	R	1928.0	
L-18.-24*	976.	-966.0	R	149.5	R	1850.0	
L-18.-25	976.	-984.0	R	149.5	R	1873.0	
L-18.-26*	958.	-888.0	R	147.0	R	1708.0	

LEGEND TA ROOM TEMPER (DEG FAREN)

TT TUNNEL = ( " )

AREA HALF-SPAN MODEL PLATFORM AREA (SQ IN)

SPAN POLE HALF-SPAN (IN)

HAC REAL CHORD, RMS. & MODEL CHORD (IN)

MAJOR VELOCITY MACHINERY BRAIDING (IN)

TWIST SHARP THRUST (DEGREES/IN-LB)

S LOAD CELL POLARITY (H-NORMAL, R-REVERSE)

LOAD CELL #1 LIPT (COUNTS)

#2 HORIZONTAL MIDCHORD (COUNTS)

PICP STATIC PRESSURE (MM HG)

PCAV CAVITY PRESSURE (MM HG)

RUN NO Q-XXX-YY: Q=POLE TESTED(S-SMALL, H-HMED, L-LARGE)  
YY=GEOMETRIC ATTACK ANGLE (DEGREES)  
MM=RUN NUMBER, THIS POLE @ THIS ANGLE

EFFECTS OF WALL EFFECTS ON SUPERCAVITATING HYDROFOILS OF FINITE SPAN

INPUT DATA CORRECTED FOR ZERO BEARINGS, SIGNS, AND HYDROSTATIC PRESSURE

RUN NO	RADIAN	θ1	θ2	θ3	P1P1P	P2P2P
L-18,-01	1150.	-2054.0	-77.3	-3175.0	218.	84.
L-18,-02	1150.	-2020.0	-78.5	-3139.6	277.	80.
L-18,-03	1152.	-1990.0	-76.2	-3109.3	264.	76.
L-18,-04	1151.	-1962.0	-71.3	-3073.9	265.	72.
L-18,-05	1150.	-1916.0	-71.1	-3048.6	251.	67.
L-18,-06	1148.	-1870.0	-68.9	-3028.2	251.	65.
L-18,-07	1142.	-1825.0	-67.4	-2967.8	235.	58.
L-18,-08	1139.	-1790.0	-67.1	-2927.5	235.	57.
L-16,-09	971.	-1585.0	-58.3	-2577.1	209.	54.
L-18,-10	971.	-1536.0	-57.8	-2521.8	208.	53.
L-18,-11	971.	-1504.0	-56.1	-2501.4	196.	51.
L-18,-12	971.	-1464.0	-55.6	-2446.0	196.	46.
L-18,-13	969.	-1376.0	-55.1	-2345.7	178.	49.
L-18,-14	972.	-1328.0	-53.3	-2285.3	178.	45.
L-18,-15	969.	-1288.0	-52.2	-2225.0	168.	43.
L-18,-16	972.	-1220.0	-51.2	-2149.6	164.	41.
L-18,-17	972.	-1200.0	-51.0	-2119.2	153.	40.
L-18,-18	973.	-1142.0	-50.7	-2028.9	152.	37.
L-18,-19	973.	-1124.0	-50.4	-2005.5	143.	32.
L-18,-20	972.	-1084.0	-49.9	-1928.2	143.	34.
L-18,-21	972.	-1080.0	-49.8	-1919.8	135.	35.
L-18,-22	973.	-1036.0	-49.8	-1852.4	135.	33.
L-18,-23	972.	-1016.0	-49.6	-1820.1	126.	33.
L-18,-24	976.	-966.0	-49.0	-1781.7	126.	33.
L-18,-25	976.	-986.0	-49.0	-1766.4	119.	33.
L-18,-26	958.	-984.0	-46.5	-1599.0	120.	33.

**REPORT INVESTIGATING THE EFFECTS OF WALL EFFECTS ON SUPERCAVITATING HYDROFOILS OF FINITE SPAN**

**HYDROFOIL DATA REDUCTION**

RUN NO.	ALPHA	LIFT-LB	DRAG-LB	BON-1BLB	VEL-TFS
L-18.-01	18.00	826.26	127.95	276.20	25.31
L-18.-02	18.00	818.90	126.53	268.13	25.31
L-18.-03	18.00	812.83	125.30	266.98	25.29
L-18.-04	18.00	802.79	123.80	258.98	25.28
L-18.-05	18.00	397.42	122.86	256.03	25.27
L-18.-06	18.00	387.78	122.04	248.04	25.25
L-18.-07	18.03	378.48	119.60	262.57	25.20
L-18.-08	18.03	371.41	117.98	241.42	25.16
L-18.-09	18.03	326.67	103.86	210.02	23.36
L-18.-10	18.03	318.76	101.63	208.15	23.36
L-18.-11	18.03	312.02	100.81	201.96	23.36
L-18.-12	18.03	303.92	98.17	200.09	23.36
L-18.-13	18.03	286.21	98.53	198.22	23.33
L-18.-14	18.03	275.97	92.10	192.02	23.37
L-18.-15	18.03	267.24	89.67	187.99	23.33
L-18.-16	18.03	250.24	86.63	184.32	23.37
L-18.-17	18.03	250.20	85.41	183.53	23.37
L-18.-18	18.03	239.51	81.76	182.38	23.38
L-18.-19	18.03	234.89	80.82	181.58	23.38
L-18.-20	18.02	226.78	77.70	179.71	23.37
L-18.-21	18.02	225.96	77.37	179.28	23.37
L-18.-22	18.02	217.16	74.65	179.21	23.38
L-18.-23	18.02	213.11	73.35	178.42	23.37
L-18.-24	18.02	203.01	70.19	176.54	23.41
L-18.-25	18.02	206.60	71.10	176.47	23.41
L-18.-26	18.02	186.10	64.94	167.40	23.21

LEGEND      VEL UPSTREAM VELOCITY (ft)

**UPPER LIVES OF WALL EFFECTS ON SUPERCAPITATING HYDROPOOLS OF FINITE SPAN**

**HYDROPOOL AREA IS NONDIMENSIONAL FORM (NO CORRECTIONS APPLIED) ..**

TEST NO.	ALPHA	CL	CDIBC	CR	L/D	D/L	Re <sup>0.105e-6</sup>
L-18--01	18.04	1.1011	0.3260	0.1192	3.3780	0.2960	1.4298
L-18--02	18.06	1.0821	0.3223	0.1119	3.3575	0.2978	1.4298
L-18--03	18.04	1.0669	0.3197	0.1146	3.3416	0.2993	1.4286
L-18--04	18.04	1.0630	0.3162	0.1112	3.2983	0.3032	1.4280
L-18--05	18.04	1.0300	0.3138	0.1090	3.2819	0.3067	1.4275
L-18--06	18.03	1.0066	0.3122	0.1068	3.2240	0.3102	1.4263
L-18--07	18.03	0.9866	0.3072	0.1048	3.2118	0.3118	1.4234
L-18--08	18.03	0.9712	0.3039	0.1047	3.1954	0.3129	1.4211
L-18--09	18.03	0.9770	0.3108	0.1057	3.2116	0.3118	1.3194
L-18--10	18.03	0.9670	0.3037	0.1087	3.1842	0.3140	1.3194
L-18--11	18.03	0.9465	0.3012	0.1016	3.1826	0.3182	1.3194
L-18--12	18.03	0.9219	0.2932	0.1007	3.1444	0.3180	1.3194
L-18--13	18.03	0.8699	0.2827	0.0999	3.0771	0.3250	1.3181
L-18--14	18.03	0.8388	0.2745	0.0965	3.0413	0.3268	1.3200
L-18--15	18.03	0.8122	0.2679	0.0948	3.0117	0.3298	1.3181
L-18--16	18.03	0.7705	0.2579	0.0926	2.9873	0.3348	1.3200
L-18--17	18.03	0.7582	0.2542	0.0922	2.9827	0.3353	1.3200
L-18--18	18.03	0.7222	0.2429	0.0916	2.9727	0.3364	1.3207
L-18--19	18.03	0.7112	0.2401	0.0912	2.9620	0.3376	1.3207
L-18--20	18.02	0.6873	0.2309	0.0903	2.9768	0.3359	1.3200
L-18--21	18.02	0.6848	0.2299	0.0901	2.9792	0.3357	1.3200
L-18--22	18.02	0.6575	0.2214	0.0900	2.9694	0.3368	1.3207
L-18--23	18.02	0.6459	0.2177	0.0897	2.9670	0.3370	1.3200
L-18--24	18.02	0.6129	0.2073	0.0888	2.9565	0.3382	1.3226
L-18--25	18.02	0.6237	0.2101	0.0884	2.9694	0.3368	1.3226
L-18--26	18.02	0.5717	0.1933	0.0883	2.9569	0.3382	1.3111

**LEGEND**

ALPHA GEOMETRIC ANGLE OF ATTACK CORRECTED FOR SHARP TWIST  
 CL LIFT COEFFICIENT, NONDIMENSIONALIZED ON UPSTREAM VELOCITY AND MODEL PLANFORM AREA  
 CDIBC CD (UNCORRECTED), THE UNCORRECTED DRAG COEFFICIENT AS COMPUTED FROM MEASURED DRAG, AND NONDIMENSIONALIZED  
 ON UPSTREAM VELOCITY AND MODEL PLANFORM AREA  
 CR HORIZONTAL COEFFICIENT, NONDIMENSIONALIZED ON UPSTREAM VELOCITY. MODEL PLANFORM AREA, AND BEAM CHORD  
 L/D LIFT-TO-DRAG RATIO = CL/CDIBC  
 D/L DRAG-TO-LIFT RATIO = CDIBC/CL  
 Re REYNOLDS NUMBER, BASED ON BEAM CHORD

## PIPE LINES OF WALL EFFECTS ON SUPERCAVITATING HYDROPOOLS OF PLUNGE SPAN

## SECTION DATA CONNECTED FOR EFFECTS OF IMAGES OF TRAILING VORTEX SYSTEM\*

TEST NO.	ALPHAT	CL	CD	CB	(D/L)	SIGC/AT	CL/AT	SIGC/AT	CL/AT	CH/AT	SIGC	CAVITY	COMMENTS/REMARKS
L-18-01	19.34	1.101	0.351	0.119	0.319	3.314	2.587	3.261	3.080	0.353	1.119	0.873	---
L-18-02*	19.32	1.082	0.387	0.115	0.320	3.304	2.630	3.209	3.046	0.361	1.114	0.867	0.92
L-18-03	19.30	1.068	0.383	0.115	0.321	3.138	2.516	3.170	3.024	0.340	1.057	0.857	---
L-18-04*	19.27	1.083	0.339	0.111	0.325	3.158	2.589	3.101	2.998	0.331	1.062	0.871	1.10
L-18-05	19.26	1.039	0.336	0.110	0.326	2.975	2.873	3.064	2.973	0.327	1.000	0.811	---
L-18-06*	19.23	1.007	0.333	0.107	0.331	2.983	2.507	2.958	2.918	0.318	1.001	0.841	0.87
L-18-07	19.20	0.986	0.327	0.105	0.332	2.782	2.399	2.943	2.914	0.313	0.932	0.804	---
L-18-08*	19.19	0.971	0.323	0.105	0.333	2.793	2.423	2.900	2.885	0.313	0.935	0.811	0.92
L-18-09	19.21	0.997	0.331	0.106	0.332	2.825	2.445	2.973	2.944	0.315	0.987	0.820	---
L-18-10*	19.18	0.967	0.323	0.105	0.318	2.814	2.449	2.889	2.884	0.313	0.992	0.820	0.90
L-18-11	19.15	0.947	0.320	0.102	0.338	2.827	2.294	2.832	2.862	0.304	0.878	0.767	---
L-18-12*	19.12	0.922	0.311	0.101	0.317	2.630	2.345	2.762	2.790	0.302	0.878	0.781	0.95
L-18-13	19.06	0.870	0.298	0.100	0.333	2.557	2.135	2.615	2.696	0.300	0.784	0.710	---
L-18-14*	19.02	0.835	0.289	0.097	0.346	2.354	2.118	2.515	2.623	0.291	0.781	0.703	1.20
L-18-15	18.99	0.812	0.282	0.095	0.367	2.140	1.935	2.451	2.563	0.286	0.709	0.641	---
L-18-16*	18.94	0.770	0.270	0.093	0.351	1.939	1.967	2.331	2.473	0.280	0.707	0.650	1.27
L-18-17	18.92	0.758	0.266	0.092	0.351	1.964	1.808	2.296	2.439	0.279	0.649	0.597	---
L-18-18*	18.88	0.722	0.254	0.092	0.351	1.949	1.843	2.191	2.336	0.278	0.682	0.607	1.68
L-18-19	18.87	0.711	0.251	0.091	0.352	1.806	1.780	2.159	2.310	0.277	0.595	0.586	---
L-18-20*	18.84	0.687	0.241	0.090	0.350	1.609	1.752	2.090	2.226	0.275	0.595	0.576	1.82
L-18-21	18.84	0.685	0.240	0.090	0.350	1.680	1.688	2.083	2.216	0.274	0.552	0.529	---
L-18-22*	18.80	0.657	0.230	0.090	0.350	1.681	1.642	2.093	2.139	0.274	0.552	0.539	2.22
L-18-23	18.79	0.646	0.226	0.090	0.350	1.538	1.500	1.969	2.104	0.273	0.598	0.492	---
L-18-24*	18.75	0.613	0.215	0.088	0.351	1.534	1.497	1.873	2.008	0.270	0.502	0.490	2.70
L-18-25	18.76	0.624	0.218	0.088	0.350	1.420	1.384	1.905	2.034	0.270	0.465	0.453	3.90
L-18-26*	18.70	0.572	0.200	0.085	0.350	1.465	1.429	1.751	1.676	0.261	0.478	0.466	---

UNLESS OTHERWISE INDICATED, ALL DATA ARE FOR:

1. SUPERCAVITATING PLOW.
2. BOTH STATIC PRESSURE TAPS OPEN.

## LEGEND

- \* ONLY UPSTREAM STATIC PRESSURE TAP UTILIZED
- PC PARTIALLY CAVITATING
- PC(TW) PARTIALLY CAVITATING (TAP WETTED)
- PW FULLY WETTED

## AT (ALPHAT) (TWO ALPHAT)\*2 ANGLE OF ATTACK, CORRECTED FOR EFFECTS OF IMAGES OF TRAILING VORTEXES

AT2 ALPHAT\*2

SIGC CAVITATION NUMBER COMPUTED WITH MEASURED CAVITY PRESSURE

SIGV CAVITATION NUMBER COMPUTED WITH CALCULATED VAPOR PRESSURE

CD DRAG COEFFICIENT, CORRECTED FOR EFFECTS OF IMAGES OF TRAILING VORTEXES

(D/L) CORRECTED DRAG-TO-LIFT RATIO = CD/CL

CAVITY LENGTH MEASURED FROM MIDCHORD AT CENTROID POSITION, NONDIMENSIONALIZED ON BEAM CHORD  
(OBTAINED FROM PHOTOGRAPHS)

**RISER RATES OF GALL EFFECTS ON SUPERCAVITATING HYDROPOILS OF PIVITE SPAN**

**HYDROPOIL INPUT DATA**

77	77	AERA	SPAN	HAC
76	62	90.0	15.0	6.03

**ZERO READINGS AND TUNNEL TEMP BEFORE AND AFTER**

BAROM 1-H	1-H	2-H	3-H	3-H
0c.	0.0	0.0	100.0	0.0
c.	0.0	0.0	102.0	0.0
CILL LBS/CF (POSSIBLY 0.0)	0.0	0.0	105.0	0.0
TESTST- 7200.0	SMART DIA.= 1.5018			

**INPUT DATA AS RECORDED\***

NUM NO	BAROM	S	SI	S	SI	S	SI	PINP	PCAV
L-21,-01	957.	-1760.0	R	168.5	R	3445.0	R	278.	91.
L-21,-02*	959.	-1780.0	R	167.3	R	3415.0	R	278.	86.
L-21,-03	966.	-1730.0	R	166.5	R	3405.0	R	262.	85.
L-21,-04*	967.	-1712.0	R	165.2	R	3370.0	R	261.	77.
L-21,-05	971.	-1676.0	R	164.6	R	3335.0	R	243.	69.
L-21,-06*	973.	-1632.0	R	163.5	R	3295.0	R	243.	63.
L-21,-07	972.	-1592.0	R	162.5	R	3250.0	R	224.	59.
L-21,-08*	972.	-1540.0	R	160.6	R	3185.0	R	224.	56.
L-21,-09	974.	-1530.0	R	160.2	R	3155.0	R	211.	48.
L-21,-10*	974.	-1486.0	R	159.5	R	3105.0	R	211.	48.
L-21,-11	978.	-1482.0	R	160.0	R	3100.0	R	206.	48.
L-21,-12*	978.	-1442.0	R	159.6	R	3035.0	R	202.	44.
L-21,-13	980.	-1428.0	R	158.9	R	3005.0	R	189.	43.
L-21,-14*	979.	-1378.0	R	158.2	R	2930.0	R	190.	40.
L-21,-15	983.	-1360.0	R	158.1	R	2910.0	R	180.	39.
L-21,-16*	983.	-1308.0	R	158.0	R	2815.0	R	180.	37.
L-21,-17	986.	-1300.0	R	157.8	R	2790.0	R	169.	36.
L-21,-18*	982.	-1250.0	R	158.1	R	2695.0	R	169.	32.
L-21,-19	982.	-1250.0	R	158.2	R	2685.0	R	155.	31.
L-21,-20*	982.	-1188.0	R	158.0	R	2585.0	R	159.	31.
L-21,-21	987.	-1198.0	R	158.1	R	2580.0	R	146.	31.
L-21,-22*	985.	-1114.0	R	156.3	R	2430.0	R	149.	31.
L-21,-23	750.	-1056.0	R	147.0	R	2270.0	R	149.	31.
L-21,-24*	752.	-1014.0	R	146.8	R	2200.0	R	148.	31.

**LEGEND**

TR BOOM TEMPER (DEG FAREN)

TT TUNNEL " ( " )

AREA HALF-SPAN MODEL PLATEFORM AREA (SQ IN)

SPAN FOIL HALF-SPAN (IN)

HAC SPAN CHORD, MMAS. 3 MODEL CANTOID (IN)

HAC VELOCITY METERETER READING (MM)

SMART TWIST TWIST (DEGREES/IN-LB)

S LOAD CELL POLARITY (+=NORMAL, -=REVERSE)

**LOAD CELL #1 LIFT (COUNTS)**

**#2 BOWEN ABOUT MIDCROSS (COUNTS)**

**#3 DRAG (COUNTS)**

**PINP STATIC PRESSURE (IN HG)**

**PCAV CAVITY PRESSURE (IN HG)**

**BUS NO 0-III-IV: 0=FOIL TESTED (S-SMALL, A-MED, L-LARGE)**

**XII-GEOMETRIC ATTACK ANGLE (DEGREES)**

**TT-SUM NUMBER, THIS FOIL @ THIS ANGLE**

EFERENT EFFECTS OF WALL EFFECTS ON SUPERCHARGING HYDROPOOLS OF FINITE SPAN

INPUT DATA CORRECTED FOR ZERO BRIDGES, SIGNS, AND HYDROSTATIC PRESSURE					
BUS NO	NAME	01	02	03	PINP PCAV
L-21,-01	957.	-1700.0	-68.5	-3305.0	271.
L-21,-02	959.	-1700.0	-67.2	-3310.0	68.
L-21,-03	966.	-1730.0	-66.3	-3300.6	65.
L-21,-04	967.	-1712.0	-68.9	-3269.3	77.
L-21,-05	971.	-1616.0	-66.3	-3236.1	69.
L-21,-06	973.	-1632.0	-63.1	-3193.9	63.
L-21,-07	972.	-1532.0	-62.0	-3168.7	59.
L-21,-08	972.	-1510.0	-60.0	-3083.5	217.
L-21,-09	976.	-1510.0	-59.5	-3051.3	208.
L-21,-10	974.	-1488.0	-58.7	-3003.0	204.
L-21,-11	976.	-1482.0	-59.1	-2997.0	195.
L-21,-12	976.	-1462.0	-58.6	-2932.6	195.
L-21,-13	980.	-1428.0	-57.9	-2992.4	182.
L-21,-14	979.	-1378.0	-57.1	-2827.2	163.
L-21,-15	983.	-1300.0	-56.9	-2807.0	173.
L-21,-16	983.	-1308.0	-56.7	-2711.7	173.
L-21,-17	986.	-1300.0	-56.4	-2666.5	162.
L-21,-18	982.	-1250.0	-56.6	-2591.3	162.
L-21,-19	982.	-1250.0	-56.6	-2581.1	152.
L-21,-20	982.	-1188.0	-56.3	-2400.9	152.
L-21,-21	987.	-1198.0	-56.4	-2875.7	141.
L-21,-22	985.	-1118.0	-54.5	-2355.4	162.
L-21,-23	750.	-1056.0	-45.1	-2165.2	162.
L-21,-24	752.	-1018.0	-48.8	-2095.0	141.

**EXPERIMENTS OF WALL EFFECTS ON SUPERCHARGING HYDROPOOLS OF FINITE SPAN**

**HYDROPOOL DATA REDUCTION\***

RUN NO	ALPHA	LIFT-LB	DRAG-LB	BOW-THR-LB	VEL-PFS
L-21,-01	21.03	365.70	139.80	266.60	23.20
L-21,-02	21.03	361.48	133.59	261.97	23.22
L-21,-03	21.03	359.26	133.17	248.77	23.30
L-21,-04	21.03	355.39	131.75	233.78	23.31
L-21,-05	21.03	348.05	130.34	231.31	23.35
L-21,-06	21.03	339.01	128.71	227.03	23.37
L-21,-07	21.03	330.80	126.89	223.12	23.36
L-21,-08	21.03	329.00	126.26	215.97	23.36
L-21,-09	21.03	317.90	123.05	216.22	23.39
L-21,-10	21.03	309.34	121.02	211.38	23.39
L-21,-11	21.03	308.23	120.81	212.87	23.83
L-21,-12	21.03	306.13	118.18	211.12	23.83
L-21,-13	21.03	297.17	116.97	201.28	23.65
L-21,-14	21.03	286.21	113.94	205.45	23.44
L-21,-15	21.03	283.38	113.12	204.78	23.49
L-21,-16	21.03	272.98	109.28	204.10	23.49
L-21,-17	21.03	271.28	108.27	203.07	23.52
L-21,-18	21.03	261.32	104.43	203.84	23.48
L-21,-19	21.03	261.33	104.02	203.89	23.48
L-21,-20	21.03	249.87	99.98	202.85	23.49
L-21,-21	21.03	250.07	99.77	202.90	23.53
L-21,-22	21.03	233.69	93.72	196.11	23.51
L-21,-23	21.02	220.22	87.26	162.31	20.71
L-21,-24	21.02	211.76	84.43	161.28	20.73

LEGEND

VEL UPSTREAM VELOCITY (U)

**EXPERIMENTS ON SUPERERODATING HYDROPOOLS OF FINITE SPAN**

**CONTINUATION DATA IN NONDIMENSIONAL FORM (NO CORRECTIONS APPLIED) ..**

Reynolds Number	Alpha	CL	CDUBC	CB	L/D	D/L	Reynolds Number
L-21.-01	21.03	1.1249	0.4099	0.1257	2.7635	0.3685	1.2848
L-21.-02	21.03	1.1092	0.4053	0.1231	2.7166	0.3554	1.2861
L-21.-03	21.03	1.0550	0.4013	0.1207	2.7280	0.3665	1.2904
L-21.-04	21.03	0.9622	0.3966	0.1181	2.7288	0.3665	1.2911
L-21.-05	21.03	1.0558	0.3907	0.1168	2.7020	0.3701	1.2935
L-21.-06	21.03	1.0264	0.3851	0.1140	2.6655	0.3752	1.2948
L-21.-07	21.03	1.0025	0.3799	0.1121	2.6386	0.3790	1.2942
L-21.-08	21.03	0.9698	0.3720	0.1085	2.6072	0.3836	1.2942
L-21.-09	21.03	0.9616	0.3676	0.1075	2.6161	0.3823	1.2954
L-21.-10	21.03	0.9357	0.3614	0.1060	2.5888	0.3863	1.2954
L-21.-11	21.03	0.9288	0.3594	0.1064	2.5841	0.3870	1.2979
L-21.-12	21.03	0.9048	0.3515	0.1055	2.5729	0.3387	
L-21.-13	21.03	0.8937	0.3472	0.1039	2.5745	0.3884	1.2991
L-21.-14	21.03	0.8616	0.3388	0.1026	2.5464	0.3927	1.2985
L-21.-15	21.03	0.8698	0.3346	0.1018	2.5397	0.3938	1.3010
L-21.-16	21.03	0.8185	0.3221	0.1015	2.5333	0.3947	
L-21.-17	21.03	0.8113	0.3191	0.1007	2.5119	0.3934	1.3028
L-21.-18	21.03	0.7884	0.3089	0.1015	2.5398	0.3937	1.3003
L-21.-19	21.03	0.7884	0.3076	0.1015	2.5501	0.3921	
L-21.-20	21.03	0.7471	0.2955	0.1010	2.5281	0.3955	1.3003
L-21.-21	21.03	0.7671	0.2935	0.1005	2.5460	0.3928	1.3034
L-21.-22	21.03	0.6995	0.2759	0.0973	2.5154	0.3944	1.3022
L-21.-23	21.02	0.6695	0.3319	0.1038	2.5555	0.3907	1.1471
L-21.-24	21.02	0.6198	0.3202	0.1029	2.5450	0.3929	1.1485

**LEGEND**

ALPHA GEOMETRIC ANGLE OF ATTACK CORRECTED FOR SHAFT TWIST  
 CL LIFT COEFFICIENT, NONDIMENSIONALIZED ON UPSTREAM VELOCITY AND MODEL PLATEFORM AREA  
 CDUBC CD (UNCORRECTED), THE UNCORRECTED DRAG COEFFICIENT AS COMPUTED FROM MEASURED DRAG, AND NONDIMENSIONALIZED  
 ON UPSTREAM VELOCITY AND MODEL PLATEFORM AREA  
 CB MOMENT COEFFICIENT, NONDIMENSIONALIZED ON UPSTREAM VELOCITY, MODEL PLATEFORM AREA, AND MEAN CHORD  
 L/D LIFT-TO-DRAG RATIO = CL/CDUBC  
 D/L DRAG-TO-LIFT RATIO = CDUBC/CL  
 Re REYNOLDS NUMBER, BASED ON MEAN CHORD

REVIEWERS' COMMENTS OF ALL ASPECTS OF SUPERCAVITATION STUDIES OF PRINTING SPOTS

APPLICATIONS OF INTEGRATING VARIOUS CONSTITUENTS FOR INFLUENCING SYSTEMS

RESULTS OF WHICH ARE PUBLISHED.

1. SUPERCAVITATING PLOW.  
2. BOTH STATIC PRESSURE TAPS OPEN.

• ONLY UPSTREAM STATIC PRESSURE TAP UTILIZED  
• ONLY DOWNSTREAM STATIC PRESSURE TAP UTILIZED

PC(11) PARTIAL CAVITATING (TAP METERS)

WILLY WELD / ALL THE TRUTH OR CONSEQUENCE

EFFECTS OF ISSUES OF ISMAILIIS PUBLICATIONS

## SIGNS CAVITATION NUMBER COMPUTED WITH MEASURED CAVITY PRESSURE

### SIGV CAVITATION NUMBER COMPUTED WITH CALCULATED VAPOR PRESSURE

CD DRAG COEFFICIENT, CORRECTED FOR EFFECTS OF IMAGES OF TRAILING VORTICES

(D/L) CORRECTED DRAG-TO-LIFT RATIO = CDCL

REVUE CANADIENNE DE L'ASSOCIATION POUR LA RECHERCHE SUR LES MÉTIERS ET LES MÉTIERS

POLITICAL PARTIES